Project B.A.G.E.L.

Conceptual Design and Feasibility Study for a Mars Ascent Vehicle using In-Situ Propellants as Part of the MSR Mission

AE3200: Design Synthesis Exercise

Project Group 20

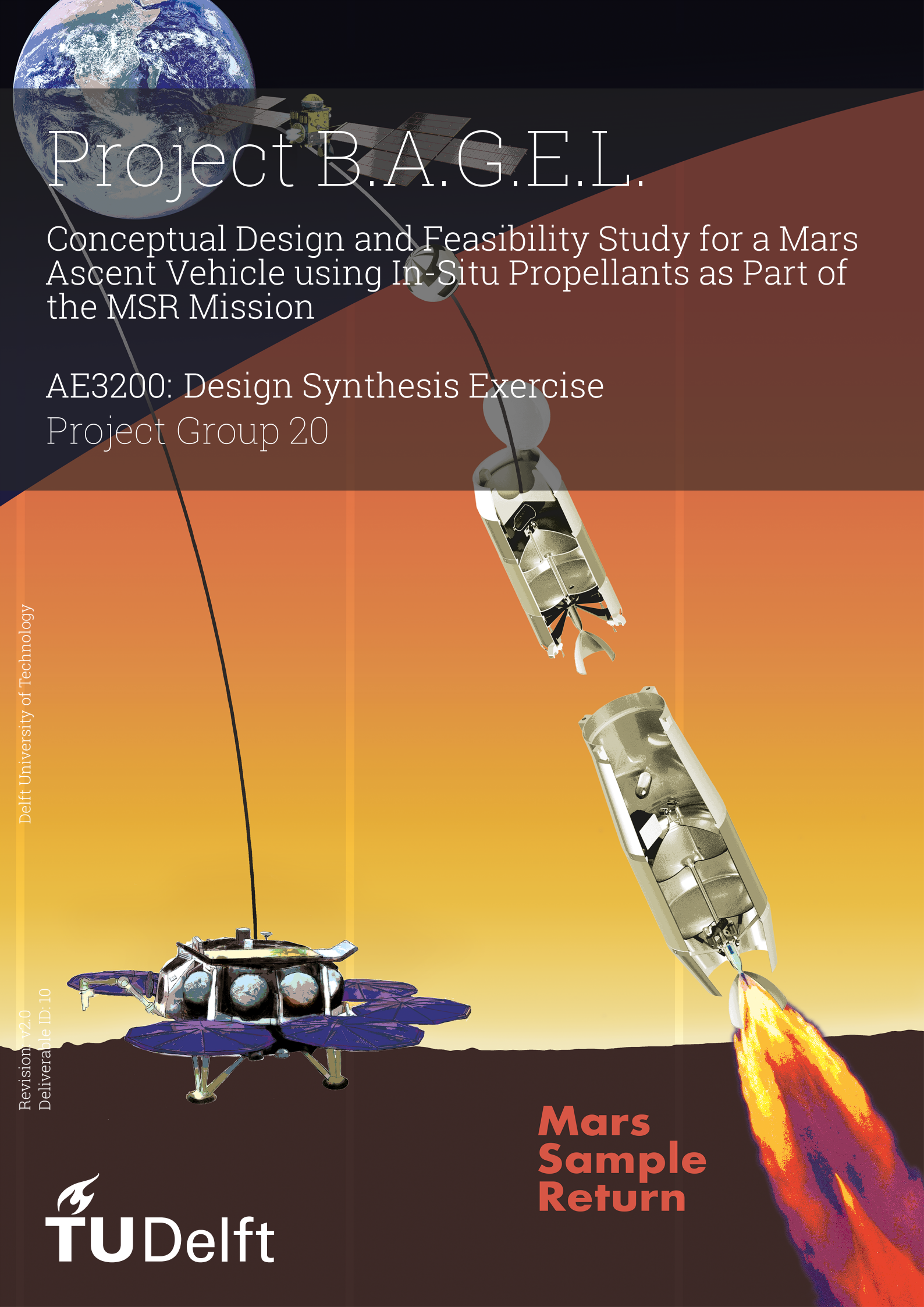

Delft University of Technology

Revision: v2.0
Deliverable ID: 10

TU Delft

Project B.A.G.E.L.

DID 10 - Conceptual Design and Feasibility Study for a Mars Ascent Vehicle using In-Situ Propellants as Part of the MSR Mission

by

Project Group 20

Student Name	Student Number
Ruán Ó hAnluain	5254965
Sven Balfoort	4669878
Dominic Campbell-Pitt	5449073
Benjamin Chen	5205379
Rune Decuyper	5528186
Alan Hanrahan	4993365
Jan Piaskowy	5446546
Jesse Rodrigo	5086019
Máté Seres	5562562
Oszkar Várnagy	5007534
Pietro Zanini	5471303

Document Revision:	v2.0
Deliverable ID:	DID 10
Tutor:	B.V.S. Jyoti (TU Delft)
Coaches:	T. Buchanan & K. Dissanayake
Company Supervisors:	M. Olde (TNO)
	D. Perigo (ESA-ESTEC)
	K. Blyth (Absolut System)
	A. Gorgeri (IoA)
Project Duration:	04-2024 to 06-2024
Faculty:	Aerospace Engineering, TU Delft

Cover: Jesse Rodrigo and Sven Balfoort
Style: TU Delft Report Style, with modifications by Daan Zwaneveld

TU Delft

Changelog

Date	Version	Changes
19-06-2024	1.0	Initial Draft
25-06-2-24	2.0	General: Minor formatting improvements. Executive Summary: Clarification of terms, Added context, Updated Figures. Introduction: Added context. Chapter 1: Corrected diagrams, Clarification and corrections in market analysis. Chapter 3: Corrected item in table. Chapter 4: Added references regarding compliance. Chapter 5: Clarification of trade-off summary. Chapter 6: Formatting, Clarification of subsystem descriptions, Updated figures. Chapter 7: Corrected error in Table 7.6, Clarification of budget contexts. Chapter 8: Clarification of sources, Updated Figures.

Deliverable Compliance

Deliverable	Page(s)
Executive Overview	ii
Functional Flow Diagram	12
Functional Breakdown Structure	12
Budget Breakdown	85
Technical Risk Assessment	16
Market Analysis	4
Operations & Logistic Concept Description	100
Project Design & Development Logic	103
Project Gantt Chart	88
Cost Breakdown Structure	89
Hardware Block Diagrams	40
Electrical Block Diagram	62
Data Handling & S/W Block Diagram	61
Sustainable Development Strategy	9
Compliance Matrix	119
Sensitivity Analysis	39
Verification & Validation	115
Production Plan	104
RAMS Analysis	109
Performance Analysis	39
Configuration & Layout	91
Structural Characteristics	57
Stability & Control Characteristics	79
Astrodynamic Characteristics	83

Executive Summary

MSR Mission

The Mars Sample Return (MSR) mission is a collaboration between NASA and ESA with the aim of retrieving the Martian rock samples gathered by the Perseverance Rover and sending them back to Earth for further study. This report outlines the design of a Mars Ascent Vehicle (MAV) and a Sample Return Lander (SRL) for this mission, with the additional consideration that in-situ resource utilisation will be performed. This means that while on Mars, carbon dioxide will be captured, and converted into liquid oxygen and liquid carbon monoxide to be used as propellants. Here one trades off a lower mass of propellant to be brought, with a larger mass of additional systems for propellant generation. This has the potential to bring net mass benefits to the mission, hence justifying a study of its feasibility.

Market Analysis

The MAV plays a crucial role in the MSR mission by launching Martian samples into orbit for retrieval and return to Earth, leveraging In Situ Resource Utilisation (ISRU) to reduce mission costs. The MAV project primarily serves scientific and exploratory markets, with potential applications in future space missions and technology developments. A Strength, Weakness, Opportunity, and Threat (SWOT) analysis identifies strengths such as adequate funding and high technology readiness while highlighting opportunities for broader applications and threats from external factors. Stakeholders include major space agencies, Original Equipment Manufacturers (OEMs), scientists, governments, manufacturers, the general public, and external collaborators, each with varying levels of interest and influence. The competitive analysis underscores the mission's cost-effectiveness, technological readiness, and potential for new market opportunities, with future market predictions indicating significant prospects in space mining, interplanetary colonisation, and ISRU technology.

Sustainable Development Strategy

Sustainability throughout the mission was of primary concern. The strategies developed covered environmental, economic, social, and safety aspects. This encompassed looking into how the development, production, operation, maintenance, and end-of-life can be made sustainable, as well as how people play a role themselves in sustainability. Another aspect covered was the potential future research opportunities that could arise from this mission. It was found that quite a number of options could be implemented to ensure a sustainable mission, both in terms of rules or policies to be followed such as those set by the Committee on Space Research (COSPAR), in addition to design features such as self-maintenance of the lander.

Functional Assessment

In order to begin the design of all the subsystems, one must have an overview of all the tasks the subsystems must undergo, necessitating a functional assessment. Here, the mission was broken down into its individual, component-level functions, and put in diagrams such that the flow of functions was clear. This was done for the phase of propellant generation and sample retrieval on Mars, as well as the launch of the MAV. These identified functions would later be used to derive subsystem requirements.

Risk Assessment

Risk assessment in the technical domain addresses potential shortcomings in performance, objectives, and requirements across safety, technical, cost, and schedule areas. Risks are mapped with prevention and mitigation strategies based on user requirements and preliminary mission architecture and then integrated into the mission requirements. These are tracked and updated throughout the design process as more information becomes available. The Baseline Report [1] established the risk assessment methodology, linking risks to stakeholder and system requirements, and has been refined to improve traceability between risks and corresponding requirements. Technical risks are categorised into domains such as SRL, MAV, propulsion etc. Risk probabilities and severities are classified, with updates and removals highlighted. New risks are listed separately, and risk maps before and after mitigation are provided.

Requirements

Requirements are the cornerstone of any project, guiding the design process to ensure successful outcomes. Each requirement in this project was given an identification code and expressed using the SMART criteria, categorised into stakeholder (STK), ISRU (ISR), Lander (LAN), MAV (MAV), and Market (MKT) requirements. Derived from user needs and risk & market analyses, the requirements emphasised interdependencies and integration. ISRU focused on propellant production and power; MAV on structure, propulsion, and avionics; SRL on thermal, power, and electronics; and Market on economic aspects. This ensured the project would be well-defined, achievable, and met stakeholder expectations.

Trade-off

All the trade-offs and sensitivity analyses done in the midterm report [2] were summarised and combined. From this, a final high-level concept design conclusion was made where the following architecture is present for both the MAV and the SRL. An artistic sketch was also made, shown in figure 1.

MAV

- **Number of Stages:** Two stages
- **Feed System:** First Stage: Electric Pump Fed, Second Stage: Pressure Fed
- **Igniter System:** Spark Torch
- **Power System:** Batteries
- **Structural Materials:** Metals and Composites. (Tanks from Al 7075-T6)
- **Communication:** Omni-Directional Radio Antenna
- **AOCS:** Determination: Star Tracker + Optical IMU's, Control: Thrust Vector Control + RCS Thrusters
- **Staging:** Cold Staging

SRL

- **Thermal System:** Passive: MLI + Heat Pipes + Reflective Paint, Active: Radiators + Cryocoolers + Fluid Loops + Electric Heaters
- **Power Generation:** Solar Cells
- **Propellant Production and Storage:** Upscaled MOXIE + Liquid storage in cryocooled tanks on SRL
- **Communication:** Omni-Directional + Directional Radio Antenna
- **MAV Launch:** Rotating Launch tower + Hot Launch
- **MAV Station keeping and Storage:** Stored Horizontally Inside the Launch Tube
- **MAV Connection to SRL:** Lugs

Figure 1: Final Design Concept

Subsystem Design and Analysis

Martian Environmental Protection

As the Martian environment is quite different to that of Earth, it had to be designed around it. Firstly, the aspect of increased radiation was looked at. This was deemed not much of an issue except for electronics, where radiation-hardened materials would be used. The additional hazard looked at was Martian dust covering solar panels. Here it was decided to use the pressurised Carbon Monoxide (CO) feed from the ISRU to blow gas over the panels, in combination with a coating over the panels which would reduce dust adhesive. Due to limited time, the analysis done here was quite limited, so it is recommended to perform a more detailed simulation on the removal of dust.

Thermal Control System

Building on the thermal environmental analysis, the thermal control system has been designed using Multi-Layer Insulation (MLI) heaters and heat pumps. With adequate insulation thickness, the lander only has to be heated and cooling can be avoided. To remain within the power budget, $56\,\mathrm{W}$ of power will be spent on heating the lander and $20\,\mathrm{W}$ of power will be allocated to cooling the cryogenic tanks, based on these values the thickness of the necessary MLI could be found. The lander main body will be covered in $47\,\mathrm{mm}$ of MLI, additionally the cryogenic tanks will be wrapped in $14\,\mathrm{mm}$ to keep them in cryogenic temperatures. The lander will be equipped with a heat pump that will cool the cryogenic tanks and heat the batteries to above $0\,^{\circ}\mathrm{C}$ to ensure ideal operating conditions for them.

ISRU

An important part of the mission was producing the propellants on Mars. It was found a 6-cell MOXIE-like design would be a good option for these purposes. Consuming less power, it would operate continuously throughout the mission lifespan. The fuel is recirculated to minimise the oxidation on the cathode, and a heat exchanger is applied to improve the efficiency. The propellants are then partially purified with a fractional distillation process, however, a more detailed analysis and design of this part would need to be performed.

Propellant Handling

The conditioning and storing of the propellants are performed on the SRL by the propellant handling subsystem. The output propellants from the ISRU are compressed to $30\,\mathrm{bar}$, filtered, and loaded into two spherical propellant tanks made of Aluminium 7075-T6. A cryocooler then cools the tanks to a cryogenic $100\,\mathrm{K}$, which liquefies both the CO and O_2 gas. These tanks are equipped with multiple safety valves and two loading paths to the MAV for redundancy. Before the MAV is launched, the propellants are loaded into its tanks using a pair of cryopumps. Finally, a couple of quick disconnects isolate the MAV right before launch.

Structural Characteristics

A structural analysis of the MAV with the incorporated tanks was performed. Three load cases were examined: the MAV under launch loads; the tank under its own internal pressure; and the MAV when using an integrated pressurised tank structure. The tanks were split between the first stage and second stage of the MAV, and the critical thicknesses, critical stresses, and final masses were found, being $2.1\,\mathrm{kg}$ and $4.3\,\mathrm{kg}$ respectively. The natural frequency of the MAV and second stage were also analysed. Finally, methods to control propellant sloshing were investigated and implemented.

The structure of the lander is heavily based on the architectures of the Insight and Phoenix lander's. This includes a $6\,\mathrm{cm}$ thick composite honeycomb lander bed, and an aluminium frame, with aluminium honeycomb shock absorbers in the legs to withstand the landing loads. The lander structure will deflect the exhaust plume of the MAV outward, away from critical components and potential piggyback payloads.

Command and Data Handling

The command and data handling systems are essential for Mars missions to transmit data, receive commands, and ensure success and safety. The mission uses BAE Systems' reliable RAD 750 CPU, proven in past missions like Curiosity and Perseverance, reducing development time and cost. The communication system, based on requirements, integrates with existing Martian architecture, enabling communication with the Deep Space Network (DSN), Mars Relay Network (MRN), and ESA's Earth Return Orbiter (ERO). The MAV has limited communication hardware but ensures a robust connection to the ERO or SRL, integrating into the DSN.

Electrical Power System

An important part of any space mission is its power production and distribution system, particularly when complex chemical processes shall be continuously operating on the lander. This will lead to a $24.2\,\mathrm{m}^2$ solar array, the largest ever brought onto Mars, and a $6\,\mathrm{kW\,h}$ lithium-ion battery. The effects of Martian dust have been detrimental to previous Mars lander missions' solar array performance, active cleaning methods are also proposed, cleaning the solar arrays using compressed gas jets from excess ISRU gases to keep the effects of dust at bay and minimise the necessary solar panel area.

Propulsion

The engine performance analysis covers several key aspects. The Chemical Equilibrium with Applications (CEA) analysis calculates chemical equilibrium compositions and properties of Liquid Oxygen (LOX) and Liquid Carbon Monoxide (LCO), showing how variations in the oxidiser/fuel ratio and chamber pressure affect performance. Specifically, the characteristic exhaust velocity (C^*) peaks around an O/F ratio of 0.43 for chamber pressures of 5.3, 10.7, and $30\,\mathrm{bar}$. Impurities in the propellants are examined, revealing that a 90% purity level in CO-feed can cause a C^* drop of $30\,\mathrm{m\,s^{-1}}$, affecting specific impulse (I_{sp}) by up to $6\,\mathrm{s}$. Theoretical analyses determine the optimal expansion area ratio, resulting in a maximum vacuum I_{sp} of $270\,\mathrm{s}$ (theoretically $306\,\mathrm{s}$) at an area ratio of 262, though practical constraints limit this. Discrepancies between theoretical and experimental values, with measured efficiencies of 86-88%, are attributed to incomplete energy release and mixing inefficiencies. Combustion chamber design is based on a characteristic chamber length of $890\,\mathrm{mm}$ for hydrogen-oxygen engines, resulting in volumes of $0.24\,\mathrm{L}$ and $0.11\,\mathrm{L}$ for the first and second stages. Nozzle lengths are $420\,\mathrm{mm}$ and $286\,\mathrm{mm}$ for the respective stages, with further optimisation needed through Computational Fluid Dynamics (CFD) analysis. The adoption of non-traditional nozzle geometries could enhance performance.

Following the engine design, regenerative cooling was looked into. For this, a simulation was created to estimate the rough temperature rise the engine as well as the carbon monoxide coolant might reach. Here, by using a coolant channel thickness of $2\,\mathrm{mm}$, the engine temperature for both the first and second stage would stay below $500\,\mathrm{K}$, and the carbon monoxide coolant for both stages would stay below its boiling point at the specified pressures for each stage.

Feed System

To achieve the chamber pressures required for the engine, an electrical pump-fed feed system was chosen for the first stage, while a pressure-fed feed system was used for the second stage. For the e-pump system, an electrical engine on each propellant turbine was used to reduce mechanical moving parts and complexity. The pressure in the first stage is kept at $7.5\,\mathrm{bar}$ by the pressurant tank and a simple regulation system. The pumps bring the pressure up to $32\,\mathrm{bar}$, where the injectors drop it to the nominal $25\,\mathrm{bar}$ chamber pressure. For the second stage, the propellant tanks are kept at $27\,\mathrm{bar}$ by the pressurant tank and are simply flowing to the injectors, where the pressure drops to about the $15\,\mathrm{bar}$ needed for the engine. Cavitation risks in the pumps are assessed using NPSH calculations, showing that at $100\,\mathrm{K}$, LCO and LOX pumps have NPSH values of $29.9\,\mathrm{m}$ and $44.3\,\mathrm{m}$, indicating cavitation is unlikely.

AOCS

Ensuring the MAV is able to successfully enter the desired orbit was crucial to the mission. To achieve this, the Attitude and Orbit Control System (AOCS) design consists of four components: a Thrust Vector Control (TVC) system, Reaction Control System (RCS) thrusters, Fibre Optic Gyroscopes (FOG), and star trackers. The first stage will use two actuators for the TVC and two FOGs. The second stage will continue using the FOGs, but not the TVC. Instead, twelve RCS thrusters are used, along with three star trackers for once its high in the atmosphere. The number of components gives consideration to redundancy in the system.

Ascent Profile

The goal of the MAV is to launch the Orbital Sample into a low Mars pick-up orbit. The ΔV budget was initially estimated to be $5000\,\mathrm{m\,s^{-1}}$, to be subsequently refined to $4500\,\mathrm{m\,s^{-1}}$ due to shorter burn times, reducing the gravity losses. Simulations and sensitivity analyses using a low-fidelity simulation tool adapted for Mars' orbital and atmospheric parameters showed the MAV is able to achieve the target orbit within the specified semi-major axis range. The MAV reaches a $502\,\mathrm{km}$ x $493\,\mathrm{km}$ orbit expelling $5380\,\mathrm{m\,s^{-1}}$ of ΔV. This is quite a bit more than the above mentioned ΔV estimation due to the better mass fractions in the final design. The simulations validate the MAV design and ascent strategy. Sensitivity analysis indicates that small changes in propulsion performance and control precision significantly impact the final orbit, necessitating precise control to meet user and mission requirements.

Pickup Orbit

The final phase of the mission involves the orbital insertion of the sample container into a $500\,\mathrm{km}$ circular orbit around Mars, with perturbances limited to $\pm 15\,\mathrm{km}$. NASA's General Mission Analysis Tool (GMAT) was used for this analysis, including the Sun and Jupiter as perturbing bodies and an exponential atmospheric model. The orbital elements are: altitude of $500\,\mathrm{km}$, eccentricity of 0, inclination of $25°$, and a Right Ascension of Ascending Node (RAAN) of $20°$.

The results, visualised over a 10-day period, show the lowest orbital altitude at $488\,\mathrm{km}$ and the highest at $512\,\mathrm{km}$, with no significant orbital decay. The inclination varies from a minimum of $18.7°$ and then increases. The orbit and ground track around Mars are illustrated, confirming stable orbital parameters within the specified constraints.

Budgets

Engineering budgets are derived for power, mass, volume and ΔV. The power generation system is designed using the power budget at a nominal usage of $465\,\mathrm{W}$. Mass breakdowns show that a total landed mass comes to $1063\,\mathrm{kg}$, a quite achievable payload mass. The use of ISRU processes is justified as the mass of propellant generation systems is less than the MAV propellant mass. The derived ΔV budget indicates stage 1 and stage 2 produce $3760\,\mathrm{m\,s^{-1}}$ and $1710\,\mathrm{m\,s^{-1}}$ of ΔV, respectively, aligning with the ascent analysis.

It is expected that it will take four years to develop and create these mission elements. The estimated costs for this mission segment are preliminary and derived from various sources. Costs are subject to revisions similar to the pre-existing MSR mission, which has seen ever-increasing estimates. The propulsion system cost is based on previous design frameworks, while the SOXIE cost mirrors the MOXIE experiment's $50 million, primarily allocated to research and development. Integration and management costs, essential for the engineering process, are also included and make up the majority of the associated costs. A large 50% contingency margin is applied to all costs, summarising the expenses for this mission segment. Following the design phase, numerous minor modifications and previously overlooked items will need to be incorporated. Although each of these additions may have a low individual cost, their cumulative expense can be substantial. Hence, a 50% redundancy is advisable to ensure a balanced approach, avoiding both over- and underestimation. Consequently, the total estimated cost of this mission segment comes to €1.2 Billion.

Final Design and Comparison

The final designs of the SRL and MAV are presented with a description of the main subsystems along with the configuration and layouts of these subsystems within the structure. It was followed by a comparison to the baseline MSR mission made by NASA, and in some parts also to the study performed by the Łukasiewicz Institute of Aviation (IoA). The comparison was made in terms of system mass, size, ΔV budget, number of MAV stages, payload mass to orbit and the overall cost. It was found that the MSR mission could greatly benefit from the option proposed in this report. However, a more thorough study would need to be performed, and a more careful cross examination of the integration with other MSR mission elements.

Figure 2 shows a render of the MAV final concept design, capable of launching the $10\,\mathrm{kg}$ Orbital Sample Container to a $500\,\mathrm{km}$ Low Mars Orbit. Figure 3 shows a render of the SRL final concept design.

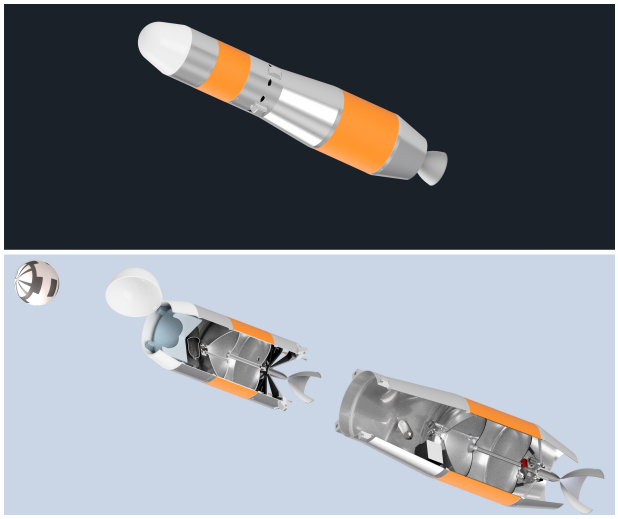

Figure 2: Overview MAV Render

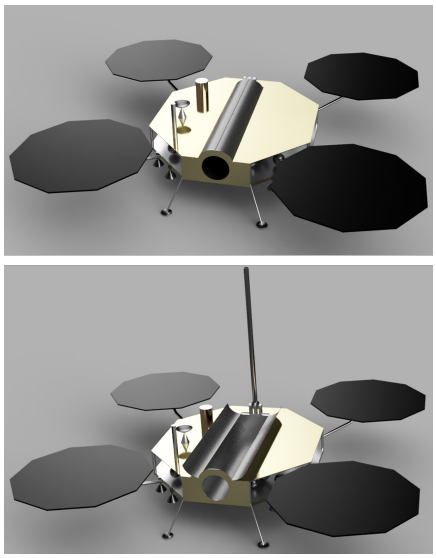

Figure 3: Overview SRL Render

Operations and Logistics

With respect to operational and logistical aspects of the MSR mission, critical elements were studied. These key elements include design and production facilities, clean room and integration facilities, the launch vehicle, mission control, communication networks, aeroshell and landing system, fetch rover, sample container, ERO, and additional scientific payloads. New elements under this study's design scope include the MAV, ISRU system, and the lander. The mission phases encompass feasibility studies, detailed design, development and integration, launch and transit to Mars, Mars landing, planet-side operations, Mars ascent, and mission end, ensuring compliance with COSPAR planetary protection policies.

Design and Development Logic

Having completed the initial phases of the design, it is important to outline the next steps that must be taken before launching. The following phase, called preliminary design, involves further design work and culminates in a preliminary design review. After that, the detailed design phase ensues, where detailed design is performed and reviewed at the critical design review. Subsequently, manufacturing and subsystem testing are carried out and reviewed at the system integration review. The final phases before the launch include integration and complete system testing.

Production

This describes what material choice was made for key mission components, and what production method will be combined with it, Split up into the MAV and the SRL.

MAV

This section details the MAV production methods and materials. The main considerations were reliability, legacy applications for the component's purpose, and resistance to the Martian Environment. The full breakdown of all components can be seen in table 1.

Component	Material	Production Method
Engine	Inconel 718	SLS 3D printing
Propellant Tanks	AA7075-T6	CNC Machining, Stir friction welding
Thrust Structure	Ti6-Al4-V	SLS 3D Printing
Interstage and Forward Structure	AA7075-T6	CNC Machining, Stir friction welding
OS Fairing	Aluminium honeycomb-graphite sheet composite	Layups of honeycomb, hand-packed with kinetic sand

Table 1: Production for Different MAV Components

SRL

For the SRL, as the systems used are more complex and intricate, it is more difficult to distinguish individual materials and production processes for certain parts. Hence, it will be relying more on outsourced systems, instead of individually produced parts. For the individual parts, the main driving components were reliability and environmental resistance. The items that will be produced directly are shown in table 2. Parts not mentioned here will either be outsourced or will be acquired as Commercial Off-The-Shelf components. These are:

- Cryogenic cooler;
- Cryogenic pumps;
- Valves;
- ISRU system;
- Thermal insulation.

As these are complex systems that have a large number of components, each going through its own production process, they are left out of the detailed descriptions.

Component	Material	Production Method/Sourcing
Storage Tanks	AA7075-T6	CNC Machining, Stir friction welding
Cryogenic Compressor	Stainless Steel, PTFE (seals)	CNC Machining
Solar Panels	Vectran Mesh	Solar Panels wafer production
Solar panel frame	AA7075-T6	CNC Machining, Stir friction welding
Lander bed	Aluminium honeycomb	Manual lay-up
Lander legs	AA7075-T6	CNC Machining, Stir friction welding

Table 2: Production for Different Lander Components

RAMS Analysis

The Reliability, Availability, Maintainability and Safety Analysis revealed some crucial information about the system. Firstly, reliability was considered. The lander design presented in this report is considerably lighter than other similar concepts, one of the reasons for this could be the reliability of the system. The lander was designed with 4 solar panels, 3 of which are necessary to operate. The reliability analysis has revealed that this leads to a 40% reliability of the solar panel assembly over the intended mission duration. This, coupled with the reliability of the other systems, leads to an overall mission reliability of about 25%, which in unacceptable for a mission of this importance. In order to remedy this shortcoming, additional solar panels have to be installed, in order to raise the reliability of the mission.

For availability and maintainability, it was found that due to the mission being unmanned and on Mars, maintenance cannot occur unless it is via software changes. The only other recoverable failures are ones where redundant hardware is available. Considering this, the calculated availability numbers were very safe, but this is mainly because there are no long maintenance periods due to very little maintenance actually being possible. For safety, it was identified that many functions during the MAV launch are crucial to Martian environmental safety due to the risk of crashing. These functions either have redundancy included or will have to be thoroughly verified and validated. It was also identified that safety needs to be considered during testing, and a list of considerations to mitigate risks here was compiled.

Verification and Validation

To validate and verify the design, a Verification & Validation plan was made to check the design with its compliance with the requirements. Firstly, methods and their description were made for the main system requirements. This created an overview of how the design can be verified compared to them. Then, a series of tests were proposed consisting of cryogenic, hotfire, and environmental stress tests. These tests are to validate that the entire system can perform the mission and meets all design requirements from the component, to the whole system level. Finally, a testing plan was proposed to create a timeline concerning the MAV and SRL Tests.

Compliance

Following the conclusion of the design, compliance matrices needed to be created such that it is ensured that all stakeholder requirements are met. When creating these tables, it was found that all requirements had indeed been satisfied, except for two which concerned ISRU. This is because quantification of ISRU purification was very difficult, as very little data was available, and it is recommended that further experiments be done for this.

Conclusion and Recommendations

This report focused on the MSR mission and aimed to test the feasibility of the in-situ generation of propellants while on Mars by developing a design. The scope of the design encompassed the MAV, the SRL, and the MOXIE system to generate propellants. It was concluded that the mission concept is viable and could potentially be more mass and cost-effective.

The report does not fully cover the detailed and worked-out design, where it would be highly beneficial for further analysis to be performed. For this reason, recommendations are also acknowledged. These cover recommendations for each subsystem analysed, as well as for the project in general, and finally looking at the general implications of this further analysis.

Contents

Nomenclature

Abbreviations

Abbreviation	Definition
ADCS	Attitude Determination and Control System
AI	Artificial Intelligence
AOCS	Attitude and Orbital Control System
BAGEL	Basis for Ascending with Gathered Exploratory Loads
CEA	Chemical Equilibrium with Applications
CFD	Computational Fluid Dynamics
CNC	Computer Numerical Control
CNSA	Chinese National Space Administration
CO	Carbon Monoxide
CO2	Carbon Dioxide
COSPAR	Committee on Space Research
CRM	Continuous Risk Management
CPU	Central Processing Unit
CV	Check Valve
DARE	Delft Aerospace Rocket Engineering
DSE	Design Synthesis Exercise
DSN	Deep Space Network
DRACO	Demonstration Rocket for Agile Cislunar Operations
DOD	Depth of Discharge
ECU	Engine Control Unit
EDL	Entry, Descent & Landing
EOL	End Of Life
EPS	Electrical Power System
ERO	Earth Return Orbiter
ESA	European Space Agency
ESTEC	European Space Research and Technology Centre
EU	European Union
FBS	Functional Breakdown Structure
FFBD	Functional Flow Block Diagram
FOD	Foreign Object Debris
FOG	Fiber-Optic Gyroscope
FV	Fill Valve
GCMS	Gas Chromatograph Mass Spectrometer
GMAT	General Mission Analysis Tool
GNP	Gross National Product
GJS	Good Jobs Strategy
Gyro	Gyroscope
H2	Hydrogen
HEPA	High Efficiency Particulate Air
IEEE	Institute of Electrical and Electronics Engineers
IMU	Inertial Measurement Unit
ISA	International Standard Atmosphere
ISRU	In-Situ Resource Utilisation
JAXA	Japanese Aerospace Exploration Agency
JPL	Jet Propulsion Laboratory
LCO	Liquid Carbon monoxide
LH2	Liquid Hydrogen
LOX	Liquid Oxygen

Abbreviation	Definition
MAV	Mars Ascent Vehicle
MECO	Main Engine Cut-Off
MEMS	Micro Electro Mechanical Systems
MLI	Multi-Layer Insulation
MOXIE	Mars Oxygen ISRU Experiment
MRO	Mars Return Orbiter
MSR	Mars Sample Return
MTBF	Mean Time Between Failures
NASA	National Aeronautics and Space Administration
NIST	National Institute of Standards and Technology
NPSH	Net Positive Suction Head
O2	Oxygen
ODE	One-Dimensional Equilibrium
ODK	One-Dimensional Kinematics
O/F	Oxidiser/Fuel
OEM	Original Equipment Manufacturer
P&ID	Piping and Instrumentation Diagram
OS	Orbital Sample
OSC	Orbital Sample Container
RAMP	Rover Avionics Mounting Panel
RAMS	Reliability Availability Maintainability Safety
RCS	Reaction Control System
RTG	Radioisotope Thermoelectric Generator
SECO	Second Engine Cut-Off
SLA	Super Light Ablator
SLS	Selective Laser Sintering
SM	Safety Margin
SMAD	Space Missions Analysis and Design
SNR	Signal-to-Noise Ratio
SOXE	Solid Oxide Electrolysis unit
SRL	Sample Return Lander
SRV	Safety Relief Valve
SWOT	Strength Weakness Opportunity Threat
TBD	To Be Determined
TCS	Thermal Control System
TDK	Two-dimensional Kinetics
TNO	Nederlandse Organisatie voor toegepast-natuurwetenschappelijk onderzoek
TT&C	Telemetry Tracking and Control
TRL	Technology Readiness Level
TVC	Thrust vector Control
UHF	Ultra High Frequency
UN	United Nations
UPS	Uninterruptible Power Supply
USA	United States of America
VV	Vent Valve

Symbols

Symbol	Definition	Unit
A	Area	m^2
A	Availability	-
$C*$	Characteristic Velocity	$\mathrm{m\,s}^{-1}$
C_F	Thrust Coefficient	-
c_p	Specific heat capacity at a constant pressure	$\mathrm{J\,kg}^{-1}\,\mathrm{K}^{-1}$
D	Diameter	m
E	Energy	J
E	Young's Modulus	Pa
f	Frequency	Hz
F	Force	N
g_0	Gravitational acceleration	$\mathrm{m\,s}^{-2}$
h	Convective heat transfer coefficient	$\mathrm{W\,m}^{-2}\,\mathrm{K}^{-1}$
I_{sp}	Specific Impulse	s
I	Current	A
I	Mass moment of inertia	$\mathrm{kg\,m}^2$
i	Current Density	$\mathrm{A/cm}^2$
k	Thermal conductivity	$\mathrm{W\,m}^{-1}\,\mathrm{K}^{-1}$
k	Number of elements needed for success functioning	-
k	Safety factor	-
L	Length	m
m	Mass	kg
M	Mach number	-
$\dot{m}$	Mass flow	$\mathrm{kg\,s}^{-1}$
n	Number of cells	-
n	Total number of elements	-
Nu	Nusselt number	-
P	Power	W
p	Pressure	bar
Pr	Prandtl number	$\mathrm{m}^2\,\mathrm{s}^{-1}$
$\dot{Q}$	Rate of heat transfer	W
q	Heat flux	$\mathrm{W\,m}^{-2}$
R	Radius	m
R	Individual gas constant	$\mathrm{J\,kg}^{-1}\,\mathrm{K}^{-1}$
R	Total reliability	-
R_i	Element reliability	-
R_p	System reliability	-
t	Thickness	m
T	Temperature	K
T	Time	s
T_{eq}	Lander surface equilibrium temperature	K
V	Velocity	$\mathrm{m\,s}^{-1}$
V	Voltage	V
V	Volume	m^3
x	Distance	m
α	Absorbtivity	-
δ	Power density	$\mathrm{W\,kg}^{-1}$
Γ	Payload Fraction	-
γ	Specific Heat Ratio	-
μ	Dynamic viscocity	$\mathrm{Pa\,s}$
ϵ	Emissivity	-
ϵ	Area ratio between chamber and throat	-
η	Efficiency	-
λ	Failure Rate	-
λ	Payload Ratio	-
ρ	Density	$\mathrm{kg\,m}^{-3}$
σ	Stefan-Boltzmann Constant	$\mathrm{W\,m}^{-2}\,\mathrm{K}$
σ	Stress	Pa

Introduction

Mars is significant in the solar system as one of the extraterrestrial bodies potentially possessing all the resources necessary to support life and develop a civilisation. It may have liquid water beneath its surface, likely locked in the permafrost [1] [2]. Additionally, Mars contains large quantities of carbon, nitrogen, hydrogen, and oxygen—essential elements for producing food, water, plastics, wood, paper, clothing, and, most importantly, rocket propellant [3].

The Mars Sample Return (MSR) mission aims to bring back Martian samples for analysis, furthering our understanding of Mars. The Mars Ascent Vehicle (MAV), the centrepiece of the mission, aims to launch the Martian samples gathered by the Perseverance rover into low Mars orbit, and transferring them to the Earth Return Orbiter (ERO) for a return to Earth. Its development marks a groundbreaking leap in engineering, enabling the first human-made product to be launched from the surface of Mars. The goal is not merely to set new records for human civilisation on Mars. Instead, the Mission Need Statement is as follows [3]:

Return Martian rock and dust samples to Earth in an effort to understand the formation and evolution of our solar system and prepare for future human explorations.

Historical exploration successes often involved adapting to local resources and methods. For example, well-prepared British naval expeditions to the Northwest Passage in the 19th century failed due to resource shortages[4], while Roald Amundsen's smaller expeditions succeeded by using local resources and travel methods [4]. This philosophy is not just relevant historically, but can also be applied to MSR. By implementing In-Situ Resource Utilisation (ISRU), and creating propellants on Mars using the carbon dioxide in the atmosphere, there is the potential to greatly reduce the total mass of the system designed for MSR. Furthermore, this would demonstrate technology crucial for expanding humanity into the solar system.

This final report, prepared by Team BAGEL, short for "Basis for Ascending with Gathered Exploratory Loads", presents the overall design of the Sample Return Lander (SRL) and MAV to demonstrate the feasibility of the ISRU approach for producing propellants on Mars. Specifically, liquid oxygen and carbon monoxide will be created from the planet's carbon dioxide-rich atmosphere. Chapter 1 starts with mission objectives and architecture, including market analysis and sustainability considerations. Chapter 2 shows the Mission phases, Project Design & Development Logic, Functional Flow Diagram, and Functional Breakdown Structure. In chapter 3, the risk assessment strategy is discussed, covering classification methods, performance and individual risks, and an overview and change log. In chapter 4, user and system requirements are categorised into functions, operations, and constraints, with an emphasis on aligning technical specifications with mission objectives, accompanied by a change log. Chapter 5 presents main trade-offs for each subsystem, with justified criteria and weights and sensitivity analysis. An overview of the conceptual sizing and analysis of all subsystems, including sensitivity analysis, is discussed in chapter 6. In chapter 7, budgeting strategies encompass mission and engineering budgets, with contingency plans for potential overruns. In chapter 8, the final layout and configuration are compared to the baseline MSR design. Chapter 9 outlines the project mission elements alongside the mission overview. Materials and production methods for each component on the Lander and MAV, as well as the final assembly method, are introduced in chapter 10. In chapter 11, quality assurance is ensured through sensitivity analysis and reasonable redundancy, with RAMS and verification and validation processes outlined to meet all requirements and verify the model. Finally, the report concludes with a summary and recommendations for future studies.

[1] https://www.nationalgeographic.com/science/article/mars-exploration-article
[2] https://www.nasa.gov/news-release/nasa-confirms-evidence-that-liquid-water-flows-on-todays-mars/
[3] https://www.nasa.gov/news-release/nasa-sets-path-to-return-mars-samples-seeks-innovative-designs/
[4] https://www.thecanadianencyclopedia.ca/en/article/sir-john-franklin

1

MSR Mission

This chapter serves the purpose of outlining the mission being designed for, and identifying the key stakeholders. Section 1.1 describes the overall objectives of the project, section 1.2 follows this by outlining the scope of the project, as well as the interfaces between subsystems. Finally, section 1.3 analyses the potential market for this mission, identifying key stakeholders and seeing how they might be affected.

1.1. Project Objectives

The MSR mission, a collaboration between ESA and NASA, is a proposed mission to return rock and dust samples gathered from the surface of Mars to Earth. Bringing Martian samples to Earth would allow for much more extensive analysis than what is possible with the onboard scientific sensors of in-situ spacecraft. The mission would see three separate sub-missions to return the samples. A sample collection rover will drill the rock and dust samples and leave the sealed samples behind. This is currently being carried out under the Mars 2020 mission by the Perseverance rover. It would be followed by the sample retrieval mission consisting of five spacecraft: the Sample Fetch Rover, SRL, MAV and two Ingenuity class helicopters. Lastly, an Earth Return Orbiter mission will bring back the samples to Earth. A critical step in the MSR mission will be the launch from the Martian surface, something that hasn't been done before. The currently proposed mission concept consists of a 2-stage solid propulsion MAV, which will serve as the baseline concept throughout the study.[1]

Other concepts have also been proposed throughout the years, like several hybrid and liquid propulsion alternatives. ESA proposed one such concept using ISRU propellants, which has the potential to significantly reduce the weight of the SRL when launched from Earth, therefore also making the EDL phase less challenging, albeit it would still be the 7 minutes of terror. Due to the abundance of CO_2 in the Martian atmosphere, it is possible to generate liquid O_2 and CO. An experiment currently ongoing on the Perseverance rover, called MOXIE, serves as a proof of concept for generating both O_2 and CO gas on Mars.

This ESA-proposed concept is currently under study by the Institute of Aviation (IoA) in Poland, TNO in the Netherlands, and Absolut System from France, to experimentally evaluate the feasibility of this mission concept. This mission concept is what is studied in this DSE, where the above companies serve as the company supervisors. The primary objective of the DSE is to execute an integrated aerospace design exercise, focusing on the early phases of the development process. The goal of this study is to develop a conceptual design for the MAV and SRL utilising ISRU propellant generation and a LOX/LCO based propulsion system and determine if this concept is feasible by comparing it to the baseline mission architecture.
This resulted in the following project objective statement:

> *To create a conceptual design and assess the feasibility of a LOX/LCO-based Mars Ascent Vehicle and its lander using locally gathered propellants, as part of the Mars Sample Return mission architecture. [5]*

1.2. Project Scope and Interfaces

This section aims to establish the scope of the project and define the interfaces between the systems. The V-model, shown in, Figure 1.1 is a useful tool that helps the systems engineer to define an effective scope.

[1] https://science.nasa.gov/mission/mars-sample-return/mission-concept

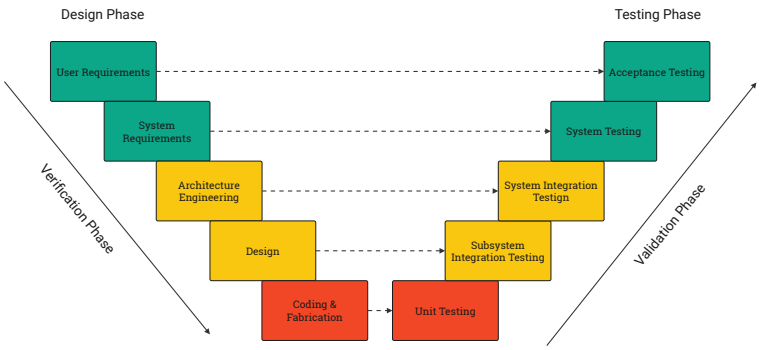

Figure 1.1: V-Model

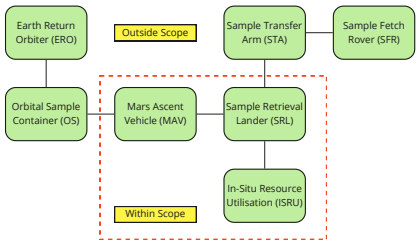

Figure 1.2: MSR High-Level Systems

Due to the large extent of the full MSR mission, it is important to establish a well-defined scope. Starting from the stakeholder requirements, they provide some initial constraints as to which parts of the MSR mission to focus on. As shown in Figure 1.1, with the user and system requirements established, the V-model can be followed down to a lower level, the system architecture. The system architecture was used as the primary method to further refine the scope and define the importance of each subsystem for the analysis. To already clearly portray the project scope from the start, the system architecture is presented here ahead of the requirements in chapter 4. The constraints stemming from the stakeholder requirements and MSR literature resulted in an initial mission scope as shown in Figure 1.2.

The mission can be broken down into two distinct major systems, the SRL and the MAV. These two systems will be interconnected and interact with each other for the majority of the mission duration through several interfaces. The SRL will house the MAV, protecting it from the Martian environment, provide power to its batteries, and load the propellants into it. After consolidating the stakeholder requirements and establishing the system requirements, several subsystems have been identified.

SRL Subsystems

- Command and Data Handling
- Thermal Control System
- SRL Structure
- Power Management
- Environmental Protection
- Propellant Handling
- Communications
- Sample Transfer
- MAV Storage and Launching

MAV Subsystems

- Thermal Control System
- Command and Data Handling
- Propellant Storage
- Power Management and Distribution
- MAV Structure
- Attitude and Orbit Control System
- Propulsion
- Communications

The major interfaces flowing from these subsystems have been visualised in Figure 1.3. The dashed boxes separate the SRL and MAV architecture. All the subsystems within these boxes are of various degrees of importance in the scope of the project. The grey boxes indicate systems that are outside the scope, but their interface with the MAV and SRL have to be considered. In Figure 1.3 the interfaces are not defined extensively, as that will be further developed in the following preliminary design step. However, it can already be seen that the SRL will have a more intricate interplay than the MAV.

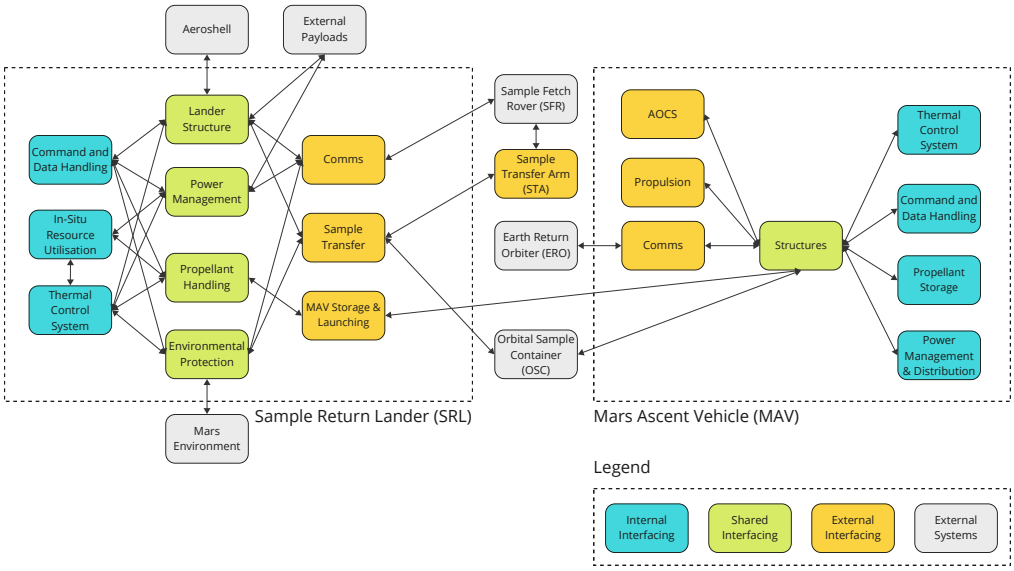

Figure 1.3: Mission Interfaces

1.3. Market Analysis

To perform a market analysis for the MSR mission architecture, one must focus on several aspects encompassing the market demand, stakeholders, competitive analysis, SWOT analysis, and the future potential market. Subsection 1.3.1 describes the market demand and the assessment on the new technology created for this mission, subsection 1.3.2 talks about the SWOT diagram, subsection 1.3.3 will introduce who the stakeholders are, subsection 1.3.4 analyses the competitiveness throughout the market, and finally subsection 1.3.5 outlines the potential future missions or markets that rely on the current mission.

1.3.1. Market Need and Value Proposition

The primary market need for the MAV is its critical role in the MSR mission, specifically, the ability to launch samples from Mars back to an orbit where they can be retrieved and brought back to Earth. Additionally, the innovative approach of ISRU to generate the propellants (LOX and LCO) is of great interest as it has the potential to significantly reduce the mass and cost associated with the mission by reducing the dependence on Earth's resources, as well as removing the need for propellant to be carried from Earth.

It is not enough to simply travel to Mars; it is also necessary to accomplish something meaningful there. A mission without capabilities holds no value [3]. The mission value should not be underestimated in the series of future deep space missions. The Mars samples provide invaluable scientific information regarding multiple aspects. For example, the rocks are preserved from when there was water on Mars, potentially providing new insights into planetary-scale formation, evolution in the inner solar system, and development of life here on Earth. Another part is that the Martian geological record represented by the samples could provide potential evidence of past life on Mars [6]. The Gas Chromatograph Mass Spectrometer (GCMS) results from previous Martian missions caused a stir, whether organic compounds were detected in the soil. If these Martian soil samples were analysed in a terrestrial laboratory, additional experiments could be conducted to resolve this debate definitively. On Earth, it is even possible to culture the samples and directly observe the results under a microscope [3].

The direct market for the MAV project is extremely niche, focusing solely on the MSR mission. However, the technology developed and the proof of concepts proposed could have broader applications. Namely: other missions requiring similar Mars ascent capabilities would have a high interest in the mission; demonstrating that the ISRU can function to incentivise further development of such technology; or even broader planetary missions where ISRU could be implemented advantageously. It is noteworthy to point out that cost of human spaceflight missions would depend on the ISRU technology, since ISRU could generate air for astronaut to breath. These aspects have the capability to establish new markets surrounding these innovative technologies and concepts.

The other primary market segments that the MAV project would serve more indirectly, are the scientific and

exploratory markets within other government-led space missions, while some secondary markets might include technology licensing for ISRU applications and educational or research collaborations. These interests are not necessarily linked to the mission itself, but may, for example, stem from the opportunity of collecting data from Mars using so-called ”piggyback” missions, or interest in researching the potential of this novel technology or understanding of the geological processes and harsh environments of Mars. Those opportunities MSR provided could characterise potential risks on Mars and prepare for future human missions [6].

1.3.2. SWOT Analysis

A mission SWOT analysis was performed to assess the strengths, weaknesses, opportunities, and threats of the MSR project itself shown in Figure 1.4. Helpful and harmful performance are divided up into internal (something we can control) and external (something that occurs out of our control) influence. Strengths define the competitive advantage or resources the mission intrinsically has. Weaknesses discusses what the mission lacks or its limits. Opportunities indicate areas in the mission that could be exploited, such as new technologies. Threats relates to any external cause that could lead to mission failure, such as changes in regulation or strong competitors.

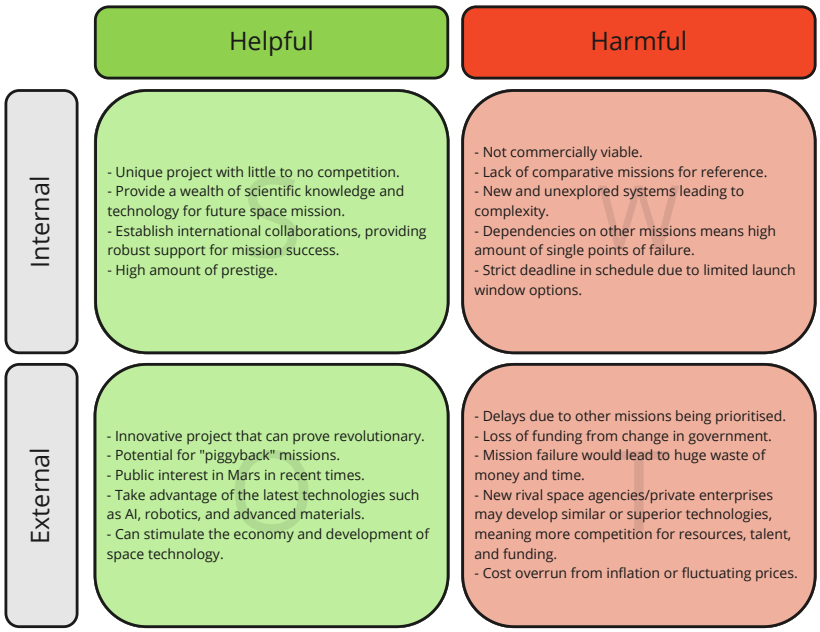

Figure 1.4: Mission Market Analysis SWOT Diagram

1.3.3. Stakeholders

A mission of such a scale has a number of stakeholders, all of whom will have separate invested interests, as well as having differing levels of influence on the project. The stakeholders of the mission can be broken down into the following groups:

- **Major Space Agencies**: This is NASA and ESA. They have been spearheading the mission with research, development, and organisation. They have committed the most and have the most control over the entire mission.
- **OEM (or integrators including launch provider)**: The manufacturers of the components used in the SRL, MAV and other mission products will have an invested interest in the success of all subsystems in the architecture.
- **Scientific Community**: Scientists of many disciplines around the globe are hoping to use the first samples of Martian soil to learn about Mars and the solar system.
- **Governments**: This is the governments of the USA and European nations. They want to stimulate the economy, demonstrate their commitment to science and develop international prestige for their scientific communities, for a reasonable price.
- **Manufacturers**: The industrial based manufacturers of mission components generate profits and have an invested interest in the success of the mission, to prove they are capable of developing Mars suitable components. They could seize the market for potential technology spin-out before others.

- **General Public**: The general public could benefit from new jobs, but would also like to see that their tax money is put to good use, and that their nation is capable of great things.
- **External Collaborators**: These are potential customers, such as private companies or other space agencies, which would like to add their experiments or components to the SRL or MAV for the opportunity to be on Mars, and are willing to pay to do so.

Each of these groups have their own varying interests and influences, these can be broken down using a stakeholder map, which is shown in figure 1.5. Influence conveys the quantity of rights and responsibilities certain parties possess over the mission, including how many changes in decisions affect them, whilst interest represents how much a party is invested into the project and stands to gain, including potential rewards or revenues.

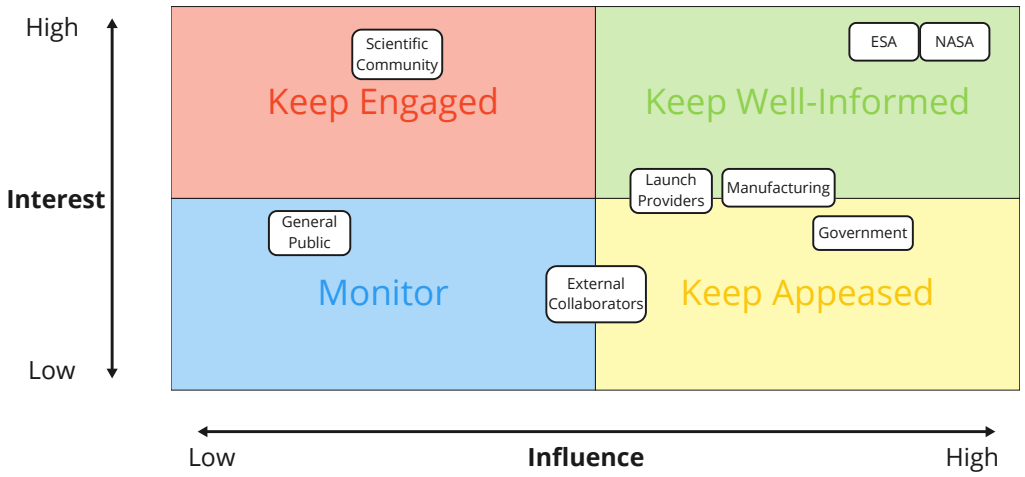

Figure 1.5: Stakeholder Map Showing Influence and Interest

As can be seen in figure 1.5, the major space agencies have the most interest and influence in the mission, essentially having full control. They have proposed, developed, and led the mission. It is their goal to facilitate scientific exploration in space, and they can make any design decisions needed.

Governments do not have as much interest in the mission as a whole or its outcomes, though they would be very invested in the rewards coming out of a successful mission, in terms of both money and fame. They also have the ability to add or cut a large amount of funding for the entire project, which offer them high responsibility.

The OEM have a fair bit of influence because they can steer system requirements. Their concern may extend to the actual performance of the mission as their components form parts of the systems. They gain by earning money by selling their products, and have an interest in showing that their products are a capable and reliable option for high-paying mission.

On the other hand, private industrial based manufacturers of the mission components have a higher degree of interest and influence. Similarly to before, they could earn profits by selling components. Additionally, it is their components which will form the physical side of the mission on the Martian surface and during the ascent, thus they have a strong influence on the mission itself.

The Scientific community has a high interest in the mission since they can earn money to carry out scientific research on the data and samples that would be gathered during the space mission, especially considering the returning samples could be revolutionary to science. However, the influence they have is not large because there is little they can demand from the SRL or MAV in terms of changes to the mission scope or design. On the other hand, the whole mission is essentially made for the scientific community within ESA/NASA for them to study the samples.

External collaborators who have the desire to pay and test their components or conduct science of their own, on the Martian environment, have a relatively lower interest in the mission because they do not explicitly earn money from the mission, though they would have the opportunity to make profit through the results of their tests.

The exact land location on Mars, and the power and mass which can be offered are all components which they rely on. The influence that they may bring is added funding and extra physical components for the mission (this would come with the requirement that they do not interfere with the mission as a whole).

The general public would typically have little interest or influence on the mission. The specific data which is hoped to be found through these samples and the technological accomplishment of their retrieval do not affect them in any significant way. They may simply receive national pride, job creation, and technology investment from this mission. For individuals, this could be highly beneficial, though for the majority of the general public, the mission will have no impact. Any influence they give could be wielded only when enough people gather to gain the governing agencies' attention.

1.3.4. Competitive Analysis

Our mission approach is highly competitive among other MSR mission methods, with distinct advantages in the following five areas: sufficient government funding, cost-effectiveness, technology readiness, capacity to carry piggyback payloads, and reusability.

First, there is adequate funding for the MSR program. Some argue that only with the financial resources of the Apollo era can we achieve great achievements in spaceflight again. However, the current government's total budget for NASA, when adjusted for inflation, is comparable to the budget during the Apollo era. Between 1961 and 1973, NASA's budget averaged 19 billion dollars per year, similar to today's budget. While NASA's budget constituted a larger share of the national fiscal expenditures in the 1960s, this was due to a smaller economy and population [3]. Despite the fact that the funding was similar, the unmanned exploration missions were more active in the past. For example, from 1961 to 1975, NASA launched eight Mars probes, six of which were successful, and from 2005 to 2020, it launched six Mars probes, all successful. These statistics prove that the initiative for the mission is not a matter of budget, but of determination to start it.

Our mission also stands out due to its low cost compared to baseline designs. In April 2024, NASA called for innovative ideas to lower costs, indicating that the baseline was not an ideal, low-cost solution [2]. This situation mirrors the 90-day report issued by President Bush in 1989, which also called for space exploration initiatives. Without using local resources, the cost of a manned mission to Mars could reach 450 billion dollars. The Mars Direct solution, proposed by Martin Marietta Corporation, changes to the use of In-Situ Resource Utilisation (ISRU) to reduce the budget to 55 billion dollars, one-eighth of the traditional plan's cost. Similarly, our proposed design also employs ISRU, which also ends up cutting costs from 2.77 billion to 0.35 billion dollars, which is also reduced to one-eighth of the traditional baseline design as detailed in chapter 7. Spreading 350 million dollars over six years represents just 0.24% of NASA's existing annual budget [3]. This amount is entirely acceptable to open up new frontiers for human civilisation.

Furthermore, current technology readiness makes this an ideal time to launch the mission. All technologies used in this mission have been validated in lab, with a minimum TRL of 4. A small scale of SOXE has been already tested on the perseverance rover, but the purification of carbon monoxide has not been tested. And the rocket engine has only been tested on Earth, but not on Mars. These are the two main points that lower the overall TRL. Half a century ago, the Apollo program achieved similar goals with far less advanced technology than we have today. With modern AI and machine learning, technological development is faster, cheaper, and more reliable. For instance, advanced flight control algorithms can optimise real-time flight trajectories, enhancing the mission's success.

We also have a head start on NASA's latest 90-day reports, having commenced our project over four weeks earlier [4]. While NASA's optimal method will be chosen after September, our design will be presented by the end of June. This early start gives us a competitive edge, embodying the old saying, "The early bird catches the worm." Additionally, our mission is positioned ahead of the Chinese National Space Administration's (CNSA) similar objective, with a more concrete timeline and readiness. This makes our mission attractive to potential new shareholders and customers, who can anticipate performing piggyback experiments by 2029. Finally, our mission is scheduled to be the first to return a sample from Mars, which will enhance our fame and prestige.

Our mission provides opportunities for other Martian missions. With fewer than five Mars landings per decade,

[2] https://www.nasa.gov/news-release/nasa-sets-path-to-return-mars-samples-seeks-innovative-designs/
[3] https://en.wikipedia.org/wiki/Budget_of_NASA
[4] https://www.nasa.gov/news-release/nasa-exploring-alternative-mars-sample-return-methods/

the chance to bring a payload to Mars is highly competitive. Our mission relies heavily on the successful electrolysis of CO_2 by MOXIE on the Perseverance rover, highlighting the importance of small, affordable demonstrations that can validate the feasibility of future, costly missions. By collaborating with other agencies and companies, our mission can provide a platform for such demonstrations, thereby strengthening technical and financial cooperation. Countries like South Korea [5] and India [6], aiming for Mars landings in the future, can use our mission as a test platform to increase their success rates. Additionally, the space and weight margins discussed in chapter 7 allow for more instruments on board, reducing the cost per user and increasing the scientific impact.

Finally, the adaptability of the MAV design is a key advantage. This flexibility allows the MAV to be repurposed for various missions or planetary bodies, saving time and resources and increasing the TRL for future missions. By maximising the use of onboard instruments for additional tasks or secondary missions after the primary objectives are completed, we extend the scientific utility and sustainable value of the MAV during its end-of-life phase. This approach prevents additional space debris in Martian orbits and ensures the mission's sustainability and competitiveness in the space market. For example, the MAV could be repurposed to conduct atmospheric studies or orbital observations after completing its primary mission, thereby extending its scientific utility and value. This will be further discussed in section 6.15.

1.3.5. Future Market Predictions and Expansion

"No space mission is just a one-off mission," Erwin Mooij reminds us. Our project builds on the success of MOXIE on the Perseverance rover, setting the stage for future missions that will rely on our developments. This section explores the future market opportunities created by our mission, including space mining, interplanetary colonisation, and innovative propellant choice.

Many objects around the solar system are composed of minerals and compounds similar to those found on Earth. This means that some asteroids, moons and planets will be rich in minerals and rare elements. The prospect of locating these resources, mining them, and ferrying them back to Earth safely attracts space agencies worldwide. This endeavour not only promises economic gains, but also opens new possibilities in manufacturing, product design, and resource management, which are crucial given Earth's finite resources. Even at this early stage of exploration, Mars is known to possess a vital resource that could become a commercial export. Deuterium, the heavy isotope of hydrogen valued at 10 thousand dollars per kilogram, is five times more abundant on Mars than on Earth. The high ratio of deuterium, needed to fuel fusion reactors, makes the prospects for generating thermonuclear fusion power on Mars excellent in the long run. Although fusion reactors do not yet exist, they could become profitable once developed [3].

Consider MOXIE, a groundbreaking mission aimed at converting Martian carbon dioxide into life-sustaining O_2. This innovative instrument is critical to future missions involving humans landing and inhabiting Mars, or simply for use in closed systems, where in-situ O_2 production could enable opportunities to carry out manned missions to other planetary bodies. If MOXIE continues to work as expected, it could pave the way for human settlement and exploration on Mars, spawning new markets for ISRU technologies.

MOXIE's output extends beyond O_2; it also generates CO, a rocket fuel providing the spacecraft with the thrust needed to navigate through Mars' atmosphere. Moreover, Mars could be a launchpad for future, potentially larger scale mission to elsewhere in our solar system. With its advantageous position over Earth, Mars offers, for example, a shorter gateway to the Oort cloud, the solar system's outermost frontier. On Mars, in addition to CH_4/O_2 or CO/O_2 propellant combinations, rocket thrust for propulsion can be generated using produced CO or raw CO_2 propellant heated in a nuclear thermal rocket engine. This aligns with NASA's current plans, where they have selected Lockheed Martin to develop and demonstrate a nuclear-powered spacecraft under the project Demonstration Rocket for Agile Cislunar Operations (DRACO) [7].

1.3.6. Additional Requirements

From the market analysis, a number of additional requirements were derived. These stemmed mainly from the fact that there was potential for "piggyback" missions which could positively affect the cost budgets for the MSR mission, as well as a more quantified requirement for the overall budget for the mission. They are listed together with the other requirements in chapter 4.

[5] https://spacenews.com/134853-2/

[6] https://www.indiatoday.in/science/story/isro-will-send-a-uav-to-fly-on-mars-with-next-mangalyaan-mission-2504224-2024-02-1

[7] https://news.lockheedmartin.com/2023-07-26-Lockheed-Martin-Selected-to-Develop-Nuclear-Powered-Spacecraft

1.4. Sustainable Development Strategy

A sustainable development strategy is essential to ensuring a mission following renewable processes and a clean working environment, while simultaneously minimising harmful emissions at all stages of the mission. It primarily focuses on the sustainability aspects intrinsic to the design and the design process, in addition to the way that the product can contribute to sustainability. The essence of sustainability goes beyond emission reduction; it is about ensuring that each process can persist indefinitely (*sustained*). This entails avoiding the depletion or irreparable damage to finite and renewable resources.

Environmental Aspects

Sustainable development and production of mission components is done in accordance with the UN 17 sustainable development goals, such that resources come from sustainable and ethical sources, and that manufacturing processes do not do undue harm to the environment. An additional objective will be to use renewable energy for all production processes. Making use of these energy sources for both daily operations (e.g. lights, ventilation) but also energy-intensive machinery (CNCs, Autoclaves) does a great deal to reduce the overall environmental impact of the project.

During operation, the mission will prioritise environmental protection as outlined in COSPAR's planetary protection policy [7], which focuses more on contamination rather than pollution. This boils down to ensuring that Mars is not contaminated by foreign terrestrial material for research and sample purity reasons, as well as ensuring that Earth is not contaminated by foreign Martian material, for safety reasons. The measures that can be implemented to safeguard the integrity of Mars-collected data and safeguard Earth include meticulously sterilising equipment headed for Mars and adhering to stringent protocols that will guarantee multiple layers of separation between items in direct contact with the Martian surface and those returning to Earth. This will prevent the exposure of unsealed Martian particles to Earth's environment, safeguarding against potentially harmful (organic) compounds. An additional way to ensure Mars is not contaminated, and to ensure that sample purity is maintained, was to minimise the use of organic materials within the MAV and SRL, as they contain carbon, as well as to minimise outgassing.

The mission takes place entirely on Mars, and thus the SRL and MAV systems need to be capable of maintaining themselves remotely. In addition to the design incorporating aspects to achieve this, certain processes can be periodically triggered from Earth to test the SRL systems to confirm they are still working. A part of the design, consists of blowing gas on the solar panels in order to remove the dust layer which will have been deposited. This will allow the solar panels to function at a higher efficiency throughout the mission. In terms of the periodic tests that could be performed, the moving of various parts on the SRL, such as the opening hatch or the rotating "rail" carrying the MAV, can be vibrated or rotated very small amounts to ensure they are still functioning, and reduce any possible degradation due to inactivity. As the SRL will be in sending system data back to Earth, another form of maintenance can also be performed. If any malfunctions are detected, software updates can be delivered to the SRL to control and fix the problems occurring, similar to what was done for the Voyager 1.

As for the end-of-life sustainability management, the topics of interest within the scope are primarily related to MAV and SRL. As this part of the mission takes place entirely on Mars, sustainability concerns will not pertain to end-of-life on Earth. In terms of the MAV, an important aspect would be the tracking of the stages jettisoned during its ascent, which was also highlighted in section 6.15. By tracking the falling segment to its crash location on Mars, the debris can be recovered in future missions, or at least the location can be recorded for future reference. In terms of the SRL, if the mission is successful, and it remains undamaged, it can continue to function as a communication hub or to gather scientific data even after the mission is deemed over, allowing for minimal wasted and disposed resources.

Economic Aspects

A part of sustainability that is not directly associated to the environment is that of economic sustainability. Also in accordance to the UN 17 sustainability development goals, guaranteeing that any produced economic growth does not compromise other community or societal aspects such as the environment, culture, or relationships to name a few. This can be accomplished by, for example, providing proper working conditions (with proper wages) to the newly created jobs, brought about thanks to the mission. Steps towards achieving this can also involve promoting and investing in sustainable practices such as those covered in this section - renewable energy, waste management, pollution, resource allocation etc.

Social Aspects

One of the most significant yet sometimes overlooked aspects is the human element. Establishing healthy and engaging work environments with motivated employees often leads to enhanced productivity, efficiency, and reduced errors. This not only minimises resource waste, but also significantly improves employees' quality of life. In all design endeavours, a system akin to the *Good Jobs Strategy*[8] will be implemented to optimise employee welfare and enhance the overall work environment. The following pillars of the GJS will guide our approach:

- **Standardise and Empower**: Individual employees are provided with clear and standardised objectives. This help to simplify their work, allowing them to focus on task execution and quality without expending energy on deciphering their responsibilities.
- **Cross-train**: Employees will undergo cross-training to specialise in various disciplines. Given the project's complexity and diverse interfaces, workload distribution across disciplines in different project phases will benefit from flexibility.
- **Operate with slack**: Ensure that the workload remains less than the total available staff at any given time. This facilitates employees in assisting others during crises or temporary unavailability. This approach, especially when combined with cross-training, proves highly effective.

Safety Aspects

Safety is a critical component of the sustainability strategy, encompassing both human and environmental considerations. Parts of safety were already touched upon in the context of COSPAR's planetary protection policy. More specifically, rigorous training, safety protocols, and emergency response plans should be in place in case of trouble. Furthermore, all personnel should be provided with the appropriate gear to intervene if required. As with any project, a detailed risk assessment should be performed specific to this portion of the MSR mission, including mitigation strategies and responsible individuals.

Future Sustainability Research

In the case of future sustainability contributions, a high-interest design feature of the MSR Mission is the carbon capture from the solid oxide electrolysis process required for the creation of the MAV propellants, oxygen and carbon monoxide. In light of this, the further research that can be triggered into this carbon capture technology is beneficial. For example, in the case of potentially up-scaling the process to fit larger applications, or when implementing the technology into other existing mechanisms to store or convert harmful emissions in-situ, or even in the case of closed-loop-life support systems. Furthermore, the storing of carbon monoxide can prove useful for other applications as it has several uses in metallurgy, and chemical industries, including the process of turning biomass fuels into diesel. This can help broaden the utility of biomass fuels, another carbon-neutral fuel source.

It should be noted that the concept of carbon capture is not central to the mission, though the process of producing the propellants from carbon dioxide is, making it an area of intensive research. Another area of interest due to the challenging Martian environment is in the power-producing systems such as solar panels. Given the abundance of dust on Mars, mitigation strategies or alternative innovative solutions will be essential to minimise the impact of dust interference on power production, which is elaborated upon in section 6.4. These solutions may not only benefit Mars missions but also have potential applications on Earth, enhancing the effectiveness and feasibility of solar panels for widespread use.

[8] https://goodjobsinstitute.medium.com/what-is-the-good-jobs-strategy-93a5c0b14980

2

Project Functional Assessment

This chapter introduces the phases of the mission and presents the various functions that the system will need to perform and how these are interconnected. In section 2.1 the phases of the mission and the high-level tasks that need to be performed are shown. Following that in section 2.2 and section 2.3 the various functions, their order, and interrelations are presented.

2.1. Mission Phases

The SRL and MAV as part of the MSR mission have to perform many different tasks divided over several mission phases. These are tasks that the vehicles need to complete themselves but are also actions that are executed upon the vehicles or actions that take place independently of the vehicles in the overall mission. Considered are the phases within the complete MSR mission that are applicable to the SRL and MAV starting with preparing on Earth and ending with the launch of the OSC into Mars orbit, resulting in the following mission phases:

1. Earth preparations
2. Earth launch
3. Earth-Mars coast
4. Mars EDL
5. System start-up
6. Mars operations
7. Mars ascend
8. Orbital payload deployment
9. Mission extension for additional scientific experiments

Only the design implications and resulting outcomes are considered starting from the Mars landing, after the EDL phase. The study includes mass and volume reservations for the landing system based on the existing MSR and Mars 2020 architecture. The fifth and sixth phases at large involve an extensive study into the complete ISRU process, payload loading and the operation of supporting systems on the SRL. The seventh and eighth phases are largely concerned with the analysis of the MAV into propulsion system architecture. In these two phases, a lot of the interactions and interfaces between the SRL and the MAV are considered together with all other parts of the MSR mission, as shown in Figure 2.1.[1] The primary mission concludes with the deployment of the payload into a Martian orbit. An extra phase has been added to consider the possibility of a mission extension for the SRL to serve as a static host for other scientific investigations.

[1] https://ntrs.nasa.gov/api/citations/20220013294/downloads/MSR%20IAC%20Presentation%20v10.pptx.pdf

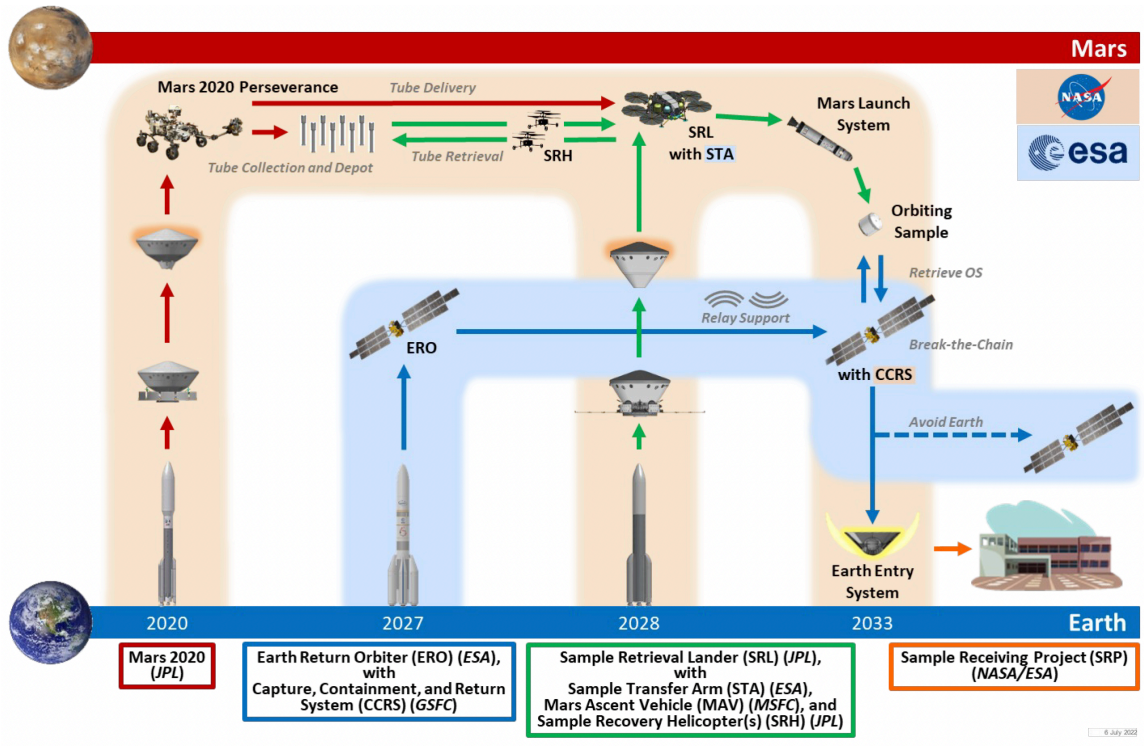

Figure 2.1: MSR End-to-End Architecture (NASA)

2.2. Functional Flow Diagram

The Functional Flow (Block) Diagram (FFBD) shows the phases of the missions considered in the study. Each phase consists of the functions that need to be performed within that phase. The diagram follows the logical order in which these functions take place. The phases and functions are represented by blocks. The first level (*FUN-#*) represents the phases. The other blocks are the functions broken down into several layers, ending in blocks that contain functions that are performed by one component and not a full (sub-)system. The arrows indicate the sequential flow, functions can also happen in parallel indicated by an AND junction or have conditional paths indicated by an OR junction. In general, the sequential functions flow downwards on the page, and when the functions break down to a lower level the arrow goes to the right. However, due to space constraints, many of the lower-level functions also flow sequentially to the right. Figure 2.2 and Figure 2.3 show the constructed Functional Flow Diagram.

2.3. Functional Breakdown Structure

The Functional Breakdown Structure represents a hierarchical view of the FFBD, that shows all the mission phases and functions as an AND tree. Figure 2.4 shows the constructed Functional Breakdown Structure. The FFBD and FBS use the same legend and colours, so *FUN-#* still represents the mission phases and the blocks representing deeper levels correspond to the system, and subsystem and end with functions performed by one component.

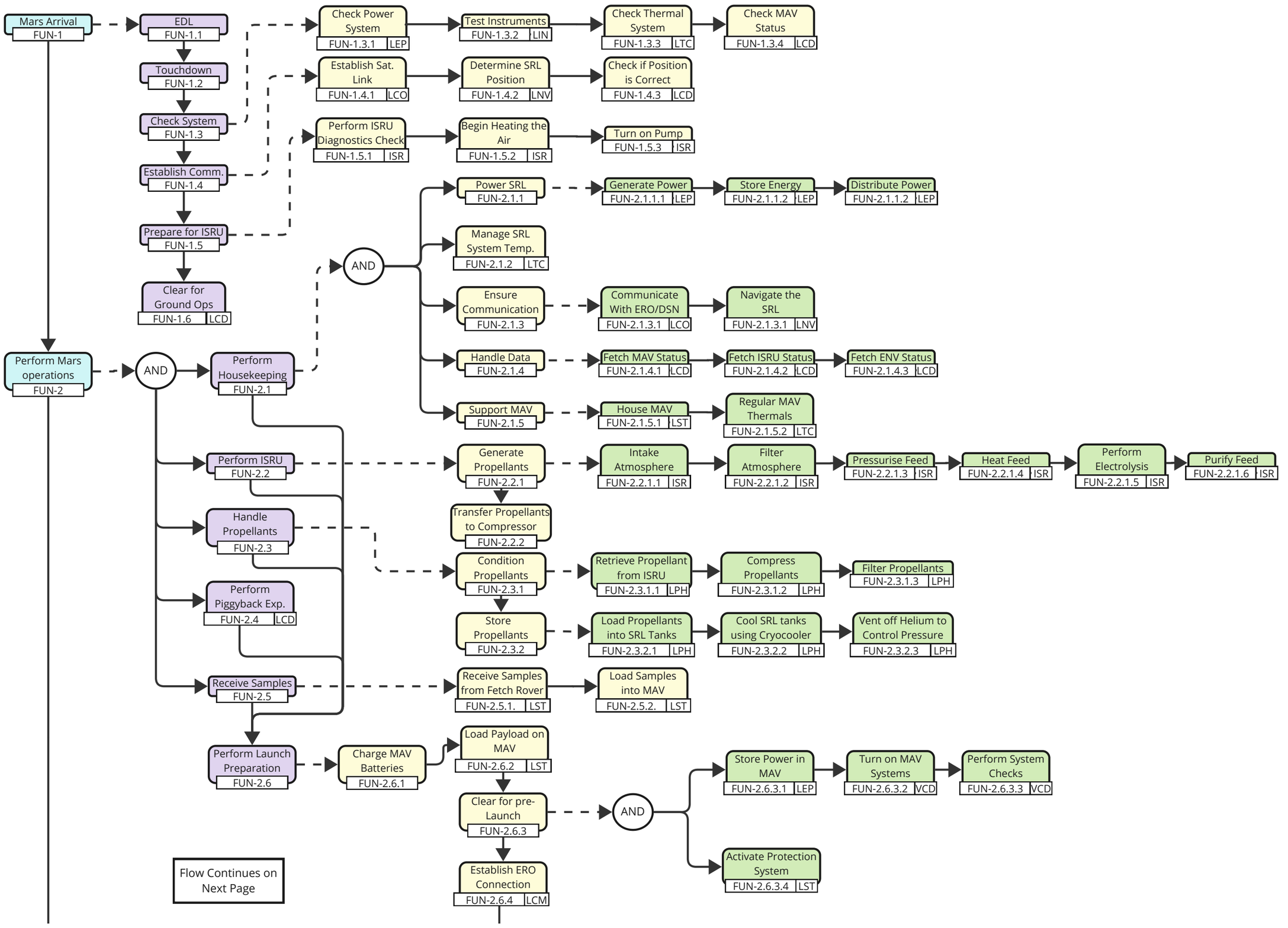

Figure 2.2: Functional Flow Diagram (Part 1)

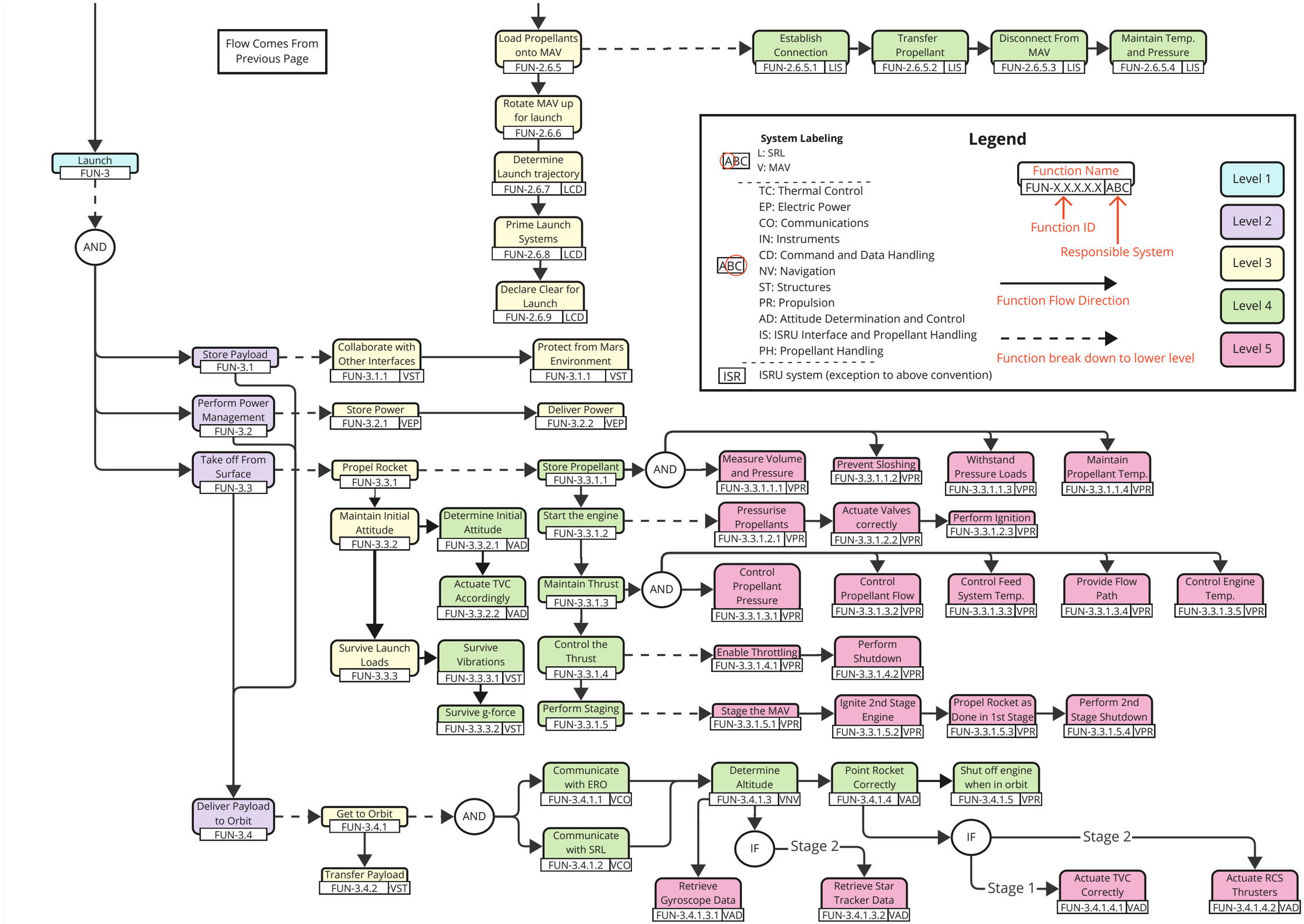

Figure 2.3: Functional Flow Diagram (Part 2)

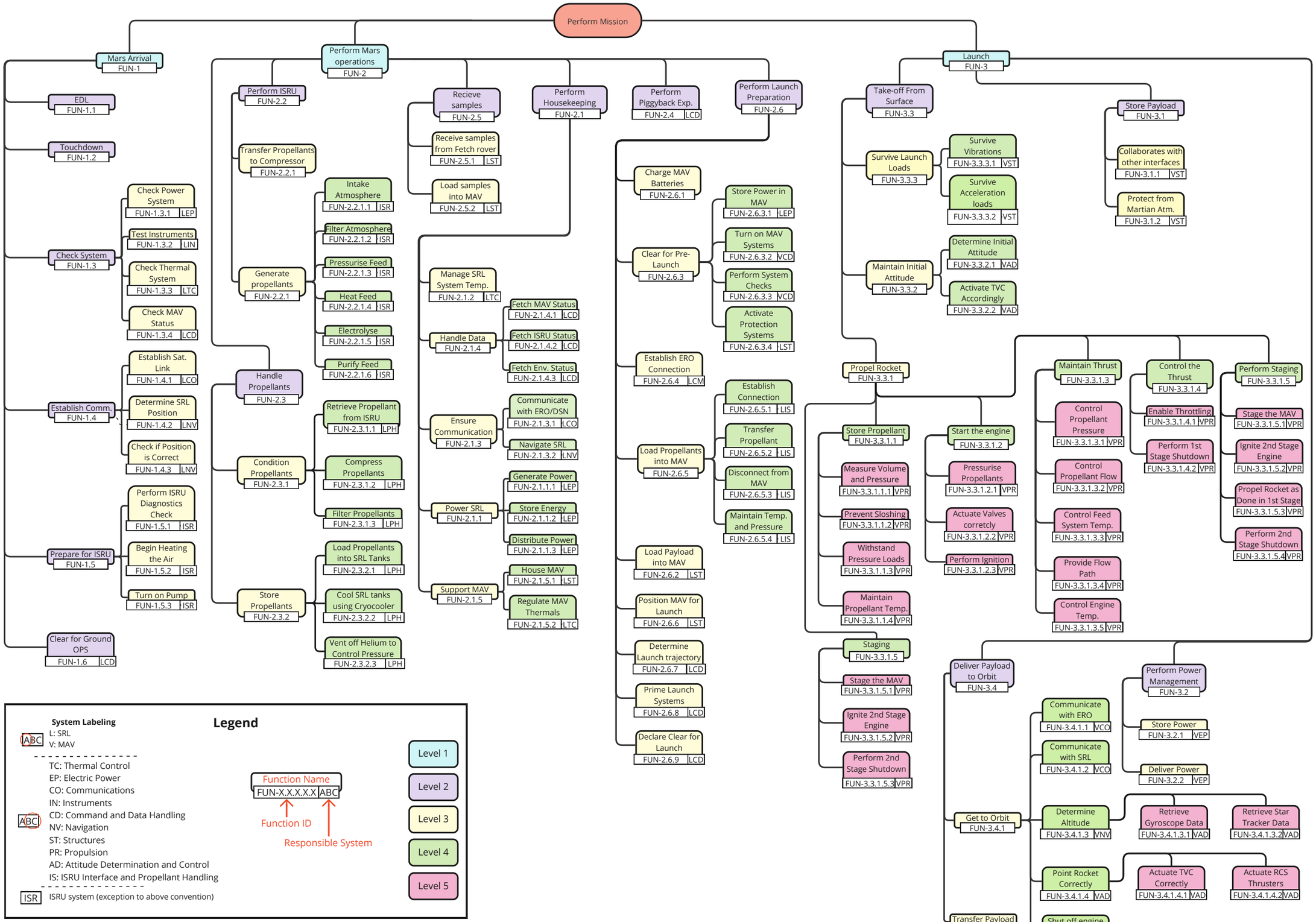

Figure 2.4: Functional Breakdown Structure

3

Risk Assessment

The technical risk assessment of the mission is discussed in this chapter. Here, section 3.1 outlines the continuous risk management method used, section 3.2 provides the categorisation of the risks, the technical risks and their risk maps are listed in section 3.3, and finally the risks changelog is provided in section 3.4.

3.1. Methodology

Risk means there is a potential for shortcomings, this can be with respect to performance goals, mission objectives and requirements. These shortcomings are usually attributed to one of the following mission domains: Safety, Technical, Cost, and Schedule. The subsequent risk assessment concerns the technical domain.

The best approach to risk assessment is often an ongoing and collaborative effort throughout the design process. Risks are initially set up based on the initial user requirements and preliminary mission architecture. These are then formed into risk maps with mitigation strategies. These risks and mitigations then flow together with the user requirements to form the full list of mission requirements. These will be constantly tracked throughout the design process, with changes made as systems become more fleshed out and more mission aspects become known. This report will mostly focus on risks that occur within the mission scope and life cycle. It can be that there are more risks that can occur after the official cycle, however, these will be outside the scope of this report.

A risk contains three aspects: scenario, probability, and consequence. The scenario is the cause leading to the shortcoming i.e. exceeding mass limits, cost overruns, and scenario causing injury [8].

The stakeholders are mostly interested in the risk of not meeting their key requirements, resulting in the mission not performing as intended. This narrows down their scope to a set of key risks, the so-called performance risks. For the engineering team, all risks are important to be identified, so that they can focus on eliminating the causes of the risks or put prevention and mitigation strategies in place.

Risk management happens in two stages. The first stage is before the risk causes a deviation, and the second stage is after the risk causes a deviation. In the first stage, risks are identified. The probability of an identified risk causing a deviation can be lowered by putting a prevention strategy in place. Of course, risks can still cause a deviation, therefore in the second stage, the consequences can be limited in terms of severity by employing mitigation strategies.

In order to mitigate the risks, two main approaches can be used. The probability can be reduced, by increasing the subsystem reliability or reducing points of failure. The severity can also be mitigated by increasing the redundancy of systems or making them easier to troubleshoot, reducing their impact if the risk event does occur. Note that redundancy can also be used as a probability prevention with systems like batteries. Using extra batteries can reduce their workload, making them less susceptible to degradation-induced failure.

A simplified risk management system based on the NASA Continuous Risk Management (CRM) will be followed throughout the full engineering process. CRM focuses on the management of risks early on in the project life cycle. CRM consists of several steps which are as follows [8, ch. 1]:

1. **Identify**: Capture the stakeholder's concerns on achieving the performance requirements. The concerns are captured as individual risks.
2. **Analyse**: For each risk the probability of a deviation and the severity of the consequence are estimated, keeping in mind the uncertainties in this process.
3. **Plan**: The next step is to decide what actions should be taken to reduce the performance risks that stem from the compounding of the individual risks. This could be accepting, mitigating, or closing the risk.
4. **Track**: The progress on implementation and effectiveness of risk management decisions is tracked continuously.
5. **Control**: When the continuous tracking indicates a risk management decision is not effective, actions can be taken to implement a revision on the plan step.

3.2. Categorisation

Risks are categorised in two ways, based on several mission domains and based on the level of the risk. In terms of risk level, a distinction is made between performance risks and individual risks. A performance risk means a performance requirement cannot be met, for example, the MAV not reaching the minimum orbital altitude. A single individual risk or a combination of multiple individual risks can cause a performance risk. The compounding of individual risks leading to performance risks is depicted in Figure 3.1. The risks have been divided over the following mission domains as listed above: Safety, Technical, Cost, and Schedule. The following sections will focus on the technical domain.

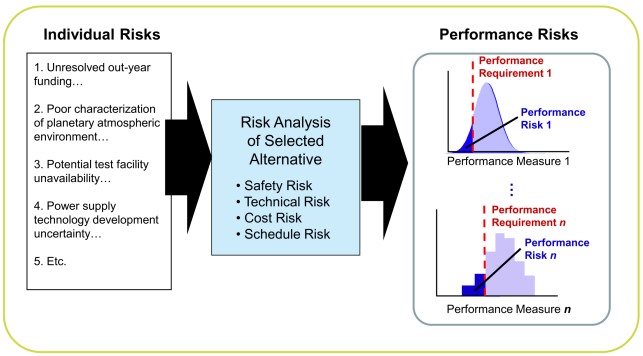

Figure 3.1: Integration of Individual Risks to Produce Performance Risks [8].

3.3. Risk Overview

The technical risks have been grouped into the following technical domains: Lander, MAV, Propulsion, Power, Avionics, ISRU, Electronics, Integration, Thermals, and Operations. The risk probabilities and severities are classified in Table 3.2 and Table 3.3. Table 3.4 shows the risk map before prevention and mitigation, Table 3.5 shows the risk map after prevention and mitigation and finally Table 3.6 provides all the technical risks.

NASA uses risk classes for their mission that indicate how much risk is accepted in the project phases depending on consequences on public safety, national science objective, schedule delay and cost. MSR is classified as Class A (Lowest risk posture by design). In this class, failure to reach the primary mission goals is deemed to have too high consequences on public safety or high-priority national science objectives. However, due to the extreme complexity and magnitude of development, it is allowed to launch the mission with many low to medium risks that could not be resolved under the mission cost and schedule constraints [9].

3.4. Changelog

Risk Assessment is a continuous process, which means throughout the project duration, more risks can be identified and prevention and mitigation strategies are altered. The initial technical risk assessment is described in detail in the Baseline Report [1]. It focused on setting up the risk assessment methodology and identifying risks from the stakeholder requirements, system requirements and market analysis. During the trade-offs in the Midterm Report [2] more risks were identified and some risks got improved prevention and mitigation strategies. To show this continuous process, a changelog is provided in Table 3.1.

Table 3.1: Risks Changelog

Date	Added		Removed	Modified
29-05-2024	RSK-LAN-OPS-001 RSK-LAN-INT-006 RSK-LAN-OPS-002 RSK-MAV-AVI-005 RSK-MAV-PRP-008 RSK-MAV-PRP-009	RSK-LAN-INT-005 RSK-LAN-INT-007 RSK-LAN-OPS-003 RSK-MAV-OPS-002 RSK-MAV-PRP-007 -	RSK-LAN-INT-002	RSK-LAN-INT-004 RSK-LAN-PRP-001 RSK-MAV-PRP-003

Table 3.2: Risk Assessment Probability Scoring. Adapted from [8].

Score	Definition	Probability
1	Not Likely	approximately **p < 20%**
2	Low Likelihood	approximately **20% < p < 40%**
3	Likely	approximately **40% < p 60%**
4	Highly Likely	approximately **60% < p 80%**
5	Near Certainty	approximately **80% < p**

Table 3.3: Risk Assessment Severity Scoring. Adapted from [8].

Score	Definition	Explanation
1	Minimal Consequences	Minimal consequences
2	Minor Consequences	Minor consequences to objectives
3	Medium Consequences	Unable to achieve a particular objective, but remaining objectives represent better than minimum success
4	Major Consequences	Unable to achieve multiple objectives, but minimum success can still be achieved
5	Destroyed	Unable to achieve objectives such as minimum success cannot be achieved

Table 3.4: Risk Map Before Prevention and Mitigation

Probability \ Severity	Very Low	Low	Medium	High	Severe
Near Certainty			RSK-LAN-ELC-001 RSK-LAN-INT-003 RSK-MAV-OPS-001 RSK-MAV-PRP-005	RSK-MAV-PRP-007 RSK-LAN-PWR-002 RSK-LAN-THM-002 RSK-MAV-INT-001 RSK-MAV-PRP-006 RSK-MAV-THM-001 RSK-LAN-OPS-001	RSK-MAV-STR-001 RSK-LAN-OPS-001
Highly Likely					
Likely		RSK-MAV-OPS-002	RSK-LAN-ISR-002 RSK-LAN-OPS-002 RSK-LAN-INT-007	RSK-LAN-INT-001 RSK-LAN-THM-001 RSK-MAV-AVI-002 RSK-LAN-OPS-003 RSK-MAV-PRP-008	RSK-LAN-PRP-001 RSK-LAN-PRP-002 RSK-LAN-PWR-001 RSK-MAV-PRP-003 RSK-MAV-PRP-004 RSK-MAV-PWR-001 RSK-MAV-STR-001 RSK-LAN-INT-006
Low Likelihood		RSK-MAV-AVI-001 RSK-MAV-INT-002	RSK-MAV-PRP-002	RSK-LAN-ELC-002 RSK-MAV-AVI-001 RSK-MAV-AVI-005	RSK-LAN-INT-004 RSK-LAN-ISR-001 RSK-LAN-INT-005 RSK-MAV-PRP-009
Not Likely					

Table 3.5: Risk Map After Prevention and Mitigation

Probability \ Severity	Very Low	Low	Medium	High	Severe
Near Certainty	RSK-LAN-ELC-001 RSK-MAV-AVI-004				
Highly Likely					
Likely		RSK-MAV-PRP-007 RSK-LAN-INT-001 RSK-LAN-INT-003 RSK-LAN-ISR-002 RSK-LAN-THM-002 RSK-MAV-OPS-001 RSK-MAV-PRP-005 RSK-MAV-THM-001 RSK-LAN-OPS-002	RSK-LAN-PWR-002 RSK-LAN-THM-001 RSK-MAV-PRP-001 RSK-MAV-PRP-006 RSK-LAN-INT-007 RSK-MAV-PRP-008	RSK-LAN-PRP-002 RSK-MAV-INT-001 RSK-MAV-STR-001 RSK-MAV-PRP-003	
Low Likelihood					
Not Likely	RSK-MAV-AVI-001 RSK-MAV-OPS-002 RSK-MAV-INT-002	RSK-MAV-AVI-001 RSK-MAV-PRP-002 RSK-LAN-OPS-001	RSK-LAN-ELC-002 RSK-LAN-ISR-001 RSK-LAN-PWR-001 RSK-MAV-AVI-002 RSK-MAV-PWR-001 RSK-LAN-INT-004 RSK-LAN-OPS-003 RSK-LAN-INT-005 RSK-MAV-AVI-005 RSK-MAV-PRP-009	RSK-LAN-INT-006	RSK-MAV-PRP-004 RSK-LAN-PRP-001

Table 3.6: Identified Technical Risks

ID	Risk	Pre-Prob.	Pre-Sever	Probability Prevention	Severity Mitigation	Post-Prob.	Post-Sever.
RSK-LAN-ELC-001	Electronics Anomaly	5	3	Choosing flight-proven electronics	Use error-correcting software and redundant hardware to keep errors in check	4	1
RSK-LAN-ELC-002	Lander Communication System Failure	2	4	Use Backup Comm Links	Use onboard automation processes to allow for continued independent operation	1	3
RSK-LAN-INT-001	MAV integration failure	3	4	Ensure individual interfaces are resistant to outer interference	Clean Areas affected by outer interference	2	2
RSK-LAN-INT-003	Launch system fails to prime	4	3	Pre-test Priming at Earth	Restart priming procedure from Earth	2	2
RSK-LAN-INT-004	Lander sample loading failure	2	5	System testing at Earth	Redundant loading paths, redundant mechanisms	1	3
RSK-LAN-INT-005	Launch mechanism jams when launching the MAV	2	5	Protect mechanical joints from Martian environment to prevent degradation	Design to allow for troubleshooting in case of component failures	1	3
RSK-LAN-INT-006	MAV storage container doesn't open	3	5	Incorporate redundant actuators	Ensure the housing can be accessed by other/external means enabling the potential for future rescue missions	1	4
RSK-LAN-INT-007	Launch exhaust damages piggyback missions	3	3	Use shielding to divert gasses away from delicate components	-	2	3
RSK-LAN-ISR-001	ISRU Failure	2	5	Use operational margin to keep ISRU running within comfortable limits	Have ISRU cells in parallel to prevent serial failure of the system	1	3
RSK-LAN-ISR-002	ISRU has lower yield	3	3	Include margin of safety for propellant production	Plan for a potential mission timeline extension	2	2
RSK-LAN-OPS-001	Contamination of Mars	4	5	Sterilise lander components	Ensure samples have contact with minimal number of surfaces	1	2
RSK-LAN-OPS-002	Launch exhaust from MAV damages lander	3	3	Divert exhaust away from vulnerable components	Enable MAV to operate without assistance from lander post-launch	2	2

Table 3.6: Continued from Previous Page

ID	Risk	Pre-Prob.	Pre-Sever	Probability Prevention	Severity Mitigation	Post-Prob.	Post-Sever.
RSK-LAN-OPS-003	MAV launch mechanism introduces unwanted rotation(s) in MAV	3	3	Thoroughly test and validate behaviour on Earth	Design for a MAV that resists disturbances, with a focus on stability characteristics	1	3
RSK-LAN-PRP-001	Propellant loading Failure	3	5	Use two propellant loading points on the lander	-	2	5
RSK-LAN-PRP-002	Propellant Leak	3	5	Have multiple points of failure such that a single faulty connection cannot cause a propellant leak.	Avoid having temperature-sensitive components next to potential leak locations. Allow time to create extra propellant to compensate for losses.	2	4
RSK-LAN-PWR-001	Power System Failure	3	5	Have an operational safety margin in the power system so the components and system do not fail from over-use. Protect fragile connections & components from Martian environment and other damages	Have UPS to keep core systems up and running, allowing for fixes to be performed from Earth if needed	1	3
RSK-LAN-PWR-002	Insufficient Power for Processes	4	4	Use a safety margin for power produced vs power needed	Use a dynamic scheduling program that can turn direct power to different systems at different times instead of running everything simultaneously	2	3
RSK-LAN-THM-001	Insufficient cooling capacity	3	4	Design the system with excess cooling capacity to handle high peak loads	Ensure systems operate with a margin w.r.t. peak thermal loads. Shut down non-essential systems if too much heat is generated.	2	3
RSK-LAN-THM-002	Insufficient thermal insulation	4	4	Perform analysis on the peak thermal cases expected for the system.	Design essential lander systems to withstand extreme temperatures expected in the Mars environment	2	2
RSK-MAV-AVI-001	ADCS System does not perform	2	4	Choose ADCS with longer MTBF & TRL	Have redundant components	1	2
RSK-MAV-AVI-002	MAV Communication System Failure	3	4	Use redundant communication systems with high TRL.	make the system compatible with DSN and existing Mars orbiters for easier comms. Have onboard computers to allow for independent operations	1	3

Table 3.6: Continued from Previous Page

ID	Risk	Pre-Prob.	Pre-Sever	Probability Prevention	Severity Mitigation	Post-Prob.	Post-Sever.
RSK-MAV-AVI-004	Electronics anomaly	5	3	Choosing flight-proven electronics	Use error-correcting software and redundant hardware to keep errors in check	4	1
RSK-MAV-AVI-005	First stage ADCS fails during launch	2	4	Validate system integrity before initiating launch procedures	Minimise complex control movements at moment of launch	1	3
RSK-MAV-INT-001	Payload fails to separate	4	4	Rigorously test system on Earth. Use high TRL separation mechanism	-	2	4
RSK-MAV-INT-002	Capture beacon malfunctions	2	2	Choose a more reliable capture beacon	Have a backup beacon	1	1
RSK-MAV-OPS-001	Hypersonic Speeds limits or damages MAV	4	3	Have the MAV fly at lower speeds in Atmosphere to limit Max Q	Have independent guidance systems that can operate under blackout. Have performance margin to overcome drag	2	2
RSK-MAV-OPS-002	Contamination of Earth	3	2	Ensure surfaces which have direct contact with Mars do not have unsealed contact with Earth	Sample handling shall follow the NASA Planetary Protection Standard (NASA-STD-8719.27)	1	1
RSK-MAV-PRP-001	Propulsion System Under performs	4	4	Design feed system with a margin. Validate systems on Earth to accurately evaluate the performance.	Ensure stages have a propellant margin to extended burns if necessary. Ensure the MAV can identify propellant margin	2	3
RSK-MAV-PRP-002	MAV feed system fails to actuate	2	3	Implement filters to reduce risk of FOD causing damage. Validate system over a large operating range	Have redundant valves and other Feed components	1	2
RSK-MAV-PRP-003	Feed failure	3	5	Validate the performance of all feed system components to beyond the expected conditions. Filters in feed lines	Redundant feed components (lines, valves, actuators)	2	4
RSK-MAV-PRP-004	Combustion chamber failure	3	5	Design the chamber with a safety factor. Perform extensive Earth side testing to validate pressure and thermal models	-	1	5
RSK-MAV-PRP-005	Propellant impurities	4	3	Validate the ability of the ISRU purification system to remove impurities.	Have filters in the relevant MAV feed system sections to deal with any impurities that got through the ISRU process	2	2

Table 3.6: Continued from Previous Page

ID	Risk	Pre-Prob.	Pre-Sever	Probability Prevention	Severity Mitigation	Post-Prob.	Post-Sever.
RSK-MAV-PRP-006	Injector failure	4	4	Avoid having a single point of failure for each injection mechanism	Spec the system to be able to inject more propellant than needed	2	3
RSK-MAV-PRP-007	Launch dynamics cause propellant sloshing	5	4	Design lander launch mechanism to minimise lateral and rotational forces on the MAV.	Incorporate components to minimise fuel movement.	3	2
RSK-MAV-PRP-008	Debris caused by launch exhaust hits MAV	3	4	Ignite engines away from likely debris sources	ADCS system should be capable of correcting for debris trajectory influences	2	3
RSK-MAV-PRP-009	Igniter timing is off and the MAV falls down onto the lander	2	5	Thoroughly test and validate behaviour on Earth	Launch mechanism allows for restraining MAV in case of ignition failure	1	3
RSK-MAV-PWR-001	Power System Failure	3	5	Have an operational safety margin in the power system so the components and system fail from over-use. Protect fragile connections & components from Martian environment and other damages.	Have UPS to keep core systems up and running, allowing for fixes to be performed from Earth if needed	1	3
RSK-MAV-STR-001	Structural Failure	3	5	Critically analyse all load cases ahead of commissioning. Design with a safety margin.	Design structures with redundancy. Use tanks and engines as loaded members to take extra structural loads	2	4
RSK-MAV-THM-001	Insufficient thermal insulation	4	4	Perform analysis on the peak thermal cases expected for the system.	Design essential MAV systems to withstand extreme temperatures expected in the Mars environment	2	2

4

Requirements

The requirements for the MSR mission were derived through two main methods. First, user requirements were analysed, clarified, negotiated, and lastly consolidated with the client. These were then used to develop system and subsystem requirements, narrowing the design scope. Secondly, the risk assessment and market analyses in chapter 3 and section 1.3 generated additional requirements. This chapter discusses the consolidated list of requirements used to guide the entire design process, as well as states if each requirement has been met in this project. In section 4.1 the changes in the requirements are documented. In section 4.2 the user requirements are presented, and in section 4.3 the system requirements are listed.

4.1. Changelog

The process for deriving all requirements is described in detail in the initial Baseline Report [1] for this study. As with any engineering design, every step is an iterative process. Thus, the requirements were repeatedly checked and improved throughout the project. For the purposes of clarity, a changelog is provided in Table 4.1

Table 4.1: Requirements Changelog

Date	Added		Removed	Modified	
16-05-2024	STK-M-009	STK-M-010	STK-M-005		
29-05-2024	ISR-019	MAV-AVI-013			
31-05-2024	ISR-020 LAN-INT-005 LAN-INT-007 LAN-INT-009 LAN-INT-011 MAV-AVI-014 MAV-INT-005 MAV-PRP-015	LAN-ENV-007 LAN-INT-006 LAN-INT-008 LAN-INT-010 LAN-THM-005 MAV-INT-004 MAV-PRP-014 MAV-PRP-016		LAN-ELC-003 MAV-AVI-013 MAV-AVI-009 LAN-PRP-001	*(Updated Traceability)*
10-06-2024			MAV-PRP-008	ISR-014 ISR-015 ISR-020 MKT-002	*(Clarified TBDs)*

4.2. User Requirements

The user requirements were originally provided with *MSR-REQ-X-###* identifiers corresponding to mission, interface, and study. This has been adapted to fit within the requirement identification system, where *STK* indicates Stakeholder and *M*, *I*, and *S* indicate Mission, Interface, and, Study requirements respectively. The tables showing these requirements have a compliance section, but compliance is discussed in section 11.3.

4.2.1. Mission Requirements

The consolidated user requirements for the mission are given in Table 4.2. Note that *STK-M-005* has been removed and replaced with *STK-M-009* and *STK-M-010* to further divide requirements into more precise goals.

4.2.2. Interface Requirements
The consolidated user requirements regarding the interfaces are given in Table 4.3. Note in the interest of keeping the numbering consistent, *STK-M-002* is kept empty.

4.2.3. Study Requirements
The consolidated user study requirements are given in Table 4.4. These requirements dictated the scope of the study, indicating what aspects of the MSR mission architecture are the most important to focus on. These requirements have not been fully met, this will be discussed in greater detail in chapter 11.

4.3. System Requirements
The system requirements were derived from the user requirements using the requirement discovery tree. These were analysed and combined with the risk analysis to determine what facets of the design are mission-critical and how they affect the design. Each requirement has an identifier, type, description, and finally, importance. The requirements are split between the ISRU process, the SRL, the MAV, and Market requirements. But firstly, higher level system requirements are defined in Table 4.5.

4.3.1. ISRU
ISRU requirements shown in Table 4.6 are simply defined by ISR-XXX. These describe the functioning of the ISRU system in order to produce the oxygen and carbon monoxide required to power the MAV ascent.

4.3.2. SRL
The requirements shown in Table 4.7 detail the requirements for the SRL system. It is split among the lander subsystems:

- LAN-ELC-XXX describing the SRL's electronic components such as communication components.
- LAN-ENV-XXX describing the SRL's ability to withstand the Martian environment.
- LAN-INT-XXX describing the SRL's ability to integrate with the rest of the mission architecture.
- LAN-PRP-XXX describing the SRL's ability to handle propellants needed for the MAV.
- LAN-PWR-XXX describing the SRL's electrical power management and distribution subsystem.
- LAN-THM-XXX describing the SRL's thermal management subsystem.

4.3.3. MAV
The MAV requirements shown in Table 4.8 describe the functioning of the MAV and its subsystems. The requirements are split the following way:

- MAV-AVI-XXX describing the MAV's avionics systems, their ability to control the MAV, and communicate with other mission elements.
- MAV-ENV-XXX describing the MAV's ability to withstand the Martian environment.
- MAV-INT-XXX describing the MAV's integration with the rest of the mission architecture.
- MAV-PRP-XXX describing the MAV's propulsion system and associated subsystems (feed, tankage).
- MAV-PWR-XXX describing the MAV's ability to power all its required functions.
- MAV-STR-XXX describing the MAV's structural components and their ability to carry the MAV through its mission cycle.

4.3.4. Market
The requirements are shown in Table 4.9 considering the economic aspects of the mission as well as the integration of market value into the mission by among other things, hosting external payloads. These requirements are derived from the analysis performed in section 1.3.

Table 4.2: Consolidated Mission Requirements

ID	Description	Trace	Compliance
STK-M-001	The system shall be able to place a 10 kg payload, consisting of Mars surface samples in the target orbit.	**MSR-REQ-M-001**	Yes
STK-M-002	The system shall place the payload in a circular orbit of greater than 500 km.	**MSR-REQ-M-001**	Yes
STK-M-003	Orbital dispersion of the payload should be below 30 km in semimajor axis.	**MSR-REQ-M-002**	Yes
STK-M-004	The system shall use a propulsion system based on Liquid Oxygen (LOX) and Liquid Carbon Monoxide (LCO) propellants for ascent.	**MSR-REQ-M-003**	Yes
STK-M-006	The system shall complete its surface mission between two consecutive Martian winters.	**MSR-REQ-M-005**	Yes
STK-M-007	The costs of the system should be comparable to existing MAV architectures.	**MSR-REQ-M-006**	Yes
STK-M-008	The system shall place the payload in a circular orbit at 25-degree inclination.	**MSR-REQ-M-001**	Yes
STK-M-009	The system shall be capable of producing the propellant to (re)fill the MAV in a maximum 12-month timeframe at the required temperatures and pressures.	**MSR-REQ-M-004**	Yes
STK-M-010	The system shall be capable of transferring the propellant to (re)fill the MAV in a maximum 12-month timeframe at the required temperatures and pressures.	**MSR-REQ-M-004**	Yes

Table 4.3: Consolidated Interface Requirements

ID	Description	Trace	Compliance
STK-I-001	The system should be compatible with the aeroshell and parachute system based on the Mars 2020 EDL system [10].	**MSR-REQ-I-001**	Yes
STK-I-003	The system shall incorporate the payload as defined for the baseline MSR mission as summarised in [11] including the samples collected by the Mars 2020 mission.	**MSR-REQ-I-003**	Yes
STK-I-004	The system shall include the payload transfer mechanism into the System but can assume the availability of a Fetch rover as defined in [11].	**MSR-REQ-I-004**	Yes
STK-I-005	The system can assume the availability of an Earth Return Orbiter capable of rendezvous with and retrieving of the payload as defined in [11].	**MSR-REQ-I-005**	Yes

Table 4.4: Consolidated Study Requirements

ID	Description	Trace	Compliance
STK-S-001	The study shall consider the size, weight and power requirements of the system and its major subsystems.	**MSR-REQ-S-001**	Yes
STK-S-003	The study shall compare blow-down, gas generator-fed, and Electric-pump-fed propulsion cycles.	**MSR-REQ-S-003**	Yes
STK-S-005	The study shall consider the sustainability aspects of the (development of the) system and identify potential contributions the development or mission might have to the UN Sustainable Development Goals.	**MSR-REQ-S-005**	Yes
STK-S-006	The study should incorporate mass and volume reservations for the landing system based on the MSR architecture defined in [11] but does not require analysis of the EDL part of the mission.	**MSR-REQ-S-006**	Yes
STK-S-007	The overall mission reliability shall be analysed quantitatively based on the TRL of different subsystems, their terrestrial analogues, and comparison with the baseline MSR architecture [11].	**MSR-REQ-S-007**	Yes
STK-S-008	The overall mission cost shall be analysed mainly by comparison with the baseline MSR architecture [11], the other components (outside the system) shall be considered outside the scope of the current work.	**MSR-REQ-S-008**	Yes
STK-S-009	The study shall evaluate the complete ISRU process.	**MSR-REQ-S-004**	Maybe (6.6)
STK-S-010	The study shall compare the LOX/LCO system solution to the baseline MSR architecture defined in [11] in terms of system weight.	**MSR-REQ-S-002**	Yes
	Continued on the next page		

	Continued from the previous page		
ID	**Description**	**Trace**	**Compliance**
STK-S-011	The study shall compare the LOX/LCO system solution to the baseline MSR architecture defined in [11] in terms of system size.	**MSR-REQ-S-002**	Yes
STK-S-012	The study shall compare the LOX/LCO system solution to the baseline MSR architecture defined in [11] in terms of number of stages.	**MSR-REQ-S-002**	Yes
STK-S-013	The study shall compare the LOX/LCO system solution to the baseline MSR architecture defined in [11] in terms of MAV Delta-V budgets.	**MSR-REQ-S-002**	Yes
STK-S-014	The study shall compare the LOX/LCO system solution to the baseline MSR architecture defined in [11] in terms of payload mass to orbit.	**MSR-REQ-S-002**	Yes
STK-S-015	The study shall evaluate the ISRU CO_2 collection process in terms of Size, Weight, Power and Propellant Throughput.	**STK-S-009**	Yes
STK-S-016	The study shall evaluate the ISRU propellant production process in terms of Size, Weight, Power and Propellant Throughput.	**STK-S-009**	Yes
STK-S-017	The study shall evaluate the ISRU propellant purification process in terms of Size, Weight, Power and Propellant Throughput.	**STK-S-009**	No (6.6)
STK-S-018	The study shall evaluate the ISRU propellant liquefaction process in terms of Size, Weight, Power and Propellant Throughput.	**STK-S-009**	Yes
STK-S-019	The study shall evaluate the propellant storage process in terms of Size, Weight, Power and Propellant Throughput.	**STK-S-009**	Yes
STK-S-020	The overall mission shall ensure the environmental integrity of Earth in accordance with COSPAR's policy of planetary protection.	**STK-S-005, RSK-MAV-OPS-001**	Yes
STK-S-021	The overall mission shall ensure the environmental integrity of Mars in accordance with COSPAR's policy of planetary protection.	**STK-S-005, RSK-LAN-OPS-001**	Yes

Table 4.5: System Requirements

ID	Description	Trace	Compliance
SYS-001	The system shall generate the propellants needed to launch a MAV to the required orbit from the Martian atmosphere.	**STK-M-004, STK-M-009**	Yes
SYS-002	The system shall maintain contact with Earth for the duration of the mission.	**RSK-LAN-ELC-002**	Maybe
SYS-003	The system shall remain fully operational for at least the duration of the mission.	**STK-M-006, STK-M-009, STK-M-010**	Maybe (11.1)

Table 4.6: ISRU Requirements

ID	Description	Trace	Compliance
ISR-005	The ISRU shall produce the propellants by electrolysis.	**SYS-001**	Yes
ISR-006	The ISRU shall liquefy the propellants after electrolysis.	**STK-S-017**	Yes
ISR-007	The propellants shall not come in contact with one another until launch.	**STK-M-004**	Yes
ISR-008	The ISRU shall produce the required propellant mass within the mission timeframe.	**STK-M-009**	Yes
ISR-012	The propellant liquefaction rate shall be greater than or equal to the propellant rate of production.	**SYS-001**	Yes
ISR-014	The ISRU shall pressurise the oxygen to $3\,\mathrm{MPa}$.	**STK-M-004**	Yes
ISR-015	The ISRU shall pressurise the carbon monoxide to $3\,\mathrm{MPa}$.	**STK-M-004**	Yes
ISR-018	The cells used in the ISRU process shall have redundancy.	**RSK-LAN-ISR-001**	Yes
ISR-019	The ISRU shall produce carbon monoxide of at least 90% purity.	**RSK-MAV-PRP-001, RSK-MAV-PRP-005**	Maybe (6.6)
ISR-020	The ISRU shall be capable of producing 20% more propellant than required for a successful flight.	**RSK-LAN-ISR-002**	Yes

Table 4.7: SRL Requirements

ID	Description	Trace	Compliance
LAN-ELC-001	The lander shall maintain communication with the Earth Return Orbiter and mission control on Earth.	**SYS-002**	Yes
LAN-ELC-002	The lander shall monitor the status of all subsystems and related processes.	**LAN-ELC-001**	Yes
LAN-ELC-003	The lander shall relay the status of subsystems to Earth for monitoring purposes.	**LAN-ELC-001, RSK-LAN-INT-005**	Yes
LAN-ELC-004	The lander shall be capable of determining its location and position on the Martian surface.	**STK-M-008**	Yes
LAN-ELC-005	The lander shall have redundant electronic hardware.	**RSK-LAN-ELC-001**	Yes
LAN-ENV-001	The lander shall monitor environmental air pressure for further analysis.	**LAN-ELC-001**	Yes
LAN-ENV-003	The lander shall withstand the low temperatures of the Martian environment.	**RSK-LAN-THM-002**	Yes
LAN-ENV-004	The lander shall utilise materials that are chemically compatible with the Martian atmosphere and surface.	**SYS-003**	Yes
LAN-ENV-005	The lander shall monitor environmental air temperature for further analysis.	**LAN-ELC-001**	Yes
LAN-ENV-006	The lander shall protect sensitive components from the negative impacts of radiation.	**SYS-003**	Maybe (6.4)
LAN-ENV-007	The lander shall shield mechanical joints from martian dust.	**RSK-LAN-INT-005**	No
LAN-ENV-008	The lander shall survive a 15g shock load upon landing on the surface of Mars.	**STK-I-001**	Maybe (6.8)
LAN-INT-001	The lander shall house and support the MAV up until the launch of the MAV.	**STK-M-006, STK-M-009, STK-M-010**	Yes
LAN-INT-003	The lander communication link system shall have redundancy.	**RSK-LAN-ELC-002, LAN-ELC-005**	Yes
LAN-INT-004	Temperature sensitive components shall not be placed within TBD m of potential leak locations.	**RSK-LAN-PRP-002**	Maybe (6.5)
LAN-INT-005	The lander Interfaces shall be resistant to degradation for the duration of the Mission.	**RSK-LAN-INT-001**	No
LAN-INT-006	The lander shall have a redundant path through which samples can be loaded.	**RSK-LAN-INT-004**	Yes
LAN-INT-007	The lander shall have redundant actuators for launching the MAV.	**RSK-LAN-INT-006**	No
LAN-INT-008	The lander shall enable the OSC to be accessed through external means, even when unpowered.	**RSK-LAN-INT-006**	No
LAN-INT-009	The lander shall direct launch exhaust away from delicate components.	**RSK-LAN-INT-007, RSK-MAV-PRP-008**	Yes
LAN-INT-010	The lander launch mechanism shall introduce minimal lateral and rotational loads on the MAV during launch.	**RSK-MAV-PRP-007**	Yes
LAN-INT-011	The lander launch mechanism shall restrain the MAV in case of an ignition failure.	**RSK-MAV-PRP-009**	Yes
LAN-PRP-001	The lander shall be able to load propellant onto the MAV through a minimum of two points.	**RSK-LAN-PRP-001, RSK-LAN-PRP-002, STK-M-010**	Yes
LAN-PWR-001	The power system shall provide power to all subsystems.	**RSK-LAN-PWR-001**	Yes
LAN-PWR-002	The lander shall provide power to the MAV.	**RSK-MAV-PWR-001**	Yes
LAN-PWR-003	The power system shall be able to provide sufficient power throughout the Sol cycle.	**LAN-PWR-001**	Yes
LAN-PWR-004	The power system shall be capable of detecting faults and relaying this information further.	**LAN-ELC-001, LAN-ELC-002, RSK-LAN-PWR-001**	Yes
LAN-PWR-006	The lander shall have a standby UPS.	**RSK-LAN-PWR-001**	Yes
LAN-PWR-007	The power system shall be able to direct power to specific subsystems at will.	**RSK-LAN-PWR-002**	Yes
LAN-THM-001	The thermal system shall provide thermal control to all subsystems.	**SYS-003**	Yes
LAN-THM-004	The thermal system shall have an array of sensors for monitoring the temperature throughout the lander and MAV.	**LAN-ELC-002**	Yes
LAN-THM-005	The Thermal system shall have excess capacity for peak loads.	**RSK-LAN-THM-001**	Yes

Table 4.8: MAV Requirements

ID	Description	Trace	Compliance
MAV-AVI-002	The MAV shall be capable of handling relevant data from sensors.	**MAV-AVI-001**	Yes
MAV-AVI-003	The MAV shall have software and hardware redundancy built into the avionics architecture to ensure reliable operations.	**RSK-MAV-AVI-004**	Yes
MAV-AVI-004	The MAV communication system shall be compatible with the DSN.	**RSK-MAV-AVI-002, STK-M-001**	Yes
MAV-AVI-001	The MAV shall establish a communication link to mission control on earth.	**SYS-002**	Yes
MAV-AVI-005	The MAV communication system shall be compatible with one or more existing Mars orbiters.	**RSK-MAV-AVI-002, STK-M-001**	Yes
MAV-AVI-006	The MAV communication link system shall have redundancy.	**RSK-MAV-AVI-002, STK-M-001**	Yes
MAV-AVI-007	The MAV shall have autonomous operation capabilities allowing for independent operation during the ascent phase.	**RSK-MAV-AVI-002, STK-M-001**	Yes
MAV-AVI-008	The ADCS shall have redundant sensors to minimise the chance of incorrect readings.	**RSK-MAV-AVI-001, MAV-AVI-011**	Yes
MAV-AVI-009	The ADCS shall have redundant control channels to ensure accurate attitude and orbit positioning.	**RSK-MAV-AVI-001, MAV-AVI-011, RSK-LAN-OPS-3, RSK-MAV-AVI-005**	Yes
MAV-AVI-010	The MAV guidance system shall be capable of operating under a communications blackout.	**RSK-MAV-OPS-001, STK-M-001**	Yes
MAV-AVI-011	The MAV shall have a redundant ADCS system.	**RSK-MAV-AVI-001**	Yes
MAV-AVI-012	The MAV shall have redundant electronic hardware.	**RSK-MAV-AVI-004**	Yes
MAV-AVI-013	The ADCS shall react within time to ensure accurate attitude and orbit positioning.	**STK-M-002, STK-M-003, RSK-MAV-PRP-008**	Maybe (6.13)
MAV-AVI-014	The MAV shall be capable of monitoring the status of all subsystems.	**RSK-MAV-AVI-005**	Yes
MAV-ENV-001	The MAV shall withstand the low temperatures of the Martian environment.	**RSK-MAV-THM-001**	Yes
MAV-INT-002	The MAV shall house and transport the Orbital Sample container to the ERO.	**STK-M-001**	Yes
MAV-INT-003	The MAV shall transmit its orbital location to the ERO for capture.	**STK-I-001**	Yes
MAV-INT-004	The MAV Interfaces shall be resistant to degradation for the duration of the Mission.	**RSK-LAN-INT-001**	Maybe
MAV-INT-005	The MAV shall have redundant ERO beacons to transmit location to the orbiter.	**RSK-MAV-INT-002**	Yes
MAV-PRP-003	The propulsion system shall be able to ignite the LOX/LCO propellants at launch.	**STK-M-004**	Yes
MAV-PRP-005	The MAV system shall deliver the OS to a 500 ± 15 km orbit around Mars.	**STK-M-002, STK-M-003**	Yes
MAV-PRP-014	The MAV shall have an initial thrust-to-weight ratio of at least 1.0.	**STK-M-002**	Yes
MAV-PRP-007	The MAV engine shall have a chamber pressure of $2.5\,\mathrm{MPa}$ with less than $0.1\,\mathrm{MPa}$ deviation.	**STK-M-004**	Yes
MAV-PRP-009	The MAV feed system shall have redundant valves.	**RSK-MAV-PRP-002**	Yes
MAV-PRP-010	The MAV engine injector shall not have a single point of failure.	**RSK-MAV-PRP-006**	No
MAV-PRP-011	The MAV feed system shall contain filters capable of filtering FOD.	**RSK-MAV-PRP-002**	Yes
MAV-PRP-012	The MAV feed system shall contain filters capable of filtering impurities from the ISRU process.	**RSK-MAV-PRP-005**	Yes
MAV-PRP-013	The MAV shall be able to have propellant loaded through a minimum of two points.	**RSK-LAN-PRP-001**	No
MAV-PRP-014	The MAV igniter should be designed such that it can be used more than once.	**RSK-LAN-INT-003**	Yes
MAV-PRP-015	The MAV Combustion chamber shall withstand pressures up to $2.5\,\mathrm{MPa}$.	**RSK-MAV-PRP-004**	yes
MAV-PRP-016	The MAV shall incorporate components to minimise fuel slosh.	**RSK-MAV-PRP-007**	Maybe (6.8)
MAV-PWR-001	The power system shall provide power to all subsystems.	**RSK-MAV-PWR-001**	Yes
MAV-PWR-002	The MAV shall be capable of receiving power from the lander.	**LAN-PWR-002**	Yes
MAV-PWR-004	The power system shall be capable of detecting faults and relaying this information for further analysis.	**MAV-AVI-001, MAV-AVI-002, RSK-MAV-PWR-001**	Maybe (6.10)
MAV-PWR-005	The power system shall have redundant capacity.	**RSK-MAV-PWR-001**	Yes

Continued on the next page

	Continued from the previous page		
ID	**Description**	**Trace**	**Compliance**
MAV-PWR-007	The MAV shall have a standby UPS.	**RSK-MAV-PWR-001**	Yes
MAV-STR-001	The MAV shall withstand launch loads.	**STK-M-001, STK-M-002**	Yes
MAV-STR-002	The MAV shall maintain aerodynamic stability during the ascent phase.	**STK-M-001, STK-M-002**	Yes
MAV-STR-003	The structural system shall be resistant to all expected cyclic loads.	**STK-M-001, STK-M-002**	Maybe (6.8)
MAV-STR-005	The MAV structure shall contain redundant members.	**RSK-MAV-STR-001, STK-M-002**	No

Table 4.9: Market Requirements

ID	Description	Trace	Compliance
MKT-001	Shall allow for $150\,\mathrm{kg}$ of External Collaborator payloads.	**MKT-005**	Maybe (7.1)
MKT-002	Shall supply $100\,\mathrm{W}$ for External Collaborator payloads.	**MKT-005**	Yes
MKT-003	Shall allow for $1\,\mathrm{m}^3$ volume for External Collaborator payloads.	**MKT-005**	Maybe (7.1)
MKT-004	External Collaborator Payloads shall not interfere with the Mars Sample Return Mission.	**STK-M-001, STK-M-002, STK-M-003, STK-M-004, STK-M-006, STK-M-007, STK-M-008, STK-M-09, STK-M-010**	Maybe
MKT-005	The added cost of the implementation of the External Collaborator Payloads shall be funded by the External Collaborator.	**MKT-006**	Yes
MKT-006	The Total Mission budget shall not exceed €10 Billion.	**STK-M-007**	Yes

5 Trade-off

Before conducting a detailed design of the mission segment, the configuration and combination of different subsystems must be selected. Different options for meeting the mission requirements were compared with one another, and traded off to create a general system configuration that can be analysed in greater detail. This chapter summarises that trade-off process in section 5.1 and subsequent results in section 5.2 before presenting the final system concept configuration upon which the design is based in section 5.3.

5.1. Trade Process

Due to the large number of trade-offs that were performed at this stage of the design, it was important to set up a consistent method that would consistently be followed.

In the first stage, the number of options being considered had to be reduced. Evaluating too many options in detail would be time-inefficient and difficult. To streamline the process, each option was initially assessed for its impact on the system —positive, neutral, or negative— represented by scores of 1, 0, and -1, respectively. Each criterion was scored, and a weighted sum was calculated using the criteria weights. The two concepts with the highest scores were then selected for further evaluation in the second stage of the trade-off.The results of the first trade-off were presented in Pugh Matrices, as shown in Table 5.1.

The second stage of the trade-off aimed to find the best option for the overall architecture of the mission. This was done by completing detailed trade-offs from the remaining options. To start, the inter-dependencies between the options that still needed to be finalised were found. Combinations of these interrelated options were created, followed by a trade-off. The final trade-off was performed simply between the best options found at the end of the first stage. In these cases, the criteria were kept consistent between the stages.

In terms of scoring, the second stage of the trade-off is much more detailed. The concepts get a score of 1-5 for subsystem trade-offs or 1-10 for the architecture trade-offs. These values were chosen for their simplicity and ease of understanding. At this stage, more detailed analysis could be performed due to the reduced number of choices. Once all the options have been scored based on the criteria, the option with the highest weighted average score was selected.

Table 5.1: Example Trade-off Pugh Matrix

Criteria	Weight (1-5)	Option 1	Option 2	Option 3
Criteria 1	1	1	1	0
Criteria 2	2	0	-1	1
Criteria 3	3	-1	0	0
Criteria 4	4	1	1	1
Criteria 5	5	0	0	-1
	No. of (+)	2	2	2
	No. of (0)	2	2	2
	No. of (-)	1	1	1
	Weighted sum:	*2*	*3*	*1*

Legend	
Positive impact on the system	1
No impact on the system	0
Negative impact on the system	-1

5.2. Trade-off Summary

5.2.1. Primary Trade-offs

Staging

For staging, an analysis was performed, and the following conclusions were made:

- **Single-Stage:** With the configuration chosen, according to calculations, a single-stage rocket is not viable. Even though it is the least risky and complex design, most sustainable and easiest to execute, it uses the most propellant mass and has the highest dry mass. Hence, a single-stage rocket was not chosen for the MAV.
- **Three Stages:** Compared to a single-stage, a three-stage rocket uses the least propellants and thus is the lightest. A big drawback to the idea however is that it is the least reliable, using three engines and lighting them while also requiring two staging mechanisms. According to the analysis performed in the midterm report, the difference with a two-stage rocket is only $24\,\mathrm{kg}$, which isn't that significant.
- **Two stages:** The two-stage rocket seemed the best middle ground between the options, being only slightly heavier than the three-stage but way more reliable. Compared to a single stage, it is able to reach the target orbit and deliver the payload to the ERO.

From the conclusions, a two stage rocket design was chosen for the MAV design.

Igniter

From the initial trade-off, laser ignition was ruled out since of its low TRL level [12] and complexity. Hypergolic propellants, pyrotechnics and spark torches are all further examined in the second stage trade-off since they are all at the same TRL level and require about the same volume. Notes were taken that hypergolics require conditioning to be a viable option.

Feed System

Analysing the feed-system options, five ideas were traded off. Gas turbine and electric pump were the best options to look into further because they are both very efficient and light options as a feed system. Closed cycle and full-flow staged combustion were also considered, but they are mainly used in high thrust cases and downscaling it to this level would take massive amounts of funding and time. Together with the fact that they are, for a LOX and LCO engine, not developed, brings the TRL level down to a point where it can't be considered any more. For the second stage of the rocket, a pressure-fed system would also be a viable option and was chosen to be considered further.

AOCS

The AOCS can be split up into two different parts, being the determination and actuation of the control of the rocket. For attitude determination, star trackers, IMU's and sun trackers were considered. Star trackers are the preferred choice when it comes to accuracy, which is one of the most important factors for the determination. The downsides are that it is less reliable while in cloudy weather or in high roll rate conditions, it requires more power and are in the middle ground in terms of weight. IMUs are a cost-effective solution and, while less accurate compared to other options, the reliability it provides is a strong case to use them as a viable option. Lastly, sun sensors were considered but eventually not chosen to be used because of their lack of accuracy together with their inability of working during eclipse or night conditions. In the end, for determination, both star trackers and IMUs were chosen as the optimal sensors for the mission.

Since IMU's were chosen as a preferred option, multiple IMU options were traded off, being quantum, mechanical and optical gyroscopes. Quantum gyroscopes are not developed enough to be considered an option in the end, since they provide a large risk in the operations of the mission. Mechanical gyroscopes require moving parts, making them less reliable compared to other options. Optical gyroscopes are the heaviest, however, in terms of stability, reliability and cost they are the best options. Combining this together with the fact that it has been flight-proven in many missions, they are chosen as the best IMU option for the MAV.

The subdivision of the optical IMUs was also considered. These consisted of MEMS or FOG gyroscopes. Although MEMS technology offers benefits in cost, size, and power consumption, it does not meet the performance and reliability standards provided by FOG, solidifying FOG as the preferred choice for critical missions.

For control, TVC systems was chosen to handle major trajectory adjustments during the first-stage burn due to their immediate response capability, while RCS were to be used for minor trajectory adjustments during

the coast period between burns. The importance of not reaching maximum dynamic pressure near first-stage burnout is noted to maintain controllability, particularly for TVC. Reaction wheels required too much mass and the least amount of torque for them to be a viable option for this mission. Due to the smaller need for control at higher altitudes and the lighter mass of the second stage, only RCS was used in the second stage, with the benefits of reduced weight and complexity.

Electric Power Systems

For power storage, by far the best option for energy storage for such a mission are batteries. Battery technology is continuing to rapidly advance in both space and terrestrial fields, leading to a dense, high-energy, tried and tested technology fit for Martian use. Following batteries are H_2/O_2 fuel cells, which have good specific energy and density qualities though not that of batteries, however, their use has mostly been as a primary energy source for manned missions, with the feasibility of them being secondary energy sources mostly being relegated to theoretical [13][14]. Flywheel Energy Storage has been used in space a number of times, however, its poor energy density has been made up for its secondary use in attitude stabilisation and control in orbit, without this secondary use, it is not competitive on a lander [15]. Compressed air and heat bank electrical storage were also considered, but are currently impractical for aerospace use.

For power generation, the options worth further analysing were Solar Panels, Radio Thermal Generators (RTGs) and Nuclear Reactors. Primary Batteries and Fuel cells will take up too much space and mass and could jeopardise the mission, as they would involve bringing the mission's entire energy requirements from Earth. Solar panels, often used in space for their high efficiency, face challenges on Mars due to Martian dust, which can reduce their reliability [1][2] and require heavy batteries and separate heating elements for lander operations. Conversely, nuclear reactors offer stable power[3] unaffected by Martian environmental conditions like dust storms and day/night cycles, but their use involves designing new systems since older models are outdated and their operation adds complexity due to criticality control. RTGs are highly reliable for deep space missions and are currently operational on Mars, but their use is constrained by the limited production of Pu-238, making them expensive and raising sustainability concerns. The two best options for power production are thus solar panels and RTGs. The implications of the choice of power production will affect the entire mission architecture, and were thus inspected later in the concept trade-off.

Propellant Storage

With regard to the storing container, the trade-off was between a freely expanding balloon-type container, and a solid tank shell container, for which the latter was decided upon. Initially, the concept of using an expanding balloon container for storing gaseous propellants on Mars was considered due to its potential benefits such as minimal space occupation when empty and no need for pressurisation. The gaseous form of oxygen and carbon monoxide could be efficiently stored at Mars' ambient temperature of $210\,\mathrm{K}$, enhancing weight and volume efficiency. However, significant drawbacks emerged, including the low TRL and potential large volume requirements, which could obstruct other lander systems and compromise the material's durability and mission reliability.

Consequently, this storage method was deemed unfeasible, leading to the dismissal of gaseous propellant storage altogether due to the difficulty of managing the required tank volumes. The following trade-off analysis focused on the phase of propellant storage, considering liquid or chemical states. Chemical storage, while theoretically possible, like adsorption of carbon monoxide to graphite[16], suffers from low TRL and adds complexity. Ultimately, liquid propellants were chosen for their balanced storage conditions and high TRL, ensuring reliability of the storage system.

ISRU Compression

For the ISRU multiple compression ways were researched. The sorption process is energy efficient, utilising energy primarily for heating the sorbent bed, and features fewer moving parts, enhancing its reliability and longevity. However, it suffers from a slow adsorption rate which limits the CO2 acquisition speed, making it less favourable for operations requiring quick supply capabilities. Mechanical compression does not involve an extended acquisition phase, allowing for a continuous CO2 supply. It was noted for its mass efficiency and does not face the challenges of slow adsorption, making it a robust choice for efficient and steady CO2 management. Although cryogenic cycling consumes more energy due to its intensive cryogenic processes, it

[1] https://www.nytimes.com/2022/12/21/science/nasa-mars-insight-mission.html
[2] https://www.nasa.gov/mcmc-dust-storms-during-northern-hemisphere-summer/
[3] https://beyondnerva.wordpress.com/tag/bes-5/

can operate multiple compressors out-of-phase to ensure a nearly steady CO2 supply. However, this method struggles with purity issues, as non-condensable gases accumulate and require additional mechanisms to vent, complicating the system.

In the end, cryogenic cycling was considered impractical for further consideration in the mission due to its high energy usage and complications in gas purity management. The decision was made to continue with sorption and mechanical compression for a more detailed evaluation.

Telemetry & Communications

As the requirements (**LAN-INT-003**) defined the lander need for redundancy, the following decision was made. As there is already a legacy of using a directional antenna to communicate both with orbiters and with Earth, this system will be used as a primary communications array. The second system will then be an omnidirectional array, as it is simpler and lighter, so it increases reliability. This will primarily communicate through Mars orbiters to lower the required power and mass budget.

For the MAV, due to the packaging and power requirements, and the need for redundancy, the choice was made to use omnidirectional antennas. Due to the Redundancy requirement (MAV-AVI-006), at least 2 omnidirectional antennae need to be used. A directional array would need a lot of compromises in packaging to keep it pointed in the right direction and to counter out all the launch vibrations. This would not be practical to include. Furthermore, as the MAV only needs to communicate to either the lander or Mars orbiters as relays, there is no need to have anything with a high enough gain to directly reach Earth.

5.2.2. Primary Trade-off Sensitivity

Staging

The trade-off for staging concludes that a two-stage MAV is the most viable. Removing the dry mass criterion makes the single-stage design the winner, and removing the volume criterion ties the single-stage option with the two-stage option. Similarly, increasing each criterion's weight to 5 has no impact on the result. Thus, a two-stage design can be confidently chosen as the optimal solution.

Igniter

Initially, the trade-off showed that the option of a spark torch and hypergolic propellants receive the highest score. Lowering the weight for reusability to 3, results in the option of hypergolic propellants and pyrotechnics receiving the same weighted sum of 10. Therefore, the sensitivity analysis reveals that it would be inappropriate to rule out the option of pyrotechnics at this stage, since it is not significantly worse than the top two scoring options. Hence, only lasers were ruled out before moving on to the more detailed stage.

Feed system

Changing the weights showed that the electric and gas turbine are still the best chosen options, since they stay close to each other and ahead of the rest. Pressure fed was also still considered for the second stage. Closed cycle and full flow staged combustion still will not be considered since their TRL level is also way too low for the mission.

AOCS

From the sensitivity analysis, for the determination, the trade-off is robust in every aspect. This has to do with how close many systems are to launch vehicles. The main note that should be taken is that reliability and accuracy will almost never drop below their assigned weights, since those criteria are the most vital to the success of MAV.

For gyroscopes, the system is robust in development cost, stability and moving parts. TRL will almost never be the least important, and mass wasn't considered as a high priority in this system. In general, the outcome of this trade-off was overall quite robust.

In terms of mass and complexity the control trade-off is quite robust, looking at capability and speed it is not so but these criteria are really important for the system, meaning that this is unlikely to shift to a lower importance. Finally, for accuracy it was deemed less important, but since a combination of both RCS and TVC was chosen, and reaction wheels never won over the other options, the trade-off choice was really robust.

Electric Power Systems

For the power storage, batteries perform best overall, and it is only when TRL is entirely excluded from the trade-off do H_2/O_2 fuel cells begin to be comparable, yet still worse than batteries. When specific energy is excluded flywheels become comparable, but worse than batteries.

For all weights except reliability, the weights were changed for power generation and the outcome stays the same. This means that the overall choice of going further with the design choices of solar or RTG is quite robust. Next to this, the reliability would generally not drop in importance, so even in that respect the choice is good as well. The choice of solar or RTGs are clearly superior, however the inter-connected-ness of this system with other systems means that the choice between these power options shall be made in the concept trade-off.

Propellant Storage

Modifying the weights for the trade-offs had minimal effect on the initial result. This is true for both the propellant storage phase and container concepts. Only when removing the reliability criteria (or removing more than one criterion) entirely are changes seen. However, as this is a long-duration long-distance space mission, reliability is key, so this weight is unlikely to change. For the storage location, this was not the case however, where changing the weights slightly saw multiple different outcomes with neither concept coming out as superior. For this case, the second stage trade-off was used to properly isolate a concept.

ISRU Compression

Since reliability, efficiency, mass efficiency and purity changes moved the ”best” option between batch sorption and mechanical compression while cryogenic cycling stays below, excluding it from further design was a very robust choice. The batch sorption does stay ahead when changing the values for the supply capacity down, so in this case it is the more robust option.

Telemetry & Communications

For the lander comms, no changes in reliability, integration or mass changed the outcome. The only parameters that influence the final outcome, were the SNR and required power whenever their weights were set below medium importance. In this case, the Omni-directional antenna would come out on top. So for shorter range transmissions, the omnidirectional antenna would be a more suitable option. This further supported the design choice made earlier to use an omnidirectional antenna to communicate with the MRO, as a backup to the main antenna.

The MAV communication trade-off was quite robust. The omnidirectional array comes out on top in all scenarios throughout all ranges, with the sole exception of the mass. If the mass weight was reduces to the least important criterion, the uni-directional array would come out on top. However, as this is a Launch Vehicle, mass will always be a limitation, hence this is a parameter that is unlikely to be reduced that far.

5.2.3. Secondary Trade-off

Igniter

For the Igniter, the stage two analysis was performed independently of other trade-offs and wasn’t considered in any architecture combination. In evaluating the systems for space missions, both spark torch and hypergolic propellants were rated highly for reliability due to extensive testing and consistent ignition capabilities. In contrast, pyrotechnic igniters scored lower because of the potential for propellant non-ignition. For reusability, spark torch and hypergolic systems are preferable as they require minimal additional space for restart capability, while pyrotechnic systems suffer from significant volume increases due to the need for multiple charges for restarts, lowering their score. In terms of complexity and volume, pyrotechnics are less complex as they involve only the charge, whereas hypergolic and spark torch systems require additional tanks, increasing their complexity and volume. However, hypergolic propellants face challenges with storability on Mars due to the risk of freezing during the Martian night without special conditioning. In the end, a spark torch was chosen as the ignition system for the engine.

Feed System

Feed systems also proved not to influence any architecture combinations and was thus done independently for the stage two trade-off. For the first stage, the feasibility of a gas turbine using LCO and LOX. This has never been done before, and the turbo machinery would have to be down-scaled to a size not really done before in outer space. This means that the efficiency will quite likely be lower than estimated and development costs would skyrocket. Therefore, the electric pump fed system was chosen. The pressure fed system was the best option for the second stage and wins over the other options overall.

Concepts

With the first stages of the trade-off completed, it is required to decide which concept to use. Many of these second-stage trade-offs had already been performed in the above sections, as those mission components were not interrelated with the rest of the system. This, however, can not be said about all the concepts that emerged from the first-stage trade-off; which resulted in highly interrelated options, needing to be assessed together. The possible options considered were:

Launch Mechanism:

- Toss MAV up
- Rotate MAV

Power Subsystem:

- Solar Panels + Batteries
- RTG

Propellant Storage:

- Store Propellant on SRL
- Store Propellant on MAV

Due to the complexity arising from eight possible combinations among three subsystems each with two options, the decision was made to simplify the trade-off analysis by reducing the number of options to four. This was facilitated by performing a preliminary compatibility analysis to identify the most incompatible options. In this analysis, each combination was scored on a scale from 1 to 10, where 1 indicated severe qualitative issues rendering the combination impractical, and 10 indicated no initial issues. This scoring was based on pairwise assessments of the subsystems, which were then aggregated to determine the overall compatibility score for each option. The total compatibility score of each option can be assessed as a simple sum of the individual compatibility. This is presented in Table 5.2.

Table 5.2: Concept Compatibility Table

	Launch Mechanism	Propellant Storage	Power Production	Compatibility Score
Concept 1	Toss MAV Up	Store Propellant on SRL	RTG	15
Concept 2	Toss MAV Up	Store Propellant on SRL	Solar Panel	19
Concept 3	Toss MAV Up	Store Propellant on MAV	RTG	20
Concept 4	Toss MAV Up	Store Propellant on MAV	Solar Panel	22
Concept 5	Rotate MAV	Store Propellant on SRL	RTG	22
Concept 6	Rotate MAV	Store Propellant on SRL	Solar Panel	21
Concept 7	Rotate MAV	Store Propellant on MAV	RTG	23
Concept 8	Rotate MAV	Store Propellant on MAV	Solar Panel	20

According to the way that the individual scores were already defined, in this table the maximum score of 30 meant that there were zero immediate qualitative issues seen with the concept combination, and a score of 3 (the lowest possible score) means that there are several immediate qualitative issues which make the concept impossible. As a result of the combined compatibility analysis, as shown in Table 5.2 above, Concept 4, Concept 5, Concept 6, and Concept 7 had emerged as the chosen options for the detailed trade-off.

From the detailed trade-off, the clear winner was concept 6. This was the only concept with a consistently good score on all the criteria. It did perform the worst on the size criterion, and as a result, this is something that will have to be monitored closely in the upcoming stages of the design. Interestingly, concept chosen does not include the toss-up launch mechanism, which is different from the baseline MSR study[4]. This however makes sense as that study was done for a solid rocket, which does not have additional sloshing and rapid start up issues like with a liquid rocket.

5.2.4. Secondary Trade-off Sensitivity

Igniter

The spark torch option received the highest overall score. Most cases lead to the same option receiving the highest score. The only case which yielded a new winner was removing the storability criteria entirely, causing hypergolic to win. This is a very drastic change, hence showing that the trade-off result is quite robust and reinforces the idea of using the spark torch. The only other change was that the pyrotechnic igniter outscored the hypergolic igniter when the reliability criterion was removed. However, this did not change the winner.

[4] https://www.jpl.nasa.gov/news/nasa-begins-testing-robotics-to-bring-first-samples-back-from-mars

Feed System

In a sensitivity analysis for the first stage rocket propulsion feed system, the electric pump consistently wins in the mass criterion. Size adjustments slightly favour gas turbines, but the differences remained marginal. The electric pump becomes increasingly preferable as complexity is considered, and its dominance extends when performance is prioritised. Gas turbines only gain an edge when the TRL is below 3. Overall, varying development costs did not significantly impact the electric pump's position as the most robust option.

For the second stage, the pressure system was the winner no matter which criterion is changed or removed while keeping the total scores the same, signifying that the pressure system is still the best option no matter the combination of weights.

Concepts

For the concepts, changing the weights had no impact on the trade-off outcome, suggesting that a very robust winner was found. Based on the derivatives, changing the weight of cost had the largest effect on the scores, but this is not too important due to the overall robustness. Not only is the assigning of the criteria weights a subjective task, but also is the scoring of each concept. For this reason, it was decided to also do a sensitivity analysis on the scores. Each score was increased and decreased by 1 and 2, and it was recorded whether the order of the outcomes of the concepts changed or remained the same.

Similar to the criteria weights, changing the scores slightly had very little effect. Adjusting each weight by +1 and -1 did not change the order of the results at all. Furthermore, changing the weights by +2 and -2 had little effect, but in certain cases, the order did change.

5.3. Final Concept Configuration

From all the trade-offs performed, a final high level design concept was derived. These design choices are split up into two parts, being the MAV and SRL respectively.

MAV

For the MAV, the following high-level design is concluded:

- **Number of Stages:** Two stages
- **Feed System:** First Stage: Electric Pump Fed, Second Stage: Pressure Fed
- **Igniter System:** Spark Torch
- **Power System:** Batteries
- **Structural Materials:** Metals and Composites. (Tanks from Al 7075-T6)
- **Communication:** Omni-Directional Radio Antenna
- **AOCS:** Determination: Star Tracker + Optical IMU's, Control: Thrust Vector Control + RCS Thrusters
- **Staging:** Cold Staging

SRL

The SRL high level design includes:

- **Thermal System:** Passive: MLI + Heat Pipes + Reflective Paint, Active: Radiators + Cryocoolers + Fluid Loops + Electric Heaters
- **Power Generation:** Solar Cells
- **Propellant Production and Storage:** Upscaled MOXIE + Liquid storage in cryocooled tanks on SRL
- **Communication:** Omni-Directional + Directional Radio Antenna
- **MAV Launch:** Rotating Launch tower + Hot Launch
- **MAV Station keeping and Storage:** Stored Horizontally Inside the Launch Tube
- **MAV Connection to SRL:** Lugs

Architecture

The SRL Architecture, shown in figure 5.1 consists of the ISRU system situated on one side while the cryogenic cooled tanks are present on the other side. In between both of them is the MAV which is kept horizontal up until the launch day when it is rotated vertically using a launch tower. Keep in mind that the sketch is based on the existing proposal from ESA/NASA, but it's purely for illustrative purposes. The hatch is there such that the arm should be able to insert the payload inside the MAV during station-keeping.

Figure 5.1: Final Design Concept

6

Subsystem Design & Analysis

This chapter covers the main subsystem designs and the analysis done to achieve these designs. It covers all the main subsystems in the SRL and MAV. Section 6.1 covers the subsystem architecture presented in an N2 chart. Section 6.2 displays the hardware block diagram which shows the physical interactions between subsystems. Section 6.3 introduces the method used throughout the following sections for the subsystem sensitivity analysis. Sections 6.4 to 6.15 then cover the design and analysis of each subsystem. This includes environmental protection, thermals, the ISRU, propellant handling, structures, command and data handling, power generation, propulsion, AOCS, ascent and astrodynamics.

6.1. Analysis and Calculation N2-Chart

Using the subsystems and system architecture, the subsystems can be organised in an N2 chart, a tool used in systems engineering to identify interfaces between subsystems. The outputs of each subsystem are displayed horizontally, and inputs are shown vertically, defining connections between subsystems. An analysis calculation N2 chart was created to identify which calculation parameters influence other sizing efforts, shown in figure 6.1. It shows the key parameters that are required to size the lander and the MAV and which parameters influence each other. It also simplifies and makes an easy overview for all team members to identify what comes next in analysing the subsystems.

Trajectory	Delta-V		AOCS requirements					Launch Heading	
	Staging	Thrust needed Burn time	Staging Architecture	Propellant mass needed				Launch forces	Launch forces
	ISP Thrust	Propulsion	Feed-System Engine system			- Feed system power - Igniter power			Propulsion Mass and Size
	MAV Structure Mass		MAV Architecture	Mass estimation					MAV Size and mass
			Tank Size	Propellants	Propellant generation rate				Propellant storage propellant conditioning
		Propellant Purity			Propellant generation	ISRU Power	Thermal needs for ISRU		ISRU Mass and Size
			Power Unit Size			Power	Thermal Needs from Power		Power Unit Size and Mass
			Thermal Unit Size and Mass			Thermal Power	Thermal		Thermal Unit Size and Mass
Attitude		Ignition Conditions	Connection Point	Sloshing/Launch propellant movement				MAV Launcher	Launch mechanism
			Connection points				Thermal Mass		Lander Architecture

Figure 6.1: Analysis N2 Chart

6.2. Hardware Block Diagram

To give an overview of the main hardware within the scope of the mission, a block diagram was created as seen in Figure 6.2. As seen in the diagram, the components are divided between the Lander and the MAV, where the interfaces between these are also highlighted. Furthermore, components are grouped into categories by colour, or visually illustrated through boxes. This diagram serves to present the physical interactions between components, and is tied with the lander and MAV layout and configuration seen in later section 8.1. The connections themselves are presented via lines or arrows, either red or black. The main part of the block diagram is the structure on which everything is connected to, and thus these connections are indicated with red lines. Moreover, the connections from the structure are either linked to the component group (full), or to the individual component (dotted). In the case of a dotted line, the other components in that group are not directly connected to the structure. There are five different types of connections indicated: Mounted, Cable, Hinge, Pipe, and Contact. **Mounted** implies that two components are rigidly fixed. **Cable** implies there is a cable connection between components. **Hinged** implies a part that can move at its attachment point. **Pipe** suggests a piped connection such as for fuel flow. Finally, **Contact** refers to physical, temporary contact with another component that is not necessarily a part of the system.

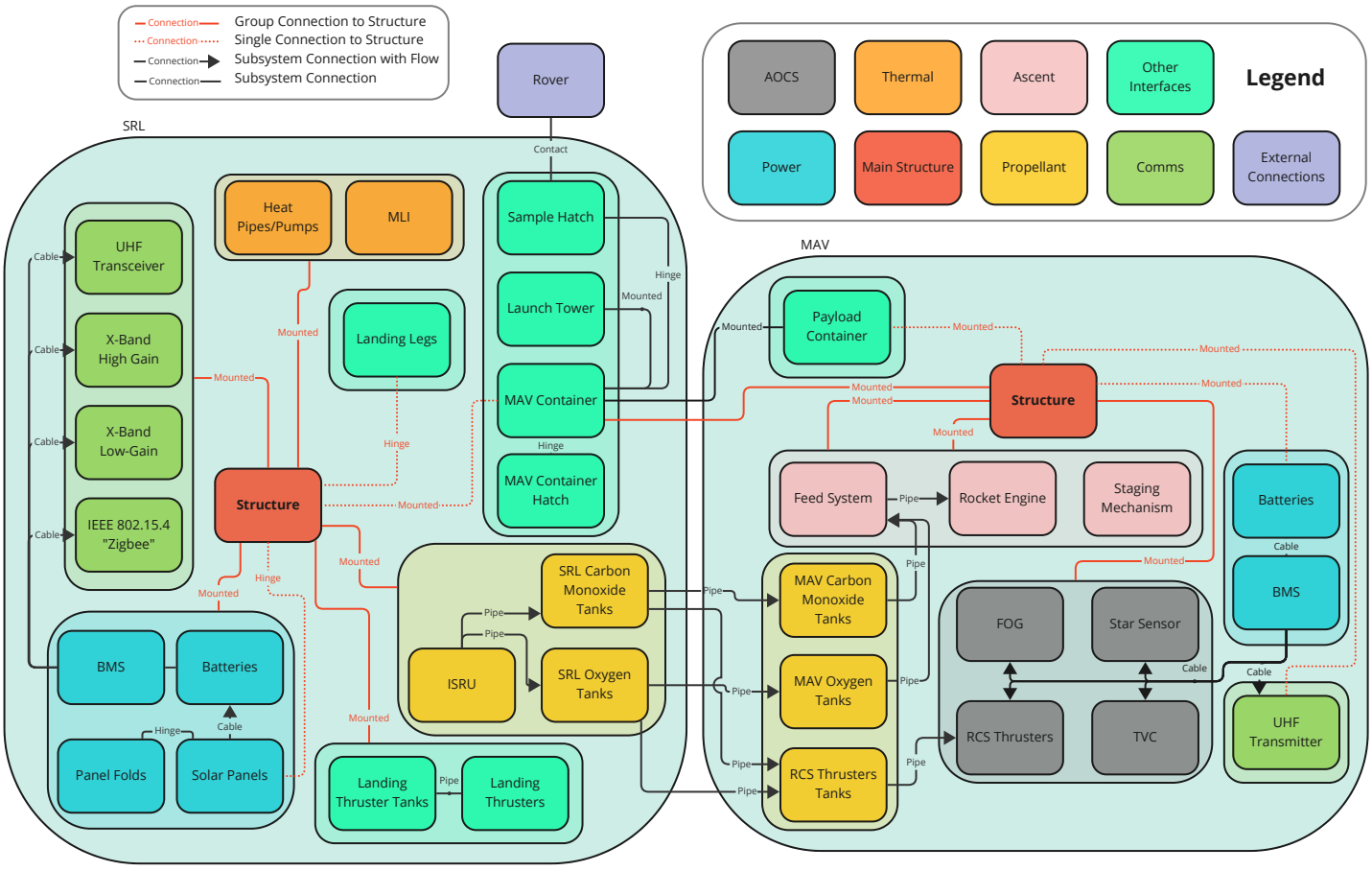

Figure 6.2: Hardware Block Diagram of the SRL and MAV Displaying Hardware Interface Connections.

6.3. Sensitivity Method

To analyse the effect of changing certain parameters on the system and its feasibility, a sensitivity analysis was performed wherever possible. This analysis aimed to assess the requirement compliance with changing the design parameters.

Due to the significantly different approach that had to be taken to design each subsystem, the approach taken for the sensitivity analysis varies slightly. However, each one identifies the affected requirements and the impact they have on the system as a whole. The scoring for the impact on the system is defined as follows:

Table 6.1: Sensitivity Impact Definition

Impact Rating	Significance
5	Makes Design Unfeasible with Current Requirements
4	Design Feasible with Smaller Compliance Margin to Requirements
3	No Effect on Compliance Margin to Requirements
2	Increase in Compliance Margin to Requirements
1	Significant Increase in Compliance Margin to Requirements

The most vulnerable parameters of the design will be identified as a result of the sensitivity analysis. Suitable mitigation and prevention strategies will be mentioned for these, as their effect on the feasibility explained.

6.4. Martian Environmental Protection

Although similar to Earth in some ways, the Martian environment introduces additional variables which must be accounted for in the design. The most significant of these are additional issues stemming from the increased radiation, and issues related to martian dust [17]. The severity of these issues as well as potential mitigation strategies will be discussed in this section. The thermal aspect of the Martian environment is also an issue, but this will be addressed in section 6.5 which focuses on thermal control.

6.4.1. Radiation

Due to its lack of magnetic field or significant atmosphere, the amount of radiation incident on the Martian surface is significantly larger than that of Earth [17], hence it must be accounted for. The first consideration to be made is the fact that significant levels of radiation can lead to the degradation of the mechanical properties of certain materials. This will be assessed for metal, polymers and ceramics. Metals will be one of the main materials used for the external structures, and it is possible that there will be composite materials which use polymers.

For metals, only neutron radiation has a significant effect on properties [18], hence this will be looked at. Based on measurements from the Curiosity rover, the Martian surface receives a neutron flux per second at the surface of approximately $0.01\,\mathrm{n/cm^2/s}$. (for neutrons above $1\,\mathrm{keV}$ [19]). Given that the mission will be performed over a maximum of 526 days (between Martian winters), this leads to a total flux of $454\,000\,\mathrm{n/cm^2}$. Metals are only significantly affected by neutron fluxes over $10^{17}\,\mathrm{n/cm^2}$ at $1\,\mathrm{keV}$ [20], hence the additional radiation will not be an issue for metals. Ceramics show a radiation sensitivity similar to that of metals [20], hence they are also safe to use for parts in the mission.

Polymers on the other hand show greater sensitivity to radiation, hence these must also be investigated. Polymers are not only sensitive to neutron radiation, but also to general ionising radiation. The Curiosity rover measured a total radiation level of on average $0.021\,\mathrm{rad/day}$ [21], leading to a total of $11\,\mathrm{rad}$ over 526 days. Even the polymers most sensitive to radiation require a dose in the order of $10^4\ \mathrm{rad}$ before any effects are noticeable [20], hence within the time-span of the mission radiation will also not be harmful to polymer materials.

While these materials may seem very safe in Mars' radiation environment, radiation can have further effects on electrical components and this must also be taken into account. For this reason, radiation hardened materials [22] will be used for the electronics to ensure that they do not significantly degrade.

6.4.2. Martian Dust

The next hazard to be accounted for is the Martian dust. The main concern here is that dust could get blown onto the solar panels, and if a significant portion remains covered then the power output could drastically decrease. This would be detrimental to the mission as power is required to produce and maintain the propellants. Specific evidence of this hazard taking shape can be seen with the insight lander which saw an approximate 90% reduction in power output due to accumulated dust on its solar panels.[1]

[1] https://www.jpl.nasa.gov/news/nasas-insight-waits-out-dust-storm

Due to requirement **STK-M-006**, the mission will be completed between two consecutive Martian winters. This already helps mitigating the dust hazard since the most severe Martian dust storms occur during its winter. That being said, NASA has still recorded many dust storms occurring in non-winter months[2], and it is also known that dust devils which lift up dust can occur at any time of the year. Therefore, the risk is not entirely mitigated and should be further accounted for.

With the insight lander, it was thought that the Martian winds would be sufficient to blow of the dust, but unfortunately they were not. From this stems the idea of using compressed gas at higher velocities to blow off the dust. This idea is often dismissed for Martian missions due to the extra mass it entails [23]. However, for this specific case compressed gases are already being generated on Mars from the ISRU. Therefore, it is likely that the additional mass brought by this solution would be less than with a regular mission, hence it was decided to look into it.

To check the feasibility of this, it was assumed that the CO feed from the ISRU would be used. The CO_2 feed is not used since the output CO_2 from the ISRU is still in liquid form, hence this would require further considerations. In addition, the unpurified CO feed would be used, so not as much propellant would be wasted. At this stage, the CO would be stored at $1\,\mathrm{bar}$ and approximately $293\,\mathrm{K}$. As carbon monoxide has a specific heat ratio γ of 1.4, its critical pressure ratio[3] to achieve chocked flow is 0.528. Since the martian atmospheric pressure is in the order of millibars [4], the pressure ratio is well below this value and hence the flow will be chocked at the outlet if vented out. This means that the gas used to clean the solar panels will leave the feed system at the speed of sound, calculated to be $348.5\,\mathrm{m\,s^{-1}}$ assuming a temperature if $293\,\mathrm{K}$ and a gas constant[5] for CO of $296.84\,\mathrm{J\,kg^{-1}\,K^{-1}}$.

In a study done on earth, it was shown that compressed air with a velocity in the order of $40\,\mathrm{m\,s^{-1}}$ would be sufficient to remove the majority of dust deposited on solar panels [24]. To properly assess the feasibility of the solution, one would have to look at the density and velocity distributions of the compressed air to be used on Mars over the solar panels, and compare this to the study done on earth. The density specifically is required to compute the drag force. Unfortunately, such detail would require rigorous simulation and is out of the scope of the project. What can instead be concluded is that by just using the ISRU feed already available, the risk of dust covering the solar panels and reducing the power output can likely be reduced based on the outlet velocity that can be achieved, and the required velocity seen in [24]. The implementation idea behind this would be that a mechanism would allow the gas to be expelled radially from the centre of the solar panels, allowing it to cover a larger area, but this again would required more analysis. Based on commercially available valves and feed lines[6] [7], and assuming 1 separate feed for each of the 4 solar panels, an estimate of $1.5\,\mathrm{kg}$ and $5\,\mathrm{W}$ can be estimated to be required for this system. While the effectiveness of this system is yet to be rigorously quantified, the estimated addition that it would bring to the mass and power budgets is tiny since the ISRU is already available. For this reason it is decided to include this system as part of the design.

In addition to the pressurised gas, there are other techniques that can be used to mitigate the dust coverage of solar panels. One such technique being the use of transparent coatings to reduce the dust adhesion. A study used a methyltrimethoxysilane coating with a transparency of 92%, and found that by slowly tilting the panels to $90°$, around 90% of solar panel dust could be removed [23]. While the solar panels used for the lander will not be rotated more than $10°$, it is clear that the use of this coating can significantly reduce the force required to remove dust, and hence aid the compressed gas system. Assuming a coating thickness of $1\,\mathrm{nm}$, combining this with the known solar panel area and density of methyltrimethoxysilane[8], this leads to a coating mass of $0.21\,\mathrm{kg}$. This is once again an insignificant addition to the mass budget, hence justifying the use of this protective system.

To conclude this section, it must be said that while these protection methods are promising, further simulation should be done on the characteristic of the compressed gas flow to see if it will be sufficient to remove the dust. Until then, this solution cannot be presented with complete certainty.

[2] https://www.nasa.gov/mcmc-dust-storms-during-northern-hemisphere-summer/
[3] https://marsed.asu.edu/mep/atmosphere
[4] https://marsed.asu.edu/mep/atmosphere
[5] https://www.engineeringtoolbox.com/individual-universal-gas-constant-d_588.html
[6] https://docs.rs-online.com/7f21/0900766b813dc1aa.pdf
[7] https://biscoair.com/double-ply-fabric-hose/
[8] https://www.chemspider.com/Chemical-Structure.13803.html

6.5. Thermal Control System

This section discusses the thermal design of the lander. The thermal design of the MAV was left as it too complex and quantifying aerodynamic heating of the martian atmosphere lies outside the scope of this report. On top of this the MAV will be operating for about $20\,\mathrm{min}$ outside of the SRL, furthermore as demonstrated by companies under terrestrial conditions, full metal ascent vehicles are a viable design solution.

6.5.1. Thermal Environment

After a preliminary research a very complex thermal environmental was outlined in the Midterm Report [2]. This proved difficult to quantify and capture in calculations, so Ines Uriol Balbin, a lecturer on spacecraft thermal design at TU Delft was approached. She helped with getting the assumptions going into the thermal analysis right, which vastly simplified the calculations needed. The assumptions used are listed below.

Thermal Analysis Assumptions

- Convection is neglected. This is due to the slight martian pressure and low atmospheric density.
- Insulators are ideal.
- Conducted heat does not influence the equilibrium temperature of the space craft.
- The lander legs are perfectly insulated and do not conduct heat between the lander and the surface of Mars.
- The environmental temperature is the atmospheric temperature.
- The ISRU is thermally isolated.

These values are based the environmental conditions recorded by Perseverance [25], the measurements were taken continously over multiple days The values used in this report are the extreme values recorded.Using these assumptions the simplified thermal values are listed in table 6.2.

Table 6.2: Surface Return Lander Thermal Environment and Lander Thermal Coefficients

Property	Minimum	Maximum	Unit
Atmospheric Temperature [25]	193	303	K
Solar Flux [26]	0	700	$\mathrm{W\,m^{-2}}$
Albedo [9]	-	0.25	-
Blackbody Radiation [10]	209.8	-	K
Stefan-Boltzmann constant	5.67e-8	-	$\mathrm{W/m^2/K^4}$
MLI Emissivity [11]	-	0.05	-
MLI Absorptivity [27] [28]	-	0.1	-
MLI Conduction Coefficient [29]	-	0.0005	$\mathrm{W\,m^{-1}\,K^{-1}}$
Solar Panel Absorptivity [12]	-	0.88	-
Solar Panel Emmisivity [13]	-	0.85	-
Rover Temperature	253	303	K

The absorbtivity was calculated based on the values found in the literature [27] and using equation (6.1), which was taken from the Spacecraft Thermal Design course [28] given at TU Delft.

$$\alpha' = \left(\frac{\alpha}{\epsilon}\right)_{outer-layer} \cdot \epsilon' \tag{6.1}$$

In equation (6.1) α stands for the absorptivity and ϵ stands for the emmisivity. The apostrophe (') denotes the effective property of the MLI. The effective values are shown in table 6.2. The lander design has been updated

[9] https://nssdc.gsfc.nasa.gov/planetary/factsheet/marsfact.html
[10] https://nssdc.gsfc.nasa.gov/planetary/factsheet/marsfact.html
[11] https://www.thermalengineer.com/library/effective_emittance.htm
[12] https://www.spectrolab.com/photovoltaics/UTJ-CIC_Data_Sheet.pdf
[13] https://www.spectrolab.com/photovoltaics/UTJ-CIC_Data_Sheet.pdf

leading to more precise knowledge about the shape and size. The SRL is designed with an octagonal shape, with solar panels around it's perimeter. The physical dimensions of the lander are shown in table 6.3. The octagonal shape is approximated by a circular shape to make updating the calculations easier.

Table 6.3: Surface Return Lander Physical Dimensions

Property	Value	Unit
Diameter	3.45	m
Width	0.57	m
Volume	5.3	m^3
Total Surface Area	24.9	m^2
Solar Panel Area	17.7	m^2
Solar Panel efficiency	32.2	%

6.5.2. Thermal Analysis

With the values established, only the equations are missing in order to begin the analysis. Equations (6.2) and (6.3) show the relevant calculations.

$$\dot{Q}_{radiation} = \sigma \cdot T_{eq}^4 \sum_{i=1}^{n} \epsilon_i A_i \tag{6.2}$$

$$\dot{Q}_{conduction} = \frac{k \cdot A}{\Delta x} \cdot \Delta T \tag{6.3}$$

In equation (6.2) σ stands for the Stefan-Boltzmann constant, ϵ_i stands for the emmisivity of the surfaces, A_i is the surface area, and T_{eq} is the equilibrium temperature of the lander surface. In equation (6.3) k is the thermal conductivity, A is the surface area, Δx is the thickness of the insulating layer, and ΔT is the temperature gradient between the two surfaces of the conducting material.

With the thermal environment and the governing equations established the spacecraft thermal properties can be investigated. From the previous analysis it was anticipated that MLI will have to be used in order to properly regulate the spacecraft internal temperature. For this analysis a difference was made between the lander and solar panel surfaces. Figure 6.3 depicts the conceptual configuration of the lander. The simplified lander model consists of the solar panels, the lander main body surrounded by MLI and the propellant tanks inside the lander which are also wrapped in MLI.

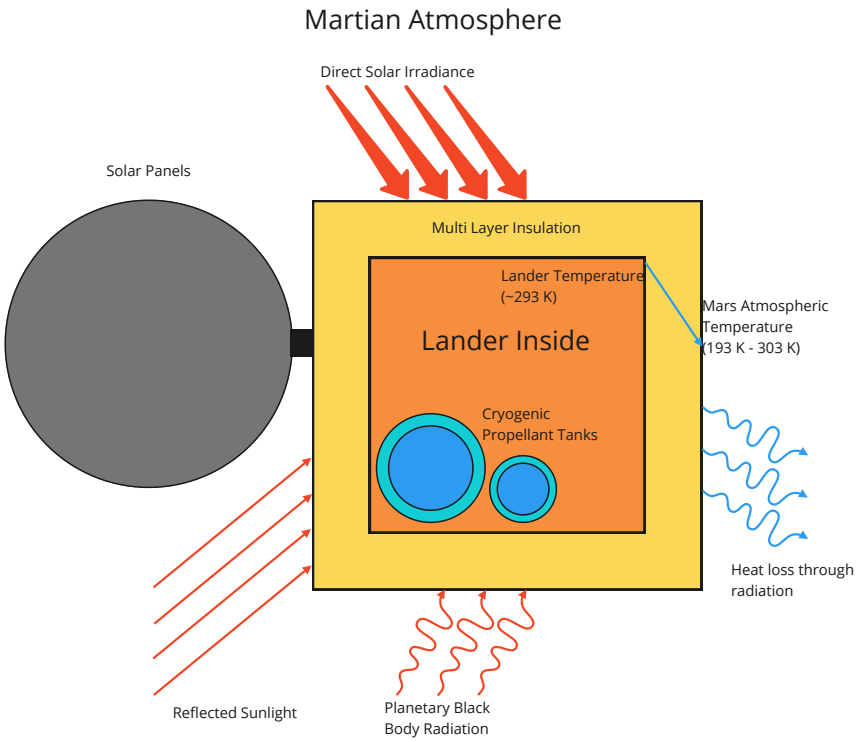

Figure 6.3: Thermal Environment of the SRL

The main purpose of this analysis is to find the MLI thickness that strikes a reasonable balance between the mass of the thermal blankets and the power consumed by the thermal system. The first step is obtaining the equilibrium temperature. Which is done by plugging in the values of table 6.4 into equation (6.2).

Table 6.4: Surface Equilibrium Temperature

Property	Min	Max	Unit
$\dot{Q}_{body}$	106	542	W
$\dot{Q}_{solar}$	0	9240	W
$\dot{Q}_{internal}$	20	20	W
$\sum Q$	126	9802	W
Equilibrium Temperature	108	273	W

The heat flow rates are calculated using the irradiated surface areas, for the $\dot{Q}_{solar}$, it was assumed that part of the surface produces electricity and part of the surface area produces heat. The ratio of these areas is calculated using the efficiency as shown in table 6.3, and the equation and calculation are shown in equation (6.4).

$$A_{Solar-Irradiated} = A_{Solar} \cdot (1 - \eta_{solar-panel}) = 17.7[m^2] \cdot (1 - 0.322) = 12[m^2] \tag{6.4}$$

The equilibrium temperatures in table 6.4 are calculated using equation (6.2), with a difference made between the emissivity of the lander main body and the solar panels. The lower value falls outside of the operational temperatures, this means that the lander requires heaters. Only a limited amount of power is available for heating which fixes the heat transfer value in equation (6.3), then the equation can be solved for the required insulation thickness Δx.

A similar analysis was completed for the propellant tanks but assuming that the lander inside temperature is the thermal environment. The cryogenic tanks also require MLI. The results of the thermal analysis are shown in table 6.5.

Table 6.5: Insulation and Power Requirement

Property	Lander	Propellant Tanks	Unit
Power	56	15	W
Insulation Thickness	47	14	mm

According to the power budget a total of $76\,\mathrm{W}$ is available for the thermal control system as shown in table 7.1. In table 6.5 the power drawn is $5\,\mathrm{W}$ lower, the reason behind this is that the cooling of the cryogenic tanks has to be done via heat pumps or heat pipes. This $5\,\mathrm{W}$ margin accounts for the mechanical thermodynamics inefficiencies. The MLI for the cryogenic tanks has been designed in such a way that $15\,\mathrm{W}$ of heat has to be removed. The hot side of the heat pump or heat pipe can be utilised to keep the batteries above 273K all the time for ideal operation. Finally, the mass of the thermal blankets has to be investigated. Assuming that the MLI blankets cover the lander body, the volume of the blankets can be estimated using the calculated blanket thicknesses. The mass can be calculated based on the volume and the density of the MLI, based on conversations with our coaches, the densities range from $40\,\mathrm{kg\,m^{-3}}$ to $70\,\mathrm{kg\,m^{-3}}$. A density of $77.1\,\mathrm{kg\,m^{-3}}$ was mentioned by Daryabeigi [30] for re-entry heat shielding. The values are shown in table 6.6.

Table 6.6: Thermal Blanket Mass

Property	Min	Max	Unit
Density	40	70	$\mathrm{kg\,m^{-3}}$
Mass	56.6	98.8	kg

Both the upper and the lower values shown in table 6.6 include the mass of five $15\,\mathrm{W}$ satellite heating pads [14]. In total, these provide 75W of power which will ensure that the lander can be rapidly heated to operational temperature after landing. The temperatures of the individual components will be monitored using thermocouples, in order to ensure that the operational temperatures are kept. In general thermocouples weigh around $4\,\mathrm{g}$ a piece, so the inclusion of these will not effect the mass budget by much.

6.5.3. Sensitivity Analysis

In order to capture the robustness of the thermal control system a sensitivity analyses is conducted. The main parameters influencing the thermal system are the lander size and the available power. The sensitivity of the system will be evaluated based on how those two parameters influence the weight of the thermal blanket. First the available power for heating and cooling is changed by $5\,\mathrm{W}$; the results of this are shown in table 6.7.

Table 6.7: TCS Sensitivity Analysis

Parameter	Power [W]	Power [W]	Diameter [m]	Diameter [m]
Change in Value	-5 (Tanks)	+5 (Lander) -5 (Tanks)	+0.17 (5%)	-0.17 (5%)
Effect on Subsystem Mass [%]	+7.4	+1.6	+12.57	-14.75
Effect on System	Mass affected	Mass affected	Mass affected	Mass affected
Requirements Affected	STK-I-001	STK-I-001	STK-I-001	STK-I-001
Impact	4	3	4	2

Table 6.7 shows that a $\pm\,5\,\mathrm{W}$ change in power leads to a maximum of 7.7% in thermal system mass. The mass values are still considered within acceptable range.

For the second part of the sensitivity analysis the diameter and the width of the lander was varied by $\pm$ 10%. The results are also shown in table 6.7. When the area is varied by 5% mass fluctuation of about 15% can be seen. The resulting values still lie within acceptable ranges for the lander, however, this highlights that thermal design and lander configuration are interdependent.

[14] https://www.satcatalog.com/component/stock-flexible-heater/

6.6. ISRU

Being a novel technology, tested on Mars only by MOXIE, the ISRU process needed some analysis early on to determine at least the preliminary values the study will have to determine later on. The two most upfront ones were acquisition and compression, and the purity level of the propellants. The former is intrinsically related to propellant production rate, power budget and the assurance of long-term work of the electrolysis. The latter related more to the propulsion capability of the MAV.

6.6.1. General Overview

Before jumping into specific parts of the ISRU process, one needs a general overview of this subsystem. The main steps are atmosphere acquisition & compression, propellant production (electrolysis), purity analysis, liquefaction, and finally propellant storage (covered in section 6.7). A general overview is shown in Figure 6.4.

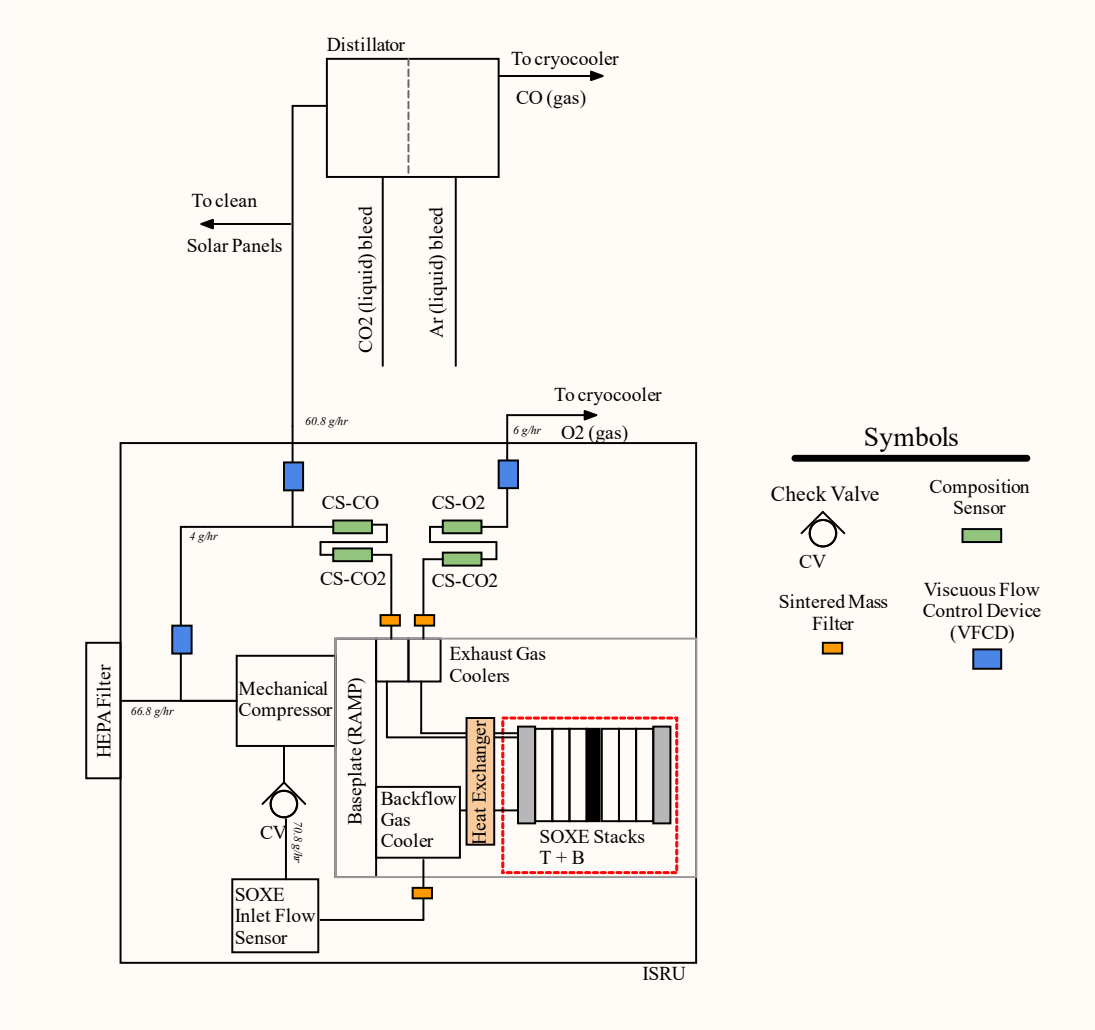

Figure 6.4: General Overview of the ISRU Subsystem

6.6.2. Propellant Production

Requirement STK-M-009 sets a maximum timeframe of 12 months for the propellant production. From the ascent analysis, the required mass of the propellants was found: $45.46\,\mathrm{kg}$ of oxidiser, and $90.91\,\mathrm{kg}$ of fuel. With a continuous propellant production rate, it would mean a constant mass flow to the tanks of $\approx 5.2\,\mathrm{g\,h^{-1}}$ and $\approx 10.4\,\mathrm{g\,h^{-1}}$ respectively.

A continuous propellant production was chosen for several reasons, two of which are linked to the preheating of the SOXE (Solid OXide Electrolysis unit) to an operating temperature of $800\,^{\circ}\mathrm{C}$. It is a very energy-consuming process, thus imposing extra hard requirements in case of cyclic operations, and being negligible if operated continuously [31]. This way, one only needs to load the batteries with lots of power at the beginning, and then operate normally in the nominal mode.

Additionally, MOXIE experienced cycle-to-cycle degradation, which is most likely caused by starting and shutting it down, which creates differential thermal stresses [32]. Important to note, however, that a continuous operational study is needed [32], something not possible and out of scope for the case of this study.

Finally, a continuous operation directly reduces the amount of propellant that has to be taken in at any point of time, impacting the atmosphere acquisition. Given that the compressor may be the biggest single source of power consumption [31], it can significantly reduce the power budget of the subsystem.

After this intermezzo, focus will be put on the design of the SOXE. MOXIE showed that a single cell can produce safely $1.2\,\mathrm{g\,h^{-1}}$ of oxygen, even with a limited $4\,\mathrm{A}$ of supplied current, and so this number was further used in the design. Given that MOXIE needs to produce the minimum $5.2\,\mathrm{g\,h^{-1}}$, it would require at least 5 cells to produce that. An extra cell was added for redundancy, and a possible increase in the CO2 utilisation ratio.

A single electrolysis cell used on MOXIE had an area of $22.7\,\mathrm{cm^2}$ [33][31], but the producing company Ceramatec estimates the surface to go up to $127\,\mathrm{cm^2}$ [34][31]. The former was used for the calculations (tested, ready and proven), as well as a conservative current density of $0.1\,\mathrm{A\,cm^{-2}}$. Using Equation 6.5 to calculate the required power:

$$P = I \cdot V = i \cdot A \cdot n \cdot v \tag{6.5}$$

, where I is current, V voltage, i current density, A cell area, n number of cells and v voltage per cell one gets the required power to perform electrolysis to be $16.3\,\mathrm{W}$.

This calculation was performed for a 6-cell SOXE, with one cell potentially producing $1.2\,\mathrm{g\,h^{-1}}$ of oxygen. Due to the fact that the production rate can be controlled, with some operating limitations, a safe $6\,\mathrm{g\,h^{-1}}$ of O2 production was chosen, which corresponds to $10.5\,\mathrm{g\,h^{-1}}$ of CO. This makes the number calculated above conservative.

Following the reaction happening in the SOXE:

$$2\,CO_2 \longrightarrow 2\,CO + O_2$$

one finds that with the chosen production rate, with a CO2 utilisation ration of 0.26 [31], and considering that the martian atmosphere is in 95% carbon dioxide, an intake of $66.8\,\mathrm{g\,h^{-1}}$ is required. This is not the total intake volume compressed by the pump, as to this one would need to add the recirculated CO.

Recirculation of part of the CO feed is primarily done to prevent oxidation of the cathode; for this work about $4\,\mathrm{g\,h^{-1}}$ of the cathode exhaust gets recirculated. Recirculating the feed could in theory also benegit the production, as it will certainly increase the utilisation rate. To produce oxygen, however, one needs a CO2-rich intake. Lowering the percentage of the CO2 in the electrolised Martian 'air' would also decrease the production rate of O2. This could potentially be mitigated by increasing the intake from the atmosphere, which would however impose extra power and reliability requirements from the compressor. Therefore only direct purification, by liquefaction, was looked in subsection 6.6.5.

6.6.3. ISRU Power Budget

The power taken by each component of the ISRU subsystem is displayed in Table 6.8.

Table 6.8: Power Breakdown

Item	Power [W]
Electrolysis	16.3
Thermal	50.4
Compressor	59.2
Electronics	25
Transducers	0.3
Composition Sensors	3
Total	**154.2**

The electrolysis power was received assuming a conservative potential of $1.2\,\mathrm{V}$ per cell [31]. When choosing operating potential, it is important to keep it above a certain value, called Nernst potential, such that the reaction of carbon dioxide decomposition can happen. There exists also an upper bound, that is a Nernst potential for when the reaction instead of producing carbon monoxide creates pure carbon. It is called coking, which coats the anode and damages its structure [31], effectively not allowing the electrolysis to happen.

MOXIE's SOXE heaters in its operational mode consume together $86.5\,\mathrm{W}$ [31]. As recommended by previous studies a continuously operating mission would benefit from a heat exchanger, which would reduce the power needed by $20\,\mathrm{W}$ [31]. Additionally, the number of cells used decreases, making SOXE smaller. As the SOXE's heat loss power scales with the surface area [33], it would additionally decrease the required energy, and finally result in the presented number.

The compressor used on MOXIE is an orbiting scroll compressor designed by Air Squared, Inc. The same company is developing a more efficient orbiting scroll compressor, which would reduce the needed power. The specific choice of a compressor must be done only after sufficient long-term testing has been performed. For the time of the study, approximations of the power needed were taken from literature [34].

The power needed for the rest of the components, that is electronics, transducers and composition sensors was copied directly from MOXIE [31]. The power needed for liquefaction is taken into account when sizing the cryocooler in the propellant handling section.

6.6.4. Acquisition and Compression

Propellants are produced from the atmosphere, and thus the Martian atmosphere needs to be acquired in the first place. As mentioned in the 'Trade-off' chapter 2 options were chosen for the subsequent phase. It was necessary to choose one of them for the final design. It was chosen to produce the propellants continuously for the reasons stated in subsection 6.6.1. This essentially kills the batch sorption option, as it operates in diurnal cycles, as it would require quite significant storage of gas if carbon dioxide was to be electrolysed continuously.

The collection of the atmosphere starts with a HEPA filter, which can reject the incoming dust, keeping the inside of the MOXIE running without problems. It has been shown that a MOXIE-like filter can work effectively for 10,000 hours [31] ($\approx$416 days), which is more than the time needed to produce the propellants.

Next is the compressor. It has been sized based on the feed flow described in subsection 6.6.2, and literature [34]. The estimates for its characteristics are shown in Table 6.9.

Table 6.9: Compressor Characteristics

Characteristic	Value	Unit
Mass	1.35	kg
Power	59.2	W
Volume	296.4	cm^3

6.6.5. Purity and Liquefaction

Unlike in the MOXIE, the products of the SOXE would be of direct benefit to another phase of the mission. As a consequence, one would require the propellants to be somewhat pure, such that they can deliver the needed performance. The mechanism of purification (of the CO-feed) was left for a later part of the study. So far it has been established that with an impurity level of up to 10%, the effect on performance was surprisingly marginal. The bigger effect was due to incomplete combustion - something that would require more testing, and it's safe to say it's outside of the scope of this study.

MOXIE has shown that the purity of the oxygen feed can be assured, and can reach levels of more than 99%. The carbon monoxide feed on the other hand has never been designed to do so. The first step in having a slightly purer carbon monoxide is the recirculation of the flow. The biggest part of purification happens however by partial distillation. By creating temperature gradient with cryocooler, and using differences in boiling points between the elements, it is possible to get rid of CO2 as well as Argon from the feed, leaving carbon monoxide mixed with a bit of nitrogen. Due to the massive time constraint of the study a more precise study was not

performed.

6.6.6. Sensitivity Analysis

To see how the change in parameters will affect the compliance, a sensitivity analysis must be performed summarised in Table 6.10.

Table 6.10: ISRU Sensitivity Analysis Table

Parameter	Time on Mars [s]	Flow Rate [$\mathrm{kg\,s^{-1}}$]	Final CO Purity
Change in Value	-10%	+10%	-10%
Effect on Subsystem Mass [kg]	+0.15	+0.1	-
Effect on Subsystem Power [W]	+6	+5	-
Effect on System	Redundancy Reduced	Redundancy Reduced	Decreased performance of the MAV
Requirements Affected	STK-M-009	STK-M-009	ISR-019
Impact	3	3	3

Due to the big uncertainties in ISRU working, big contingencies both in propellant production and fuel purity were taken, making the design ultimately very redundant to any changes. It obviously raises the question whether it is then an efficient design - further work is left for future studies.

6.7. Propellant Handling

Another critically important subsystem for the mission is the collection, conditioning, and transfer of the propellants on the Martian surface. The propellants have to be delivered from the ISRU to the MAV tanks. As decided in the trade-off presented in chapter 5, it was chosen to store the propellants on the SRL during the time on Mars. For this reason, the conditioning is also done as part of the propellant handling subsystem. The various elements, including the cryogenic cooler, compressor, and SRL tanks have been designed, which is presented below.

6.7.1. Cryogenic Compressor

The first stage of propellant handling is compressing it into the SRL tanks. A high pressure is required to make liquefaction easier and to prevent the need for further compression once loading the propellants into the MAV. As calculated in section 6.6 the output pressure of the ISRU is $0.555\,\mathrm{bar}$. The tank pressure was decided to be nominal $30\,\mathrm{bar}$, as this is slightly above the $27\,\mathrm{bar}$ MAV second-stage tank pressure. Since this is a significant compression, a compressor is required.

After performing research on existing compressors, it became clear that no commercially available compressors were suitable for the required compression due to the very low flow rate combined with the high compression ratio. For this reason, it was decided to design a custom compressor for the SRL.

The compressor design that was chosen, is a Teflon-sealed piston driven by an electric motor, that compresses the gasses into their respective propellant tanks. The piston moves left and right in a steel cylinder, alternatively compressing oxygen and carbon monoxide. For redundancy, a set of 2 electric motors will be installed, each being able to fully drive the piston independently. To size and select the motor required some calculations had to be performed.

Several assumptions were made during the design of the compressor to ensure that it was capable of compressing the received propellants with a sufficient margin. These assumptions are:

- The cryocooler is designed for the worst-case atmospheric temperature, which is around $293\,\mathrm{K}$[15], from the range of $120\,\mathrm{K}$ - $293\,\mathrm{K}$. This provides a conservative estimate for the amount of compression power required.
- It was assumed that the compression is done under adiabatic conditions since no heat is added or removed from the system.
- Due to the assumption above, the following equation holds: $P \cdot V^{\gamma} =$ constant.
- It was assumed that a compression cycle is 10 seconds.
- The propellants are compressed to $35\,\mathrm{bar}$ to ensure that they can be compressed into the $30\,\mathrm{bar}$ tanks.

Based on these assumptions, the NIST database [16], the following data was obtained for the propellants:

Table 6.11: Propellant Properties Required for Compression Calculation

Property	Value for Oxygen	Value for Carbon Monoxide	Unit
Mass Flow Rate	1.80	2.47	$\mathrm{mg\,s^{-1}}$
Volume Flow Rate	2.47	5.65	$\mathrm{cm^3\,s^{-1}}$
Ratio of Specific Heats γ	1.4	1.4	-

The data in Table 6.11 above can be used to calculate the energy required for the adiabatic compression of the propellants.

$$E = -\frac{P_1 \cdot V_1 - P_2 \cdot V_2}{\gamma - 1} \tag{6.6}$$

Equation 6.6 above, calculates the work performed on a gas during an adiabatic process[17]. This equation, in combination with the above data, was used to calculate the Energy and Power required for the adiabatic compression.

Table 6.12: Compression Calculation for Propellant Handling

Property	Value for Oxygen	Value for Carbon Monoxide	Unit
Initial Volume	24.7	56.4	$\mathrm{cm^3}$
Final Volume	1.28	2.92	$\mathrm{cm^3}$
Initial Pressure	55.5	55.5	kPa
Final Pressure	3.5	3.5	MPa
Work Done	7.8	17.8	J
Power	0.78	1.78	W

The results in Table 6.12 show a very low power required for the adiabatic compression of the propellant gasses. However, this is due to the propellants' low flow rate. To arrive at the total amount of energy required by the compressor, the work done by the pistons must be calculated. This is presented in Table 6.13 below.

Table 6.13: Results for Compressor Piston Calculation

Property	Value for Oxygen	Value for Carbon Monoxide	Unit
Time for 1 cycle	10	10	s
Radius of Chamber	150	150	mm
Length of Chamber	21.7	49.7	mm
Maximum Force	3969	3969	N
Power Required	13.10	14.97	W

[15] https://science.nasa.gov/solar-system/temperatures-across-our-solar-system/
[16] https://webbook.nist.gov/chemistry/
[17] http://hyperphysics.gsu.edu/hbase/thermo/adiab.html

With the data presented in the previous tables, the total output power that the motor has to provide is the sum of the adiabatic compression power and the power the piston needs to move. This comes out to be around $30W$.

Using Maxon's[18] configurator, the ECX SPEED 19 was selected as the motor for the compressor. It provides $30\,\mathrm{W}$ of output power, with an efficiency of $82\,\%$ and a mass of only $78\,\mathrm{g}$. As mentioned before, 2 of these motors will be used for redundancy reasons.

Due to the high pressure and temperature created inside the compression chamber, it was decided to make the cylinder out of thick stainless steel. This resulted in a mass estimate for the cylinder and Teflon-sealed pistons to be $0.52\,\mathrm{kg}$.

A summary of the power and mass requirements will be given at the end of this section.

6.7.2. Cryocooler

Once the propellants have been compressed and loaded into the SRL tanks, they need to be liquefied. This is done by a high-capacity cryocooler. Such a cryocooler has been in development by Lockheed Martin, who also released a detailed design and scaling model for their design [35]. The design of the cryocooler for the SRL was thus based on this design.

As for the compressor, a number of assumptions have to be made to ensure that the cryocooler performs its intended purpose with sufficient margins. These are:

- The cryocooler is designed for the worst-case atmospheric temperature, which is around $293\,\mathrm{K}$[19], from the range of 120-$293\,\mathrm{K}$. This provides a conservative estimate for the amount of cooling power required.
- The liquefaction is an isobaric process, as it is done in a tank at a controlled pressure.
- A safety margin of 1.25 is used for the mass flow rate, providing sufficient capacity to handle inconsistencies in flow rates.
- A safety factor of 1.25 is used for the cooling power, as this compensates for degradation over time and peak power requirements.
- The liquefaction is done at $30\,\mathrm{bar}$, which is the nominal pressure in the SRL tanks.
- The liquefaction is progressively done throughout the entire terrestrial year spent on Mars, which is 365 days or 8760 hours or, 31536000 seconds.

Using this set of assumptions, the amount of energy, and thus power, for the liquefaction of the propellants could be calculated. This was done with the help of the NIST database on the thermophysical properties of fluid systems. Here, the properties of the propellants could be evaluated at cryogenic and isobaric conditions. The following table was constructed, containing the necessary data for the calculation of the cooling power:

Table 6.14: Propellant Properties Required for Liquefaction Calculation

Property	Value for Oxygen	Value for Carbon Monoxide	Unit
Mass	45.5	90.9	kg
Mass 1.25 SM	56.8	113.6	kg
Cp Gas (avg)	1100	1150	$\mathrm{J/kgK}$
Cp Liquid (avg)	1950	2800	$\mathrm{J/kgK}$
Lv	213000	215000	$\mathrm{J/kgK}$
Starting Temperature	293	293	K
Boiling Temperature	141	129	K
Final Temperature	100	100	K

In Table 6.14 above, the previously mentioned safety margin is applied to the propellant masses. Cp was retrieved from the NIST database and represents the specific heat capacity at constant pressure. Lv is the

[18] https://www.maxongroup.net.au/maxon/view/configurator/BOM:IDX56MA0STPET558B:::
[19] https://science.nasa.gov/solar-system/temperatures-across-our-solar-system/

latent heat of vaporisation, followed by the relevant temperatures for the liquefaction. It is important to note that all values for heat capacities were taken at $30\,\mathrm{bar}$, which is the final pressure in the tank, and results in the conservative estimate. Using the data above, the energy, and thus power needed for the liquefaction was calculated.

Table 6.15: Energy Required for Phases of Cooling Propellants

Phase	Oxygen: Energy Required	Carbon Monoxide: Energy Required	Unit
Cooling to Boiling Point	9.5	21.5	MJ
Liquefaction	12.1	24.4	MJ
Cooling to Final Temperature	4.5	9.2	MJ
Total	26.2	55.1	MJ

These calculations used specific heat capacities, latent heat, temperature changes, and masses. From this, the constant power required during the mission to remove energy from the propellants was calculated to be approximately $2.6\,\mathrm{W}$. Including the safety margin mentioned above, this results in a required cooling power of $3.25\,\mathrm{W}$.

To size the cryocooler, the high-capacity cryocooler model developed by Lockheed Martin was used [35]. This is a design using a cold head inline pulse-tube design, which can be scaled as explained in the design report. This enabled the sizing of the cryocooler needed for the propellant handling subsystem based on the following graphs.

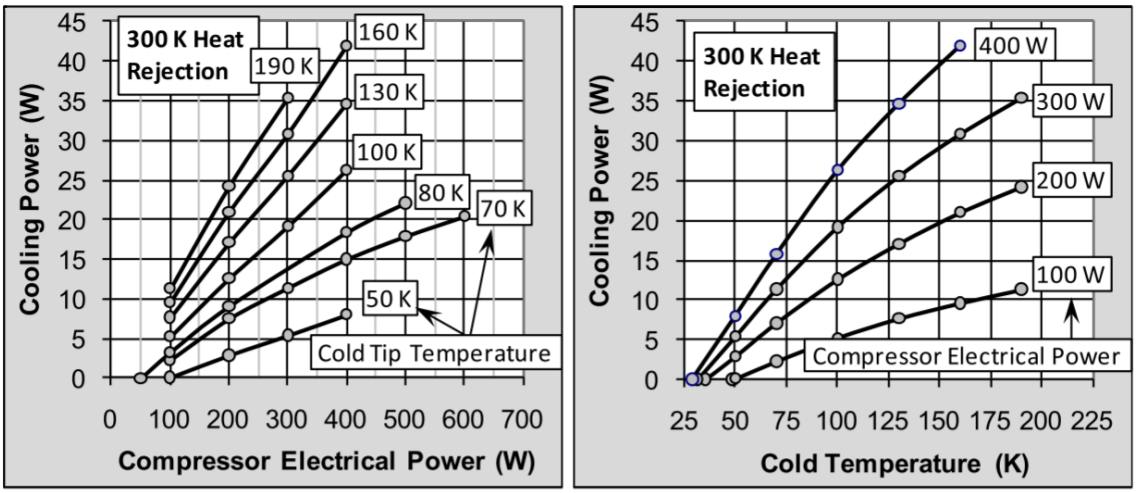

Figure 6.5: Cooling Power as a Function of Compressor Electrical Power and Cold Tip Temperature [35]

Figure 6.5 above is taken from the model presented by Olson et. al. [35]. It is appropriate for heat rejection at $300\,\mathrm{K}$, which is very close to the $293\,\mathrm{K}$ experienced by the SRL. It is also important to note that rejection at this atmospheric temperature is the worst-case scenario, as the colder ambient temperature would result in less heat needing to be rejected. Using these graphs, it is clear that the cryocooler required is at the lower end of the spectrum in terms of size and power requirements. In the case of the SRL, a cold tip temperature of $100\,\mathrm{K}$ is required, along with a cooling power of $3.25\,\mathrm{W}$. This leads to a compressor electrical power of approximately $75\,\mathrm{W}$. Furthermore, a conservative estimate, due to the limited applicability of downward scaling, resulted in a mass of $1.3\,\mathrm{kg}$ for the cryocooler.

6.7.3. SRL Tank Sizing

Once the cryocooler and the compressor have been designed and sized, a tank is required for the storage of the propellants while the MAV is on the surface of Mars. This tank needs to keep the propellants contained, and under cryogenic conditions throughout the entirety of the stay on Mars.

Due to the relatively low pressure that needs to be sustained by the pressure vessels ($30\,\mathrm{bar}$), they would have to be significantly overdesigned if transported unpressurised, due to the risk of buckling. For this reason, it was decided to pressurise both of the tanks with $7\,\mathrm{bar}$ of Helium for the duration of the launch. This would enable the tanks to withstand the launch loads without the risk of buckling. Furthermore, this relaxes the cooling requirements of the tanks.

The cooling requirement is relaxed due to both of the propellants liquefying at a temperature higher than $100\,\mathrm{K}$, when under a pressure of $7\,\mathrm{bar}$. This prevents a build-up of latent heat that needs to be removed, allowing for constant liquefaction of the propellant flow. This would not be possible without the pressurisation of the tanks with Helium. The reason for the choice of helium is that it is an inert gas with a much lower mass than the propellants themselves, meaning that this design offers the greatest weight reduction.

As with the previous components of the propellant handling subsystem, a number of assumptions were made before the tanks were designed. These are as follows:

- The tank material used is Aluminium 7075 T-6 as decided in trade-off process [2], with a cryogenic yield stress of $528\,\mathrm{MPa}$ and density of $3000\,\mathrm{kg\,m^{-3}}$.
- The design tank pressure is $30\,\mathrm{bar}$.
- A safety margin of 1.25 is used for the tank thickness.
- The tanks are filled to 98% to allow for unexpected expansion [36].
- To be conservative, the density taken is midway between boiling point and final temperature.
- The tanks are designed to be a sphere as this is the most efficient shape given the abundance of available space.

With the above assumptions and the volume formula for a sphere, the tank was sized. The intermediate steps and data found are presented below:

Table 6.16: SRL Tank Sizing Calculations

Property	Value for Oxygen	Value for Carbon Monoxide	Unit
Mass with SM	56.8	113.6	kg
Specific Volume	1.1	1.7	$\mathrm{dm^3\,kg^{-1}}$
Volume of Propellant	62.5	193	$\mathrm{dm^3}$
Tank Volume	63.8	197	$\mathrm{dm^3}$
Tank Radius	248	361	mm
Tank Thickness	0.88	1.28	mm
Assumed Thickness	1.0	1.3	mm
Material Volume	0.78	1.14	$\mathrm{dm^3}$
Tank Mass	2.33	6.41	kg

Table 6.16 above concludes the sizing of the structural components of the tank. Due to the pre-pressurisation of the tanks with Helium, an additional $0.87\,\mathrm{kg}$ of mass will be taken to Mars.

6.7.4. Valves and Propellant Transfer

For the separate parts of the propellant handling subsystem to be connected and work together as intended, a series of valves, pipes, and pumps are required. It was decided that the following set of valves would be used for each SRL tank.

- Check Valve (CV) X1: A check valve is needed after the compressor piston to enable it to operate correctly.
- Safety Relief Valve (SRV) X1: A safety relief valve is needed to passively protect against overpressurisation.
- Rupture Disk X1: A rupture disk is installed in case the SRV fails and serves to protect piggyback experiments on the SRL.

- Vent Valve (VV) X1: A manual valve that is controlled by the SRL on-board computer to control the tank pressure.
- Fill Valve (FV) X2: Two fill valves provide two separate paths for the propellant to be loaded from the SRL tanks onto the MAV.
- Pressure Sensor X2: Two pressure sensors for redundancy serve to measure the pressure inside the tanks.
- Temperature Sensor X2: Two temperature sensors for redundancy serve to measure the temperature inside the tanks.

As listed above, each of the two tanks will be equipped with all of these valves and sensors. The mass and power of each of these valves are presented Table 6.17 below.

Table 6.17: Valve and Sensor Data

Component	Mass [g]	Power [W]
Check Valve[20]	74	0
Safety Relief Valve[21]	100	0
Rupture Disk[22]	20	0
Vent Valve[23]	510	16.7
Fill Valve	510	16.7
Pressure Sensor[24]	22	0.01
Temperature Sensor[25]	20	0.01

Apart from the valves, the tubing, which includes the low and high-pressure lines, had to be sized. It was assumed that each cryogenic high-pressure line going between the SRL and the MAV was $1\,\mathrm{m}$ in length. Using a cryogenic high-pressure line suitable for this application[26], with a per-meter mass of $4.75\,\mathrm{kg\,m^{-1}}$, a total mass of $19\,\mathrm{kg}$ was calculated. Furthermore, low-pressure lines are also required, which lead from the ISRU to the SRL tanks. The length of piping required for this was estimated to be $1.2\,\mathrm{m}$, due to the proximity of the two systems to each other. A suitable low-pressure line[27] was chosen with a per-meter mass of $0.75\,\mathrm{kg\,m^{-1}}$, leading to a total mass of $0.9\,\mathrm{kg}$.

Moving the propellants from the SRL tanks to the MAV has a negative pressure differential, meaning that the propellants should initially flow on their own. However, this cannot be guaranteed and therefore pumps will be installed which aid the propellants in moving to the MAV. Both the LOX and LCO cryogenic lines are installed with a Thomas 107Z1[28] pump. These are $1.95\,\mathrm{kg}$ each and use $45\,\mathrm{W}$ of power. It is important to note that when these pumps are operated, the ISRU is no longer running, so power will be sufficiently available without increasing the power requirements.

Finally, the last component of the propellant handling is the ability to disconnect from the MAV when it is ready to launch. To enable this, a quick disconnect is required to remove the physical connection of the propellant transfer lines. Due to the lack of available information online about the mass of such a valve, the quick disconnect valves used on Delft Aerospace Rocket Engineering's (DARE) Stratos IV were measured on a scale. The resulting mass of one of these quick disconnects was found to be $0.45\,\mathrm{kg}$. Two of these valves are required for the MAV, one for each propellant.

With the individual components being sized and designed, a sensitivity analysis and an overview will follow.

[20] https://nl.rs-online.com/web/p/check-valves/4586788
[21] https://produkte.herose.com/eng/products/cryogenic-services/06001_dt.php
[22] https://produkte.herose.com/eng/products/cryogenic-services/06001_dt.php
[23] https://www.emerson.com/documents/automation/data-sheets-cash-valve-cryogenic-valves-controls-cash-valve-en-en-5432348.pdf
[24] https://www.pcb.com/products?m=102b11
[25] https://www.scientificinstruments.com/product/model-ro-215-100k/
[26] https://www.bruggpipes.com/fileadmin/user_upload/downloads/produkte/03-industrie/01-flexwell-cryo-pipe/dokumentation/FCP_DatBl_EN_13aug21_FINAL.pdf
[27] https://www.toscelik.com.tr/uploads/file/9c26f2896543ff973bd8abbb110ec7a2-1616657905116.pdf
[28] https://www.thomaspumps.com/en-nl/diaphragm-pumps-compressors/107z1-series

6.7.5. Sensitivity Analysis

To assess the effect of parameter changes on requirement compliance, a sensitivity analysis was performed on the propellant handling subsystem, as prescribed in section 6.3.

Table 6.18: Propellant Handling Sensitivity Analysis Table

Parameter	Time on Mars [s]	Flow Rate [$\mathrm{kg\,s^{-1}}$]	Final Temperature [K]	Storage Pressure [Pa]
Change in Value	-10%	+10%	-10%	+10%
Effect on Subsystem Mass [kg]	+1	+0.5	+0.4	+0.7
Effect on Subsystem Power [W]	+9	+3	+15	0
Effect on System	Redundancy Reduced	Redundancy Reduced	Increased Size of Power Subsystem	Reduced Margins
Requirements Affected	STK-M-010 LAN-ELC-05	STK-M-010 LAN-ELC-05	STK-I-001	STK-I-001
Impact	4	4	4	3

After performing the sensitivity analysis as shown in Table 6.18 it is visible that changing various parameters will make the design have smaller margins and redundancy. In case the Time on Mars or Flow Rate is changed as specified in the table above, both motors would be required to drive the compressor, thus reducing redundancy. This may seem like a great issue, but due to the worst-case assumptions in terms of temperature and mass flow during the design, it is very unlikely to affect the effectiveness of the compressor even in case one of the motors fails.

Due to the large margins available in terms of the mass budget, the $0.7\,\mathrm{kg}$ added by the increase in storage pressure has a negligible effect on requirement compliance.

Overall, the changes in parameters do not have a major effect on the requirement compliance of the propellant handling subsystem. Due to the significant margins included in the design itself already, even if there are peak increases in mass flow or extreme conditions, the mission will not be put in jeopardy.

6.7.6. Overview of the Propellant Handling Subsystem

After performing the design, selection, and sizing of all the components of the propellant handling subsystem, they were interlinked and presented in a P&ID. This is presented below and represents the interfaces and arrangements of the components.
As can be seen in Figure 6.6 above, the propellant handling subsystem interfaces with the ISRU and MAV through a series of low and high-pressure lines. The entirety of the propellant handling is performed on the SRL and is left on Mars once the MAV departs.

To conclude this section, an overview of the mass and power contributions of the propellant handling subsystem is presented below.

Table 6.19: Summary of the Propellant Handling Subsystem

Component	Mass [kg]	Power [W]
Cryocooler	1.30	75.00
Compressor	0.68	74.70
SRL Tanks	9.61	0
Valves	3.62	100.2*
Pipes	20.8	0
Pumps	3.9	90*
Total	39.90	149.70

The entries marked with an asterisk (*), in Table 6.19 above, represent power requirements for components that

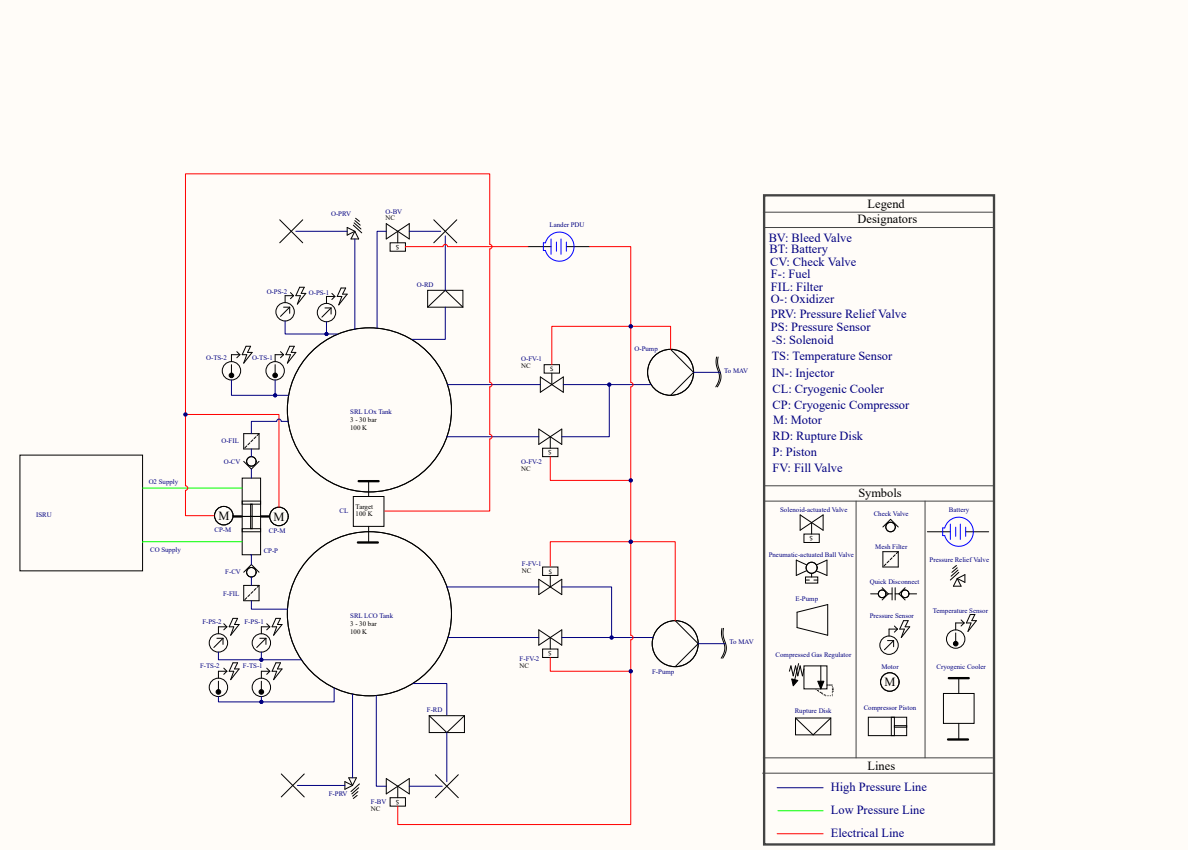

Figure 6.6: P&ID for the Propellant Handling Subsystem

are only used after the ISRU process has been finished. For this reason, and since their operation is limited to a short time, their contribution to the total power has not been included.

6.8. Structural Characteristics

6.8.1. Lander Structure

The structure of the lander is heavily based on the Phoenix and Insight landers; this reduces the cost of the development and increases the reliability of the design. However, due to the slightly larger estimated budget than Insight's $360\,\mathrm{kg}$ [29], as seen in subsection 7.1.2, and the shifting centre of mass that is to be expected once the MAV is lifted from loading into its launch configuration, 4 legs shall be used to support the structure of the SRL, instead of 3 as in Insight and Phoenix.

Structural components of the SRL shall be made primarily from honeycomb composite with aluminium panels, this is due to its very low mass and high strength characteristics, and shall form a $6\,\mathrm{cm}$ thick bed, which shall carry the lander subsystems during the $150\,\mathrm{m\,s^{-2}}$ EDL loads. The landing legs shall use an aluminium honeycomb crush core as a single-use shock absorber for the impact of landing, similar to that of Insight[30].

The launch tower shall consist of a $101\,\mathrm{mm}$ diameter, $4\,\mathrm{mm}$ thick, hollow cylindrical aluminium beam, this will hold the MAV horizontally for much of the length of the mission, including during the immense EDL loads. Once the MAV is fully loaded, the launch tower shall erect the MAV into its launch position.

The MAV storage bay, the igloo as seen in Figure 6.7b, shall isolate the MAV from the rest of the lander thermally so that thermal insulation is not necessary on the MAV for the loading phase. Once loaded, the igloo doors shall open outward and the MAV will be raised into launch configuration. During launch, the MAV's rocket plume shall be guided by the igloo out of the lander via the payload access hole, protecting the lander.

[29] https://science.nasa.gov/mission/insight/spacecraft/
[30] https://spaceflight101.com/insight/insight-spacecraft/

The igloo doors shall guide the plume into the igloo further as the rocket ascends. The igloo and its doors shall have an outer layer of Rhenium to be able to ensure they may withstand the temperatures of the rocket exhaust.

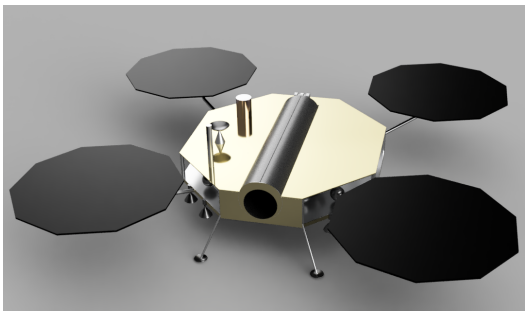

(a) Lander in production and loading phase

(b) Lander in launch configuration

Figure 6.7: Lander Configurations

6.8.2. MAV Propellant Tank Structure

The launch vehicle tank structure was divided into two parts, the first stage and second stage, where the tanks were assumed to be a single, long, thin-walled cylinder composed of both oxygen and carbon monoxide propellant tanks (in a tandem tank formation). Depending on the load case, the end caps of the tanks, assumed to be hemispherical, were also considered. Three main load cases were analysed: the MAV during peak launch conditions; the tanks under maximum pressure; and the MAV structure thanks to the integrated tank internal pressure. The purpose of this analysis was to identify the minimum thicknesses required for the tank walls, and thus the skin of the MAV, such that the structure could survive the stresses, in addition to finding the masses of the tank structure.

The first load case, concerning the launch loads, involved analysing the thin-walled cylindrical structure due to the acceleration of the MAV. Fundamentally, this acceleration would induce a force on the MAV, which in turn results in stresses flowing through the structure. The second load case, with the tanks under pressure, looked at the axial and hoop stresses (radial stress is assumed negligible) the tanks experience. It should be noted that the two tanks were assumed to be one singular tank for this load case (without a bulkhead). Additionally, for this case, the thicknesses of the hemisphere end caps were also analysed to match the pressure conditions inside the tank. The final and third load cases focused on estimating the stresses the MAV tank structure could withstand as a result of the pressurised tanks being integrated with the structure. By integrating the tanks with the structure, the pressurised tanks become load-bearing and thus potentially reduce the required thicknesses of the MAV walls, or in other words, increase the stress the structure can withstand.

As for the tank material, following the trade-off performed in the previous report [2], Aluminium 7075-T6 was selected. Importantly, further design iterations for the MAV led to different structures for the first and second stages. This in turn affected the diameters and lengths of the tanks. These new values are summarised in Table 6.20.

Table 6.20: New MAV Upper and Lower Stage Dimensions and Properties.

Parameter	1st Stage	2nd Stage	Unit
Oxidiser Tank Length	142	97	mm
Fuel Tank Length	372	254	mm
Total Tank Length	515	351	mm
Diameter	570	450	mm
Pressure	7.5	30	bar

Similarly to the analysis done in the previous report, the critical thickness t_1 was found to be for the hoop stress as seen in Equation 6.7, and the spherical end cap thicknesses t_s were found with Equation 6.8, where R is the

radius, σ is the material yield stress, and Δp is the pressure differential. Concerning the pressure differential, the internal pressure is significantly larger than the pressure of the Martian atmosphere. As such, the pressure differential is assumed to be equal to the internal pressure.

$$t_1 = \frac{\Delta p R}{\sigma} \tag{6.7}$$

$$t_s = \frac{\Delta p R}{2\sigma} \tag{6.8}$$

The new thicknesses can be calculated for both MAV stages from the critical stresses, further leading to the masses of both stages being calculated. These values are presented in Table 6.21.

Table 6.21: Summary of the Material Characteristics Including Stresses, Safety Factors, Masses and Critical Thicknesses.

Parameter	1st Stage	2st Stage	Unit
Hoop (Critical) Thickness	0.540	1.943	mm
End Cap Thickness	0.270	0.972	mm
Critical Stress Experienced	42.75	153.9	MPa
Total Mass	2.1	4.3	kg

Given the cryogenic yield strength of Aluminium 7075-T6 being approximately equal to $528\,\mathrm{MPa}$ [31][32], it can be noted that neither of the critical stresses within the structures exceed or even approach the yield stress. The calculations were performed using a 25% safety factor, meaning that even with a yield strength of $396\,\mathrm{MPa}$, the structure is still considerably sound, with a factor margin of 2.57 $(= \frac{Yield\ Stress}{Critical\ Stress})$.

The natural frequency is a parameter that, while on its own is not too important, in interaction with other systems, it can be devastating. Rockets experience a lot of vibrations during ascent for a large variety of reasons. This can be due to aerodynamic effects, engine vibrations, RCS inputs or vibrations of components like pumps. If these are similar to the natural frequency of the vehicle, this can lead to oscillations in the body, which can lead to an eventual break-up [37]. Hence, it is important to determine the natural frequency to determine if there is any risk of this occurring. From this, one can determine if the subsystems or the MAV structure itself requires a redesign.

The natural frequencies of the two stages were calculated using the new dimensions. The first stage alone is not considered as, during launch, it will never be an isolated structure, but rather will be connected to the second stage. Thus, the natural frequency will be calculated for both the whole MAV, and the second stage using the model assumption seen in Figure 6.8[33].

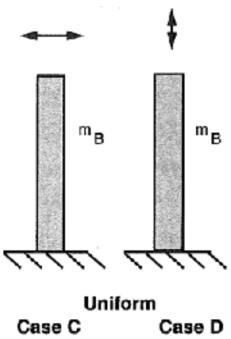

Figure 6.8: Model MAV Tank Structure Used for Natural Frequency Calculations.

$$f_{nat_C} = 0.56\sqrt{\frac{EI}{m_b L^3}} \tag{6.9}$$

$$f_{nat_D} = 0.25\sqrt{\frac{EA}{m_b L}} \tag{6.10}$$

From this assumption, two equations can be utilised to approximate the natural frequencies in the lateral (f_{nat_C}) and axial (f_{nat_D}) directions, as presented in Cases C and D. Equation 6.9 was used for the lateral natural frequency (Case C), while Equation 6.10 was used for the axial natural frequency. In these equations, E refers

[31] https://www.makeitfrom.com/material-properties/7075-T6-Aluminum
[32] https://www.totalmateria.com/en-us/articles/properties-of-aluminum-at-cryogenic/
[33] AE1222-II: Aerospace Design & Systems Engineering Elements I, Part: Launch Vehicle design and sizing, By B.T.C. Zandbergen

to the material's Young's Modulus, I to the cross-section area moment of inertia, m_b to the uniform mass, L is the supposed beam length, and A the cross-sectional area, all in standard SI units. When calculating I and A, as usual, the thin-walled assumption was used, leading to $I = \pi R^3 t$, and $A = 2\pi Rt$. Table 6.22 and Table 6.23 present the natural frequencies calculated for the whole MAV, along with the parameter values, while Table 6.24 and Table 6.25 presents the same but for the second stage.

Table 6.22: Whole MAV Case C Calculations for Natural Frequency.

Parameter	Value	Unit
Youngs Modulus	70	GPa
Area Moment of inertia	9030	cm^4
Uniform mass	6.4	kg
”Beam” length	3.3	m
Lateral Natural Frequency	*92.9*	Hz

Table 6.23: Whole MAV Case D Calculations for Natural Frequency.

Parameter	Value	Unit
Youngs Modulus	70	GPa
Cross-sectional area	22.2	cm^2
Uniform mass	6.40	kg
”Beam” length	3.30	m
Axial Natural Frequency	*679*	Hz

Table 6.24: Second Stage Case C Calculations for Natural Frequency.

Parameter	Value	Unit
Youngs Modulus	70	GPa
Area Moment of inertia	14100	cm^4
Uniform mass	3.34	kg
”Beam” length	1.60	m
Lateral Natural Frequency	*476*	Hz

Table 6.25: Second Stage Case D Calculations for Natural Frequency.

Parameter	Value	Unit
Youngs Modulus	70	GPa
Cross-sectional area	34.8	cm^2
Uniform mass	3.34	kg
”Beam” length	1.60	m
Axial Natural Frequency	*1690*	Hz

6.8.3. Propellant Sloshing

A detailed analysis of the sloshing induced disturbances on MAV during its ascent is out of the scope of this project. Nonetheless, a number of potential methods to control this effect were explored. Some passive methods to control the propellant make the use of surface tension systems, and given that the values of surface tension of liquid carbon monoxide [38] are somewhat similar to that of liquid oxygen [39], which is a frequently used oxidiser, means that a common apparatus would work for both. This consists of using vane structures inside the propellant tanks to draw off the liquids into the tank outlets [40]. To prevent the build up of moments or fluctuating forces inside the propellant tank, baffles can be installed to generate turbulence and break up the flowing liquid [40]. Finally, to prevent the vortexing of the propellants as they pass through the tank outlet, often taking down gas bubbles with it, anti-vortex baffles can be installed to break up the whirlpool formation [40]. The uses of bladders or diaphragms cannot be reliably used due to their polymeric materials, and thus their inability to properly withstand the cryogenic temperatures in the tanks.

6.9. Command & Data Handling

The command and data handling systems are vital for any Mars mission to transmit data, receive commands, and ensure mission success and safety. The block diagram presented in Figure 6.9 shows the links between the central processing unit (CPU) and all other subsystems. The arrows represent different inputs and outputs from each system.

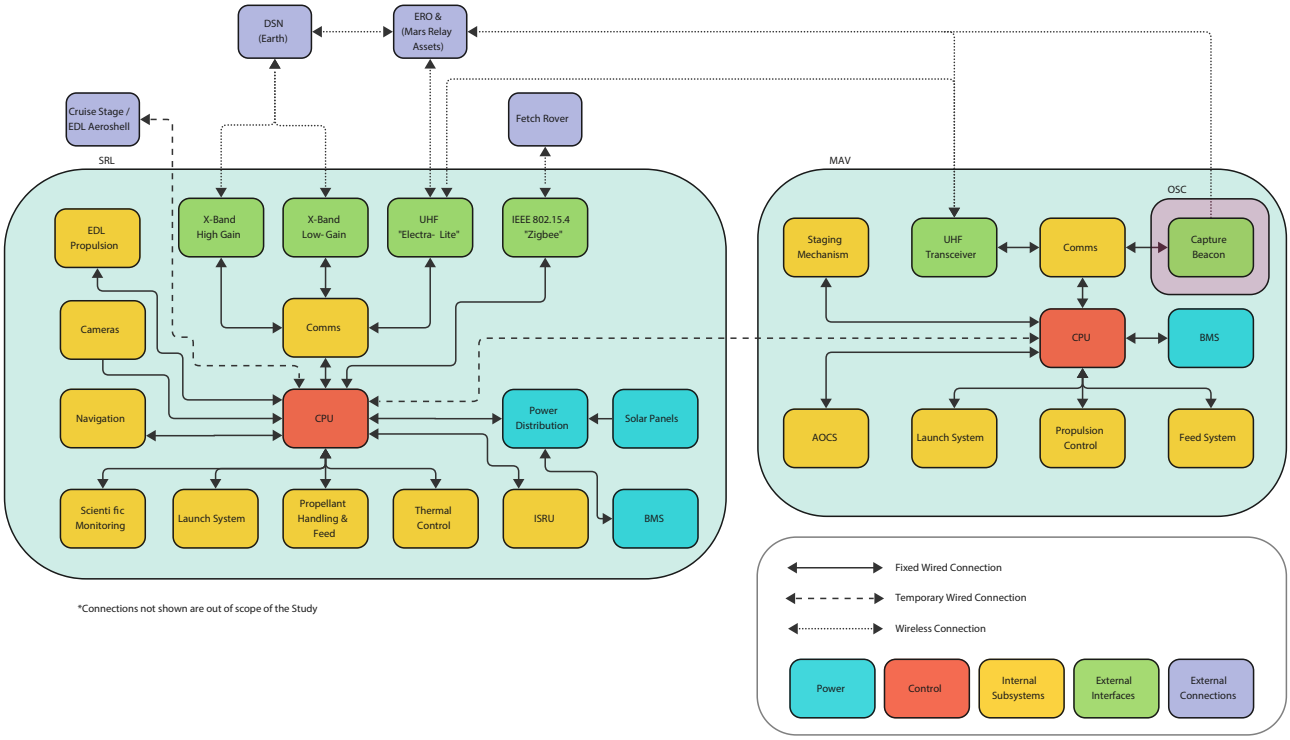

Figure 6.9: Block Diagram of the SRL and MAV Displaying Data Links Between Different Subsystems.

The Central Processing Unit is key to any electronic system. In this instance, an architecture similar to past Mars missions was chosen. BAE Systems' radiation hardened *RAD 750* [41] is the CPU at the hearts of the Insight lander and the Curiosity and Perseverance rovers. While this processor is not as powerful as one found in a modern smartphone, it has proven time and time again to be very reliable. Furthermore, building upon past mission designs allows for a shorter, and cheaper, development time. Future missions to Mars may want to invest in a more powerful and contemporary CPU, but as this mission's core goal is not about gathering and processing data, such investment is deemed unnecessary for now.

Building from requirements **LAN-ELC-001**, **MAV-AVI-001** and **MAV-AVI-005**, a communication system was designed. An important characteristic of this system design is its ability to integrate with preexisting Martian architecture. As such most of the components are derived from the Curiosity and Perseverance rovers. With nearly identical architecture to the Perseverance rover, the SRL will be able to communicate with the Deep Space Network (DSN), the Mars Relay Network (MRN) and ESA's ERO. Using a simple off-the-shelf Zigbee module, local wireless communication can be established with the Sample Fetch Rover for loading samples into the MAV.

The MAV, by comparison, has a rather limited suite of communication hardware. It has two ERO beacons to comply with requirement **MAV-INT-005**, and has multiple UHF communication antennae to ensure a robust connection to either the ERO or the SRL can be established. This connection link, with the lander or orbiter acting as a relay, can incorporate the MAV into the DSN, complying with requirement **MAV-AVI-004**.

Table 6.26: SRL Communication System Overview

Component	[kg]	[W]
X-Band High-Gain Antenna	1.4	0
Antennae Gimbal	6.6	7
X-Band Low-Gain Antenna	0.4	0
RF Waveguides	3.7	0
X-Band Transceiver (Receiving)	5.3	13
X-Band Transceiver (Transmitting)	0.0	7
X-Band LNA	1.4	63
UHF Antenna	0.6	0
UHF Transceiver (Receiving)	3.0	15
UHF Transceiver (Transmitting)	0.0	50
Zigbee Transceiver	0.1	1
Zigbee Antennae	0.1	0
Total	**22.5**	**156**

Table 6.27: MAV Communication System Overview

Component	[kg]	[W]
UHF Transceiver	0.1	6
UHF Antennae x2	0.2	0
ERO Beacon x2	0.4	5
Total	**0.7**	**11**

6.10. Electrical Power System

This section covers the electrical power system of the mission. The complex chemical processing described in section 6.6 will occur continuously to minimise fatigue loading. Consequently, the Mars lander will have substantial power requirements, necessitating the largest power system ever sent to Mars. A block diagram of the electrical power system highlighting the links between each subsystem is shown in Figure 6.10 for reference.

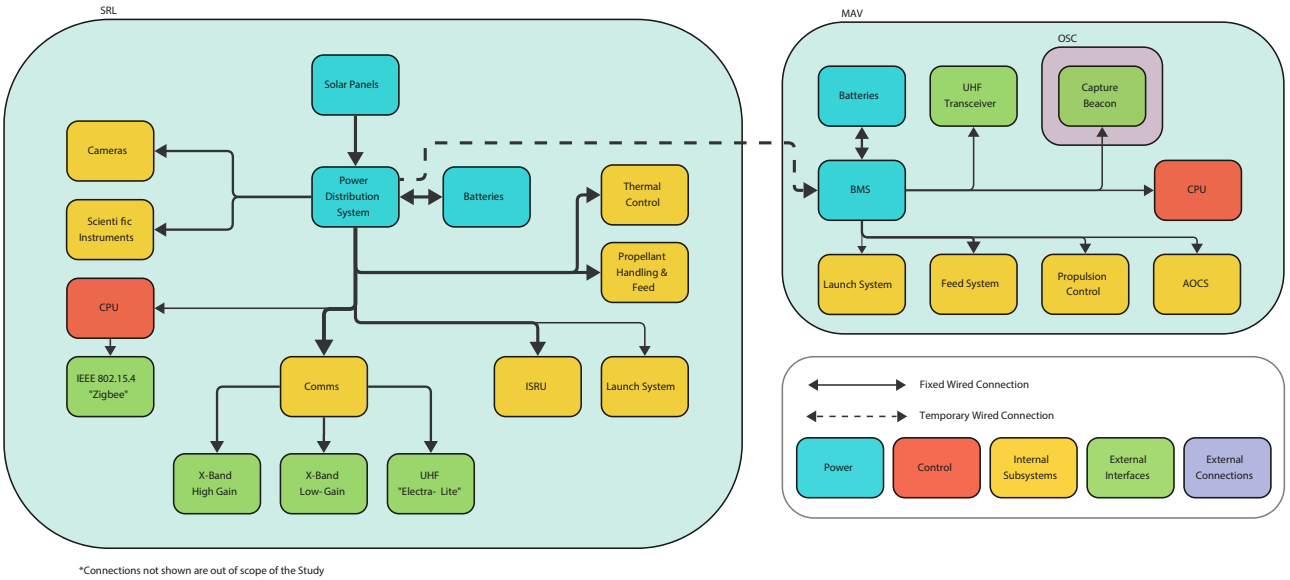

Figure 6.10: Block Diagram of the SRL and MAV Displaying Electrical Power Connections.

6.10.1. Solar Panels

Solar panels were chosen as the means of power generation after a thorough trade-off against commonly used Radioisotope Thermal Generators, as outlined in the Midterm report [2], primarily due to the reduced cost and mass, and increased sustainability. The solar panel architecture is inspired by The Insight Lander launched in 2018, this reduces the amount of testing and ensures reliability in the design. Using solar irradiance measurements from the Viking 1 lander[42], which is at a similar latitude as the lander, an irradiance of $3200\,\mathrm{Wh/m^2/sol}$ may be expected for the solar array. Highly efficient flight-proven solar cells would allow for a 32.2% cell

efficiency [34].

6.10.2. Dust Accumulation

The accumulation of dust on Martian landers is a common issue and can even be catastrophic to a mission [35]. Dust accumulation on solar panels typically decreases power generation by 0.2% per sol [43]. Fortunate weather can lead to cleaning events, which may extend the lifespan of the mission, however, these are not guaranteed and the mission's success should not be dependent on something as unpredictable as Martian weather. As explained in subsection 6.4.2, the use of compressed gas jets and anti-adhesion coatings would drastically reduce this accumulation. The exact effectiveness of these methods is out of the scope of this study, but a conservative estimate dictates a degradation rate decreasing from 0.2% to 0.13%

6.10.3. Batteries

The constant propellant production leads to significant power requirements at night, without solar power to keep the lander running, substantial batteries are necessary. Lithium-ion battery performance has improved drastically in recent years and a specific energy of 300Wh/kg can be expected from the batteries used [44]. As described in section 6.5 The lander shall maintain a temperature above 0° C, combined with a relatively low number of cycles (360 sols producing propellant), which can allow the batteries to have 100% DOD [45].

6.10.4. Sizing

The power budget of the lander is outlined in section 7.1. The Electrical Power system is sized according to the daily constant power requirements, leading to a constant power demand of $465\,\mathrm{W}$. Considering the solar irradiance, cell efficiency and corrosion rate outlined, the expected solar cell area is$17.9\,\mathrm{m}^2$. With a solar panel packing efficiency of 74% as used on the Insight lander [46] and solar panel mass of $43\,\mathrm{kg}$. The battery mass and volume are expected to then be $24.3\,\mathrm{kg}$ and$13.3\,\mathrm{L}$. This uses the assumption of 100% efficiency, as any energy losses from the electrical power system will be in the form of heat, leading to a corresponding lower power requirement for the thermal control system.

6.10.5. Sensitivity Analysis

In order to analyse the effect of changing parameters on requirement compliance, a sensitivity analysis was performed on the Electrical Power System. This is outlined in Table 6.28.

Table 6.28: Electrical Power System Sensitivity Analysis

Parameter	Solar Irradiance $\mathrm{W\,h\,m^{-2}}$/sol	Deterioration Rate [%/sol]	Solar Panel Efficiency	Power Budget[W]
Change in Value	-400	+0.04	-10%	+50
Effect on Subsystem Mass [kg]	+6	+6.73	+4.4	+7.2
Effect on Solar Panel Area [$\mathrm{m^2}$]	+3.5	+3.8	+1.84	+2.6
Effect on System	Larger EPS	Larger EPS	Larger EPS	Larger EPS
Requirements Affected	LAN-PWR-001	LAN-PWR-001	LAN-PWR-001	LAN-PWR-001
Impact	3	3	2	3

The sensitivity analysis Table 6.28 shows that with a 10% or more change in Solar Irradiance, Solar Panel Efficiency or Power Budget, the main effect is the need for a larger subsystem as a whole. The effect shown for the solar cell deterioration rate is that if unfortunate weather and an under-performing cleaning system lead to a deterioration rate of 0.17%/sol, instead of 0.13%/sol. This is where the redundancy of the EPS design lies, very few of the many Mars landers have had no cleaning events[43], and with the hard-to-quantify performance of the dust cleaning mechanism, 0.13%/sol should offer a significant margin.

[34] https://www.spectrolab.com/photovoltaics/XTE-SF_Data_Sheet.pdf
[35] https://www.space.com/scientists-hail-science-legacy-insight-mars-lander

6.11. Propulsion System

From the design options, the conclusion was made to have two separate systems for the stages. The first stage will consist of an electric pump feed system, with a general layout of such a system shown in figure 6.11. The choice was made to use separate engines for the pumps to reduce the risk of mechanical failures due to gear systems. Another reason for this design decision was that the main other e-pump fed rocket, Rocket Lab's Electron rocket also uses this design and is flight-proven. For the second stage, a simple pressure-fed feed system is used with its layout shown in figure 6.12.

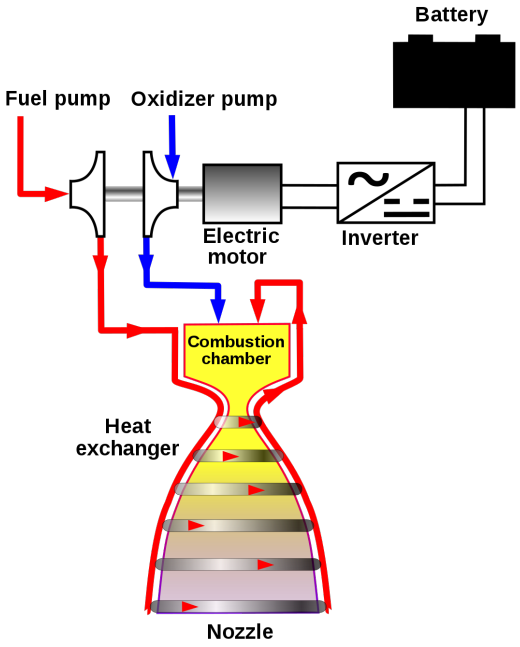

Figure 6.11: Electric Pump-Fed Feed System Layout [36]

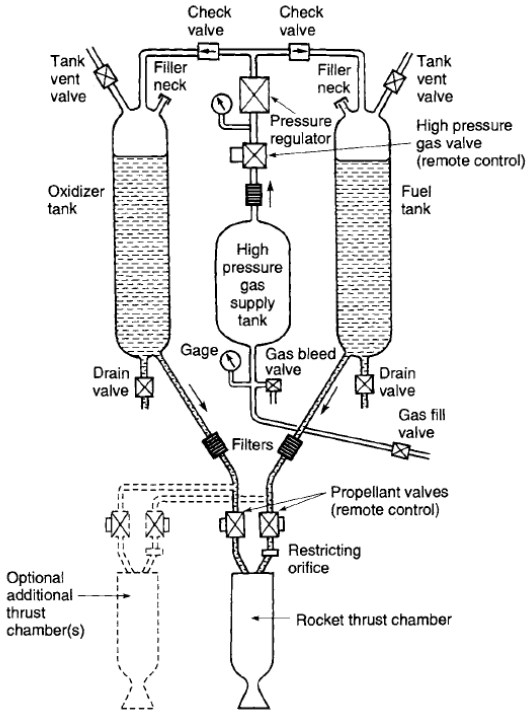

Figure 6.12: Pressure-Fed Feed System Layout [37]

For the combustion chamber sizes and nozzle designs, a cylindrical chamber and bell nozzle were chosen. The main reasons being that the manufacturing of such a chamber is simpler and a bell nozzle was the chosen design option from the design trade-offs. The further sizing, analysis and detailed layout are explained and shown in subsection 6.12.4 and chapter 8 as well as researching regenerative cooling and possible cavitation.

6.12. Engine Performance Analysis

This section will go into the performance analysis of the engine. First, a Chemical Equilibrium with Applications of will (CEA) be carried out in subsection 6.12.1, and the result are verified and validated with existing NASA report. Next, the impurities impact will be analysed based on engine performance in subsection 6.12.2. Section 6.12.3 will talk about the expansion ratio ratio and corresponding specific impulse. In subsection 6.12.4, feed system sizing will be address. The throat area and chamber sizing will be executed in subsection 6.12.5 and subsection 6.12.6. Following by that, nozzle sizing is discussed in subsection 6.12.7. Cavitation is addressed in subsection 6.12.8. And in subsection 6.12.9, regenerative cooling analysis is shown. Finally, a sensitivity analysis will be carried out in subsection 6.12.10.

6.12.1. Chemical Equilibrium with Applications

The NASA python code CEA is used to calculate chemical equilibrium compositions and properties of liquid oxygen and liquid carbon dioxide. Figures 6.13 and 6.14a were generated through the code. Figure 6.14a shows how the characteristic exhaust velocity varies with the oxidiser/fuel ratio (O/F ratio) for three different chamber

[1] https://en.wikipedia.org/wiki/Electric-pump-fed_engine
[2] https://aerospacenotes.com/liquid-propellant-feed-systems/

pressures: $5.3\,\mathrm{bar}$ (blue), $10.7\,\mathrm{bar}$ (orange), and 30bar (green). C^* reaches a peak around 0.43 O/F ratios for each pressure setting, suggesting the stochastic ratio 0.5 is not the optimal mixture ratio for performance. Additionally, the values generated by the code are verified with the theoretical values calculated in Figure 6.14b.

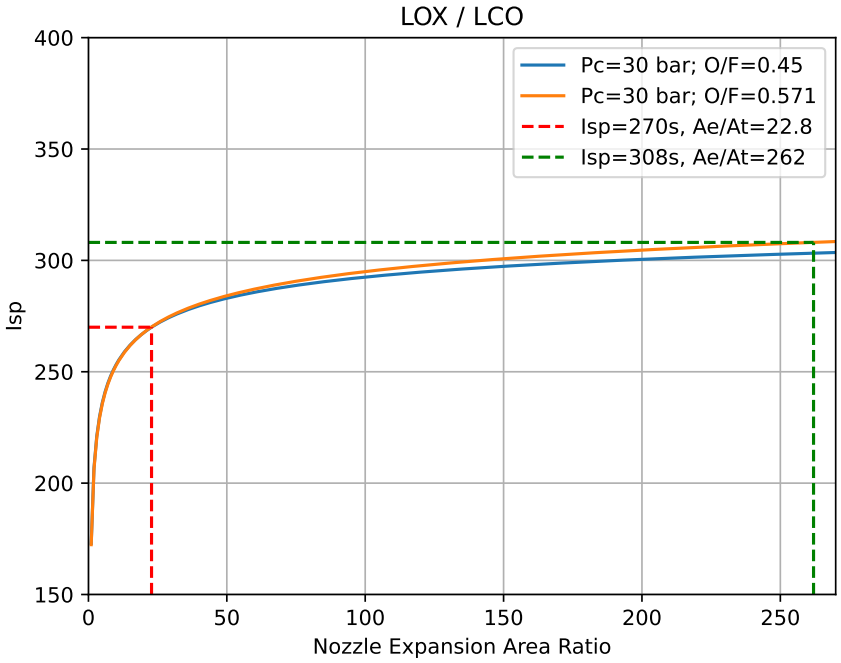

Figure 6.13: I_{sp} Against Nozzle Expansion Area Ratio for Two Different O/F Ratio

One possible cause of the efficiency decrease could be incomplete energy release. The magnitude of its effect can be seen in Figure 6.14b. It is important to note that the difference between the maximum theoretical and experimental C^* due to incomplete energy release is around $120\,\mathrm{m\,s^{-1}}$. In the simulation, the reaction is assumed to be complete combustion without heat loss. In the figure, two types of injectors can lead to different C^* due to their mixing capability, but the design of the injector could be looked further into. This qualitative analysis can be visualised clearly on the overall efficiency, by quantifying the maximum specific impulse, I_{sp} change in the engine. The relation between the characteristic velocity and specific impulse is, as written, in Equation 6.11. where C_F is the thrust coefficient, which reasonably speaking has values around $1.5 - 2.0$, which verified to be 2.0. Assuming g_0 to be around $9.81\,\mathrm{m\,s^{-2}}$, a $120\,\mathrm{m\,s^{-1}}$ change in C^* will mean a maximum I_{sp} variation of $24\,\mathrm{s}$.

$$C^* = \frac{I_{sp} \cdot g_0}{C_F} \tag{6.11}$$

Figure 6.13 illustrates the relationship between I_{sp} and the nozzle expansion area ratio (A_e/A_t), which is the ratio of exit area over throat area, for a rocket engine using LOX/LCO as propellants, with an assumed chamber pressure of $30\,\mathrm{bar}$ at different oxidiser/fuel ratios. The graph demonstrates how the specific impulse, a measure of engine efficiency, increases with the expansion area ratio of the nozzle, depicted for theoretical and experimental optimal O/F ratios: 0.45 and 0.571. For an O/F ratio of 0.45, the specific impulse reaches about $270\,\mathrm{s}$ at an area ratio of 22.8, whereas for an area ratio of 262, it achieves approximately $308\,\mathrm{s}$ (relevant later for subsection 6.12.3). This visualisation effectively shows variation in low area ratio despite fuel mixture and variations in fuel mixture for high area ratio has an impact on the engine's performance, indicating optimal configurations for achieving higher I_{sp}. The similar area ratio is found in the only tested liquid carbon monoxide and liquid oxygen rocket engine, verifies our design [47].

6.12.2. Impurities impact on engine performance

Even the MOXIE experiment wasn't producing 100% pure oxygen - it ensures maintaining a >98% purity throughout its work [31]. The CO-feed on the other hand was not analysed thoroughly by the researchers, thus an analysis of a CO fuel stained by CO_2 (most likely unwelcome guest) has been performed. The work here was

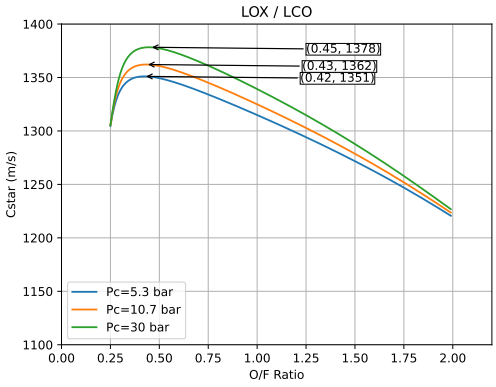

(a) Various Chamber Pressure in the Engine Theoretically

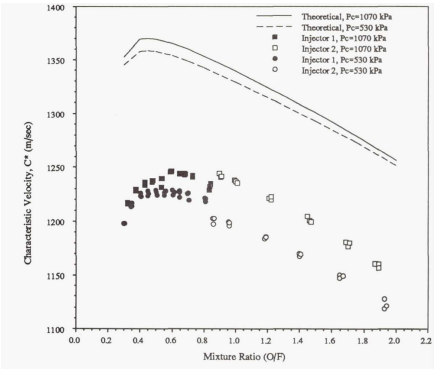

(b) Gaseous O_2/CO_2 Combustion Experimental vs. Theoretical Data[47]

Figure 6.14: Graph Representing Value of C^* Against O/F Ratio for LOX/LCO Mixture

meant to be qualitative - exact procedures on how the purification and liquefaction will be performed in this project is part of detailed work and analysis which will be executed in the later part of the project.

First, the attention is brought to impurities in the CO-feed, as this is the biggest unknown. The contamination (the remaining per cent of the fuel) was modelled as CO_2, which could potentially hide among carbon monoxide molecules. The effect, as predicted by the CEA program, is displayed in Figure 6.15a. The form and magnitude of the results are similar to the ones found in the literature [47].

At this stage, the worst-case impurity level was deemed to be 90%. Later on, if found needed, this qualitative analysis can be broadened. Looking at the graph can reveal that the difference between absolute pure CO and the 90% is $30\,\mathrm{m\,s^{-1}}$, of C^*. To visualise this effect better on the overall efficiency, quantifying the I_{sp} potential change will be useful. The relation between the two is, as written in Equation 6.11, where C_F is the thrust coefficient, which reasonably speaking has values around $1.5 - 2.0$. Assuming g_0 to be around $10\,\mathrm{m\,s^{-2}}$, a $30\,\mathrm{m\,s^{-1}}$ change in C^* will mean a maximum variation of $6\,\mathrm{s}$ in I_{sp}.

Second, a look into the performance change due to impurities in the oxygen feed was theoretically analysed, again using the CEA. Thanks to MOXIE's performance, the purity of O_2 down to 98% was looked into. Contamination was once again modelled with CO_2. The effect is visualised in Figure 6.15b. The differences in this range are minute, and thus omit able in the performance analysis and its effect on the I_{sp}.

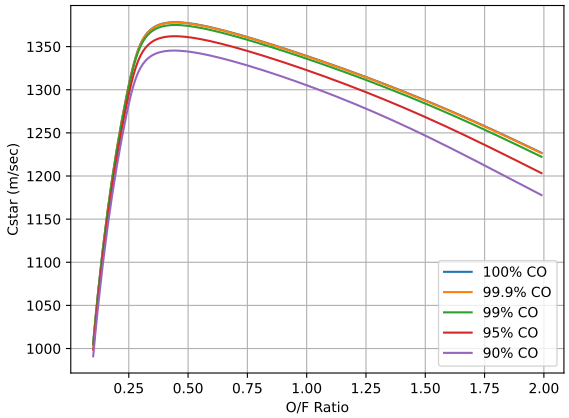

(a) C^* Against O/F Ratio for Various Concentrations of LCO in the Fuel

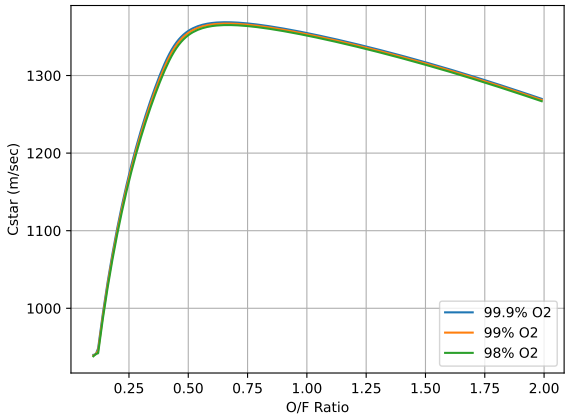

(b) C^* Against O/F Ratio for Various Concentrations of LOX in the 0xidiser

Figure 6.15: Propulsive Performances for Expansion Area Ratio and Propellant Concentrations

6.12.3. Area ratio and theoretical attainable I_{sp}

Following the theoretical analysis, some performance of the MAV engine can be executed. Assuming an isentropic frozen flow in the nozzle, with a reasonable chamber pressure p_c of $30\,\mathrm{bar}$, exit pressure p_e equal to Mars ambient pressure of $700\,\mathrm{Pa}$ (adapted nozzle), and a conservative heat capacity ratio γ of 1.17 for CO_2, and applying them in Equation 6.12 and Equation 6.13[48] :

$$\frac{A_e}{A^*} = \frac{\Gamma(\gamma)}{\sqrt{\frac{2\gamma}{\gamma-1}(\frac{p_e}{p_c})^{\frac{2}{\gamma}}[1-(\frac{p_e}{p_c})^{\frac{\gamma-1}{\gamma}}]}} \tag{6.12}$$

$$\Gamma(\gamma) = \sqrt{\gamma(\frac{1+\gamma}{2})^{\frac{1+\gamma}{1-\gamma}}} \tag{6.13}$$

It will yield an aspect ratio of 262 approximately. From Figure 6.13, one can read off a corresponding I_{sp} value of $306\,\mathrm{s}$. Looking at the manufacturable side: the nozzle will most likely not be bigger than the MAV itself, and the current MAV baseline design predicts a diameter of $57\,\mathrm{cm}$ [11], which can be therefore taken as a first-order estimate of the nozzle. This would imply the maximum throat diameter of $3.5\,\mathrm{cm}$, a reasonable and manufacturable size.

Looking at the performance and validity of the staging analysis performed for the trade-off: the impurities effect ($\approx 6\,\mathrm{s}$) and the incomplete energy release effect ($\approx 24\,\mathrm{s}$) combined are contained within the contingency taken. An I_{sp} of $270\,\mathrm{s}$ was used, while a theoretical possible value of $306\,\mathrm{s}$ was found.

The discrepancy between the theoretical and experimental values is likely due to incomplete energy release in the combustion chamber. Based on combustion experiments with gaseous oxygen and carbon dioxide, the measured combustion efficiency was 96%, indicating relatively complete combustion [49]. Therefore, incomplete combustion is not the cause of the observed low efficiency. The discrepancy between theoretical analysis and experimental results from small-scale combustion tests suggests that slow kinetics or uneven gas mixing may be key factors in the efficiency problem. In this scenario, the high combustion gas temperature causes severe decomposition in the combustion chamber, while slow kinetics hinder the recombination that typically occurs in the combustion chamber and nozzle. This combination of high decomposition and slow recombination likely results in the measured specific impulse efficiency of only 86% to 88% [49]. Although this experiment involved gaseous carbon monoxide and liquid oxygen, the mixing of two liquids is worse than that of a gas and a liquid, as the liquid must vaporise before mixing. Therefore, it is assumed that similar efficiency losses occur in LOX/LCO cases.

6.12.4. Feed system sizing

Currently, not many electrical pump sizing methods are available but a general approach of feed system design sizing can be used. [50] has been chosen as the main point of sizing the electrical feed system. For this, some numbers have been taken over from the paper and are shown in table 6.29.

First Stage

To calculate the entire system mass for the first stage, equation (6.14) [50] is used.

$$m_{First} = m_g + m_{tg} + m_{pu} + m_{ee} + m_{inv} + m_{bat} \tag{6.14}$$

Where m_g and m_{tg} are the pressurant gas and tank masses, m_{pu} is the pump mass, m_{ee} the electric engine mass, m_{inv} is the inverter mass and m_{bat} is the battery mass
The pressurant gas and tank mass are calculated using equations (6.15) and (6.16).

$$m_g = k_g k_p k_u \gamma_g \alpha \frac{M_g}{R_u T_0}\left(\frac{m_p p_C}{1-k_p\frac{p_C}{p_0}}\right) \tag{6.15}$$

$$m_{tg} = \frac{3\rho_t}{2\sigma_t} k_g k_p k_u \gamma_g \alpha \left(\frac{m_p p_C}{1-k_p\frac{p_C}{p_0}}\right) \tag{6.16}$$

Where: γ_g is the pressurising gas specific heat ratio, m_p being the propellant mass, p_C is the chamber pressure, R_u is the universal gas constant, M_g is the Pressurising gas molar mass, ρ_t is the tank material density, σ_t is the ultimate tensile strength of the tank material and k_g is a safety constant to account for left over gas at the end of the cycle. α, k_p and k_u are calculated using equations (6.17) to (6.19) while k_{tg} is the safety margin for

Table 6.29: Assumed Values for Calculating Feed System Mass from [50]

Parameter	Assumed Value	Unit
Pressurant Gas Pressure	200	bar
Pump Power Density	40	$\mathrm{kW\,kg^{-1}}$
Pump Efficiency	0.8	-
Electric Engine Power Density	3.8	$\mathrm{kW\,kg^{-1}}$
Electric Engine Efficiency	0.8	-
Inverter Power Density	60	$\mathrm{kW\,kg^{-1}}$
Inverter Efficiency	0.85	-
Battery Sizing Margin	1.2	-
Battery Power Density	400	$\mathrm{W\,kg^{-1}}$
Battery Energy Density	250	$\mathrm{W\,h\,kg^{-1}}$
Tank Pressure 1st stage	0.3*Chamber Pressure	-
Tank Pressure 2nd stage	1.8*Chamber Pressure	-

the estimated mass.

$$\alpha = \alpha_o + \alpha_f = \frac{OF}{\rho_o}\left(\frac{1}{1+OF}\right) + \frac{1}{\rho_f}\left(\frac{1}{1+OF}\right) \tag{6.17}$$

$$k_p = \frac{p_g}{p_C} \tag{6.18}$$

$$k_u = \frac{V_{tf}}{V_f} = \frac{V_{to}}{V_o} \tag{6.19}$$

Where OF is the oxidiser-fuel ratio, ρ_o and ρ_f are the densities of the propellants, V_f and V_{tf} are the fuel and fuel tank volume, same with the oxidiser and oxidiser tank volume.
For the pump, electric engine and inverter mass estimates, equations (6.20), (6.22) and (6.23) are used with the design choice of an engine and inverter for each pump.

$$m_{pu} = m_{puf} + m_{puo} = (1 + k_{pi} - k_p)\frac{\alpha_f p_C m_p}{\delta_{puf} t_b} + (1 + k_{pi} - k_p)\frac{\alpha_o p_C m_p}{\delta_{puo} t_b} \tag{6.20}$$

Where: k_{pi} is calculated by equation (6.21), δ_{pu} is the pump power density and t_b is the burn time.

$$k_{pi} = \frac{\Delta p_i}{p_C} \tag{6.21}$$

At which Δp_i is the pressure fall in the injector.

$$m_{ee} = m_{eef} + m_{eeo} = (1 + k_{pi} - k_p)\frac{\alpha_f p_C m_p}{\delta_{eef} t_b \eta_{puf}} + (1 + k_{pi} - k_p)\frac{\alpha_o p_C m_p}{\delta_{eeo} t_b \eta_{puo}} \tag{6.22}$$

Where: δ_{ee} is the electric engine power density and η_{pu} is the pump efficiency.

$$m_{inv} = m_{invf} + m_{invo} = (1 + k_{pi} - k_p)\frac{\alpha_f p_C m_p}{\delta_{invf} t_b \eta_{puf} \eta_{eef}} + (1 + k_{pi} - k_p)\frac{\alpha_o p_C m_p}{\delta_{eeo} t_b \eta_{puo} \eta_{eeo}} \tag{6.23}$$

Where: δ_{inv} is the inverter power density and η_{ee} is the electric engine efficiency.
For the battery masses, two possible limitations are possible. They are either power or energy limited, with their masses calculated using equations (6.24) and (6.25)

$$m_{bap} = (1 + k_{pi} - k_p)\frac{p_C m_p}{t_b}\left(\frac{\alpha_f}{\eta_{puf}} + \frac{\alpha_o}{\eta_{puo}}\right)\frac{k_b}{\eta_{ee}\eta_{inv}\delta_{bap}} \tag{6.24}$$

$$m_{bap} = (1 + k_{pi} - k_p)\frac{p_C m_p}{t_b}\left(\frac{\alpha_f}{\eta_{puf}} + \frac{\alpha_o}{\eta_{puo}}\right)\frac{k_b}{\eta_{ee}\eta_{inv}\delta_{baw}} \tag{6.25}$$

With k_b being the sizing safety factor, δ_{bap} is the battery power density and δ_{baw} being the battery energy density. For all these equations the chamber pressure was kept a variable to optimize for weight together with the chamber and nozzle sizes.

Second Stage

For the pressure fed second stage, equations (6.15), (6.16) and (6.26) are used. The main difference here is that the pressure in the propellant tanks is higher than the chamber pressure compared to the electric pump fed system.

$$m_{Second} = m_g + m_{tg} \tag{6.26}$$

Results

For the first stage, the relationship between the subsystem mass and the chamber pressure is roughly linear, shown in Equation 6.27 with mass in kg and chamber pressure in bar. A breakdown of this mass is shown in Table 6.30. For the second stage, the relationship is not linear, and is shown Figure 6.16.

$$m_{FS} = 0.154 P_C + 0.138 \tag{6.27}$$

Table 6.30: Component Mass Distribution of the First Stage

Component	Fraction
Batteries	56.6%
Electric motors (2)	19.8%
Inverters (2)	1.6%
Pump Mass (2)	1.5%
Pressure Gas	9.5%
Pressure Tank	11.0%

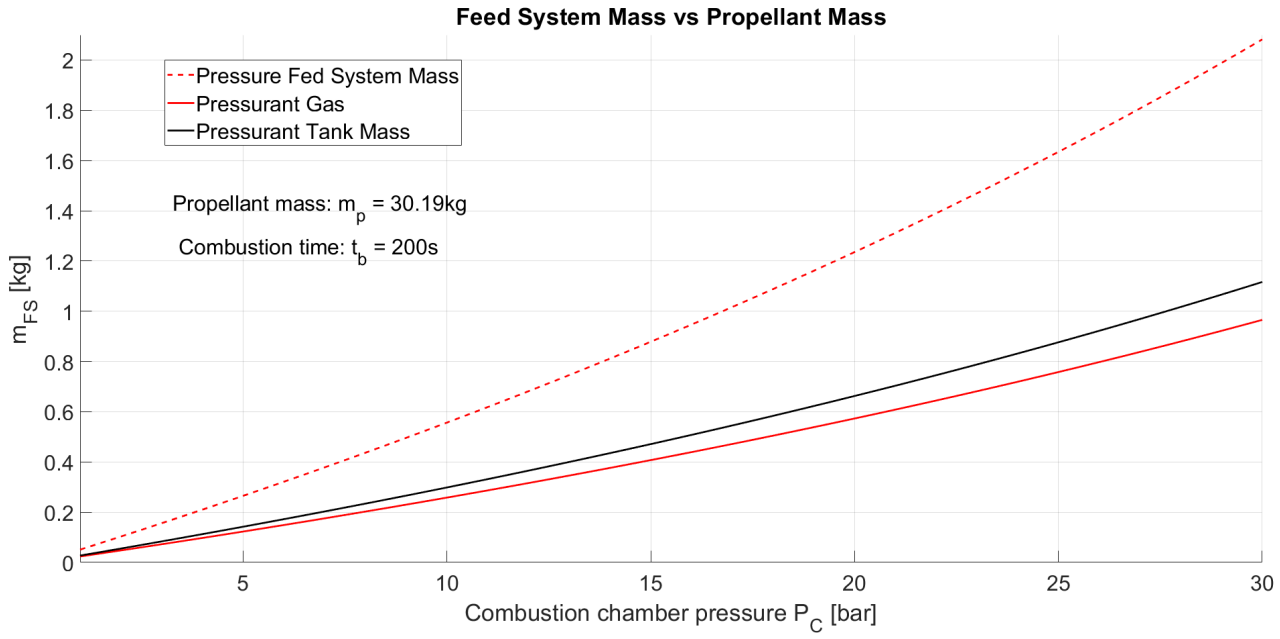

Figure 6.16: Second Stage Mass Estimates

These graphs show the minimum mass required to achieve the performance needed, set by the requirements. To achieve a final chamber pressure optimised for mass, the chamber, throat and nozzle sizing should also be considered. This is done in the following subsections.

6.12.5. Throat area calculation

Following the design of the feeding system, the throat area of the MAV engine can be determined. Firstly, we assume isentropic frozen flow in the chamber and nozzle. Given the relatively low atmospheric pressure on Mars compared to Earth, the atmospheric pressure is considered negligible. A thrust-to-weight ratio of 2 is set to allow a margin for additional mass, meeting the thrust requirements for two stages as shown in Table 4.8. The experimental specific impulse of $270\,\mathrm{s}$, as discussed in subsection 6.12.3, is chosen for the design. Consequently, the mass flow can be calculated using Equation 6.28 [38]. The mass flow for the first stage is $0.529\,\mathrm{kg\,s^{-1}}$, while for the second stage it is $0.151\,\mathrm{kg\,s^{-1}}$. The total propellant mass is known, with burn times of $201\,\mathrm{s}$ for the first stage and $200\,\mathrm{s}$ for the second stage.

$$F = \dot{m} \cdot I_{sp} \cdot g_0 \tag{6.28}$$

From the CEA analysis discussed in subsection 6.12.1, the chamber pressure, chamber temperature, heat ratio, and gas constant are calculated. Using these values, along with the previously calculated mass flow rate in Equation 6.28, the cross-sectional area of the throat can be sized using Equation 6.29 [39].

$$A^* = \frac{\dot{m}}{\frac{p_t}{\sqrt{T_t}} \cdot \sqrt{\frac{\gamma}{R}} \cdot \left(\frac{\gamma+1}{2}\right)^{-\frac{\gamma+1}{2(\gamma-1)}}} \tag{6.29}$$

Since the throat and chamber are designed to be circular, the throat and outlet diameters can be determined based on the calculated cross-sectional area. Varying the chamber pressure affects the dimensions and mass of the nozzle. Higher chamber pressure results in a lower nozzle mass. However, increasing the pressure also raises the pump mass linearly as shown in Figure 6.16. This inverse relationship between pump mass and nozzle mass leads to an optimal design to minimise the overall mass. By evaluating combined pump and nozzle masses at pressures ranging from 15 to $30\,\mathrm{bar}$, in increments of $5\,\mathrm{bar}$, the optimal pressure was identified at $25\,\mathrm{bar}$. At this pressure, the calculated throat diameters for the first and second stages are $18.52\,\mathrm{mm}$ and $12.63\,\mathrm{mm}$, respectively, while the nozzle exit diameters are $299.8\,\mathrm{mm}$ and $204.5\,\mathrm{mm}$, respectively.

6.12.6. Chamber sizing

The first step in designing a combustion chamber is to determine its characteristic chamber length, which ensures the combustion flame does not damage the injector and that the fuel and oxidiser are fully vaporised. The characteristic chamber length varies between different propellant combinations [51]. Since liquid oxygen and liquid carbon monoxide engines are not a mainstream rocket fuel combination on Earth, it is challenging to derive the characteristic chamber length from statistical data. We attempted to predict the characteristic chamber length using a linear relationship with fuel characteristics such as flame temperature and molar mass. However, after examining the relationships between characteristic chamber length and these fuel characteristics for various fuels, no strong linear correlation was found.

The characteristic chamber length is highly dependent on the injector used, as different types of injectors result in different Sauter mean diameters of the mixture in the chamber. A high degree of mixing is preferred [52]. Injector design and combustion stability require further research. To ensure feasibility and avoid unexpected issues, we defaulted to using concentric tube injectors, based on the only tested liquid oxygen and liquid carbon monoxide engines [53].

After selecting the injector, and without experimental data to support its performance, the characteristic chamber length issue remains unresolved. Since there is no commercial carbon monoxide and oxygen engine to reference, we based our design on the commercial hydrogen and oxygen engine, following the same procedure to be safe, as two NASA reports [47] [54] had already made this assumption and conducted experiments and analysis. The experimental engine size was not used as a reference because this is the first engine built, designed to prevent the flame from burning the injector. For safety reasons, researchers designed the combustion chamber to be longer than necessary, avoiding combustion and liquefaction problems. However, this thin

[38] https://www.grc.nasa.gov/www/k-12/airplane/rktthsum.html
[39] https://www.grc.nasa.gov/www/k-12/airplane/astar.html

tube design introduces boundary layer effects, as reflected in TDK (Two-dimensional kinetic) analysis [47].

Referencing hydrogen-oxygen is not a random act because NASA also used the RL10 rocket engine [47] and RS25 (or SSME) [54] as prototypes for developing this new propellant combination engine. Both referred engines are hydrogen-oxygen engines, with a characteristic chamber length of $890\,\mathrm{mm}$ [51]. Using Equation 6.30 where L^* is characteristic chamber length, V_c is the chamber volume, and A_t is the throat area obtained from subsection 6.12.3, L^* and A_t can be used to calculate the required combustion chamber volume. The combustion chamber volumes for the first and second stages are $0.24\,\mathrm{L}$ and $0.112\,\mathrm{L}$, respectively.

$$L^* = \frac{V_c}{A_t} \tag{6.30}$$

Equation 6.31 in SI unit where ϵ is area ratio between chamber and throat, D_t is throat diameter demonstrates the relationship obtained from Figure 6.18. The throat diameter obtained from subsection 6.12.3 can be used to calculate the ratio of the combustion chamber area to the throat area.

$$\epsilon = 1.302 \cdot {D_t}^{-0.481} \tag{6.31}$$

The diameters for the first and second stage combustion chambers are $55.16\,\mathrm{mm}$ and $41.25\,\mathrm{mm}$, respectively. Using the volume formula for a cylinder, the lengths of the combustion chambers are $100.36\,\mathrm{mm}$ for the first stage and $83.49\,\mathrm{mm}$ for the second stage. These calculations align with statistical relationships Figure 6.17.

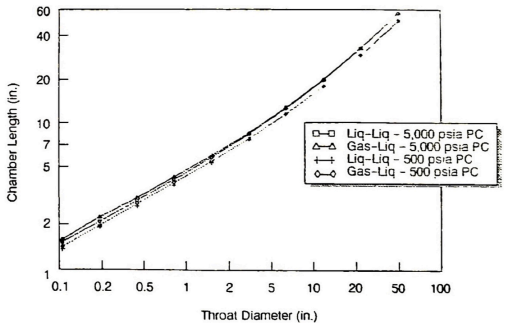

Figure 6.17: Chamber Length Against Throat Diameter [51]

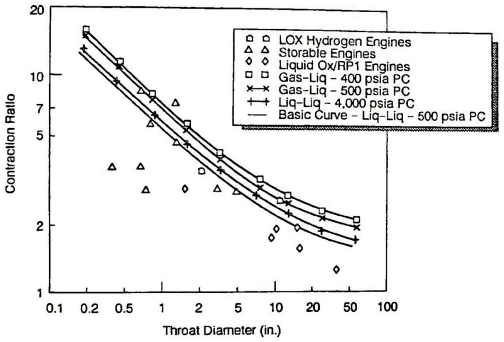

Figure 6.18: Area Ratio Against Throat Diameter [51]

The engine throat is designed with a convergent-divergent nozzle. The nozzle inlet angle was chosen to be $25°$, based on the only existing liquid oxygen and liquid carbon monoxide engine using this angle [51]. The injector took up 10% of the chamber length. The final design of the combustion chamber will be shown in Figure 6.19 and Table 6.31.

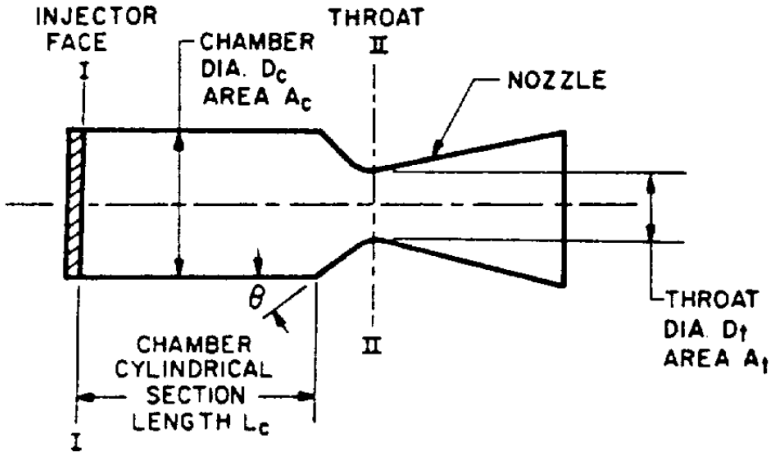

Figure 6.19: Combustion Chamber Dimension [51]

Table 6.31: Dimension of the Combustion Chamber

Parameter	Value - 1st stage	Value - 2nd Stage	Unit
Chamber Length	100.4	83.4	mm
Injector Length	10.0	8.30	mm
Chamber Diameter	55.2	41.3	mm
Throat Diameter	18.5	12.6	mm
Nozzle Diameter	300	205	mm
Nozzle Inlet Angle	25	25	°

In summary, the engine design is heavily based on the injector. Once the injector is tested, the combustion chamber dimensions will be further refined. Also, experiments with carbon monoxide and oxygen in the calorimetric chamber show that slow dynamics may need to be considered when determining the appropriate combustion chamber length. The chamber heat flux did not level out until $7\,\mathrm{cm}$ downstream of the injector, indicating continued combustion [49], which suggests the current designed chamber length is sufficient. Future injector design research is essential to ensure the chamber dimensions are compatible with the chosen injector.

6.12.7. Nozzle sizing

To achieve better performance and a shorter length, a bell-shaped nozzle was chosen. Engine performance was further enhanced by improving the actual Isp through graphical optimisation using the Rao's program [55]. Figure 6.20 shows the shape of the first stage engine nozzle, while Figure 6.21 illustrates the second stage engine nozzle. The nozzle lengths for the first and second stages are $420\,\mathrm{mm}$ and $286\,\mathrm{mm}$, respectively. Future designs will be refined based on experimental data and CFD analysis to develop more efficient nozzle shapes.

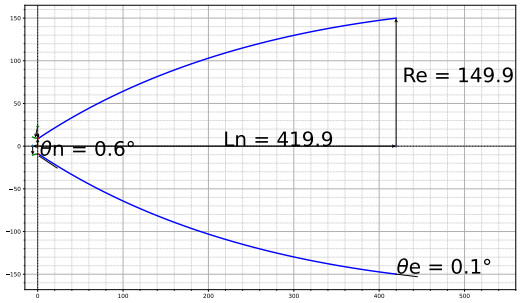

Figure 6.20: First Stage Nozzle Dimension

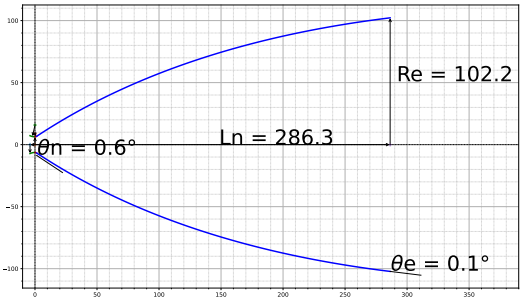

Figure 6.21: Second Stage Nozzle Dimension

As mentioned in subsection 6.12.3, LOX and LCO do not mix well in practice. One-dimensional equilibrium (ODE) analysis is not recommended for evaluating LOX and LCO engines, as it overestimates the recombination of CO2 in the throat compared to one-dimensional kinematics (ODK) and two-dimensional kinematics (TDK). A large divergence immediately behind the throat is not advisable due to high relative pressure and rapid expansion, which can cause separation in this region. Figure 6.23 shows that the mass fraction of CO2 increases from the combustion chamber to an area ratio of 2, then levels out as it enters a slow expansion zone without reaching the combustion temperature. Interestingly, as the radius of the downstream nozzle throat increases, the mass fraction of CO2 also increases. This indicates that a larger downstream nozzle throat radius allows for slower gas expansion, providing more time for recombination before the temperature drops too low. This finding may suggests that non-traditional nozzle geometries can enhance performance, potentially increasing specific impulse by approximately 2 seconds [47].

In Figure 6.22, the top design represents a new nozzle geometry developed by NASA, where the downstream throat arc transitions to a shallow cone instead of directly to a bell nozzle. Once the cone reaches an expansion area ratio of 4, the optimal Rao nozzle is added. Although the exit angle of this non-conventional nozzle is larger at $8.8°$ compared to the optimal bell-shaped geometry at $6.8°$, leading to greater divergence losses, ODK and TDK analysis still indicate that this new nozzle still achieves a higher specific impulse than the traditional bell-shaped nozzle [47]. Further optimisation of this nontraditional design could yield even better performance in

the future through CFD analysis.

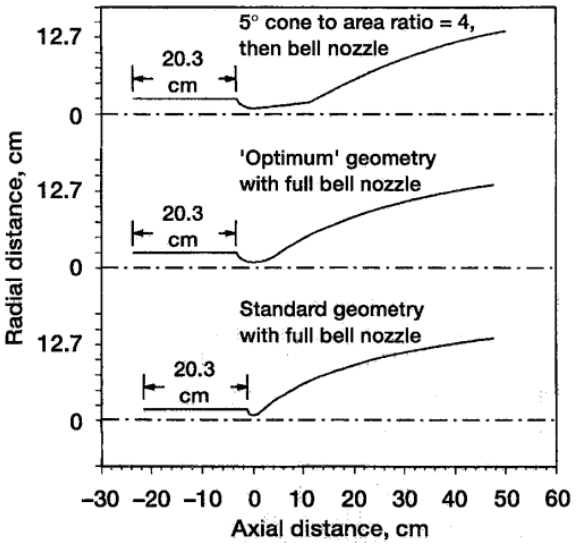

Figure 6.22: Graphical Representation of the Bell, Optimum Bell, and Cone-With-Bell Engine Geometries [49]

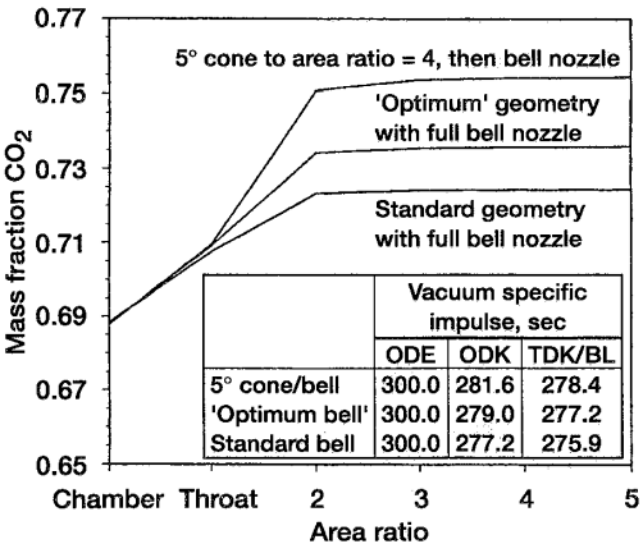

Figure 6.23: Comparison of Optimum Bell Nozzle with Nozzle that Begins with a 5° Cone [49]

6.12.8. Cavitation

Following from the design choices, with an engine as small as this, possible cavitation could occur and create critical damage in the pumps. To analyse if cavitation occurs, something called Net Positive Suction Head (NPSH) [m or ft] is calculated which is required to be above a required value to prevent cavitation. According to Cannon [56], equation Equation 6.32 can be used as a simple estimation method.

$$NPSH = \frac{p_i - p_v}{\rho * g_0} \tag{6.32}$$

Where p_i is the inlet pressure, p_v and ρ are the vapour pressure and density of the liquid and g_0 is the gravitational constant.

At $100\,\mathrm{K}$, the properties of both propellants are given in table 6.32

Table 6.32: Results for Compressor Piston Calculation

Property	LCO	LOX	Unit
Density	793	1140	$\mathrm{kg\,m^{-3}}$
Vapour Pressure	518	255	kPa
Inlet Pressure	750	750	kPa

Using these values together with g_0 equalling $9.81\,\mathrm{m\,s^{-1}}$. The NPSH of the LCO and LOX pumps are 29.9 and $44.3\,\mathrm{m}$. Comparing this to Campbell [57], where they say that generally the NPSH is between 6 and $40\,\mathrm{m}$.

In conclusion, cavitation would generally not occur at the current configuration of the turbopumps. It should be noted that the rotation speed and cryogenic conditions of both pumps were not considered due to time constraints and should be investigated in further studies.

6.12.9. Cooling Design

As part of the engine design, it is important to consider how it will be cooled and the temperature it will maintain. For a cooling method, it was decided to look into the option of regenerative cooling by writing a simulation in Python. In reality, regenerative cooling is very complex, and extremely accurately modelling it is beyond the scope of the project. Hence, it must be emphasised that this model was created with the intention of getting a ballpark figure to assess feasibility, rather than to retrieve the exact temperatures the engine reaches during combustion.

For regenerative cooling, the thermophysical properties of carbon monoxide and oxygen were compared to determine the most suitable coolant. The comparison showed that the density, viscosity, and thermal conductivity of both fluids are similar over a wide range of temperatures and pressures. The Prandtl Number values indicate that it is not explicitly clear which fluid is a better coolant. However, their specific heats vary considerably. CO fuel has a larger specific heat capacity and will hence be less prone to when absorbing heat during the process.

Assuming two-phase flow in the cooling channels, carbon monoxide generally resulted in a higher coolant pressure drop while maintaining a lower hot-gas-side wall temperature for the same geometry configuration. Despite this pressure drop, carbon monoxide can be considered a better coolant than oxygen under most conditions [58].

Model Set-Up

To create the model, 3 main heat exchanges of heat were looked at: convection between the gas in the combustion chamber and the chamber walls, conduction from one side of the chamber wall to the other, and convection between the coolant channel. It will now be explained how each of these heat transfers was estimated in the model. For a general convection process, the heat flux q in $\mathrm{W\,m^{-2}}$ is given by Equation 6.33 [59],

$$q = h(T_1 - T_2) \tag{6.33}$$

where h is the convective heat transfer coefficient in $\mathrm{W\,m^{-2}\,K}$ and T_1 and T_2 are the temperatures of the surfaces between which the convection is taking place. To use this equation, one must also know the values of h for each convective process. For the convection h_{hot} between the combustion chamber and the chamber walls, Equation 6.34 can be used [59],

$$h_{hot} = 0.01975 \frac{k^{0.18}(\dot{m}c_p)^{0.82}}{D_c^{1.82}} \left(\frac{T_{hotgas}}{T_{wall}}\right)^{0.35} \tag{6.34}$$

where k is the thermal conductivity of the combustion gas in $\mathrm{W\,m^{-1}\,K}$, $\dot{m}$ is the mass flow in $\mathrm{kg\,s^{-1}}$, c_p is the constant pressure heat capacity of the gas in $\mathrm{J\,kg^{-1}\,K}$, D_c is the diameter of the combustion chamber and T_{wall} is the temperature of the wall on the side of the combustion chamber in K. T_{hotgas} is given by Equation 6.35 [59].

$$T_{hotgas} = T_{local} + 0.8(T_\infty \eta_c^2 - T_{local}) \tag{6.35}$$

Here, T_∞ is the combustion temperature, and the local temperature T_{local} can be assumed equal to T_∞ [60]. Furthermore, the combustion efficiency η_c is assumed to be 0.92. A final consideration to make for convection on the hot gas side is the calculation of adiabatic wall temperature T_{aw} which can be done with Equation 6.36 [59],

$$T_{aw} = T_\infty \left(1 + r\frac{\gamma - 1}{2}M^2\right) \tag{6.36}$$

where M is the Mach number of the combustion gas. Equation 6.36 captures the fact that as the gas slows down near the chamber walls, its static temperature increases. This is the temperature used in Equation 6.33 when finding heat transfer. Furthermore, the value r in Equation 6.36 is given by $Pr^{\frac{1}{3}}$, where Pr is the Prandtl number as defined in Equation 6.37,

$$Pr = \frac{c_p \mu}{k} \tag{6.37}$$

where μ is the gas dynamic viscosity of the gas in $\mathrm{Pa\,s}$. All the properties of the combustion has mentioned here are found using the Rocketcea python package. This covers the convective heat transfer on the hot side. On the cold side (between the cooling fuel and the engine walls), the convective heat transfer coefficient h_{cold} can be found using Equation 6.38 [59],

$$h_{cold} = \frac{kNu}{D} \tag{6.38}$$

where D is the diameter of the coolant channels, and Nu is the Nusselt number of the fuel. Nu can be found using Equation 6.39 [59],

$$Nu = 0.023 Re^{0.8} Pr^{0.4} \tag{6.39}$$

where Re is the Reynolds number of the fuel flow. This summarises the convection on the cold side. The conduction within the engine wall itself q_{cond} is given simply by Equation 6.40,

$$q_{cond} = \frac{k(T_1 - T_2)}{t} \tag{6.40}$$

where T_1 and T_2 are the temperatures on either side of the wall, k is the thermal conductivity and t is the thickness. With this, all the governing equations for the model have been defined. It will now be explained how the model was actually set up, and what the main assumptions were. Figure 6.24 attempts to illustrate this.

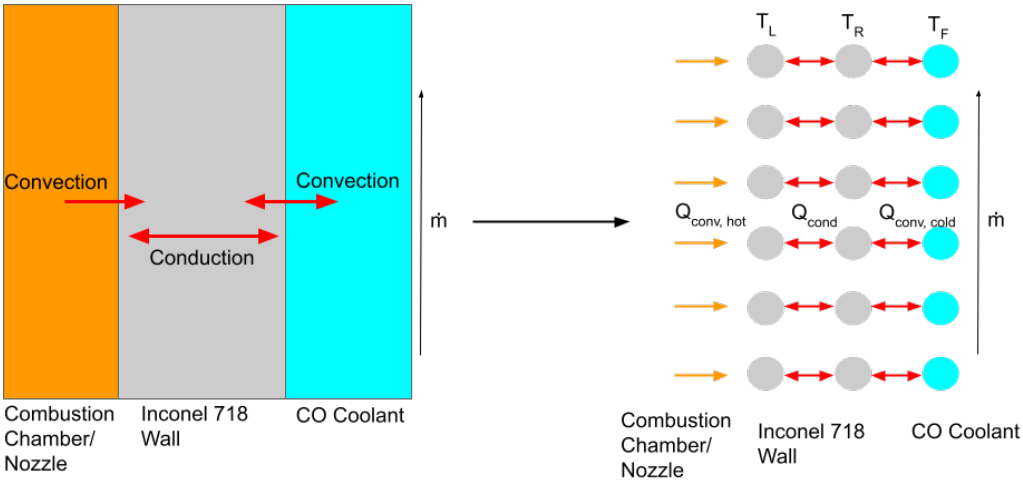

Figure 6.24: Regenerative Cooling Model

The left-hand side of the figure shows the idea behind the model in a more physical sense. On one side, the combustion chamber transfers heat to the inconel wall via convection. Any change in temperature of the combustion gas due to this phenomena is neglected. On the other side, heat is exchanged between the inconel wall and the cooling channel via convection, and in this case the increase in temperature of the cooling fuel cannot be neglected. Finally, the wall conducts heat from one of its sides to the other. Other simplifying assumptions made here are that there is no 'vertical' heat transfer within the wall, similarly that the fluid only exchanges heat with the wall next to it, and there is no heat exchange within the fluid, or between the fluid and other walls surrounding it. Furthermore, the cooling fluid is assumed to remain at a constant pressure, as defined by the required chamber pressure, and the entire engine (combustion chamber and nozzle) is assumed to be a cylinder with a diameter equal to the actual average engine diameter.

With these assumptions in mind, the simulation itself can be further explained. As shown on the right side of Figure 6.24, the system is split up into n nodes vertically. This shows how the fuel flows from the bottom of the engine wall to the injector. The wall itself is also split into to sets of vertical nodes, to model the temperature difference between either side of the wall. At the start of the simulation, a cooling channel pitch is input. From here, the total cooling channel length could be calculated based on the engine geometry. With the total channel length, as well as the input wall thickness, the mass and area of each node for the wall could be calculated. The same could be done for the nodes representing the fluid since the fluid channel diameter and fluid density is known.

As the simulation starts, an array of temperature values is created for each set of vertical nodes, containing all the initial temperatures at each node. Following this, the convective and conductive properties are all estimated based on the temperatures and the fluid properties at that temperature found with the Coolprop and Rocketcea libraries. The heat transfer coefficients are also stored in arrays, and with this the net heat gain or loss at each node is calculated, this depends on the time-step as the heat transferred is power multiplied by time. Finally, with the heat gain/loss known, the change in temperature of each node for that time-step can be calculated. This represents the process for a singular time step. Following this, the same process repeats with the new initial temperature arrays as inputs. This continues for the entire burn time.

Another crucial aspect of the simulation to mention is the modelling of fluid flow. At the start of the simulation, a time-step is calculated such that for in 1 time-step, a mass equal to the mass per node of fluid travels between

fluid nodes. This may sound confusing, but what it means is that at the end of each time step, to model the flow of fluid each temperature value in the array of fluid temperatures is shifted to the right by 1 spot, and the new first value becomes the initial temperature value of the fluid (because new fluid at that temperature is flowing in).

Considering all this, the main aspect left to address is that the simulation assumes the whole engine is in contact with the cooling channel. Of course, this is not the case in reality, as the channel spirals around the engine but does not cover the entire surface area. Based on the assumed channel pitch and channel diameter, it could be seen that roughly 10% of the engine surface area is 'covered' by cooling channels. To attempt to account for this in the model, the heat transfer via convection with the combustion gas is multiplied by 10. This is an extremely non-rigorous way of accounting for the assumption in the model. That being said, it must again be emphasised the aim here is to assess the feasibility of the regenerative cooling, rather than get extremely accurate temperature values, since the later would require a far more in-depth simulation.

Simulation Results

Having explained the model, the results can now be outlined. The simulation was done for both the first and second stage engines. The main inputs for each simulation are shown in Table 6.33. Furthermore, the simulation outputs of interest are displayed in Table 6.34.

Table 6.33: Inputs for Regenerative Cooling Simulation

Input	Value - 1st Stage	Value - 2nd Stage	Unit
Coolant channel diameter	2	2	mm
Channel pitch	20	20	mm
Wall thickness	1	1	mm
Fluid pressure	25	15	bar
Engine diameter	159	109	mm
Burn time	200	170	s

Table 6.34: Outputs of Regenerative Cooling Simulation

Output	Value - 1st Stage	Value - 2nd Stage	Unit
Maximum wall temperature	369	498	K
Maximum coolant temperature	119	115	K

The maximum wall temperatures reached seem safe since the Inconel 718 used has a maximum operating temperature[40] of $978\,\mathrm{K}$. Due to the rudimentary nature of the simulation, it is possible that higher temperatures will be reached in real life. However, with the current geometry there is quite a healthy margin which accounts for this. With regard to coolant temperature, LCO at $15\,\mathrm{bar}$ and $25\,\mathrm{bar}$ boils at approximately[41] $115\,\mathrm{K}$ and $125\,\mathrm{K}$ respectively. Considering this along with the results in Table 6.34, one sees that the fuel will not boil during the regenerative cooling process. One could argue that both temperatures are somewhat close to the boiling points, which isn't great considering the rudimentary nature of the simulation. However, even if the boiling points are reached, the required latent heat must also be overcome. This adds additional margin and reassures that boiling of fuel will not happen during regenerative cooling.

Considering that the inputs here align with the assumed engine dimensions, and that the output temperatures for both the fuel and engine wall are comfortably within the required ranges, it can be concluded that regenerative cooling would be a viable option for cooling of both engines.

6.12.10. Sensitivity Analysis

To see the effects of changing certain values, for example, burn time of the first and second stage, a sensitivity analysis was performed. Tables 6.35 and 6.36 show the results of the analysis and their impact on the

[40] https://www.specialmetals.com/documents/technical-bulletins/inconel/inconel-alloy-718.pdf
[41] https://webbook.nist.gov/chemistry/fluid/

requirements. The combustion time will be decreased by 10% to see what the changes of a higher fuel flow, the propellant mass is increased by 10% to see the effect of more ΔV needed. The pressurant tanks have some weight, so decreasing the pressure to reduce that mass may have an effect and is lowered by 10%. Finally lowering the propellant tanks may decrease structural weight but a decrease of 0.1 times combustion pressure is simulated to see the effects on the first stage.

Table 6.35: First Stage Sensitivity Analysis

Parameter	Combustion Time [s]	Propellant Mass [kg]	Pressurant Gas Pressure [bar]	Propellant Tank Pressure Fraction
Change in Value	-20	+10	-20	-1.0 · chamber pressure
Effect on Subsystem Mass at 30 bar [g]	+37.6	+73.8	+25.2	+16.7
Effect on Subsystem Mass at20 bar [g]	+25.4	+49.4	+17.0	+11.9
Effect on Engine Performance	Higher mass flow means Higher Thrust but also different nozzle shape	Higher mass flow means Higher Thrust but also different nozzle shape	None	None for the engine but turbopumps have to be larger
Requirements Affected	MAV-PRP-014	MAV-PRP-014	MAV-PRP-014	MAV-PRP-014
Impact	4	4	4	4

Table 6.36: Second Stage Sensitivity Analysis

Parameter	Combustion Time [s]	Propellant Mass [kg]	Pressurant Gas Pressure [bar]
Change in Value	-20	+3	-20
Effect on Subsystem Mass at 15 bar [g]	-2.5	+7.1	-0.9
Effect on Subsystem Mass at 10 barr [g]	-6.7	-0.7	+-6.2
Effect on Engine Performance	Higher mass flow means Higher Thrust but also different nozzle shape	Higher mass flow means Higher Thrust but also different nozzle shape	None
Requirements Affected	MAV-PRP-014	MAV-PRP-014	MAV-PRP-014
Impact	2	4	2

As seen in the tables above, no design becomes infeasible, the only changes are that the margins are smaller than before but are still large enough to not pose any threats to the requirements.

6.13. AOCS

The AOCS system was made up of 4 parts: the thrust vector control (TVC) system, the reaction control system (RCS) thrusters, the fibre optic gyroscope (FOG), and the star tracker. The masses and powers derived from the design are summarised in Table 6.37.

6.13.1. First Stage

In the context of the the first stage of the MAV, and it's ascent, the disturbances in low Martian atmosphere were found to be minimal, as estimated from literature [27] (primarily due to the fact that that Mars has a weak internal magnetic field, and a considerably low density atmosphere), and thus the use of TVC was sufficient for

the control of the MAV. Thus, RCS thrusters were not used in the first stage. Furthermore, the use of the FOG to determine the attitude of the MAV was dominant over the star sensor at this stage. The TVC system was sized using off-the-shelf electromechanical actuators, designed specifically for this purpose, collected from a provider[42]. As these components were originally designed for Earth launch vehicles with significantly larger thrusts than those of the MAV, all of the options were scaled to match the smaller thrust, whilst still applying a safety factor of 20%. This meant the power, mass, and volume for each option would become smaller. From this, a single actuator type was selected based on a compromise of mass and power. The volume was not as critical of a criteria due to the scale of the actuators already being reduced to an acceptable minimum size. It was decided that only two of these actuators were required to handle the TVC, leading to a total mass and power of $1.05\,\mathrm{kg}$ and $90.18\,\mathrm{W}$ respectively, using the RCS thrusters from the second stage as redundancy.

The selected FOG was also an off-the-shelf component that did not require extensive designing thanks to it being proven technology (and the providers being reliable[43]), but rather a simple selection based on certain parameters. The selected component was the FOG80N[44] which provided the highest accuracy available for that provider, despite weighing $5\,\mathrm{g}$ more than the other options. There was no specific constraining requirement for accuracy, which makes the decision somewhat arbitrary. As two FOGs were used, the total mass and power derived here was $0.09\,\mathrm{kg}$ and $1\,\mathrm{W}$.

6.13.2. Second Stage

For the second stage, TVC is no longer used due to weight considerations. Furthermore, as the MAV will be higher into the atmosphere and already almost into orbit, star sensors could now be used alongside the FOGs, given their ability to give absolute rather than relative pointing knowledge from the FOG [61]. This accuracy is required as the MAV would need to be able to navigate to the required orbital altitude given by the stakeholder requirements more reliably. The star sensor was selected after collecting a range of different star sensors with different designs and characteristics. The lowest mass sensor was the selected choice as mass was crucial for the second stage ascent, further leading to the design choice to use three for redundancy. This led to a total mass and power of $0.126\,\mathrm{kg}$ and $1.8\,\mathrm{W}$ respectively[45].

In place of the TVC system, cold gas RCS thrusters were used. Similarly to before, a range of cold gas thrusters were collected and a specific thruster was chosen. Due to the minimal disturbances and lack of constraining requirements, the trade-off was not as critical: the mass, power and thrust were looked at. To ensure full and more delicate control over the MAV second stage, a total of 12 thrusters were designed for. With regards to the propellant for the RCS thrusters, it was decided to utilise the helium initially used to pressurise the oxygen and carbon monoxide tanks within the lander. This way, as the tanks in the lander are filled with propellant generated from the MOXIE system, instead of venting the displaced helium out into the environment, it can be fed into the tanks for the RCS thrusters. The use of helium as the pressured cold gas was also relatively beneficial in terms of the I_{sp}, with it being measured at $165\,\mathrm{s}$ [62], compared to other potential options. The physical thruster selected was an existing off-the-shelf component that was designed to be compatible with helium gas[46], leading to a total mass and power of $2.88\,\mathrm{kg}$ and $90\,\mathrm{W}$ respectively.

Table 6.37: Summary of Mass, Power, and Number of Components Stemming from the AOCS Design

Property	TVC System	FOG System	Star Sensors	RCS Thrusters	Unit
Mass	1.05	0.09	0.126	2.88	kg
Power	90.18	1.00	1.8	90.0	W
Number used	2	2	3	12	-

6.13.3. Sensitivity Analysis

To analyse the effects of discrepancies in the parameters or characteristics of the AOCS components, a sensitivity analysis was performed. The results are presented in Table 6.38. It can be seen that the main problems arise with the TVC actuators due to their weight and power requirements. Small increases in this may have

[42] https://www.moog.com/products/actuators-servoactuators/space/launch-vehicles/electromechanical-actuators.html
[43] https://www.nidv.eu/en/industry-guide/patria-netherlands-b-v-formerly-nedaero/
[44] https://nedaero.com/wp-content/uploads/2022/07/FOG-Family-130722.pdf
[45] https://www.satcatalog.com/component/st-200-1/
[46] https://www.ibb.ch/products-services/propulsion/cold-gas-thrusters/

snowball effects on the overall MAV design. The other issues may arise with regards to the RCS thrusters increase in propellant mass. Though the mass is not large, it will require the resizing of its propellant tanks which will increase the weight in other ways, and, just like before, may lead to a snowball effect. This is the case not only for the mass, but for the power too, where the battery may need resizing and thus the whole mass begins to increase. To deal with these issues, safety margins were included in the mass and power margins, as well as in the parameters of the components themselves.

Table 6.38: AOCS Sensitivity Analysis

Parameter	TVC Scale [%]	FOG Bias Stability [°/h]	Star sensor accuracy [arcseconds]	RCS Thrusters Propellant [%]
Change in Value	+20	+25	+15	+20
Effect on Subsystem Mass [kg]	+0.21	0	0	+0.174
Effect on Subsystem Power [W]	+18.0	0	0	+6
Effect on System	Higher mass and power	Inaccurate attitude determination	Inaccurate attitude determination	Slightly greater mass and power usage
Requirements Affected	MSR-REQ-S-001	STK-M-002, MSR-REQ-M-002	STK-M-002, MSR-REQ-M-002	MSR-REQ-S-001
Impact	4	2	2	4

6.14. Ascent Profile

The goal of the MAV is to launch the Orbital Sample Container into a circular Martian orbit, with such precision that the ERO can rendezvous with the OSC and capture it. In the Baseline Report [1] the initial ΔV budget for the MAV was estimated to be $5000\,\mathrm{m\,s^{-1}}$. This initial estimate was based on the velocity needed for the $500\,\mathrm{km}$ orbit and gravity loss for a total burn time of $9\,\mathrm{min}$ plus a margin to account for gravity losses, which were not further analysed at that point.

For the Midterm Report [2] this estimation was further refined during the preliminary MAV staging analysis. The ΔV budget was reduced to $4500\,\mathrm{m\,s^{-1}}$, as it became clear the burn time would be shorter, leading to a lower gravity loss.

6.14.1. Staging Strategy

An identical architecture for both stages was assumed, where each stage has the same Isp, structural coefficient ϵ, and mass ratios M_{Oi}/Mfi. These assumptions simplified the analysis by standardising the stage designs and performance metrics. An equal ΔV contribution per stage leads to an optimised payload fraction [63]. Table 6.39 shows the result of preliminary staging analysis, indicating that a single stage to orbit was not feasible unless a higher Isp or more efficient structural coefficient could be achieved. The result will later be used to compare with the final MAV design and simulated ascent profile.

6.14.2. Ascent Simulation

The analysis up until the Midterm Report was limited to ”back of the envelope” estimations on the ΔV budget and required propellant mass and staging division so that the preliminary design could be made. With the preliminary MAV design done, it is time to see if the previously made assumptions hold and if the MAV can deliver the OSC to orbit fulfilling its requirements.

As per requirements **STK-M-001**, **MAV-PRP-005**, and **STK-M-008** the MAV shall deliver the OSC to a $500\,\mathrm{km}$ $\pm 15\,\mathrm{km}$ Martian orbit at a $25°$ inclination. To determine this a simulation was needed that can simulate the MAV ascent in 3D considering the following aspects:

- Simulate the drag loss through the thin Martian atmosphere.
- Lift off from the SRL landing site and execute the in and out of plane manoeuvres in a single profile.
- Simulate the gravity loss throughout from the vertical burn component until horizontal ascent.
- Basic vehicle guidance, sufficient to reach a precise target orbit.
- Support launch vehicles with multiple stages and liquid propulsion.

Multiple different existing simulation toolkits were evaluated, NASA’s General Mission Analysis Tool and the TU Delft Astrodynamics Toolbox. Both these tools fulfil the above requirements, however, both are very complex and feature a steep learning curve. It was deemed these tools were too complex for the needed assessment but could be useful for future steps.

Table 6.39: MAV Staging Comparison - from Midterm Report [2].

Property	1 Stage	2 Stage	3 Stage	Unit
Payload Fraction Γ	-0.02	0.0809	0.0969	-
Payload Ratio λ	-0.02	0.397	0.850	-
M_O/M_f	5.47	2.34	1.76	-
M_{OSC}	10	10	10	kg
$M_{\text{interface}}$	5	5	5	kg
M_{PL}	15	15	15	kg
M_{On}	-696.46	52.74	32.65	kg
M_{Pn}	-569.17	30.19	14.12	kg
$M_{O(n-1)}$		185.46	71.08	kg
$M_{P(n-1)}$		106.17	30.74	kg
$M_{O(n-2)}$			154.73	kg
$M_{P(n-2)}$			66.92	kg
Total Dry Mass	-127.29	49.09	42.95	kg
Total Propellant Mass	-569.17	136.37	111.79	kg
Lift-off Mass	-696.46	185.46	154.73	kg

A low-fidelity launch vehicle simulator based on the work of B. Luke[47] was used. This simulation tool can simulate two stage orbital launch vehicle trajectories in 3D and fulfils most of the above requirements except for simulating at Mars.

Now just any simulation tool from the internet should not be trusted blindly to use a good model and yield accurate results. The following steps were taken to verify to some extent the credibility of this tool. Firstly the tool came with examples of existing launch vehicles like RocketLab's Electron and SpaceX's Falcon 9. For both these example cases, the results are in the same order of magnitude (or closer) as the stated parameters of these rocket's payload user guides. Secondly, the expelled ΔV from the MAV simulation will be compared to the ΔV budget.

The simulation tool was adapted for running ascent simulations from Mars. To calculate the drag losses the Earth atmospheric model was replaced with a model based on the NASA Mars Atmosphere Model[48]. This model is similar to the ISA and features two-atmosphere layers with a non-zero temperature lapse rate. The gravity model parameters were changed with values for Mars [64]. This gravity model takes into account a WGS-84 ellipsoid to reflect the Ellipticity of Mars.

[47] Source code: `https://github.com/BrendanLuke15/Launch-Sim`
[48] Taken from: `https://www.grc.nasa.gov/www/k-12/airplane/atmosmrm.html`

Table 6.40: Ascent Profile Simulation Inputs

Parameter	Value	Unit
Launch Site Location	[18.38, 77.58]	[lat, lon] °
Altitude Target	500	km
Semi-major axis tolerance	5	km
Orbital Inclination	25	°
Constant pitch angle	1.37	°
Staging coast period	80	s
Vertical trajectory height	500	m

Table 6.41: Ascent Profile Vehicle Parameters

Parameter	Value	Unit
Stage 2 propellant	30.2	kg
Stage 2 total mass	63.4	kg
Stage 2 thrust	400	N
Stage 1 propellant	106.2	kg
Stage 1 total mass	140.11	kg
Stage 1 thrust	1400	N
Specific Impulse	270	s

Table 6.40 shows the set orbital parameters and Table 6.41 shows the set MAV parameters. The values for the staging coasting period, constant pitch angle and vertical trajectory height were found by using an initial estimate and tweaking them by running the model multiple times to find the values that had the most optimal effect on the final orbital altitude precision.

The ascent model runs in an iterative integration loop of the position and velocity vector of the MAV, shown in Figure 6.25. The model will run through the following steps as indicated by the numbers on the plot:

1. Launch of the MAV from the SRL landing location in the vertical direction. After an initial vertical trajectory of $500\,\mathrm{m}$ a constant pitch angle manoeuvre will kick in.
2. The pitch program will continue until stage one runs out of propellant. After stage burnout, stage one will be jettisoned.
3. After staging, the second stage will coast for a set amount of time before second stage ignition.
4. The second stage will start with a prograde burn program to bring the apoapsis node to the target orbital altitude.
5. The second stage will switch to a horizontal burn program once the apoapsis node is close to the target orbital altitude to start circularising the orbit.
6. The second stage will then coast to apoapsis and execute a short horizontal burn to finish circularising the orbit.

6.14.3. Simulation Results

Figure 6.25 shows the output of the simulation. The vertical lines indicate the following important events following the shown numbering:

1. MECO; First stage separation (T+ $201\,\mathrm{s}$).
2. End of coast; Second stage ignition 1 (T+ $281\,\mathrm{s}$).
3. SECO-1; Apoapsis node on target (T+ $454\,\mathrm{s}$).
4. Second stage ignition 2; Circularisation burn (T+ $1894\,\mathrm{s}$).
5. SECO-2; Reached Low Mars Orbit (T+ $1913\,\mathrm{s}$).

With the given simulation inputs the MAV reaches a $502\,\mathrm{km}$ x $493\,\mathrm{km}$ x $25.3°$ low Mars orbit, this is within the allowed semi-major axis margin. The total burn time over the ascent comes down to $6.6\,\mathrm{min}$, this is in accordance with the initial estimation of having less than $9.0\,\mathrm{min}$ total burn time. The total expelled ΔV is $5378\,\mathrm{m\,s^{-1}}$, this is about $100\,\mathrm{m\,s^{-1}}$ less than the total ΔV budget of the MAV shown in subsection 7.1.3. This means the MAV has enough propellant to deliver the OSC into the pick-up orbit, in fact the second stage has $1\,\mathrm{kg}$ of propellant left at the end of ascent.

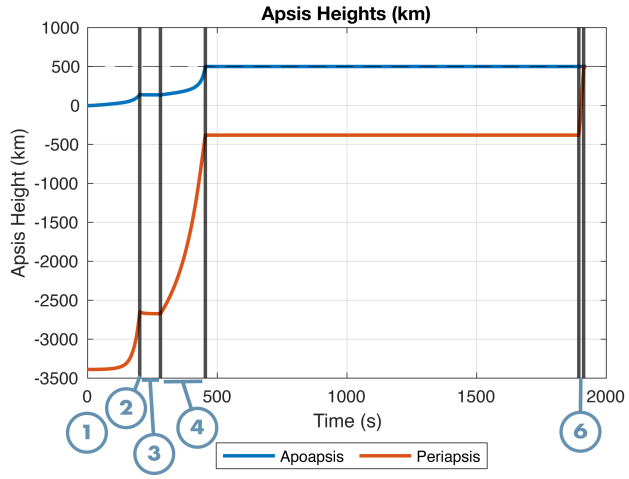

(a) Ascent Apsis Progression

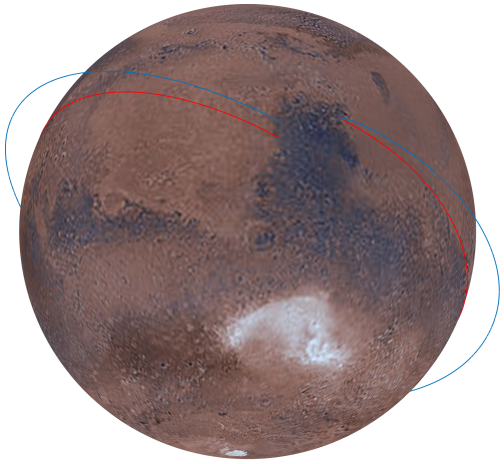

(b) 3D Ascent Profile Visualisation

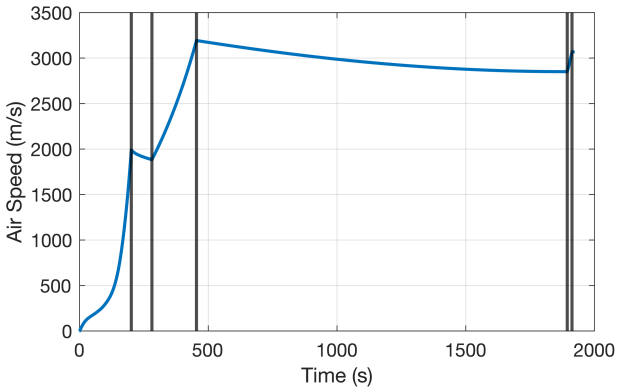

(c) Ascent Velocity Progression

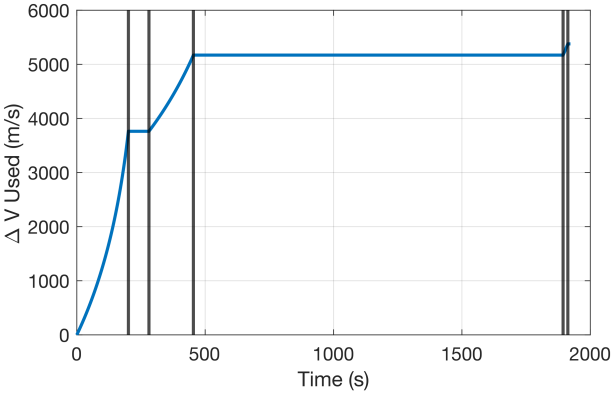

(d) Ascent Expelled ΔV Progression

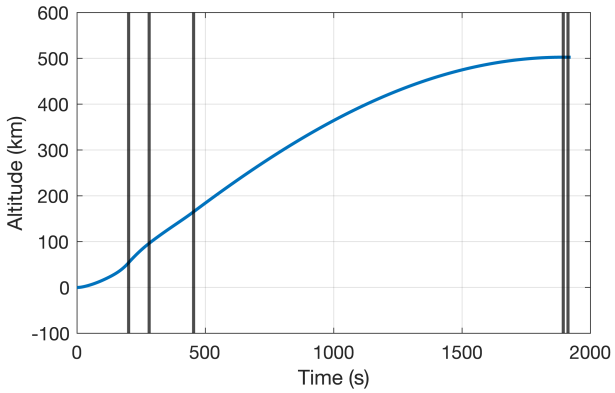

(e) Orbit Altitude Progression

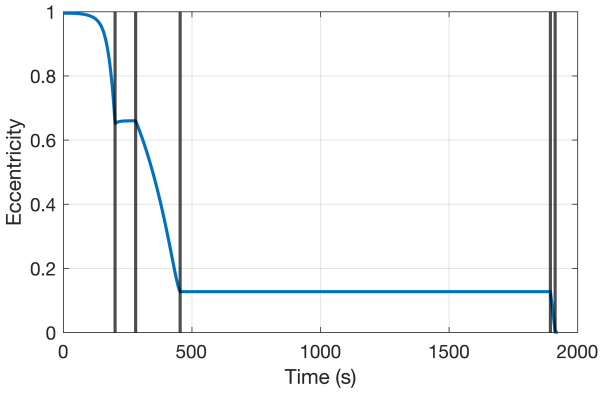

(f) Orbit Eccentricity Progression

Figure 6.25: Ascent Profile Simulation Output

6.14.4. Sensitivity Analysis

To analyse the effects of changes in propulsion performance and control precision of the first stage TVC on the final orbit dimensions, a sensitivity analysis was performed. The results are presented in Table 6.42. It can be seen that small deviations to the propulsion performance have a large impact on the final orbit. In this situation a $-20\,\mathrm{N}$ thrust deficiency would be over the average of the burn for both stages. It should be noted that for smaller changes in Isp or thrust it could still be possible to reach the orbit if the AOCS system compensates adequately be changing the TVC pitch. The AOCS needs to be able to maintain an average TVC pitch range of about $0.15°$ to ensure reaching the pick-up orbit with a semi-major axis range of $30\,\mathrm{km}$.

Table 6.42: Ascent Profile Sensitivity Analysis

Parameter	Isp [s]	Thrust [N]	TVC Pitch [°]	TVC Pitch [°]
Change in Value	-10	-20	+0.1	-0.1
Effect on orbit [km]	502 x 400	1433 x 71	894 x 92	520 x 473
Effect on expelled ΔV [$\mathrm{m\,s^{-1}}$]	-2	+99	+98	-18
Effect on leftover propellant [kg]	-1[49]	-1[49]	-1[49]	0
Effect on System	Trajectory, AOCS	Unstable orbit	Unstable orbit	Trajectory, AOCS
Requirements Affected	MAV-PRP-005, MAV-AVI-013			
Impact	4	5	5	4

6.15. Astrodynamics

In this section, the astrodynamics of the pick-up orbit are outlined and discussed. Furthermore, the sustainability approach is discussed.

6.15.1. Pick up orbit parameters

The final phase of the mission discussed in this report is the orbital insertion of the sample container. As specified in the user requirements, the orbit shall be a $500\,\mathrm{km}$ circular orbit with perturbances limited to $\pm 15\,\mathrm{km}$. In order to accurately analyse the orbit NASA's General Mission Analysis Tool (GMAT)[50] was used. GMAT allows the user to specify perturbing bodies in the orbit and to visualise the effects of changing conditions. Using GMAT is a tedious business, and even setting up a simple orbit can take a long time, as all coordinate frames have to be defined individually. However, once the setup is done a lot of interesting elements can be included. for this analysis, the Sun and Jupiter have been used as perturbing bodies, alongside an exponential atmospheric model. The inputs are shown in table 6.43 and the results are presented in figure 6.26

Table 6.43: Orbital Elements of the Final Orbit

Property	Value	Unit
Altitude	500	km
Eccentricity	0	-
Inclination	25	°
Right Ascension of Ascending Node	20	°

The Right Ascension of Ascending Node (RAAN) was chosen to minimize the fluctuations in orbit.
Figure 6.26 shows plots of the target orbit over a period of 10 days. Over this period of time, the lowest point in orbit will be at $488\,\mathrm{km}$ and the highest point will be $512\,\mathrm{km}$, which is shown in figure 6.26a. The same sub-figure shows no discernible orbital decay over the 10-day time period displayed. Figure 6.26b shows the change in inclination over the same 10-day time period. Over this time period a minimum inclination of $18.7\,°$ is reached, after which the inclination increases. In figures 6.26c and 6.26d the orbit around Mars and the ground track are displayed.

6.15.2. Sustainability

It is important to ensure that Martian discovery can continue in the future. The 7 minutes of terror is a well known phenomena to every space engineer. Large amounts of space debris could worsen the risk involved in landing on Mars. If the debris around Mars increases indefinitely, the planet is at risk of developing Kessler Syndrome. To avoid the scenarios described above, BAGEL is committed to keeping the Martian orbits pristine. Once the MAV has delivered its payload to the pick up orbit, it will deorbit and break upon landing. The crash site of both

[49] MAV runs out of propellant
[50] https://software.nasa.gov/software/GSC-18094-1

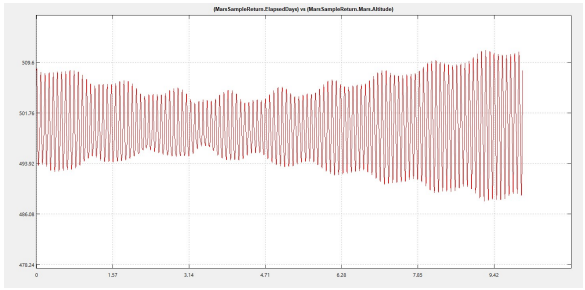

(a) Altitude

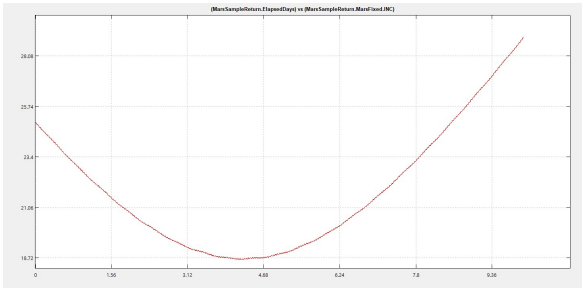

(b) Inclination

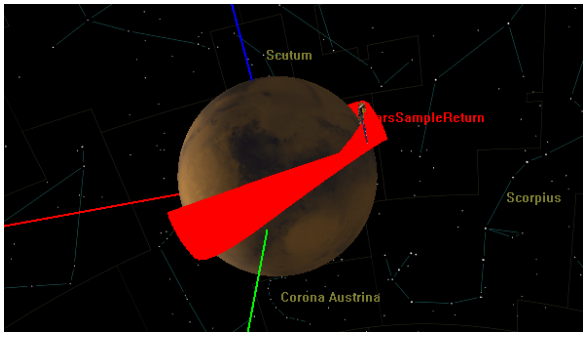

(c) Orbit

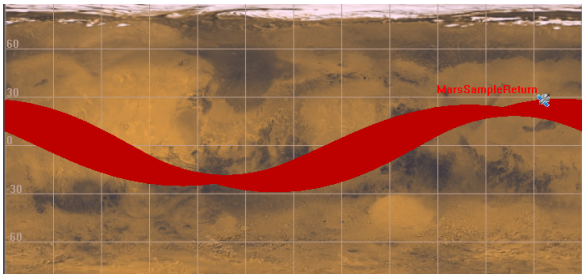

(d) Groundtrack

Figure 6.26: Sample Container Retrieval Orbit

stages will be tracked, marked and noted for future reference. Future missions then have the opportunity to pick up the debris for further analysis.

7 Budgets

This chapter presents a revised version of both engineering and mission budgets, building upon the initial estimates presented in the Baseline Report [1], and subsystem designs shown in chapter 6. The power, mass, $\triangle V$, and volume budgets are shown in section 7.1 and the costs associated with the mission as well as the estimated timeline are discussed in section 7.2.

7.1. Engineering Budgets

When designing each subsystem, a contingency margin was included in the sizing process, as discussed in chapter 6. As such, the final values presented in the tables throughout this section already include some flexibility allowance. To avoid inflating the figures unnecessarily, no additional contingency margin is added in these budgets.

7.1.1. Power

The power budget shown in Table 7.1 details the needs of individual subsystems aboard the lander. These values were used to size the power generation and distribution system discussed in section 6.10. It's important to note that these values do not all represent constant power usage, and not all subsystems will operate simultaneously. As such, the power generation system is not sized based on the total shown. Similarly, the power requirements needed by the MAV shown in Table 7.2 are not considered significant for sizing the power generation system, as the MAV can be charged after the propellant production and loading is complete.

Table 7.1: SRL Power Budget Breakdown

Subsystem	**Power [W]**	**Comment**
Communications	40	*Daily Average*
SOXIE	95	
Intake Compressor	59	
Cryo-Cooler	75	
Cryo-Compressor	75	
Valves	100	*Only very briefly utilised*
Pumps	90	*Only very briefly utilised*
Data Processing Unit	15	
Thermal System	76	
Dust Removal System	5	
Scientific Instruments	20	
Structures & Mechanisms	5	
Total	**655**	*465 Nominal*

Table 7.2: MAV Power Budget Breakdown

Subsystem	Power [W]	Comment
Stage 1 TVC	75	
Stage 1 Feed System	10250	*Maximum Power, Only Briefly Used*
AOCS	10	
Communications	11	
Data Processing System	10	
Total	**106**	*Excluding Feed System*

7.1.2. Mass

The mass breakdowns shown in Table 7.3 and Table 7.4 show the masses of each subsystem. Any space mission must pay close attention to the mass of all components because every extra kilogram of payload requires much more propellant in order to launch it from earth. It's good to note that the mass of the propellant generation and processing systems are less than the mass of the MAV propellant, which vindicates the use of ISRU processes.

Requirement **STK-I-001** dictated that the maximum mass deliverable to Mars is $2400\,\mathrm{kg}$, of which $200\,\mathrm{kg}$ is reserved for the Sample Fetch Rover and $300\,\mathrm{kg}$ is reserved for the EDL system. The total mass of the SRL, and the dry mass of the MAV come to a total of $563\,\mathrm{kg}$, and an overall landed mass of $1063\,\mathrm{kg}$ which is $\approx 1300\,\mathrm{kg}$ less than required. This is clearly a lot less than expected, which can be attributed to the very preliminary analysis that has been performed

Table 7.3: SRL Mass Budget Breakdown

Subsystem	Mass [kg]
Communications	22.5
SOXIE	17.7
Intake Compressor	0.2
Cryo-Cooler	1.3
Cryo-Compressor	0.7
LOX Tank	2.3
LCO Tank	6.4
Helium Pressurant	0.87
Valves	3.62
Pipes	20.8
Pumps	3.9
Data Processing Unit	2.0
Thermal System	104.0
Solar Panels	42.2
Batteries	24.3
Dust Removal System	1.7
Cabling	21.5
Scientific Instruments	20.0
Structures & Mechanisms	200.0
Total	**495.9**

Table 7.4: MAV Mass Budget Breakdown

Subsystem	Mass [kg]
Propellant stage 1	106.2
Engine 1st Stage	12.1
Feed System	1.8
Batteries	2.1
TVC	3.4
Structures	10.0
Mechanisms	2.3
Prop Tanks	2.1
Cables	0.1
Subtotal Stage 1	*140.1*
Payload	10.0
Propellant stage 2	30.2
Engine 2nd stage	10.4
Feed System	0.9
AOCS	0.4
Batteries	0.3
Telecom	0.7
Structures	7.0
Prop Tanks	1.2
Harness	1.5
Data Processing Unit	0.5
Cables	0.4
Subtotal Stage 2	*63.4*
Total	**203.5**

7.1.3. ΔV

A ΔV budget is derived from Table 7.4 using the Tsiolkovsky rocket Equation 7.1. The result of this analysis show that stage 1 produces $3755\,\mathrm{m\,s^{-1}}$ of ΔV and stage 2 produces $1714\,\mathrm{m\,s^{-1}}$ for a total of $5470\,\mathrm{m\,s^{-1}}$. This aligns with the ascent analysis performed in section 6.14.

$$\Delta V = I_{sp} g_0 \ln \frac{M_1}{M_2} \tag{7.1}$$

7.1.4. Volume

It's important that all subsystems can fit inside the aeroshell as dictated by requirement **STK-I-001**, meaning a total allowable volume of $13\,\mathrm{m^3}$. The upper estimates for the subsystems are shown in Table 7.5 and Table 7.6. Note that these volume budgets can be further refined down during the integration phase as different components can likely fit together more efficiently.

Table 7.5: SRL Volume Budget Breakdown

Subsystem	Volume [dm^3]
Communications	29.4
SOXE & Compressor	16.7
Cryo-Cooler	0.3
Cryo-Compressor	0.1
LOX Tank	64.0
LCO Tank	197.0
Valves	1.5
Pipes	33.1
Pumps	0.2
Data Processing Unit	4.8
Thermal System	1500.0
Solar Panels	447.1
Batteries	13.3
Dust Removal System	3.2
Cabling	5.9
Scientific Instruments	48.0
Structures & Mechanisms	9576.0
Total	**11938.8**

Table 7.6: MAV Volume Budget Breakdown

Subsystem	Volume [dm^3]
Propellant stage 1	131.3
Propulsion 1st Stage	146.8
Batteries	6.3
TVC	0.5
Structures	108.7
Mechanisms	10
Prop Tanks	13.1
Subtotal Stage 1	*416.7*
Payload	2.1
Propellant stage 2	55.8
Propulsion 2nd stage	66.8
AOCS	1.1
Batteries	1.0
Communications	2.0
Structures	53.1
Prop Tanks	5.6
Harness	1.0
Data Processing Unit	0.2
Subtotal Stage 2	*188.8*
Total	**605.5**

7.2. Mission Budgets

7.2.1. Development Schedule

The project schedule is based on previous and mission analyses and project setup experience. Figure 7.1 shows the high level project timeline; is worked out in more detail for the near future and gets less detailed further in the future. In figure 7.1 uses the ESA definitions for the phases.

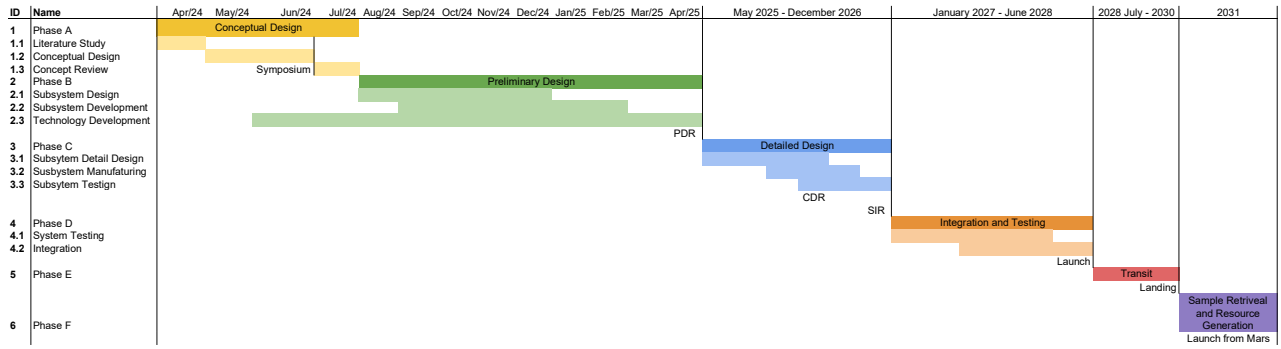

Figure 7.1: Development Schedule

The concept generation part of Phase A comes to an end with the DSE symposium; after this a 1 month review period was planned in where the customer can review the concept and evaluate it. August marks the beginning

of Phase B, where the detail design and development of the subsystems takes place along side with technology development. In the scope of this report, technology development covers the engine development and testing along side with researching CO separation technologies for the ISRU.

In May of 2025 Phase C, the detail design is projected to start, this phase will last 19 months and cover the detail design of all parts, and manufacturing and testing of the subsystems.

Finally Phase D, the system testing and integration will start in January of 2027 and ends in June 2028. In reality the Mars Launch window opens in 2028 December and ends in 2029 January. This gives a 6 month contingency period, which will surely be utilised to it's fullest.

Phase E covers the Transit including the Mars EDL and ends once the lander is operational. Finally in Phase F the lander will produce the necessary resources, the fetch rover will collect the samples, load them and the MAV will ascend into the pick up orbit. This phase ends when the Earth Return Orbiter departs for Earth.

This timeline was based on the assumption that the project will be approached with a Skunk Works like mentality. The design team now realises that this will not be the case, adn lengthy contract negotiations will delay the timeline.

7.2.2. Cost Budget

The pre-existing MSR mission itself has had many budget revisions, leading to an ever-ballooning cost estimate [65]. Furthermore, it is very difficult to derive a cost estimate without first-hand industry experience. Thus, the estimated costs presented in this section are merely presented as an initial estimate of costs and only apply to the mission segment explored in this report. For all cost estimates in this section, inflation is taken into account and final values are presented for the financial year 2024.

Subsystem Development

The costs of each subsystem are derived from multiple places. Most costs are calculated from the engineering budgets shown previously, and the corresponding relations documented in the SMAD [27]. A 2015 paper detailing a design framework for rocket engines was used to estimate the cost of the propulsion system [66].

The cost of the SOXE is assumed to be the same as that of the MOXIE experiment, this is deemed to be a valid estimate as the vast majority of this $50 Million price-tag was devoted to research and development [67] that can be leveraged for development of the SOXE. Since both experiments utilise similar solid oxide electrolysis technology, only minor modifications are needed for the SOXE, significantly reducing additional R&D expenses. The proven success of MOXIE means that SOXE can benefit from reduced learning curve effects and streamlined regulatory processes, collectively minimising costs associated with development, validation, and testing.

Table 7.7: SRL Cost Budget Breakdown

Subsystem	Cost [$M]	Comment
Communications	60	
SOXE	50	*Same as MOXIE*
Cryo-Cooler	7	
Cryo-Compressor	7	
LOX Tank	1	
LCO Tank	1	
Valves	1	
Pipes	2	
Pumps	1	
Data Processing Unit	9	
Thermal System	89	
Solar Panels	13	
Batteries	10	
Dust Removal System	6	
Cabling	9	
Scientific Instruments	15	
Structures & Mechanisms	30	
Total	**316**	

Table 7.8: MAV Cost Budget Breakdown

Subsystem	Cost [$M]
Propulsion 1st Stage	24
Structures	2
Mechanisms	1
Prop Tanks	1
Cables	2
Subtotal Stage 1	*30*
Payload	5
Propulsion 2nd stage	12
AOCS	3
Batteries	2
Communications	8
Structures	1
Prop Tanks	1
Harness	1
Data Processing Unit	3
Cables	2
Subtotal Stage 2	*38*
Total	**68**

Mission Integration Costs

The expenses associated with a complex space mission are not limited to the costs of developing each individual component. There are additional costs associated when it comes to integration and management of the entire engineering process. Estimates for these costs are shown in Table 7.9. A summary of all costs for this segment of the MSR mission, including a 50% contingency margin is presented in Table 7.10.

Table 7.9: Additional Cost Breakdown

Engineering Element	Cost [$M]
System Engineering	77
Project Management	58
System Integration & Testing	58
Product Assurance	12
Configuration Management	77
Contractor Fees	46
Data Management	8
Development Support Facility	15
Hardware/Software Integration	62
Integrated Logistics	23
Safety & Mission Assurance	27
Total	**462**

Table 7.10: Mission Segment Cost Summary FY2024

Engineering Element	Cost [M]
Subsystem Development	$384
Additional Costs	$462
Contingency (50%)	$423
Total	$1,269
	≈ €1,185

8

Final Design

The 'Final Design' chapter starts with presenting a more detailed definite configuration chosen for SRL and MAV in section 8.1. In section 8.2 it then goes into more detail about the interior of the ascent vehicle, specifically the propulsion system design. It concludes with a comparison of the chosen final design, to other designs of the MSR mission, namely the one from NASA in section 8.3.

8.1. Layout & Configuration

This section will highlight the main layout of components within the Lander and the MAV, presenting how each subsystem physically interfaces with another internal, external, or separate system. The lander layout and configuration are described first, followed by the MAV.

8.1.1. Lander

The lander design had comparatively more freedom than the MAV design when it came to the layout of components, and placement of subsystems. Given the scope of this project, a detailed design of the lander being able to survive various launch and landing loads was not looked into, though still considered to some extent. Thus, the design was mostly qualitative, inspired by the previous Mars InSight mission[1], with the underlying support structure being similar to a moon lander [68], and other literature [69].

The main components that made up the lander are listed below. Each component is also numbered and seen in Figure 8.1, excluding the thermal system. CAD renderings of the lander are seen in Figure 8.2a and Figure 8.2b.

1. **Support Structure:** The lander was required to have a support, load-bearing structure to which different subsystems would be connected. This consisted of a main aluminium honeycomb structure bonded with a truss structure.
2. **MAV Container:** By definition, the MAV would have to be stored on the Lander for almost the entirety of the mission. Thus, due to its size, the protective container of the MAV was a major factor affecting the layout of the lander.
3. **Sample Hatch:** Along with, and perhaps built into, the MAV container, a hatch door needed to be present. This hatch would serve as the entrance point for the collected samples to be placed inside the MAV.
4. **Launch Tower:** Also directly related to the MAV container, the rotating launch tower lifting the MAV was designed for. This tower would necessarily have a strengthened base where the tower hinges to deal with the loads.
5. **Propellant Tanks:** Crucial to the mission, the propellant tanks which would initially store the LOX and LCO produced from the SOXE, before being transferred to the MAV, occupied a certain volume on the lander. The fact that they would need to be kept cryogenic meant that their location in the lander was significant from the perspective of thermal management.
6. **SOXE:** The SOXE itself would be located on the lander. Due to its operating temperature, its location was important in terms of its effect on the cryogenic components within the lander. Though simultaneously, as the SOXE was tasked to produce propellants, it would benefit from being located near the tanks.

[1] https://www.jpl.nasa.gov/news/press_kits/insight/launch/mission/spacecraft/

7. **Battery:** Storing power was designed to be done with a battery. As there was no specific need to have more than one battery (with smaller volumes) spread out through the lander, only a single larger battery pack was used. Power generated from the solar panels would be stored here.
8. **Solar Panels:** To generate power in situ, as with many other space missions, solar panels are used. In this case, four solar panels were used, each being able to fold away such that the lander can fit in the Mars entry capsule.
9. **Communication Devices:** To communicate back to Earth or with other vehicles (such as orbiters or future landers), communication devices are used. Four different kinds were used: a UHF Transceiver; a high gain antenna; a low gain antenna; and an IEEE 802.15.4 ”Zigbee” (though ”Zigbee” is not seen in Figure 8.1).
10. **Landing Legs:** The lander will not be moving throughout the mission, and thus was designed to have stiff landing legs to support the structure on the ground. The detailed design of these was not within the scope of the mission, and thus was mostly inspired by the InSight lander. The lander was designed to have four separate landing legs, each being foldable to fit in the entry capsule.
11. **Landing Thrusters:** Unlike some other Mars missions, the lander would have to land using its own thrusters, without a sky crane. Therefore, the lander had to fit thrusters along with additional propellant tanks that came with them.
12. **Thermal System:** To manage the temperature throughout the lander, a thermal system was included. It encompassed two main parts, being heat pumps and MLI.

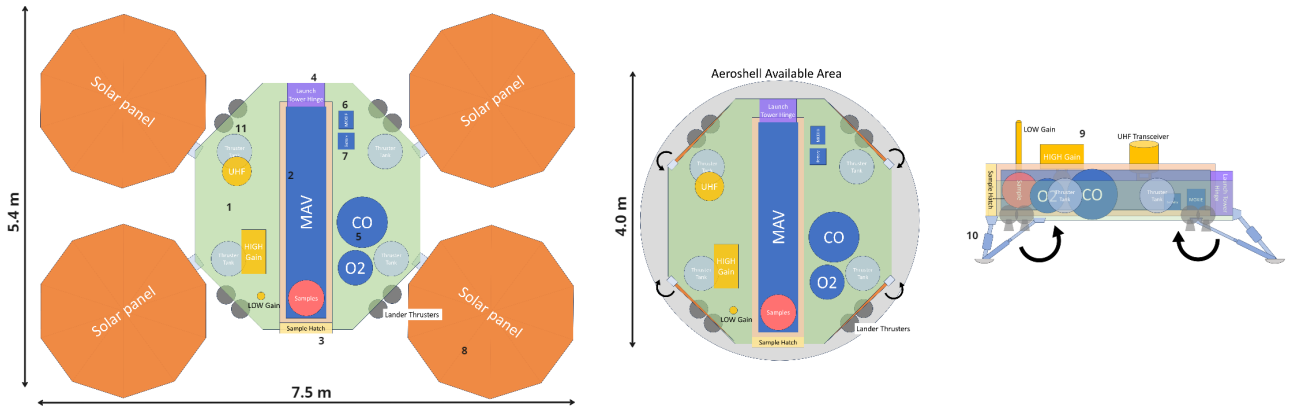

Figure 8.1: Conceptual Lander Layout Diagram. Top View Deployed Lander (Left), Top View Lander in Capsule (Centre), Side View Deployed Lander (Right)

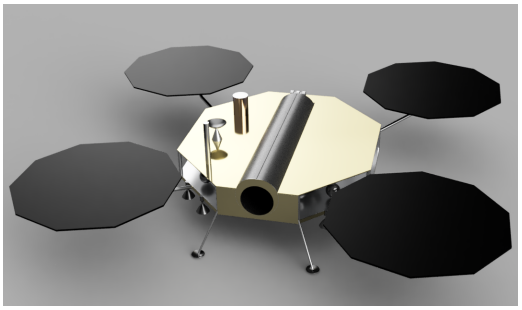

(a) Lander in Production and Loading Phase

(b) Lander in Launch Configuration

Figure 8.2: Lander Configurations

Not included in Figure 8.1 are all the cables and pipes connecting each subsystem together, as well as the MLI which covers almost the entirety of the lander. Furthermore, delving into the details for some of the components, the solar panels were designed in a decagon, capable of folding in a fan like manner into a triangular shape. Moreover, the folded solar panel would be capable of then rotating at its base to hug the lander, such that it would be able to fit in the lander capsule. The MAV container was the main constraining factor when it came to

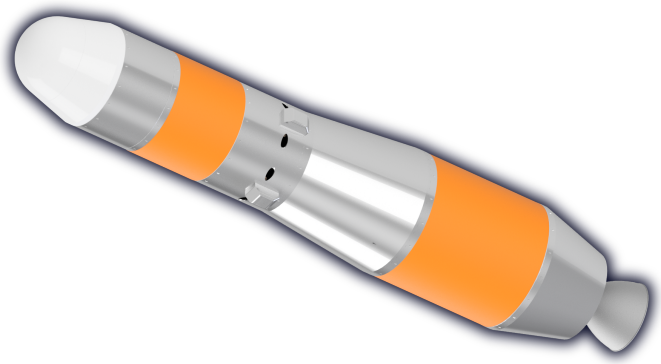

Figure 8.3: Full MAV Render

sizing the overall dimensions of the underlying structure. Its relative size and location on the lander - located centrally for the centre of mass - would mean that the container had to be designed to be load-bearing as well. Finally, with regards to the landing legs, they would be stowed beneath the lander during its journey in the entry capsule, and deployed during landing. The legs themselves each consisted of three single struts, either damped with a spring or a fluid damper and merged into a crushable honeycomb structure to absorb the impact of landing.

8.1.2. MAV

The MAV's main mission is ascending from the Martian surface. It consists of two stages, with each its separate feed system. To stay within the scope of the project and with the limited time, the main research was done into the propulsion and tank designs, AOCS and payload. Other systems, like telecommunication and control, were just estimated using high-level estimations. A full render of the MAV with the stages and OS housing deployed is shown in Figure 8.3.

The main components are listed below, split up between the first and second stage. These components are also numbered and visible on figure 8.4.

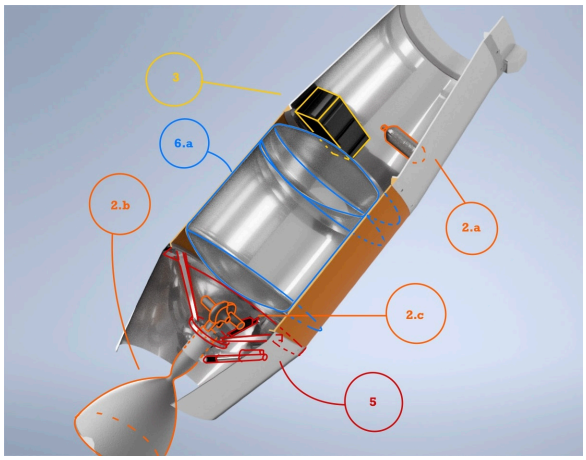

(a) MAV First Stage Breakdown

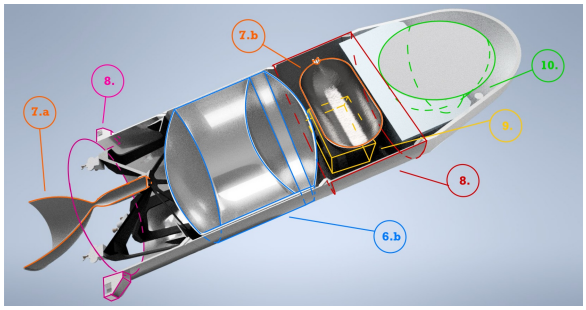

(b) MAV Second Stage Breakdown

Figure 8.4: MAV Breakdown

1. **Support Structure:** To withstand the launch loads of Earth and Martian ascent and survive EDL, a supporting, load-bearing structure is used to connect all subsystems.

2. **First Stage Propulsion System:** To propel the first stage, an engine with an electrical pump feed system is used to pressurise the propellants. The top bottle is the helium pressurant tank to keep the propellant tanks under pressure. Propulsion elements are denoted as 2 in Figure 8.4a, with $2.a$ being the pressurant tank, $2.b$ the engine chamber and bell, and $2.c$ the turbopumps.
3. **First Stage EPS:** Because the power requirement of the feed system is quite high, batteries are also present on the first stage, which is dead weight after the first stage is empty. This element is denoted by 3 in Figure 8.4a.
4. **Staging Ring:** Since the system consists of 2 stages, a staging ring is present to kick the first stage away from the second stage when the stage is empty. This is shown by element 8 in Figure 8.4b
5. **TVC:** Thrust Vector control is used to keep the MAV on its trajectory and pointed the same way. The system includes the actuators, gimballing mechanism and thrust structure. This element is denoted by 5 in Figure 8.4a.
6. **Propellant Tanks:** To keep the propellants pressurised and at temperature, propellant tanks are used to withstand the pressure loads as well as help as a load-bearing structure for the MAV. They use a common bulkhead to save weight. For both stages, the LOX tank is above the LCO tank. The first stage tank system is denoted by $6.a$ in Figure 8.4a, and the second stage is denoted by $6.b$ in Figure 8.4b.
7. **Second Stage Propulsion System:** For the second stage, a smaller engine is used together with a pressure-fed feed system to provide the required thrust, with the top tank being the pressurant tank. As seen in Figure 8.4b, $7.a$ denotes the second stage engine, and $7.b$ denotes the helium pressurant tank.
8. **Avionics Bay:** In this part of the MAV, all the AOCS sensors and TT&C are placed together in a central space. This bay also houses the pressurant tank, and is denoted by $8.$ in Figure 8.4b.
9. **Second Stage EPS:** Batteries to power the avionics bay, TT&C and propulsion systems are present here. The batteries are in the container highlighted by $9.$ in Figure 8.4b.
10. **Payload:** On top, the payload containing the samples are placed inside the fairing. These are eventually released to the ERO when in orbit. The Orbital Sample container can be seen in Figure 8.4b as 10.

8.2. Propulsion System

The description of the propulsion system can be split up into the first stage and the second stage. The main reason being that the first stage uses an electrical pump-fed feed system while the second stage uses a simple pressure-fed feed system. For each stage a piping and instrumentation diagram (P&ID) was created. Next to this, mass estimations, power budgets and a cost estimation was performed for the entire system. The P&ID for the entire system is presented in Figure 8.5.

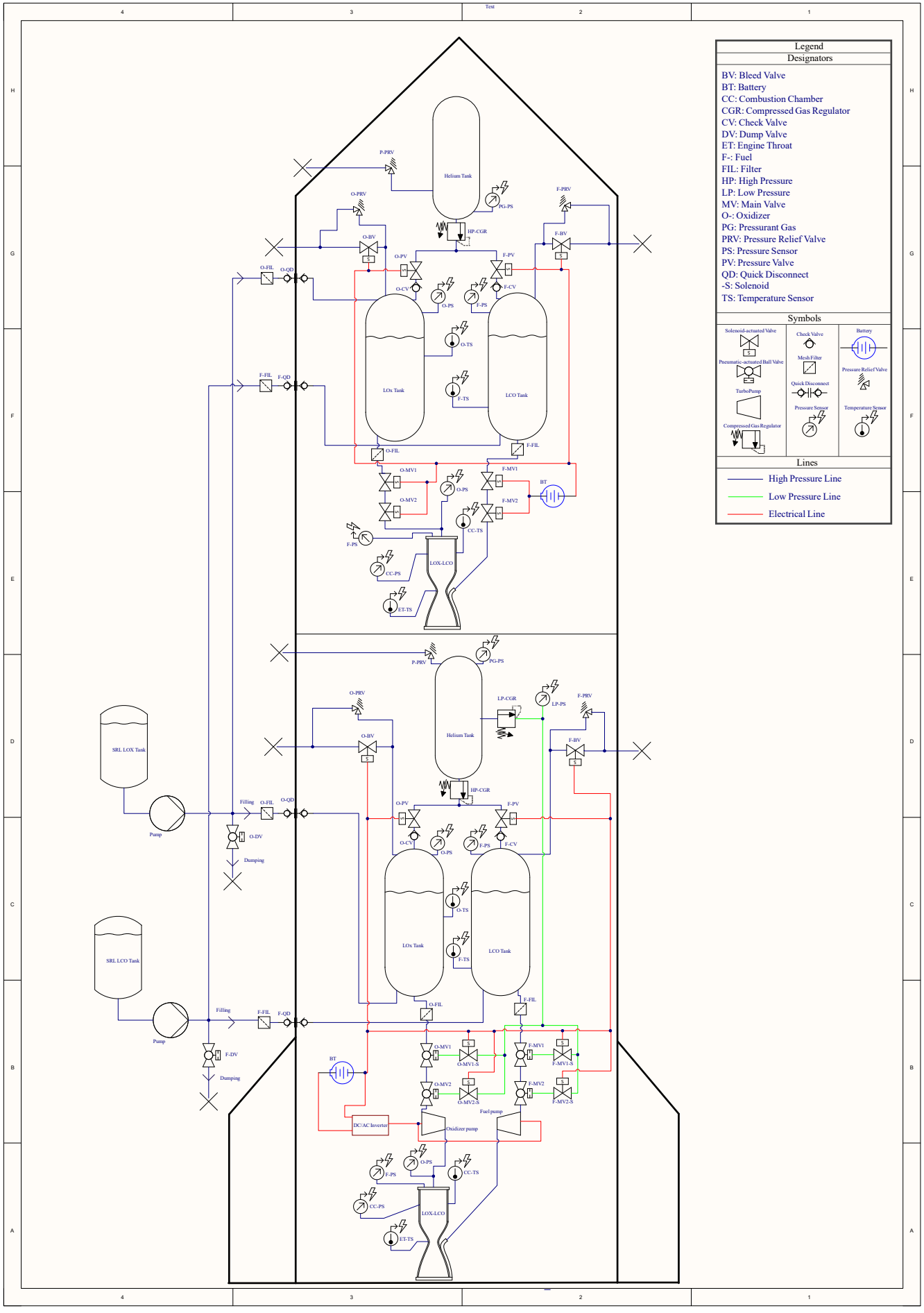

Figure 8.5: P&ID of the MAV Feed System

The schematic can be split up into two parts, being the first and second stage.

8.2.1. First Stage

Propellant Loading
The MAV Tanks are connected to the SRL via quick disconnects where the propellants are pumped into them. In between are filters to limit the amount of unwanted particles to get into the tanks.

Feed System
From the tanks, another filter is present to prevent impurities to enter the feed system. After the filters, two pneumatic valves are present. These are in series to prevent leaks to pass through, as well as redundancy in the system for if a valve would open in any way. These are powered by low pressure controlled by solenoid valves. After the main valves, the propellants are brought up to pressure by the pumps where they enter the combustion chamber. To keep the pressure in the propellant tanks the same, a $200\,\mathrm{bar}$ helium tank with a gas regulator is used.

Relieve System
Next to the feed system, a relief system is also required for the MAV. For all tanks, pressure relieve and bleed valves are present to bleed off any gasses that would occur during propellant loading or launch conditions. Check valves are used to prevent any propellants to flow into the pressure valves at the helium tanks. All these are actuated when the pressures reach a maximum measured by the multiple sensors present in the system.

Pressure overview
The pressure in the system starts with the helium tank, kept at a pressure of $200\,\mathrm{bar}$ which is regulated in the piping to $7.5\,\mathrm{bar}$, keeping the pressure in the propellant tanks. This pressure is then increased to $31.5\,\mathrm{bar}$ using the electronic pumps while accounting for pressure losses in the main valves. After this, the pressure drops by an estimated 20% to $25\,\mathrm{bar}$, where the combustion chamber operates nominally.

8.2.2. Second Stage

For the Second stage, the propellant loading and relieve systems are the same as the first stage. The feed system consists of the pressure tank, at $200\,\mathrm{bar}$, keeping the propellant tanks, which operate at $27\,\mathrm{bar}$, at their operating pressure. From this, the fuel flows directly through the main valves into the engine at the required pressure for the injectors to achieve nominal chamber pressure at $15\,\mathrm{bar}$.

8.2.3. Regenerative Cooling

For part of the engine design, it is important to assess the feasibility of regenerative cooling and whether this is a viable way to keep the engine within reasonable temperatures. To do this, it was decided to create a simulation in python. Regenerative cooling is a very complex process, and extremely accurate modelling of these phenomena is beyond the scope of the project. That being said, it was desired to at least model it to a degree which allows for assessment of its feasibility, even if the output values are not entirely accurate.

8.3. Comparison With Baseline MSR

After completing the design, it is time to compare it to the mission proposed by NASA, with the information known so far. It is a crucial step to convince the reader that the mission designed and recommended by the BAGEL team is competitive, after having convinced it is feasible.

8.3.1. System Mass

The overall design masses are presented in Table 8.1. A more detailed comparison would be impossible, given the insufficiency of information provided by NASA on these systems.
When praising the obvious lower mass of BAGEL's team MAV, in the same breath one should focus the reader's attention on the fact that it is the *landed* mass. A grand difference with the baseline is that in the mission proposed by this paper, the propellants are produced on Mars, which drastically reduces the mass that has to be taken on the MAV on the way to the Red Planet.

This fact goes even further - a lower Earth-lunch mass means that for the same launch loads, the vehicle struc-

[1] Private communication, slides from the IoA/ TNO/ Absolut ESA Collaboration, received 14/06/2024
[2] Private communication with M. Olde from TNO, 02/05/2024

Table 8.1: High-Level Mission Mass Breakdown

System	Baseline MSR mission mass [kg]	BAGEL mission mass [kg]	IoA 2 stage solid MAV mass[1] [kg]
SRL	1900[2]	795.9*	-
MAV (as landed)	400-500 [70]	67.1	197
Total	**2300-2400**	**863**	-

ture would be allowed to be lighter. To be blunt and open, one needs to point at the limitation of the study, which focused on Mars operations and only glossed over the other parts of the whole mission.

Equally important is referring to the elemental character of the study in the early development, which may have omitted some more detailed parts of the MAV. A potential more technical reason for the mass may be in part due to the solids requiring heavier insulation, adding to the baseline's mass. It is unknown how much of its mass is taken by them. Set side by side with another study performed by IoA in Poland, with a comparative 2-stage solids design, NASA's design numbers show a sign of over-engineering.

Looking at the **lander**, the mass change is obvious and drastic, which may raise some eyebrows. To not deny our design capabilities, and at the same not to defame NASA and its scientists' work, one must put the blame on the very early design stage of the SRL.

As such this case might be seen, after taking into account the little official information on SRL's design - mass and structure breakdowns are to be found nowhere, hence the comparison must operate within the mist of ignorance.

A cause might also be the rudimentary nature of the study. *The value given in Table 8.1 takes into account the mass of the tanks needed for the EDL part of the MSR mission, however, a detailed landing structure was not designed as it was outside the scope of this report. It is hard to estimate this fact's significance, given yet again the scarcity of NASA's information.

The advantages of lower overall mass that has to be sent to Mars to perform the same mission are of plenty. Every kilogram saved at this stage of analysis comes back as a contributor to the margin for the future phases; comes back, in an iterative process, in the form of a reduced load on every system in the MSR mission architecture; and it comes back as potential millions of euros saved, that could be used on other missions.

8.3.2. System Size

After visiting mass, a look at dimensions shall be made, with the high-level systems' information specified in Table 8.2.

Table 8.2: High-Level Systems Size

System		BAGEL	NASA
Lander	Dimensions	$3.85\,\mathrm{m}$ x $3.53\,\mathrm{m}$ x $0.57\,\mathrm{m}$	-
	Volume	7.7	13.6[11]
MAV	Dimensions	$3.3\,\mathrm{m}$ x $0.57\,\mathrm{m}$	$3\,\mathrm{m}$ x $0.57\,\mathrm{m}$ [70]
	Volume	0.842	0.766

As can be concluded by comparing two numbers, the proposed MAV is longer. The unknown interference length between the stages can explain the extra in the dimension. A 'bonus' was added to the used dimensions as a conservative approach, in view of not finding any rationale for the dimensions used in the original MAV.

Great difference in used propellants' state, comes with great (magnitude-wise) changes to the architecture. The addition of a needed feed system component may have added extra space and certainly changed the packaging inside the vehicle.

The tendency of a liquid-propellant MAV to be longer corresponds with other studies consulted[1]. A more quantitative comparison will need to wait till the full MSR mission architecture is designed.

A disadvantage of a longer MAV is the valuable extra space it takes in the aeroshell. It forces the SRL to be larger and imposes an extra size constraint for other potential systems.

As communicated in 8.3.1, more specific and final information on SRL is uncommon to come by. This does not mean a comparison cannot be made, but rather that it should be taken with a grain of salt. All that is known is that such a lander must fit within the aeroshell, meaning size-wise it should not differ too much from the proposed one.

Just as in the case of the MAV, a smaller SRL would mean more space for other potential co-systems of the mission. The more space is saved on SRL, the more room to breathe is given to other design teams, leading to a more friendly and happy co-existence of the teams.

8.3.3. System Capabilities

What truly matters in the end is what the designed creation able to do. Different requirements will lead to different capabilities and of course different architecture. The following subsections will address by comparing the ΔV budgets of the MAV (with its designed required orbit), the payload mass it is able to place on the desired orbit around Mars, and finally, the number of stages it requires.

Astro & ΔV Budgets

The overall MAVs required performance is summarised in 8.3.

Table 8.3: Astro Comparison

	BAGEL	**NASA**	**IoA**
Altitude km	500	300 [70]	500
Maximum Dispersion in Semi-Major Axis km	15	30 [70]	-
Inclination	25	25 [70]	25
ΔV $\mathrm{m\,s^{-1}}$	5470	$\approx$ 4000[1] [71]	4117

Due to the lack of similarity in the altitude of the target orbit, the ΔV budgets of both proposed MAVs will obviously vary. The BAGEL team vehicle will need to be more precise in its orbit determination - a feat that is supported by using the liquid propellants, instead of solid core. The simulation run modelled with multiple burns allowed to reach the desired altitude within the range. Please keep in mind that no requirement on orbit inclination was made for the study.

As to how this budget divides per MAV's stage: as mentioned in subsection 7.1.3, the 1st stage provides $3755\,\mathrm{m\,s^{-1}}$, and the second one covers $1715\,\mathrm{m\,s^{-1}}$. In the case of the solid MAV, a rough estimation based on other studies[421], the division is as follows: 1st stage gives a kick of $\approx 2400\,\mathrm{m\,s^{-1}}$, second is a lighter $\approx 1700\,\mathrm{m\,s^{-1}}$. The change of the magnitude of the kick needed lays in the different altitude needed. The similarity of ΔV of the second stage can be seen as more of a coincidence than convergence.

Number of Stages

The difference in stages is summarised in Table 8.4.

[1] Private communication, slides from the IoA/ TNO/ Absolut ESA Collaboration, received 14/06/2024

[421] Private communication, slides from the IoA/ TNO/ Absolut ESA Collaboration, received 14/06/2024

Table 8.4: Comparison MAV Stages

	BAGEL	NASA
Stages	2	2
Propellant	LOX/LCO	Solid

Even with different propellant types used, both studies ended up with a 2 stage rocket. It is a perfect equilibrium between mass efficiency and staging complexity for this type of mission.

Payload Mass To Orbit

A key aspect of the mission is putting the desired package in orbit, such that it can be later collected by ERO, and safely transported back to Mother Earth. Numbers on the amount of payload that can be taken is shown in Table 8.5.

Table 8.5: Payload to Orbit Comparison

	BAGEL	NASA	IoA
Number of Samples	30	20-30 [70]	-
Mass to Orbit kg	10	8	17

The mass provided is the mass of the whole Orbital Sample Container. The exact number of possible samples the BAGEL mission could carry would be an aspect of an analysis and design in a later stage. So far, importance was put into making it possible to deliver the given mass to the orbit.

The higher mass from the IoA study can come from the higher maturity of the study, which allows smaller margins and contingencies, leading to a not-overengineered MAV, with possible increased performance. BAGEL already at this stage, however, shows a higher capability from NASA's option.

8.3.4. Cost Budget

It is said that NASA's MSR mission will require a cost of 11 Billion American Dollars [65], yet a more detailed breakdown is impossible to come by. The cost shown in Table 8.6 has been estimated based on literature [72]. The estimate was then appropriately modified to account for the inflation and then scaled to the aforementioned 11 Billion American Dollars.

Table 8.6: Cost Comparison

	Cost [€M]	
Cost Item	**BAGEL**	**NASA**
MAV	64	588.5
SRL	295	1472.6
Additional	430.4	696
Grand Total (+50% contingency)	1,185	4,155

The division of the costs for the comparison follows the same philosophy presented in subsection 7.2.2. The cost estimate for NASA is very rough, however, it is known for a fact that MSR has faced some considerable delays and it needs extra funding from the Congress[65].

Private-owned companies have shown that it's possible to drastically reduce the cost of any launch or mission. Not being bound by any political requirements allows more flexibility in the operations, design and manufacturing choices that a government-owned entity does not have. The BAGEL-proposed mission has a real possibility of doing the same task, but cheaper.

9 Operations

This chapter aims to describe the operational side of the mission. Firstly, section 9.1 describes the different phases and elements of the mission itself. Following this, section 9.2 gives an overview of the phases that need to be carried out between completion of this DSE project, and the actual launch.

9.1. Operation and Logistical Concept

The MSR mission is scheduled to return in 2040. As the date is currently assumed by NASA, it has also been used for this study[1]. This chapter will give an overview of the mission elements, and mission life cycle. The mission elements will talk about which elements are involved in the mission, which existing infrastructure will be used, and which actual parts this project will specifically design. Then, the mission life cycle will detail the full mission, including development phases onwards and into EOL and post mission operations.

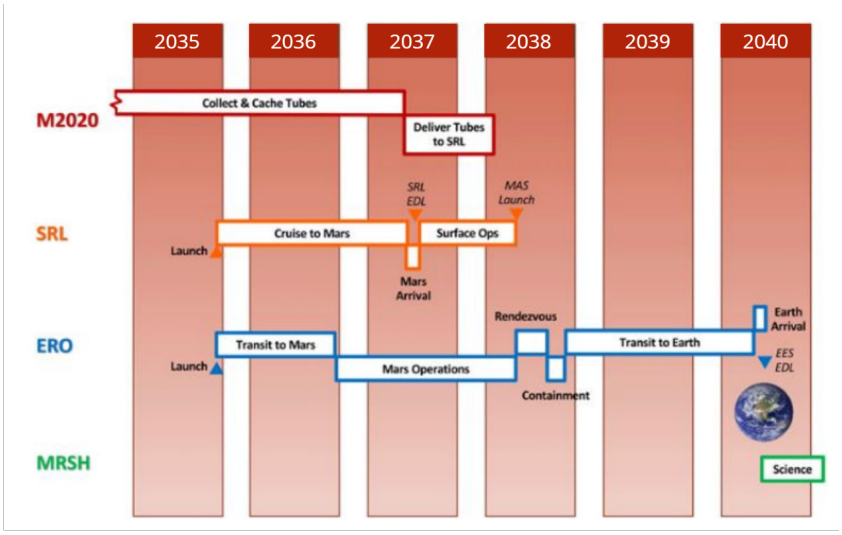

Figure 9.1: Notional Mission Timeline

9.1.1. Mission Elements

This section will describe with mission elements that will make up the mission. Initially, a description will be given of the elements that are already present, after which new aspects that this study will bring will be discussed. Mission elements from all phases will be used. Note that any design on these systems is considered to be outside the scope of this project. All key elements and their interactions are shown in Figure 9.2.

[1] https://spacenews.com/nasa-to-look-for-new-options-to-carry-out-mars-sample-return-program/

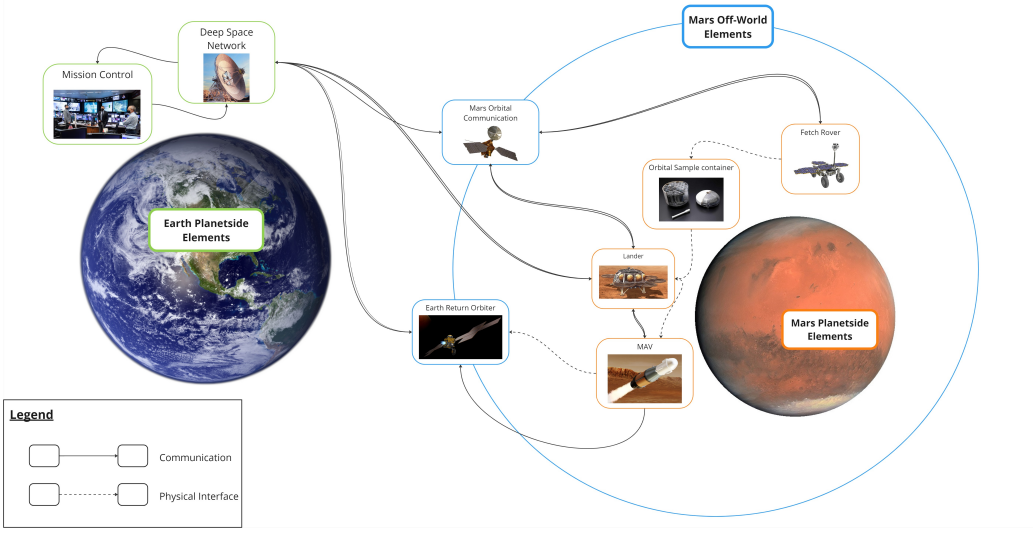

Figure 9.2: Operational Concept Description

Existing Elements

These elements will be mission parts that are already assumed to exist or be operational by the time of the mission launch, or whenever they are relevant. This chapter will describe what these systems are, and how they fit into the mission.

- **Design and Production facilities:** The new Concurrent Design Facility will be used for the ideation and initial production test runs. This location will also be used to develop the systems, and receive and assemble the prototypes. The relevant concepts will be designed, developed and tested here. Production of subsystems will likely be outsourced to external contractors across the EU. This is both to ensure that the parts will be manufactured by the experts in the field, and ensure that value is returned to ESA member states in terms of jobs.
- **Clean room and integration facilities:** For integrating the final components for the actual mission hardware, the ESTEC Testing facility will be used. This has a large suite of testing facilities to validate the systems and perform the final assembly in a clean environment to avoid contaminating the Mars surface. The benefits of this facility are that it has been used for a long time for both orbital and interplanetary missions. This means that there is a large amount of experience already present in using these facilities, allowing them to deliver the most value to the testing and integration process.
- **Launch Vehicle** This is the vehicle that will carry the mission vehicles to Mars. It will influence the real design in terms of launch loads and natural frequency. The launch vehicle will provide limits for the maximum aeroshell diameter and the maximum system weight. Fortunately, there is a large variety of heavy-lift launch vehicles on the market nowadays, so the launch mass is not currently a design requirement.
- **Mission Control:** As this mission will make use of a large variety of existing NASA assets on Mars, it makes sense it uses the JPL Space Flight Operations Facility in Pasadena, California for optimal integration between all mission elements. This Control Center has a long history of interplanetary missions and often handles control of missions using the Deep Space Network (DSN). As this mission will likely use this network as well for communications, and other mission architecture elements (MRO, Perseverance) are already run from the DSN, it only makes sense to use this control centre.
- **Communications Network (Earth Side):** As mentioned earlier, a lot of the existing Mars infrastructure is being operated through the DSN. Hence, it only makes sense to use this system for this mission as well. Not only does it reduce operating costs as no new ground systems need to be built, but its long legacy also ensures that there is a good amount of experience in using it. This helps to reduce development costs and troubleshooting times for communication subsystems, as one can rely on tried and tested designs and procedures.
- **Communications Network (Off-world):** Communication can happen directly to Earth, but to simplify matters and reduce overall communication costs, the choice was made to rely on existing Mars orbiters like the MRO to relay communications. These already have existing interfaces with the DSN, making it easier to integrate into the overall mission architecture.
- **Aeroshell & Landing system:** For the aeroshell, an existing aeroshell concept will be used. The aeroshell will handle interplanetary transit, orbital course corrections, aero-capture, orbit insertion and

then finally the full EDL part. It will guide the mission to the correct location on Mars, slow it down to a normal speed, and then deploy the landing system. Once the SRL is deployed, its propulsive landing system will slow the SRL down further and set it down in its final location.

- **Fetch Rover** The Fetch Rover developed by ESA will retrieve all the samples left behind by the Perseverance rover, and drive them to the SRL. Additionally, as it will already have an arm to pick up the sample capsules, the fetch rovers arm will also be used to load the samples into the OS container. So, the insertion of the samples from the rover into the MAV will be handled by the Rover. The fetch rover is not assumed to fly in the same aeroshell as the SRL and MAV, and is assumed to already be present and operational on Mars by the time of the Landers arrival.
- **Sample Container:** The sample container will house the surface samples collected by perseverance. The container and its interface with the ERO are assumed to already have been designed by ESA.
- **ERO:** The Earth Return Orbiter will collect the orbital sample container after it has been injected into its target orbit by the MAV. This system is developed by ESA and is assumed to arrive in Mars orbit to pick up the sample once it has been deployed.
- **Additional Scientific Payloads:** As mentioned in [1], additional scientific payloads can be carried by the lander onto Mars, to increase the mission value. These will be provided by external customers, and can either use small amounts of Lander power or just use their own onboard power and thermal systems.

Project Elements

These are the elements that this study is aiming to design. The aspects mentioned here will be part of the design scope of this study unless mentioned otherwise.

- **MAV** The MAV will be powered by a CO-O_2 bipropellant. This will integrate the payload on the Martian surface, take off from the SRL, and then deploy the Orbital Sample Container into the target orbit. After this, the container will be picked up by the ERO from said orbit. The study will provide a full design for the MAV, including size, architecture, detailed propulsion and feed system design, and a packaging and integration breakdown. While the Orbitals Sample Container is assumed to be designed, the MAV design will prescribe its housing within the MAV, aerodynamic fairing, and deployment system once in orbit. The design will also contain the propellant loading solution from the Lander into the MAV.
- **ISRU** The ISRU system will generate the propellant for the MAV. This design will detail the total mass of the system, its total propellant and thermal output, and rough volume and feed descriptions. It will also detail the cycles in which the system will operate to generate the required propellant without overly degrading the synthesis module or draining too much power. The interactions between this system and the lander power will be an important outcome of this study.
- **Lander** The lander system itself will handle the vast majority of the described tasks. This will include providing power to the ISRU system, managing waste heat and storing the generated propellant. Next to that, it will also interface with the MAV, through tasks like housing the MAV and managing its temperatures, loading the propellant and providing the launch infrastructure. It will also house the payload arm to load the soil samples from the Fetch Rover into the MAV. The study will detail the general size and volume of these subsystems, and provide a general layout of how all these systems will be integrated.

9.1.2. Mission overview

It is scheduled to arrive at the end of a Martian summer and remain there for up to 12 months. After this time, the samples will be loaded onto the MAV, and the MAV will launch into a Martian orbit. Here, it will deploy the payload sample, to be picked up by the ERO module. This overview will specifically detail the development and operation of the SRL, MAV and ISRU systems throughout the mission cycle. It does not detail the full MSR mission, just the roles of the systems discussed within this study within the full system. The mission phases are based on the phases as described in the Baseline Report [1]. However, they now also take into account the design, production and testing phases. The mission shall be performed in compliance with the COSPAR policy of planetary protection.

- **Phase 0: Design Feasibility Study** This phase will investigate the feasibility of this mission. This will include assessments of the technology, trade-offs, low-level sizing and detail design on select subsystems. It will give an overall idea of the mission scale in terms of mass budgets, operational risks and general mission outline. It can be compared with the baseline Mars Sample Return as outlined in [70], to see if this architecture has significant benefits over the current system, and what systems would have to be changed to get a measurable improvement. This phase will also design the full concept, mission breakdown (i.e. propellant generation cycles, propellant loading architecture) and a high-level design of the MAV, SRL and ISRU cycles.

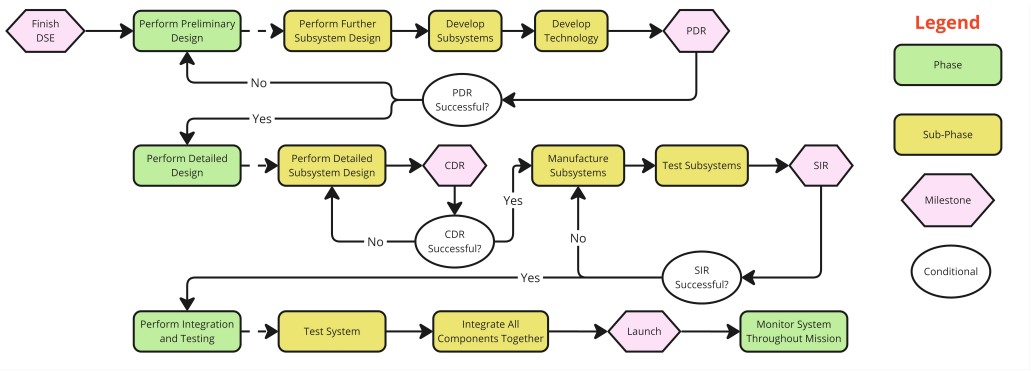

Figure 9.3: Project Design and Development Logic Flow Diagram

- **Phase 1: Mission design** Once Phase 0 has fully developed the concept, and determined if it is even feasible, the detail design phase will start. This is fairly self-explanatory. This phase will fully design all relevant mission systems and subsystems down to the part level. Critical systems that require further testing and validation will be identified together with their appropriate verification&validation method. It will also fully develop operations procedures for how the systems will operate on Mars. This will entail the full order of system start-up, propellant cycles and troubleshooting for expected problems. This phase will also select a launch provider and make a definitive choice on the ground station and mission control segment.
- **Phase 2: Development, Production and Integration** This phase will test the concept relevance to the mission. It includes testing things like deployment mechanisms, validating the expected efficiency and degradation of the ISRU, and testing the relevant propulsion systems. Once these have been verified, the full system can be produced and integrated in the ESA Clean Room at the ESTEC Testing Facility and shipped off to the launch provider, where it will be integrated into the Launch Vehicle.
- **Phase 3: Launch, Transit and Mars Arrival** This phase is the full journey from the surface of Earth to the surface of Mars. The Launch Vehicle will take off from Earth, and make the interplanetary transit similarly to the other Mars missions like perseverance. When arriving at Mars, the aeroshell will use the Mars Atmosphere to aerobrake and lower its orbit until it can make a full descent. At this point, the EDL phase will start with the goal of delivering the SRL to the surface of Mars.
- **Phase 4: Mars Landing** Once the system has landed, it will start running diagnostics and setting up crucial systems like establishing communication links with the ERO and Fetch Rover. Any issues that arise will be subject to troubleshooting procedures. Once everything has been confirmed to be up and running, the planet-side operations can start.
- **Phase 5: Planet Side Operations** The goal of this phase is to make all the necessary preparations for the MAV to deliver the payload sample to orbit. This includes integrating the samples from the Fetch Rover into the MAV, keeping the MAV in a survivable environment, and generating the required amount of propellant for the MAV to take off.
- **Phase 6: Mars Ascent** This phase will dictate the full launching and take-off procedure. The MAV will then traverse through the Mars atmosphere and into orbit. This phase will include the rocket staging and burn profile. Finally, the MAV will reach the target orbit.
- **Phase 7: Mission end** In this phase, the payload will be deployed into the orbit for pickup by the ERO. This phase will also dictate EOL procedures for both the Lander and MAV. This is the difference between the MAV either going to a graveyard orbit or deorbiting, and the Lander's continued operation in support of any potential scientific payloads or future missions.

9.2. Project Design & Development Logic

In the previous sections, much detail was provided regarding the phases of the mission itself. However, this leaves out the crucial phase that occurs between the end of the DSE project and the launch. Here, much further detailed design must be performed, in addition to manufacturing and testing. These specific phases as well as the activities to occur in the phases are compiled into a project design and development logic flow diagram in Figure 9.3 to show the order of activities.

10 Production

This chapter will identify some key system components, explain what materials they would be made of, and what production process would necessitate. Components were picked based on how important they are to the overall structure, and on how much their performance is dependent on their material choice and available options. For example, a bolt is such a simple component, with such simple and well-understood production methods, there is not much of a point in giving it an analysis. section 10.1 presents the production plan for the MAV, which is followed by the SRL production plan in section 10.2. Finally, the plan for assemblies is given in section 10.3.

10.1. Components MAV

The section will outline the production and integration plan of the most critical components of the MAV. Each time it will give materials and manufacturing methods used.

10.1.1. Engine

The engine chamber is one of the most important parts of the MAV. It needs to be able to handle large temperature differences, from cryogenic temperatures in the injector and cooling channels to around 3000 K inside the main chamber. This requires materials with good thermal properties, and high strength, and all of this while still needing to be as light as possible. It will also handle high loads, with it having to handle all the engine vibrations, chamber pressure and generated thrust and easily transfer this into the rest of the MAV. Both its materials and production processes will need to account for this.

Materials

The engine will be made of Inconel 718. This has been successfully used LOX-based rocket engines in the past. It has good strength properties and excellent heat resistance. This makes it very suitable for this purpose.

Production Method

The engine will be manufactured using Metal 3D printing. This allows for complex features, like cooling channels or complex wall curves, to be easily integrated into the chamber directly. It could even allow the full engine including the injector to be printed in one part, reducing the risks of leaks or failed components, and allowing for easier integration. This technology has again been proven to work for LOX-based rocket engines, giving a high degree of confidence that it is suited for this application as well.

10.1.2. Tanks

The tanks will be some of the most important structural components of the MAV. It will be one of the primary load-bearing components for both stages, taking up engine loads, and transferring them to the other rocket system. It will also have to store the propellants at pressure and cryogenic temperatures. Finally, it needs to be adaptable enough to attach mounting points for connecting elements.

Materials

As mentioned in the previous structural analysis [2], the tanks will be made out of Aluminium 7075-T6. This is due to the materials legacy in use for cryogenic (LOX) tanks in spaceflight applications. It can also be easily passivated to reduce the risks of long-term corrosion over time.

Production Method

As 7075-T6 cannot be reliably welded using traditional means. However, stir friction welding can be used to connect the parts. The tank cylinder and endcaps can be CNC'd. This allows for good dimensional accuracy, and for components line RadAx connectors or fitting connectors to be machined directly into the tank bulkheads for easy integration with the rest of the structure. CNC-ing will also allow for Isogrid patterns to be machined on the inside of the tank wall for further weight saving. The tank and bulkheads would then be integrated together using stir-friction welding.

10.1.3. Thrust structure

This structure will need to transfer all loads and vibrations from the engine chamber into the tank structure or connecting elements. Next to that, it may also have to function as a mounting system for the turbopumps and other engine bay systems. In the first stage, the thrust structure also needs to be able to incorporate the TVC actuators and their required range of motion. Together with the necessity to package engine subsystems, it means this structure will require a large amount of flexibility in the shapes and patterns of the structure to allow for all of these systems. This will be a driving need when selecting a production method and associated material. Next to that due to the light weight, a high specific strength is needed. Additionally, to have high pointing accuracy of the thrust, a relatively high stiffness is needed. Finally, for high dimensional consistency in take-off, high thermal resistance is needed to handle the heat from the drive plume.

Materials

This could be made in multiple ways. It could simply be machined out of 7075-T6 at all the other components. However, as engines are quite small, a more optimised design could be chosen. For this reason, the thrust structure will be made out of Ti6-Al4-V, as this allows for high strength, good temperature resistance, and the ability to be 3D printed.

Production Method

The titanium thrust structure will be 3D printed. This has been done a lot on smaller satellite thrusters, so it has a legacy in spaceflight systems. Additionally, 3D printing allows for a larger flexibility in forming the structure to handle the load most optimally and make it more weight-optimised. Additionally, it also allows for greater flexibility in designing hardpoints for mounting TVC linkages or feed system components. This technology has been used for space propulsion, hence it should be a reliable choice.

10.1.4. Interstage and Forward structure

The interstage and forward structures will be mounted directly on top of the first and second-stage tanks, respectively. These parts will have to house avionics like the flight computers or ECU, EPS components like batteries, communication subsystem, and in case of the interstage, space allocation for things like the second stage engine bell. These sections do not need to handle extremely high loads, aside from the thrust loads. Instead, most of its needs relate to its ability to house the aforementioned subsystems. This means easy integration with other MAV sections and stable mounts for the systems. This requires low weight, high strength, ease of production, and finishing for integrating threads and other mounting mechanisms. These will be the driving needs for these segments.

Materials

Aluminium 7075-T6 will again be used for the following reasons. For one, it will allow connecting features like RadAx elements to be easily integrated into the component. Next to that, having the interstages and tanks be made out of the same components will reduce the risk of galvanic corrosion between two different materials. This is also one of the reasons why Composites are not considered for the interstage, as they could galvanically corrode the aluminium connecting elements.

Another thing to note is that composites were not often considered for structural components in the system. The first is the risk of contamination of the Mars environment. If the first stage of the MAV crashes back into Mars after it has burned out in ascent, this risks spreading a large amount of carbon fibres and resin over the surface of Mars. This can damage the ability of other science missions to find organic matter on the surface of Mars. Next to that, especially in cryogenic conditions, it is very difficult to perform accurate calculations on the structural properties or even determine feasibility in the Mars environment without extensive testing and modelling. As those activities are outside the scope of this report, composites will not be considered for certain areas.

Production method

These components will once again be machined, likely by CNC. This allows for easy integration of the connecting features into the structure itself. It also allows for easy integration of cutouts for hatches etc. Finally, again weight saving patterns like isogrids can be easily implemented into the components. To avoid the risk of cold welding between the parts and components integrated into it, the forward structure and interstage will be anodised.

10.1.5. OS fairing

The OS fairing is slightly different from the other components. For one, due to its placement all the way at the MAV nosecone, it will only have to support its own weight, leading to low launch loads. On the other hand, it will be subject to aerodynamic heating sustained in take-off. This gives the need for a material with relatively high stiffness and good thermal properties, while still having a low weight. Luckily strength is less of an important parameter here, increasing the range of viable materials. Note that as this material has been used before on aeroshells, and is also an ablative material, its risks of contaminating the MAV atmosphere have been already quantified and deemed acceptable, unlike other composites.

Materials

The OS fairing will be made out of a similar material to the EDL Aeroshell. This is because both systems will face similar aerodynamic loads and heating, and as the material has been applied before, it should limit developmental issues and other problems. The fairing will thus be made of a honeycomb composite developed by Lockheed Martin. Lockheed describes it as "*an aluminium honeycomb structure sandwiched between graphite-epoxy face sheets and hand-packed with SLA-561V — a low conductivity ablative material whose texture has been compared to kinetic sand*" [1].

Production Method

The production process is quite an involved one. First, the inner structure will be made. Then the Aluminium honeycomb will be bonded to this structure. Then these will be packaged between the graphite-epoxy face sheets, and finally, the outer SLA hand packed on top of this. This is a manual process that will have to be performed in a specialised facility. However, as an aeroshell will be produced for this mission anyway, such a facility should be operational and equipped during the manufacturing process regardless. Hence, it is assumed that the fairing could also easily be produced without too much additional costs.

10.2. Components SRL

The section will outline the production and integration plan of the most critical components of the SRL.

10.2.1. SRL tanks

Similarly to the MAV, the tanks in the SRL area are very critically important components of the mission. They primarily have to bear load while launching from Earth and when landing on Mars. It furthermore needs to be mounted to the structure of the SRL.

Materials

The chosen material for the tanks is Aluminium 7075-T6 for the same reasons as stated above.

Production method

The only difference between the SRL tanks and the MAV tanks in terms of production method is that a cylindrical section does not need to be combined with a spherical one for the SRL, since both tanks are spheres. CNC machines will also be used for the manufacture of the tanks, as this allows for connection points and fitting to be integrally machined into the structure. The two halves of the sphere will be machined and then joined together using stir-friction welding.

10.2.2. Cryogenic Compressor

The cryogenic compressor is made up of multiple components. It consists of the two motors, which will be acquired from Maxon[2] as an off-the-shelf component, the compression cylinder, and pistons. The 2 latter components will be custom manufactured.

[1] https://www.lockheedmartin.com/en-us/capabilities/space/aeroshell-space.html
[2] https://www.maxongroup.net.au/maxon/view/configurator/BOM:IDX56MA0STPET558B:::

Materials
Both the pistons and the compression cylinder will be made out of stainless steel, as they need to withstand substantial temperatures (up to $800\,\mathrm{K}$) and pressures (up to $35\,\mathrm{bar}$). Aluminium could not be used as in most other components, due to its lower melting temperature. The pistons and cylinder will feature Teflon seals, which can withstand the harsh conditions.

Production Method
The cylinder and pistons will also be produced using CNC machining, as this allows for the most flexibility in design and allows for the connection points to be integrally machined.

10.2.3. Cryocooler
The cryocooler is based on the design given by Olson et al. [35]. Due to the resized design, Lockheed Martin will be commissioned to make a custom design for this mission. Due to the complexity and lack of publicly shared information about the exact design of the cryocooler, it is out of the scope of the project to design a custom one.

10.2.4. Cryogenic Pumps
For the pumps that aid the propellant transfer from the SRL onto the MAV, a pair of off-the-shelf pumps will be used. These are produced by Thomas[3] and are readily available. Mounting options are already available, and they can also be directly welded to the structure.

10.2.5. Valves and Tubes
The valves and tubes used in the propellant handling subsystem are all off-the-shelf components and thus do not require production. They will be ordered from the suppliers specified in section 6.7.

10.2.6. ISRU
Components used in the process are not planned to be produced in-house. Due to the readiness of each piece and its complexity, they are produced by already-known subcontractors - acquisition & compression unit by Air Squared, powered by a motor from Avior Control Technologies, providing feed to the cells produced by Ceramatec (OxEon Energy).

10.2.7. Thermal Insulation
Adequate quality multi-layer insulation, heating elements, and heat pump will be acquired from external sources, as designing these is out of the scope of this project, and multiple options are already available from suppliers.

10.2.8. Power
The power subsystem shall procure a number of its main components from private contractors, due to the complexity of the components involved. With the innovations occurring in battery and solar cell technology at the moment, a number of companies would be capable of manufacturing them to the necessary standard[4][44], this competition shall reduce the price of these components. The solar panel shall be manufactured using a Vectran mesh, similar to that of the Insight lander, this is a very light material with advantageous thermal properties that can be woven into a sheet which may be both very strong and thin[5]. Each solar wing shall be folded up during launch and cruise, into 10 segments, once landed the solar panels will be deployed outward. The arm and frame for these wings shall be made from an aluminium frame for rigidity.

10.2.9. Structure
The structure is the primary load-carrying component of the lander, it includes the lander bed, frame and legs. The structure must carry all the components and subsystems which make up the lander and MAV, it must be built to withstand the intense loads of EDL.

Materials
The lander bed, upon which the majority of the subsystems will be loaded, will be composed of AL3/16-5052-.003 aluminium honeycomb[6]. This is a readily available material which performs well under sheet bending.

[3] https://www.thomaspumps.com/en-nl/diaphragm-pumps-compressors/107z1-series

[4] https://www.spectrolab.com/photovoltaics/XTE-SF_Data_Sheet.pdf

[5] https://www.kuraray.com/products/vectran

[6] https://www.phys.hawaii.edu/~idlab/taskAndSchedule/iTOP_Commissioning/mechanics/Showa%20Aluminum%20Honeycomb.pdf

The legs shall be made from aluminium, including an aluminium honeycomb crush column in order to absorb the impact.

The frame of the lander shall be made out of Aluminium 7075-T6, this is used for its advantageous specific strength. The lander frame is a very large component, weight optimising it shall offer significant mass savings.

Production Method

The structural components shall be primarily commissioned from high-quality, low-tolerance suppliers. Honeycomb aluminium can be readily produced from sheet aluminium, with aluminium welded onto its ends to offer rigidity. Stir friction welding shall be used to fix the frame and bed to one another. The legs will be held using hinge joints to the lander frame and bed. The aluminium crush core will be manufactured to maximise energy and impact absorption, instead of strength as is the rest of the structure.

10.3. Assemblies

This section will go into what parts need to be put together and how this will be done.

10.3.1. Sub-assemblies

This will be the sub-assemblies making up each section of the MAV. It will detail what these sections are, which components they house, and how these will be integrated.

Engine bays

The engine bay will consist of a bay fairing, engine, E-pumps, and thrust structure including TVC linkages. The engine will be bolted to the TVC links in the thrust structure. The engine part moving with TVC will also mount the turbopumps. This entire assembly will then move when the TVC is actuated. The TVC links will then be bolted to the top of the engine bay and bay fairing. The bay fairing will have a RadAx connector machined into it, which attaches it to the tank. The thrust structure will also be bolted to the fairing, to allow all loads to be properly introduced into the MAV through the RadAx connector.

Interstage/Forward Structure

The interstage and forward structure will house the avionics and other stage subsystems for the first and second stages respectively.

The interstage will house the first-stage avionics, ECU, and batteries. These will be bolted either directly to the interstage or to a small adapter plate. This architecture is similar to what is proposed in the 2-stage solid MAV concept [73].

Separation Mechanism

The separation mechanism for both stages will use a pre-existing NASA system, this being the LSSN (Low Shock Separation Nut). This system has been in use for a while and has also already been considered for the 2-stage Solid Motor MAV concept [73]. 4 of these will be used for the Stage separation and 2 for the OS separation. These will be used to connect the first and second stages, and also to hold the OS container.

10.3.2. Connectors

The sections themselves will be joined using RadAx connectors. These have a long history of use in Launch vehicles and present the best compromise in structural rigidity and minimal weight. They are also relatively easy to integrate, as they are basically a simple bolted connection. This will be used to join all the major sections together. As mentioned in the previous section, the parts will have this connection machined into it, allowing for fewer joints, and reducing weights and possible weak points.

10.3.3. Integration

The RadAx connectors also allow the MAV to be easily split up into several sections that can all have their respective integration performed separately. This allows for easier testing and troubleshooting, as a failed component would not require the entire MAV to be disassembled. Once all sections have been tested and certified individually, they can be combined together into a full stage. These will then also be tested independently, and only once those have been successfully tested the MAV will be assembled for a full stack test. Once this is completed, the MAV can be integrated into the lander, which will then in turn be integrated into the aeroshell.

11

Quality Assurance

This chapter first delves into the Reliability, Availability, Maintainability, and Safety (RAMS) analysis for the Sample Return Lander (SRL) and Mars Ascent Vehicle (MAV) in section 11.1. It outlines the reliability estimates based on literature values and current data, discusses the availability and maintainability strategies, and addresses safety concerns for both Martian and Earth environments. Additionally, section 11.2 provides a comprehensive verification and validation (V&V) plan to ensure all mission requirements are met. Section 11.3 culminates a compliance matrix that maps how each requirement has been satisfied through the design process.

11.1. RAMS

This section presents the Reliability, Availability, Maintainability and Safety Analysis of the SRL and the MAV.

11.1.1. Reliability

SRL

The reliability analysis is done using the approach suggested in the literature [27]. At this point in the study, the failure rate of the majority of components is unknown, so the generic values from the SMAD have been used, and are shown in Table 11.1.

Table 11.1: Component Failure Rate and Reliability

Components	Failure rate	Reliability
Control Processor	0	1
Mechanisms	0.1	0.9
Thermal	0.1	0.9
Structures	0.1	0.9
Batteries	0.02	0.98
Solar Panels	0.17	0.83
TTC	0.23	0.77
Unknown	0.06	0.94

The values presented in Table 11.1 are based on about 1600 earth-orbiting satellites, which means that the values are lower than what can be expected of the components mounted on the SRL and MAV. The lander reliability diagram is shown in Figure 11.1.

The final reliability score is reached assuming that all 8 highlighted assemblies have to be functional in order to complete the mission. In some cases, like for the solar panels the total reliability was calculated using Equation 11.1, where n is the total number of elements, k is the number of elements needed for successful

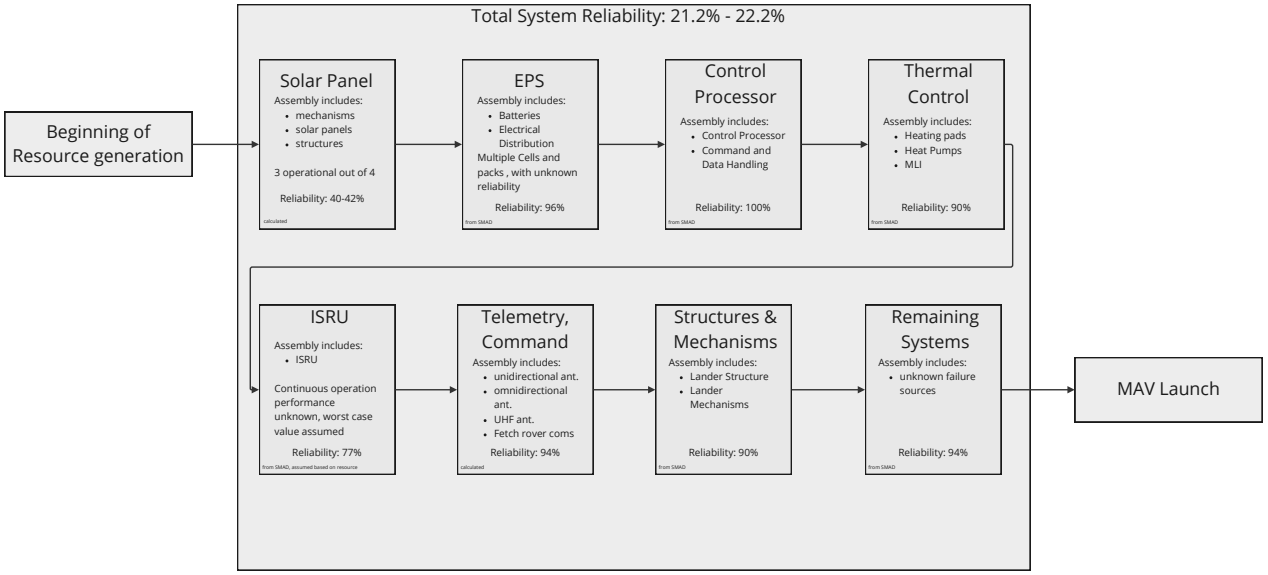

Figure 11.1: Lander Reliability

functioning, and R_i is the element reliability.

$$R = \sum_{k}^{n} \frac{n!}{k! \cdot (n-k)!} R_i^k \cdot (1 - R_i)^{(n-k)} \tag{11.1}$$

For the solar panels the reliability was calculated based on the fact that a solar panel element consists of structures, mechanisms, and the solar panel. Since the mechanism only has to open the solar panels once, the reliability was calculated twice, once with including the mechanism reliability, once excluding it.

For the telecommunications assembly it was assumed that all sub-elements have a 77% reliability, but the lander is capable of operations with any of the long distance communication antennas. The fetch rover communications include redundant systems.

A shown on top of figure 11.1 the overall reliability for the 1 year operational duration of the lander is about 22%, which is very low for a mission of this calibre. As pointed out at the beginning of this section, the values for reliability are underestimated. However not all shortcomings can be explained with this. The reliability of the solar panels decreases the overall mission reliability significantly, additional, redundant solar panels have to be added in order to decrease the mission failure probability.

The ISRU presents the second largest risk; here the lowest reliability listed in the SMAD [27] was used, because research into continuous operation and failure rates is lacking at the time this report is written, as pointed out by Hoffman et. al. [32].

At this point in time it is recommended to investigate the viability of adding a second redundant ISRU.

MAV

It was assumed for the MAV that it's reliability decreases over the transit and propellant production time similarly to a satellite in Earth orbit over a year. Based on this assumption, the failure rates are taken from the SMAD [27], and shown in table 11.2.

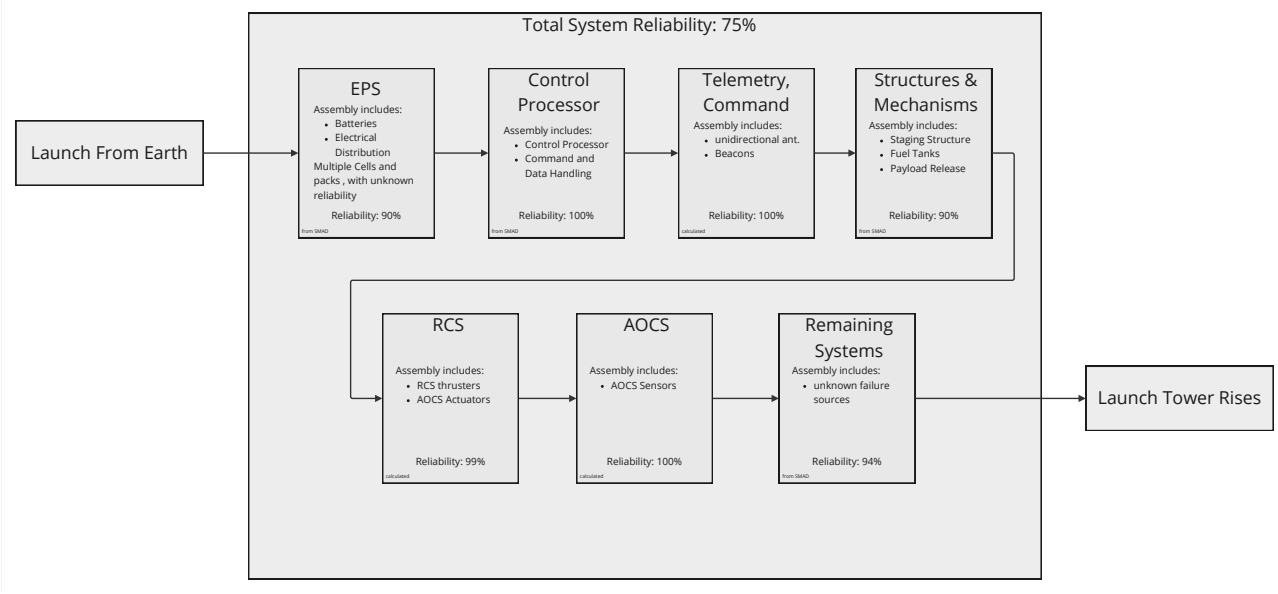

Figure 11.2: MAV Reliability

Table 11.2: MAV Component Reliability

Components	Failure rate	Reliability
Attitude Control	0.12	0.88
RCS	0.2	0.8
Control Processor	0	1
Structures	0.1	0.9
Batteries	0.1	0.9
TTC	0.22	0.78
Unknown	0.08	0.92

Based on the values in table 11.2 a reliability analysis was conducted, the overview of which is presented in Figure 11.2.

The MAV has a number of fully redundant systems, like the TT&C; to calculate the reliability of these systems Equation 11.2 was used.

$$R_p = 1 - (1 - R_i)^n \tag{11.2}$$

As shown in figure 11.2, the chance of the MAV functioning properly at the time of the launch tower erection is 75%. Due to time constraints and lack of data, the reliability analysis of the launch was not taken into account. It's also assumed that the sample container is sufficiently simple to ensure proper functioning after the storage and sample loading period.

11.1.2. Availability and Maintainability

The next two aspects of RAMS analysis are availability and maintainability. Availability concerns the downtime when there are failures which one can recover from. Subsystems which take longer to fix, hence having a longer downtime, have a lower availability. Furthermore, maintainability aims to outline which parts of the overall system can be maintained, and in the case of planned maintenance, when this is scheduled for. While these are separate aspects of RAMS analysis, there is much overlap between them, since the downtime due to a failure can relate to its maintainability. For this reason, these aspects are both addressed in the same subsection.

Starting with availability, it must be acknowledged that due to the nature of the mission it is quite difficult to fix things in case of failure, mainly because one can't simply go to Mars to perform maintenance. However, there are three main scenarios which failure can be recovered from, and hence availability must be considered.

1. Recovery from hardware failure via redundant hardware.
2. Recovery from software failure via remote software updates.
3. Partial recovery from hardware failure via remote software updates.

The final item on the list may seem confusing, but an example of this can be seen through the Curiosity Rover. When the drill on the rover suffered a hardware failure, drilling operations were halted. Engineers were not able to fix the main issue, but they were able to re-programme the drilling software in a way that allowed for the broken drill to work, just with a different and less optimal method that still allowed for a continuation of the mission[1]. This is a scenario which is possible for this mission, for example with the sample loading mechanism, hence it must be considered.

All the specific scenarios which fall under the three just mentioned are shown in Table 11.3. The standard failure rates λ are retrieved from the SMAD [27], based on similar missions. The recovery times are an order of magnitude estimate, and the availability A is found with Equation 11.3 [27],

$$A = \frac{MTBF}{MTBF + MTTR} \tag{11.3}$$

, where $MTBF$ is the mean time between failures, calculated as the reciprocal of λ, and $MTTR$ is the mean time to repair.

[1] https://science.nasa.gov/resource/curiositys-new-drilling-technique/

Table 11.3: Availability Values

Failure	Recovery	Downtime [s]	Failure Rate	Availability
ISRU cell	Redundant cell nominally operating	0.2	0.01	1
Lander electronic hardware	Redundant hardware nominally operating	0	0.08	1
Lander Communications	Redundant communication hardware started up	5	0.23	1
Sample loading mechanism	Redundant loading mechanism used instead	10	0.1	1
MAV launch mechanism	Redundant launch mechanism used	10	0.1	1
Propellant storage sensors	Redundant sensors nominally operating	0	0.1	1
Propellant Storage motor	Redundant motor already operating	0	0.1	1
MAV fill line	Filling done through redundant feed line	10	0.1	1
Lander software	Software update from earth	$1.3 \cdot 10^7$	0.06	0.976
Lander hardware	Software update from earth	$1.3 \cdot 10^7$	0.1	0.96
MAV avionics	Redundant hardware nominally operating	0	0.12	1
MAV communications	Redundant communication hardware started up	5	0.23	1
ADCS sensors	Redundant hardware nominally operating	0	0.12	1
ADCS actuators	Redundant actuators started	5	0.12	1
MAV electronic hardware	Redundant hardware nominally operating	5	0.08	1
MAV-ERO beacon	Redundant hardware nominally operating	0	0.1	1
MAV feed valve	Redundant valve used	5	0.1	1

A trait immediately noticeable from Table 11.3 is the fact that most of the failures have an availability of 1. This is a result of two things. Firstly, some failures which are recovered via redundant hardware already have the redundant hardware nominally operating, hence after the failure, there is no downtime while the redundant hardware starts up and the availability is 1 according to Equation 11.3. Secondly, even if there is downtime due to redundant hardware start-up, the downtime (in the order of seconds) is minuscule in comparison to the mean time between failures (in the order of years) calculated from the failures rates. Therefore, even though the availability is slightly less than 1, the difference is so insignificant that it makes more sense to leave the number as 1.

The only cases where the availability is noticeably below 1 are the ones where a software update is sent from Earth. Here, the downtime is significantly larger since a team must actually write, verify and validate new software, rather than just have redundant hardware startup. The numbers in the table are taken from the example of Voyager 1 which required 5 months for a software update due to a malfunctioned chip[2]. Although noticeable, these availability values are still very high and hence not concerning.

Overall, Table 11.3 has shown that all the availability values are very high, and hence this is not a huge issue. That being said, it must be acknowledged that Table 11.3 only concerns recoverable failures. Due to the mission

[2] https://www.jpl.nasa.gov/news/nasas-voyager-1-resumes-sending-engineering-updates-to-earth

nature, most of the recoveries are via redundant hardware and hence have a low downtime. In another mission, downtime might be much higher for recoveries that require physical maintenance from humans, something not possible for this mission. While this is good for availability values, it must still be acknowledged that failures can occur, and there is less room for recovery.

Regarding maintenance, this has largely been summarised in the previous few paragraphs. Due to the mission being on Mars, humans cannot perform physical maintenance. The only scheduled maintenance activity is the cleaning of the solar panels with the compressed gas system. The only unscheduled maintenance that could happen is a software update used to fix either a software or hardware issue.

11.1.3. Safety

The fourth and final aspect of the RAMS analysis is safety. Depending on the aerospace mission being carried out, it is typically crucial to consider how humans and other life-forms might be harmed during the mission, and how this can be best mitigated. However, for this specific mission, it is slightly different. Since the mission is unmanned and on Mars, there is no risk to human life during the mission itself. During the launch phase on Earth, a control issue could cause the launch vehicle to crash in a populated area, but this is outside the scope of the project.

Although the typical human safety aspects during the mission do not apply to this project, there is still more to be considered. Firstly, the aspect of Martian environmental safety. While there will be no humans on Mars, the mission could still cause damage to the Martian environment if something goes wrong, hence making it a safety hazard in that sense. Furthermore, it is also within the scope to consider the testing of the system on earth. If this is not handled properly, people could get put in serious danger, hence this will also be addressed.

Firstly, regarding the Martian environment, Table 11.4 gives a list of safety critical functions and the reason why they are critical.

Table 11.4: Safety Critical Functions

Function/Component	Reason
MAV igniter	If the second stage engine fails to ignite, the MAV will not reach orbit and fall back down to Mars.
MAV injector sealing	If there is leakage of LOX into the combustion chamber then this could lead to an explosion.
MAV attitude determination	Failure to determine attitude/incorrect attitude determination could lead to an incorrect trajectory.
MAV attitude control	Failure to control attitude could lead to an incorrect trajectory into Mars
MAV exhaust chute	If during launch the exhaust of the MAV is not correctly redirected it could damage part of the Martian surface.
MAV feed system control	If the MAV feed system is not controlled correctly, this could lead to an incorrect burn profile and hence an incorrect trajectory.
MAV feed system and tank sealing	If there is fluid leakage within the MAV during flight, other safety critical hardware (e.g. attitude control) could be damaged beyond use.

For the specific functions of MAV attitude determination and control, the issue is already addressed through the use of redundant hardware as outlined in subsection 11.1.2. For the other functions, redundancy has not been implemented either because it is not possible for the specific case, or because significant verification and validation can be done to the point where redundancy is not required. That being said, it is important that all the functions mentioned in Table 11.4 undergo particularly rigorous verification and validation, as they are critical to the mission. The specific techniques used to verify and validate these functions will be outlined in section 11.2.

As mentioned earlier, the aspect of safety during testing must also be addressed. To mitigate any potential

hazards, it is important that specific considerations be made, and protocols be implemented. Table 11.5 shows a list of these considerations. If all the considerations here are followed, then a good standard of safety will be maintained for each test. That being said, these considerations are just general. For each specific test, when the details of the test are known, further safety considerations should be derived to properly ensure safety.

Table 11.5: Testing Safety Considerations

Consideration	Explanation
Use correct PPE	Wearing the right personal protective equipment (PPE) is essential to mitigate the harm done to people. This could include safety glasses, safety shoes, helmets, gloves, coats, all to be implemented where necessary.
Fire extinguishers	It is important to have fire extinguishers on hand in case a fire must be quickly put out.
Keep away from pressurised systems	Depending on the pressurised volume, a burst could be very dangerous hence personal should stay away.
Check rating of components	It is important that the wires are all rated for the expected current, and the valves are all rated for the expected pressure. The same can be said for many other components such as pipes and seals.
Implement kill switch	There should always be a button which one can press at any time which stops the test and purges the system in case anything goes wrong.
Electrical isolation	Electrical systems that could be harmful if electrical discharge occurs must be isolated such that no one accidentally touches them during the test.
Data monitoring	Many temperature and pressure sensors should be implemented throughout the system and the test should be programmed to automatically stop if any of the readings surpass a critical value.
Use distance protocols	For something like an engine hotfire, it is very important that personal maintain a minimum distance in case of an explosion. This distance should be worked out beforehand and well enforced.
Clean the system beforehand	It is important that the system is thoroughly cleaned to avoid any malfunctions. Furthermore, LOx cleaning is particularly important to implement to make sure the LOx doesn't undesirably react with anything during the test.
Use appropriate test environment	For example, a hotfire should not be performed in an open space surrounded by many buildings an people, but rather in a testing bunker designed to withstand an explosion.
Pre-test risk assessment	Before testing, the safety risks should be identified, a risk map should be made, and mitigation strategies should be applied. It is good practice to derive a list of successive failure modes for the system and assess whether the list is desirable from a safety standpoint.
Train personal for emergency	It is important that the people performing a test know what to do in case of a fire or another emergency. That way everyone can act fast to remove the hazard or at least safely evacuate the area.
Contact local authorities	Depending on the nature of the test, it could make sense to have local authorities block off a certain area from civilians/cars/boats/aircraft.
Contact emergency services	To be safe, it would be good to have emergency services on standby so that anyone in need of medical attention due to an accident can receive it as soon as possible.

11.2. Verification & Validation

To ensure the correct functioning of the system, a Verification and Validation procedure is planned. The V-model as shown previously in figure 1.1, it's used to effectively identify where validation and where verification is required. This chapter focuses on introducing the Verification and Validation methods undertaken to ensure

the product complies with the customer's specifications. Hence, the section about verification, section 11.2.1, primarily focuses on the user and system requirements, whereas section 11.2.2, Validation, mainly discusses acceptance and system testing.

11.2.1. Verification

Four methods are used to verify the design to the requirements. These are either done through inspection, analysis, demonstration, or testing. Inspection is done by checking with design documentation for compliance. Analysis is done through mathematical or other models, while demonstrations are checked through operations. Finally, testing is done by checking compliance under operating conditions. The verification method for the various requirements can be found in Table 11.6.

11.2.2. Validation

To validate the assumptions and models used, several tests are proposed to ensure the proper functioning of the entire system or several sub-systems. These are then combined into a testing campaign to ensure all tests are done sufficiently and within the time frame. It is important to note that, in the context of risk when developing new technology, testability is more important than maturity (TRL) [3]. Furthermore, it is also crucial to highlight the fact that (sub)systems/components with high TRLs do not need as extensive component testing.

Proposed Tests

These tests are placed in order of priority, in terms of which tests are the most necessary.

1. **Hotfire Testing (Validation)**: The engine will be mounted to a set stand and will be fired for the projected burn time. This will assure the thrust, I_{sp}, thermal and ignition conditions of the engine.
2. **Shake 'n' Bake Tests (Validation)**: The entire structure will be placed on a vibration plate to test for vibrational modes on Earth, as well as EDL conditions on Mars. The MAV is also subjected to high temperatures to make certain that the system can handle the large temperature changes that it is likely to be exposed to on Mars and during flight.
3. **Environment Tests (Validation)**:
    - **Thermal Vacuum Testing**: All parts will be tested to ensure they survive in the conditions of space and near-vacuum conditions in the Martian atmosphere. This will be done in a thermal vacuum chamber that simulates these low pressures and extreme temperature variations that the spacecraft will encounter.
    - **Wind tunnel test**: Place the MAV model in a supersonic and a hypersonic wind tunnel using nitrogen gas. Schlieren photography can be used to identify shock wave and stability characteristics.
    - **Electromagnetic testing**: Electrical and magnetic components that make up the MAV are compatible and don't interfere with the martian magnetic field. As well as the increased exposure to radiation and their resistance to it.
4. **Drop Testing (Validation)**: Stage separation often requires pyrotechnics, which impose an impulse on the MAV. Dropping the MAV from a certain altitude allows for an easy way to measure the effects of the impulse.
5. **Acoustic testing (Validation)**: The MAV and lander are put in an acoustic chamber, strapped in, and blasted with noise a hundred times louder than a typical rock concert. The MAV needs to withstand the noise of launch, where the rumbling of the rocket can be loud enough to damage the hardware.

All the validation tests are important to the mission. If the budget is sufficient, conducting all the tests is advisable to minimise the mission risk. The static fire test comes first in the list, since this LCO/LOX engine is unprecedented, and MAV relies on it to achieve to the target orbit. The Shake 'n' Bake Tests rank second in importance because heat and vibration are two key factors that could easily lead to launch failure. Also, this test is cost-effective, as it requires no new test equipment. Environmental testing follows, given the mission's equipment must endure a year on Mars, making it essential to anticipate any potential issues during this period that could lead to the failure of the entire mission. Finally, drop testing and acoustic testing are equally critical. The more affordable one would be more prioritised. Drop testing involves simple strain sensors and a dropping location, whereas acoustic testing is more costly and requires advanced sound equipment to mimic extreme launch noise.

11.2.3. Testing Campaign

Mars Ascent Vehicle (MAV):

The testing plan for the Mars Ascent Vehicle (MAV) includes component testing with hotfire tests to validate engine performance and various pressure vessel tests (burst, vacuum, chemical compatibility, and impulse response/vibration) to ensure the tank's integrity and confirm the operational limits. Subsystem testing involves shake 'n' bake tests for structural integrity under vibrations and thermal stresses. Integrated system testing includes acoustic testing to ensure the MAV can withstand high noise levels during launch. Environmental testing involves thermal vacuum tests, electromagnetic and radiation tests and wind tunnel tests to validate performance under space and Martian conditions. Drop testing is also performed to simulate landing and stage separation impacts. Finally, a series of roll-out tests where the MAV is mounted to the ground is conducted to perform the simulation of all MAV mission sequence.

Sample Return Lander (SRL):

For the Mars Lander, the testing plan starts with environmental tests such as thermal vacuum testing, electromagnetic tests, and wind tunnel tests to simulate conditions on Mars and assess aerodynamic stability. Subsystem testing includes shake 'n' bake tests for structural integrity. Integrated system testing involves acoustic testing to ensure the lander can withstand the noise levels during launch. Drop testing is used here as well to simulate stage separation and landing impacts. Next to this, the ISRU is also tested to ensure its production capabilities and purity of the propellants. The plan culminates in a mission simulation to validate the lander's performance throughout the entire mission sequence, ensuring readiness for deployment on Mars.

Table 11.6: Requirement Verification

Identifier	Requirement	Method	Method Description
STK-M-001	The system shall be able to place a 10 kg payload, consisting of Mars surface samples in the target orbit.	Analysis	Perform Ascent Analysis with appropriate software and analytical methods.
STK-M-003	Orbital dispersion of the payload should be below 30 km in the semi-major axis.	Analysis	Perform Ascent Analysis with changes in parameters to simulate situations.
STK-M-004	The system shall use a propulsion system based on Liquid Oxygen (LOX) and Liquid Carbon Monoxide (LCO) propellants for ascent.	Testing	A series of test campaigns will be used to analyse the behaviour of the rocket engines.
STK-M-006	The system shall complete its surface mission between two consecutive Martian winters.	Analysis	Based on terrestrial tests and performance of MOXIE predict the propellant production time to check achievable time frame.
STK-M-007	The costs of the system should be comparable to existing MAV architectures.	Demonstration	Perform a cost analysis of the entire system and compare it to other architectures.
STK-M-008	The system shall place the payload in a circular orbit at a 25-degree inclination.	Analysis	Analyse the TVC capabilities and the ΔV budget.
STK-M-009	The system shall be capable of producing the propellant to (re)fill the MAV in a maximum 12-month time frame at the required temperatures and pressures.	Analysis	Analyse the scaled-up propellant production rates based on the performance of MOXIE on MARS.
STK-M-010	The system shall be capable of producing and transferring the propellant to (re)fill the MAV in a maximum 12-month time frame at the required temperatures and pressures.	Demonstration	Demonstrate that propellant transfer is possible at maximum rate under Martian conditions.
STK-I-001	The system should be compatible with the aeroshell and parachute system based on the Mars 2020 EDL system [Ref 5].	Demonstration	Place the system in the aeroshell.
STK-I-003	The system shall incorporate the payload as defined for the baseline MSR mission as summarized in [Ref 1] including the samples collected by the Mars 2020 mission.	Demonstration	Demonstrate payload compliance.
STK-I-004	The system shall include the payload transfer mechanism into the System but can assume the availability of a Fetch rover as defined in [Ref 1].	Demonstration	Demonstrate the functionality of the transfer mechanism.
ISR-007	The Propellants shall not come in contact with one another until launch.	Demonstration	Demonstrate the fully separated propellant tanks.
ISR-008	The ISRU shall produce the required propellant mass within the mission time frame	Analysis	Analyse the scaled-up propellant production rates based on the performance of MOXIE on MARS.
ISR-012	The propellant liquefication rate shall be greater than or equal to the propellant rate of production	Testing	Test the performance of the liquefaction process.
ISR-014	The ISRU shall pressurise the Oxygen to 3 [MPa]	Testing	Test the performance of the pressurisation system.
ISR-015	The ISRU shall pressurise the Carbon Monoxide to 3 [MPa]	Testing	Test the performance of the pressurisation system.
LAN-INT-004	Temperature sensitive components shall not be placed within TBD m of potential leak locations.	Testing	Record the leak rates of the system under simulated Martian conditions.
LAN-PWR-001	The power system shall provide power to all subsystems	Testing	Test the performance of the power system.
LAN-PWR-002	The lander shall provide power to the MAV.	Demonstration	Demonstrate the power transfer from the lander to the MAV.
LAN-THM-001	The thermal system shall provide thermal control to all subsystems.	Demonstration	Demonstrate that the system is capable of providing adequate thermal control.
MAV-ENV-001	The MAV shall withstand the low temperatures of the Martian environment.	Testing	Test the performance of the Thermal Control System under simulated Martian conditions.
MAV-PRP-003	The propulsion system shall be able to ignite the LOX/LCO propellants at launch.	Testing	Test the ignition system.
MAV-PRP-014	The MAV shall have an initial thrust-to-weight ratio of at least 1.0 [-]	Analysis	Compare the mass of the MAV to the Thrust of the engine.
MAV-STR-003	The structural system shall be resistant to all expected cyclic loads.	Testing	Test the performance of the systems under cyclic loading.
SYS-001	The system shall generate the propellants needed to launch a MAV to the required orbit from the Martian atmosphere.	Analysis	Analyse the scaled-up propellant production rates based on the performance of MOXIE on MARS.
SYS-002	The system shall maintain contact with Earth for the duration of the mission.	Analysis	Analyse the performance of the communication system.
SYS-003	The system shall remain fully operational for at least the duration of the mission.	Analysis	Analyse the expected lifetime under simulated Martian conditions.

11.3. Compliance

In order to show that the design indeed meets the original user requirements, it is necessary to create a compliance matrix which shows how each requirement has been satisfied. Table 11.7 shows this for the mission requirements, Table 11.8 for interface requirements, and Table 11.9 for study requirements.

Table 11.7: Mission Requirements Compliance Matrix

ID	Compliance	Explanation
STK-M-001	Yes	Section 6.14 shows that with the given payload mass, an orbit with an apoapsis of $502\,\mathrm{km}$ and a periapsis of $493\,\mathrm{km}$ is achieved.
STK-M-002	Yes	Section 6.14 shows that with the given payload mass, an orbit with an apoapsis of $502\,\mathrm{km}$ and a periapsis of $493\,\mathrm{km}$ is achieved.
STK-M-003	Yes	Section 6.14 shows a semi-major axis range of $7\,\mathrm{km}$. Section 6.15 shows that over time there is a dispersion of $24\,\mathrm{km}$ in semi-major axis.
STK-M-004	Yes	Section 6.12 uses LCO and LOx for the propulsion analysis, and parameters from this analysis are used in the ascent analysis.
STK-M-006	Yes	Section 6.6 shows that the propellants can be produced in 12 months, which fits within the time-frame between Martian winters. Furthermore, the power calculations in Section 6.10 considered the Martian environment between winter periods.
STK-M-007	Yes	Section 7.2.2 predicts a total cost of 1.2 billion euros. Section 8.3 shows that NASA made a prediction in the order of 4.2 billion euros.
STK-M-008	Yes	Section 6.14 shows that the final inclination reached is $25°$.
STK-M-009	Yes	Section 6.6 shows that O_2 can be produced at $6\,\mathrm{g\,h^{-1}}$ and CO at $10.5\,\mathrm{g\,h^{-1}}$. Over 12 months this gives $52.6\,\mathrm{kg}$ of O_2 and $131.4\,\mathrm{kg}$ of CO, more than the required propellant masses of $45.56\,\mathrm{kg}$ O_2 and $90.91\,\mathrm{kg}$ CO.
STK-M-010	Yes	Section 6.7 shows that the propellant handling system is capable of transferring the propellants at $100\,\mathrm{K}$ and $30\,\mathrm{bar}$

Table 11.8: Interface Requirements Compliance Matrix

ID	Compliance	Explanation
STK-I-001	Yes	Section 7.1 derives total mass and volume budgets of $570\,\mathrm{kg}$ and $12.1\,\mathrm{m^3}$, fitting within the aeroshell requirements of $1900\,\mathrm{kg}$ and $13.61\,\mathrm{m^3}$.
STK-I-003	Yes	Section 9.1.1 outlines how the payload is incorperated into the system.
STK-I-004	Yes	Section 9.1.1 considers the payload transfer mechanism, while assuming the availability of the fetch rover.
STK-I-005	Yes	The availability of the earth return orbiter was assumed, and no additional design was done for this.

It can be seen that the majority of the stakeholder requirements are met. However, two of them are not met, these being **STK-S-009** and **STK-S-017**. The later requirement specifies that the study should evaluate the ISRU purification process. This was done for the O2 ISRU feed since there were numbers available for this from the MOXIE experiment. However, for the CO feed there were no studies done on the purification. While in theory it would be possible to remove all the CO here, theoretical analysis of this is quite tricky, and to get meaningful values it would need to be tested in real life, hence a conclusion is not drawn at this stage.

STK-S-009 states that the study shall evaluate the complete ISRU process. **STK-S-017** flows from this requirement, hence the fact that **STK-S-017** was not met as just explained implies that **STK-S-009** will also not be met.

Table 11.9: Study Requirements Compliance Matrix

ID	Compliance	Explanation
STK-S-001	Yes	Section 7.1 summarises the size, weight and power of all systems.
STK-S-003	Yes	Section 5.2.3 summarises the comparison between the pressurisation methods, and it is outlined in more detail in the midterm report [2].
STK-S-005	Yes	Section 1.4 outlines the specific implementation of sustainability into the design.
STK-S-006	Yes	Section 7.1 incorporates mass and volume reservations for the landing system.
STK-S-007	Yes	Section 11.1.1 quantifies the mission reliability.
STK-S-008	Yes	Section 7.2.2 shows the analysis of the mission cost.
STK-S-009	No	Not possible to complete since **STK-S-0017** was incomplete.
STK-S-010	Yes	Weight comparison is performed in Section 8.3.1.
STK-S-011	Yes	Size comparison is performed in Section 8.3.2.
STK-S-012	Yes	Comparison of number of stages is performed in Section 8.3.3.
STK-S-013	Yes	MAV Delta-V budget comparison is performed in Section 8.3.3.
STK-S-014	Yes	Payload mass to orbit comparison is performed in Section 8.3.3.
STK-S-015	Yes	The ISRU CO_2 collection process is evaluated in Section 6.6.
STK-S-016	Yes	The ISRU propellant production process is evaluated in Section 6.6.
STK-S-017	No	ISRU propellant purification is not evaluated.
STK-S-018	Yes	The ISRU propellant liquefaction is evaluated in Section 6.6.
STK-S-019	Yes	The propellant storage process is evaluated in Section 6.7.
STK-S-020	Yes	The environmental integrity of Earth is ensured according to COSPAR's policy of planetary protection, as specified in Section 1.4.
STK-S-021	Yes	The environmental integrity of Mars is ensured according to COSPAR's policy of planetary protection, as specified in Section 1.4.

Conclusion and Recommendations

In this chapter, the conclusions of this study shall be discussed first. Then, the recommendations for future studies which were not in the scope of this project are outlined. Finally, the general implications of this study are concluded.

Conclusion

The MSR mission's final report set out to create a comprehensive and cost-effective design suitable for the retrieval of Martian samples. By dividing the mission into subsystems and conducting market and risk analyses, a foundation for a sustainable and feasible final design was created. The mission's design was optimised through detailed subsystem analyses and integrated through interface, block and piping and instrumentation diagrams, for both the MAV and the SRL.

Key findings from our analyses include a design that operates within Martian environmental constraints, such as radiation and thermal extremes, while incorporating solutions like blow down systems for dust mitigation. The structural, propulsion, and thermal systems were tailored to meet the set requirements, culminating in a design that is not only feasible but also four times cheaper than existing options. The propulsion system in particular was designed using an e-pump fed bipropellant engine, which is the only liquid engine option designed currently for the mission.

Future steps include the implementation of the verification and validation plan and the outlined production plan to transition from conceptual design to reality. RAMS analysis ensured the reliability, availability, maintainability and safety of the design, and its testing procedures.

Recommendations

With the completion of the preliminary design, as carried out in this report, a final version of the concepts has been settled on. Despite this, it remains clear that further iterations and modifications can be made to improve the design and arrive at a final and fully defined system. This section is dedicated to the recommendations that have been derived during the design process. They aim to share the problems, potential solutions, and further ideas that have been encountered by the engineering team, that due to time constraints could not be further explored or analysed. By no means is it an exhaustive list or a checklist of items that need to be completed to get to the final design; it merely represents the items that were found to be of particular interest yet could not be completed in the scope of this project.

The recommendations are given in the form of specific recommendations for each subsystem analysed, followed by general recommendations for the overall project. It is important to note that this chapter and the project Gantt chart presented in Figure 7.1 complement each other in laying out the plan for the future of the project.

Subsystem Recommendations

The recommendations for each subsystem are presented separately below:

Martian Environment Protection

For the Martian environmental protection, a large issue with the work done is that the dust removal capabilities of the compressed air system were not rigorously quantified. It is possible to estimate the properties of the compressed air at its outlet, but one must have a more accurate estimate of the density and velocity distributions of the gas over the solar panels to make sure that it is enough to remove the dust. It is hence recommended that a more rigorous simulation be made to model this behaviour.

Thermal Control System

The thermal control system analysis builds on the approach presented in the new SMAD [27] and incorporates aspects from the Spacecraft Thermal Design course and personal discussions with tutors and coaches. How-

ever, this analysis concentrated only on the lander due to time constraints. In order to fully design the thermal control system for the entire mission, the ascent phase of the MAV would have to be investigated. It was also assumed that the payload container is appropriately designed, with the beacons properly shielded and kept at operating temperatures. Furthermore, it's assumed that the samples can either survive in the temperatures in space or that they are maintained at Martian temperatures by the payload capsule.At the current stage, only a uniform temperature lander interior and the cryogenic tanks are included in the analysis.
Further analysis steps should focus on a nodal analysis of a more complete model. Then to further refine the design, thermal analysis software like ESATAN-TMS should be utilised.

ISRU
The ISRU shall be treated much more in detail in a more advanced study. Because of only recent use of that type of system, a lot of trial and testing still needs to be done. The emphasis should be put on the things that differ the most between this mission and MOXIE: the purification of the carbon monoxide feed, and assurance of long-term functioning. Even though batch sorption was discarded for this study, it is recommended to look into it as it may hold a better solution for a long-term operating mission, considering it has fewer moving parts than a mechanical compressor. Additionally, because of its working process, it may give an extra benefit of getting rid of the inert gases, allowing the gas that is taken in to be almost perfect carbon dioxide. Due to the large time constraint, this study could not come up with a sensible purification method for the CO feed. A thorough look should be done in this field to ensure even the 90% of purity that was chosen before.

Propellant Handling
One recommendation for the propellant handling subsystem is to explore the idea of conjoined or concentric tanks, as this could reduce the cooling requirements. Another recommendation is to analyse the idea of only cooling the propellants until liquefied in order to store on the SRL, and then cooling to the final temperature prior to loading onto the MAV. This would decrease the amount of thermal insulation needed, but increase the cooler mass, potentially leading to improvements.

Structural Characteristics
A more thorough structural analysis of the lander would be necessary in future studies, including supporting piggyback payload mass. An analysis into a leg configuration which remains balanced when bringing the MAV into launch configuration should also be done in future studies. Further studies should also study the loads of the plume being deflected by the lander to a more quantitative degree, as the exact mechanisms of this feature are difficult to quantify without a rigorous aerodynamic model.

Command and Data Handling
To enhance the command and data handling subsystem for future Mars missions, several areas of research and analysis could be pursued. Firstly, evaluating the performance and reliability of the off-the-shelf Zigbee module in the harsh Martian environment would be a worthwhile investment, while the Ingenuity Helicopter was able to work with one, specific details on the long term-reliability are unclear. Exploring advanced communication technologies and protocols could also offer improvements in data transmission rates and robustness and would have benefits reaching far beyond the MSR mission, though it is important that any new advances remain compatible with other mission elements.

Electrical Power System
The solar array needed for the SRL is going to be more than double that of the largest solar array put on Mars further analysis into the deployment of such an array would be necessary, as the solar panel configuration of 4 wings varies rather significantly from the typically 2 wing approach. Potentially adverse effects of such large arrays should be investigated, in particular for thermal management. Further studies into how well the staggering advancements in battery technology of recent years can be implemented for Mars applications should be investigated.

Propulsion System
For the propulsion system, in particular the feed system, a possibility of a "bang-bang" system to keep the propellant tanks pressurised was found but was due to time constraints not looked into. This is one of the design options that should be further looked into. Next to this, research into combustion instabilities and a further in-depth study on cavitation should be performed. Lastly, due to the scope of the project, no research was done into the effects of cryogenic temperatures on pump performance and is a vital next step into designing the feed system.

Engine Performance Analysis

Our engine design is currently based solely on theoretical analysis and has not undergone further testing. For future research on rocket engines, several suggestions are proposed. First, the bell nozzle requires CFD analysis and actual testing to determine a more optimised shape. Previous testing has indicated that a conventional bell nozzle may not be as efficient as non-conventional designs. Second, the combustion chamber design relies on assumptions, computer simulations, and limited experimental data, necessitating further research and experimentation. Known experiments suggest that the liquid fuel requires a specific length to evaporate fully; thus, testing should verify whether the current combustion chamber length prevents injector burnout and ensures a better homogeneous fuel mixing. Additionally, the choice of injector and potential combustion instability, which could lead to pressure drops and issues such as pogo instability, should be investigated further. Alternative cooling methods, including regenerative and radiation cooling (using refractory materials), should also be considered and tested. Although film cooling and ablative cooling were not selected in the initial design, experiments should still be conducted to validate these trade-off decisions. Lastly, the re-entry conditions on Mars have not been addressed in this report; further analysis on engine due to re-entry for Mars missions is required.

AOCS

This study used mainly off-the-shelf components for the AOCS system, which does not provide the most efficient solution for the components used. Especially for the TVC system, a more beneficial approach would be to design the actuators specifically for the MAV, rather than scaling down actuators designed for Earth based launchers. Another improvement to the study would be to make a more detailed analysis of the potential disturbances on the MAV during its ascent, perhaps using simulation software rather than general equations.

Ascent Profile

As mentioned in the ascent analysis, a low-fidelity tool was used in favour of a more advanced tool like GMAT or Tudat Space. The sensitivity analysis showed that small changes in propulsion and TVC performance can have large influences on the final orbit size, if not adequately compensated by the AOCS system. The used tool only featured basic guidance constant guide control that does not respond to any feedback. It is recommended to use a more advanced simulation where the guidance control takes feedback to compensate and establish the required control precision and authority for the first stage TVC and second stage RCS.

Astrodynamics

The pickup orbit was analysed using NASA's GMAT software, where the parameters, like the RAAN has been adjusted in order to minimise the orbital decay and the fluctuation in inclination.

GMAT offers the possibility to automatically optimise the trajectory for a given mission. This has not been utilised for this analysis due to the complexity and steep learning curve of the software. It is recommended that future analyses try and optimise the trajectory for less inclination variation.

RAMS Analysis

The Reliability analysis has shown that the mission failure probability is at about 75%, this is of course unacceptable. The low reliability can be traced back to the ISRU and the power generation.

Research should be aimed at quantifying the reliability of the ISRU in continous operation. In order to increase the reliability of the solar panels, it's recommended to increase the redundancy.

Engineering Budgets

The current estimates for the mass, power, and volume budgets are preliminary and require further iteration. Historical data shows that mission estimations can vary significantly over time. Some figures may be inaccurate, and certain components, particularly those related to integration, might be missing. Additional testing is necessary to identify and account for any support systems that may be discovered during the process. Despite these uncertainties, the presented numbers are precise and indicate that this mission segment is highly achievable, warranting serious consideration and further investigation.

Mission Budgets

The cost estimates provided are preliminary and based on outdated methodologies. A comprehensive audit or detailed estimation by experts with relevant experience is recommended, as the current report was prepared by individuals without industry or political experience. Additionally, the schedule budget is an approximation and requires input from all stakeholders and contractors involved in the mission. Accurate timelines can only be established with their collaboration and insights.

General Recommendations

Throughout the course of this analysis, a few topics kept coming back to complicate the generation of the design concept. These two topics were identified as essential research and analysis topics. The ISRU presented one of the reoccurring hurdles. CO2 electrolysis is a well-established concept, with a lot of research going into it. Unfortunately, almost all the research is focused on the purification of oxygen and treats CO as a waste product. The Perseverance lander equipped MOXIE has proven that CO2 electrolysis is possible in the Martian environment. However, MOXIE had an on-off operation, the ISRU on the BAGEL mission is intended to work continuously, research has to be conducted on the degradation rates associated with continuous operation, in order to increase the reliability of the process. Additionally, there are no go to or off-the-shelf solutions for separating the carbon monoxide from the other waste gasses. The engine performance relies on the purity of the propellants. Future analyses should concentrate on the options or development of viable CO separation methods. The purity of the propellants is not the only difficulty that arose during the analysis of the engine. There is only a small amount of data on LCO-LOX engines and the combustion mechanisms behind them. Due to this reason, the residence time and characteristic chamber length had to be taken from LH2-LOX engines. This could lead to the engine under-performing significantly. It's crucial for the mission success to start engine development and experimental data gathering as soon as possible in order to converge on a viable engine design.

General Implications

The successful completion of this project paves the way for future advancements in Martian exploration, setting a precedent for propulsion based on in-situ propellant creation. The scaling up of the MOXIE provides extra data and knowledge into creating a system capable of creating breathable air on Mars, as well as implication of carbon capture on earth. The blow down system will provide ways to clean dust off solar panels on Mars, which has been an issue in the past when bad weather occurs. Lastly, the feed system design using e-pumps for low thrust applications provide essential data into downsizing turbomachinery and technical advancements in turbomachinery design.

References

[1] R. Ó. hAnluain, S. Balfoort, D. Campbell-Pitt, B. Chen, R. Decuyper, A. Hanrahan, J. Piaskowy, J. Rodrigo, M. Seres, O. Várnagy, and P. Zanini, "Project mars lox/lco dse group 20 baseline report," TUDelft, Tech. Rep., 2024.

[2] R. Ó hAnluain, S. Balfoort, D. Campbell-Pitt, B. Chen, R. Decuyper, A. Hanrahan, J. Piaskowy, J. Rodrigo, M. Seres, O. Várnagy, and P. Zanini, "BAGEL: Mars LOX/LCO DSE Group 20 Midterm Report," Tech. Rep., 2024.

[3] R. Zubrin, *The Case for Mars: The Plan to Settle the Red Planet and Why We Must*. 1996.

[4] T. K. Derry, *A History of Scandinavia: Norway, Sweden, Denmark, Finland, and Iceland*. 1979, ISBN: 0-8166-0936-5.

[5] B. Jyoti, "Project Guide Design Synthesis Exercise," 2024.

[6] NASA, *Mars Sample Return Science*. [Online]. Available: https://science.nasa.gov/mission/mars-sample-return/science/.

[7] COSPAR, *Cospar policy on planetary protection*, 2021. [Online]. Available: https://cosparhq.cnes.fr/assets/uploads/2021/07/PPPolicy_2021_3-June.pdf.

[8] H. Dezfuli, A. Benjamin, C. Everett, G. Maggio, M. Stamatelatos, R. Youngblood, S. Guarro, P. Rutledge, J. Sherrard, C. Smith, and R. Williams, "NASA Risk Management Handbook," NASA, Tech. Rep., 2011. [Online]. Available: https://ntrs.nasa.gov/citations/20120000033.

[9] J. Leitner, *Risk classification and risk-based safety and mission assurance*, 2014.

[10] A. Nelessen, C. Sackier, I. Clark, P. Brugarolas, G. Villar, A. Chen, A. Stehura, R. Otero, E. Stilley, D. Way, K. Edquist, S. Mohan, C. Giovingo, and M. Lefland, "Mars 2020 entry, descent, and landing system overview," *2019 IEEE Aerospace Conference*, pp. 1–20, 2019. DOI: 10.1109/AERO.2019.8742167.

[11] B. Muirhead, A. Nicholas, and J. Umland, "Mars sample return mission concept status," *2020 IEEE Aerospace Conference*, pp. 1–8, 2020. DOI: 10.1109/AERO47225.2020.9172609.

[12] S. O'Briant, S. Gupta, and S. Vasu, "Review: Laser ignition for aerospace propulsion," *Propulsion and Power Research*, vol. 5, no. 1, pp. 1–21, 2016.

[13] K. A. Burke, "Fuel cells for space science applications," Glenn Research Center, Cleveland, Ohio, Tech. Rep., 2003.

[14] M. C. Guzik, "Regenerative fuel cell power systems for lunar and martian surface exploration," Glenn Research Center, Cleveland, OH, Tech. Rep., 2017.

[15] G. M. R. Bob G. Beaman, "Hybrid battery and flywheel energy storage system for leo spacecraft," Goddard Space Flight Center Greenbelt, Tech. Rep., 1998.

[16] B. Marchon, W. Tysoe, J. Carrazza, H. Heinemann, and G. Somorjai, "Reactive and kinetic properties of carbon monoxide and carbon dioxide on a graphite surface," *The Journal of Physical Chemistry*, vol. 92, pp. 5744–5749, Oct. 1988. DOI: 10.1021/j100331a039.

[17] D. on Engineering and P. Sciences, *Safe on Mars: Precursor Measurements Necessary to Support Human Operations on the Martian Surface*. Washington, DC: The National Academies Press, 2002.

[18] C. L. Younger, "THE INFLUENCE OF NUCLEAR RADIATION ON THE CORROSION CF METALS," [Online]. Available: https://www.osti.gov/servlets/purl/4070524#:~:text=Nuclear%20radiation%20studies%20of%20damage,only%20heat%20to%20the%20metal..

[19] M. Litvak, A. Sanin, and I. Mitrofanov, "Mars neutron radiation environment from hend/odyssey and dan/msl observations," *Planetary and Space Science*, vol. 184, 2020.

[20] *Nuclear and space radiation effects on materials*, Jun. 2015. [Online]. Available: https://www.nrc.gov/docs/ML1533/ML15334A202.pdf.

[21] D. Hassler, "Mars' surface radiation environment measured with the mars science laboratory's curiosity rover," *Science*, vol. 343, 2013.

[22] A. Keys and M. Watson, “Radiation hardened electronics for extreme environments,” NASA, Tech. Rep., 2007.

[23] J. Zhang, W. Wang, and S. zhou, “Transparent dust removal coatings for solar cell on mars and its anti-dust mechanism,” *Progress in Organic Coatings*, vol. 134, pp. 312–322, 2019.

[24] D. Li, “Study on the cleaning and cooling of solar photovoltaic panels using compressed airflow,” *Solar Energy*, vol. 221, pp. 433–444, 2021.

[25] J. G. Kempenaar, K. S. Novak, M. J. Redmond, E. Farias, K. Singh, and M. F. Wagner, *Detailed Surface Thermal Design of the Mars 2020 Rover*, Jul. 2018. [Online]. Available: http://hdl.handle.net/2346/74064.

[26] V. M. L. Yang, “A high-efficiency, small, solid-state laser for pyrotechnic ignition,” *JPL Quarterly Technical Review*, vol. 2, no. 4, 1973.

[27] J. R. Wertz, D. F. Everett, and J. J. Puschell, *Space mission engineering : the new SMAD* (Space technology library ; v. 28), eng. Hawthorne, CA: Microcosm Press, 2011, ISBN: 9781881883159.

[28] I. Urial Balbin and N. van der Pas, *Spacecraft Thermal Design*.

[29] S. L. Bapat, K. G. Narayankhedkar, and T. R. Lukose, “Performance prediction of multilayer insulation,”

[30] K. Daryabeigi, “Thermal Analysis and Design of Multi-layer Insulation for Re-entry Aerodynamic Heating,” ISSN: 2001-2834.

[31] M. Hecht, J. Hoffman, D. Rapp, J. McClean, J. SooHoo, R. Schaefer, A. Aboobaker, J. Mellstrom, J. Hartvigsen, F. Meyen, E. Hinterman, G. Voecks, A. Liu, M. Nasr, J. Lewis, J. Johnson, C. Guernsey, J. Swoboda, C. Eckert, C. Alcalde, M. Poirier, P. Khopkar, S. Elangovan, M. Madsen, P. Smith, C. Graves, G. Sanders, K. Araghi, M. de la Torre Juarez, D. Larsen, J. Agui, A. Burns, K. Lackner, R. Nielsen, T. Pike, B. Tata, K. Wilson, T. Brown, T. Disarro, R. Morris, R. Schaefer, R. Steinkraus, R. Surampudi, T. Werne, and A. Ponce, *Mars Oxygen ISRU Experiment (MOXIE)*, Feb. 2021. DOI: 10.1007/s11214-020-00782-8.

[32] J. A. Hoffman, M. H. Hecht, D. Rapp, J. J. Hartvigsen, J. G. SooHoo, A. M. Aboobaker, J. B. McClean, A. M. Liu, E. D. Hinterman, M. Nasr, S. Hariharan, K. J. Horn, F. E. Meyen, H. Okkels, P. Steen, S. Elangovan, C. R. Graves, P. Khopkar, M. B. Madsen, G. E. Voecks, P. H. Smith, T. L. Skafte, K. R. Araghi, and D. J. Eisenman, “Mars Oxygen ISRU Experiment (MOXIE)-Preparing for human Mars exploration,” Tech. Rep., 2022. [Online]. Available: https://www.science.org.

[33] D. A. Aboobaker, *Moxie: Generating oxygen on mars*, 2017.

[34] M. Nasr, F. Meyen, and J. Hoffman, “Scaling the Mars Oxygen ISRU Experiment (MOXIE) for Mars Sample Return,” Tech. Rep., 2018.

[35] J. R. Olson, P. Champagne, E. Roth, and T. Nast, “Very high capacity aerospace cryocooler,” in *AIP Conference Proceedings*, vol. 1434, 2012, pp. 161–167, ISBN: 9780735410206. DOI: 10.1063/1.4706917.

[36] “International standard: Cryogenic vessels - transportable vacuum insulated vessels of not more than 1 000 litres volume,” p. 10, 2018, Second Edition - Part 1.

[37] M. C. Olde, R. Wubben, E. Gilleran, K. de Kievit, B. Kevers, and M. van Heijningen, “Investigation of the in-flight failure of the stratos iii sounding rocket,” Delft Aerospace Rocket Engineering, Tech. Rep., 2019.

[38] P. Jianxin and L. Yigang, “Estimation of the surface tension of liquid carbon dioxide,” *Physics and Chemistry of Liquids - PHYS CHEM LIQ*, vol. 47, pp. 267–273, Jun. 2009. DOI: 10.1080/00319100701824389.

[39] J. M. J. J. Hartwig and J. M. Jurns, *Liquid oxygen liquid acquisition device bubble point tests with high pressure lox at elevated temperatures*.

[40] B. T. C. Zandbergen, *Course ae4s01 thermal rocket propulsion (version 2.09)*, Sep. 2022.

[41] D. Rea, D. Bayles, P. Kapcio, S. Doyle, and D. Stanley, “PowerPC ™ RAD750™-A Microprocessor for Now and the Future,” Tech. Rep., 2005.

[42] J. Appelbaum and D. J. Flood, “Solar radiation on Mars,” *Solar Energy*, vol. 45, no. 6, pp. 353–363, Jan. 1990, ISSN: 0038-092X. DOI: 10.1016/0038-092X(90)90156-7.

[43] R. D. Lorenz, G. M. Martínez, A. Spiga, A. Vicente-Retortillo, C. E. Newman, N. Murdoch, F. Forget, E. Millour, and T. Pierron, “Lander and rover histories of dust accumulation on and removal from solar arrays on Mars,” *Planetary and Space Science*, vol. 207, p. 105 337, Nov. 2021, ISSN: 0032-0633. DOI: 10.1016/J.PSS.2021.105337.

[44] F. M. U. Khan, M. G. Rasul, A. S. Sayem, and N. Mandal, “Maximizing energy density of lithium-ion batteries for electric vehicles: A critical review,” *Energy Reports*, vol. 9, pp. 11–21, Oct. 2023, ISSN: 2352-4847. DOI: 10.1016/J.EGYR.2023.08.069.

[45] B. V. Ratnakumar, M. C. Smart, C. K. Huang, D. Perrone, S. Surampudi, and S. G. Greenbaum, “Lithium ion batteries for Mars exploration missions,” Tech. Rep., 2000. [Online]. Available: www.elsevier.nl/locate/electacta.

[46] C. Romero-Guzmán, I. Pérez-Grande, and J. A. Rodríguez-Manfredi, “Thermal model of InSight solar panels in Martian conditions,” *Acta Astronautica*, vol. 202, pp. 476–484, Jan. 2023, ISSN: 0094-5765. DOI: 10.1016/J.ACTAASTRO.2022.10.045.

[47] D. L. Linne, “Carbon Monoxide and Oxygen Combustion Experiments: A Demonstration of Mars In Situ Propellants,” Tech. Rep., 1991.

[48] A. Cervone, “AE2230-II Propulsion and Power, Lecture RP2-1,” 2023.

[49] D. L. Linne, “A Rocket Engine for Mars Sample Return Using In Situ Propellants,” Tech. Rep., 1997.

[50] P. Rachov and H. T. D. Lentini, *Electric feed systems for liquid propellant rocket engines*, Dec. 2010. DOI: 10.13140/2.1.4431.9042. [Online]. Available: https://www.aacademica.org..

[51] D. K. Huzel and D. H. H. Huang, *DESIGN OF LIQUID PROPELLANT ROCKET ENGINES*, 2nd ed. 1967.

[52] M. S. Gontijo, G. A. A. Fischer, and F. D. S. Costa, *Characteristic lengths of liquid propellant rocket engines and the influence of chemical reactions*, Dec. 2021. DOI: 10.26678/abcm.cobem2021.cob2021-2105.

[53] D. L. Linne, *Performance and heat transfer characteristics of a carbon monoxide/oxygen rocket engine*, Feb. 1993.

[54] E. S. Armstrong, *Cooling of in-situ propellant rocket engines for mars mission*, Jan. 1991.

[55] G. V. R. Rao, “Exhaust nozzle contour for optium thrust,” *Jet Propulsion*, Jun. 1958.

[56] J. L. Cannon, “Chapter 2.3.11 Liquid Propulsion: Propellant Feed System Design,” Tech. Rep.

[57] W. E. Campbell and J. Farquhar, “Centrifugal Pumps for Rocket Engines,” Tech. Rep.

[58] E. S. Armstrong, “Cooling of In-Situ Propellant Rocket Engines for Mars Mission,” Lewis Research Center, Ohio, Tech. Rep., Jan. 1991.

[59] L. Denies, “Regenerative cooling analysis of oxygen/methane rocket engines,” M.S. thesis, TU Delft, 2015.

[60] J. Grobusch and F. Kesteren, “Dlx-150a ”battleship” & dlx-150b ”firebolt” design report,” Delft Aerospace Rocket Engineering, Tech. Rep., 2022.

[61] S. Lee, G. G. Ortiz, and J. W. Alexander, “Pointing knowledge accuracy of the star tracker based atp system,” vol. 5712, SPIE, Apr. 2005, p. 255. DOI: 10.1117/12.612037.

[62] H. Nguyen, J. Köhler, and L. Stenmark, *The merits of cold gas micropropulsion in state-of-the-art space missions*, 2002.

[63] G. Sutton and O. Biblarz, *Rocket Propulsion Elements*. John Wiley & Sons, 2010, ISBN: 9780470080245. [Online]. Available: https://books.google.nl/books?id=1Sf6eV6CgtEC.

[64] NASA, *Mars Facts*. [Online]. Available: https://science.nasa.gov/mars/facts/.

[65] NASA Office of Inspector General, “Audit of the Mars Sample Return Program,” Tech. Rep., 2024. [Online]. Available: https://oig.nasa.gov/hotline.html..

[66] C. P. Frank, C. M. Tyl, O. J. Pinon-Fischer, and D. N. Mavris, “New design framework for performance, weight, and life-cycle cost estimation of rocket engines,” Tech. Rep., 2015.

[67] NASA Office of Inspector General, “NASA’S Mars 2020 Project,” Tech. Rep., 2017. [Online]. Available: https://oig.nasa.gov/hotline.html..

[68] K. C. Wu, J. Antol, J. J. Watson, R. J. Saucillo, D. D. North, and D. D. Mazanek, “Lunar lander structural design studies at nasa langley,” vol. 2, American Institute of Aeronautics and Astronautics Inc., 2007, pp. 1579–1591, ISBN: 1563479079. DOI: 10.2514/6.2007-6137.

[69] M. K. Biswal and R. N. Annavarapu, *Conceptual design of mars lander with novel impact intriguing system*.

[70] B. K. Muirhead, A. Nicholas, and J. Umland, *Mars Sample Return Mission Concept Status*. 2019, ISBN: 9781538668542.

[71] R. Shotwell, J. Benito, A. Karp, and J. Dankanich, “Drivers, developments and options under consideration for a Mars ascent vehicle,” in *IEEE Aerospace Conference Proceedings*, vol. 2016-June, IEEE Computer Society, Jun. 2016, ISBN: 9781467376761. DOI: 10.1109/AERO.2016.7500822.

[72] R. Zubrin and S. Price, “Mars Sample Return mission utilizing in-situ propellant production,” NASA, Tech. Rep., 1995. [Online]. Available: https://ntrs.nasa.gov/citations/19950021840.

[73] M. S. Yaghoubi D, *Integrated Design Results for the MSR SRC Mars Ascent Vehicle*. Huntsville, Alabama, 2021.